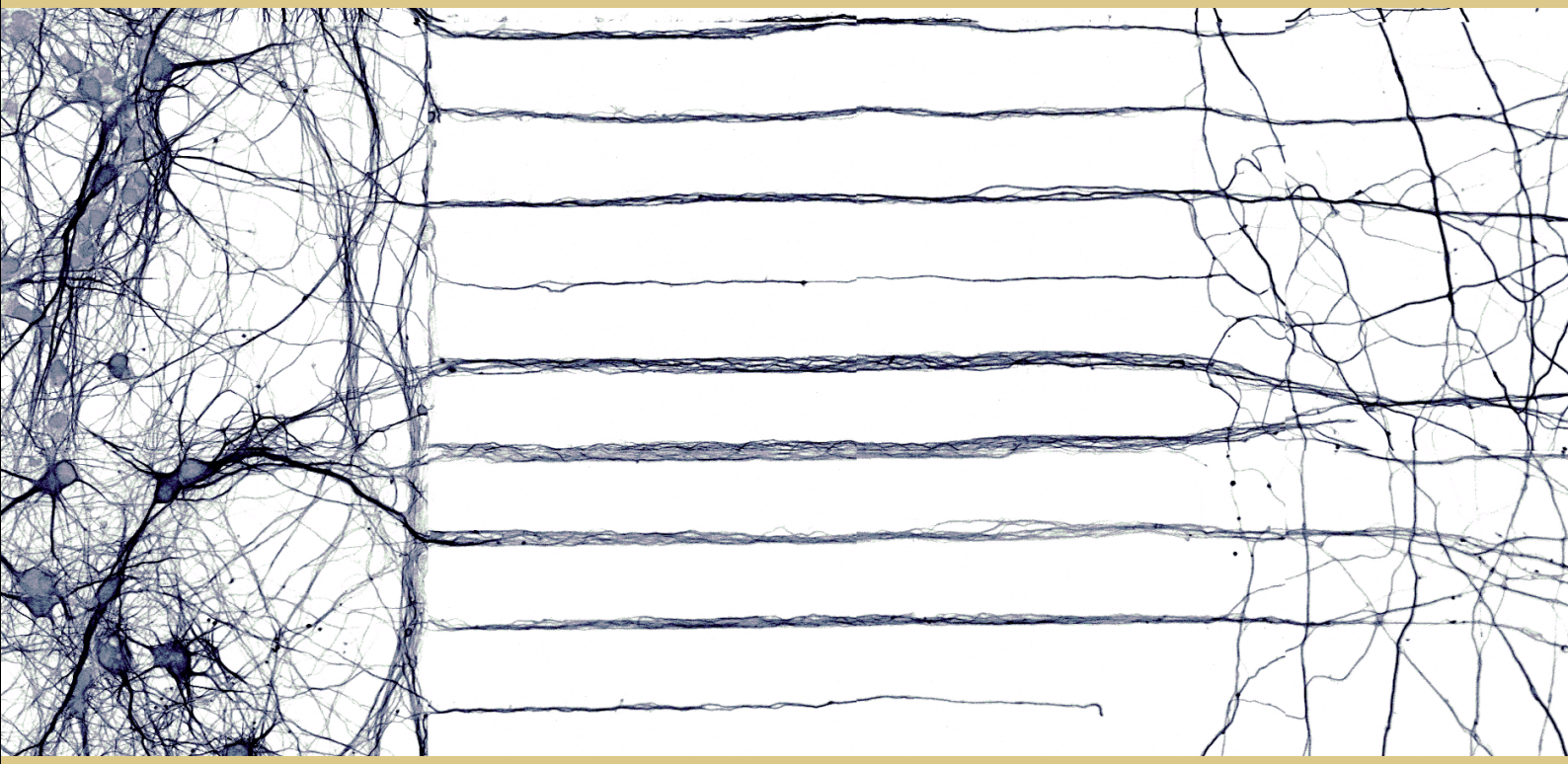

Maria Joana Guimarães Pinto

PRESYNAPTIC FORMATION AND FUNCTION UNDER THE CONTROL OF UBIQUITIN AND THE PROTEASOME

Tese de Doutoramento em Biologia Experimental e Biomedicina, Ramo de Neurociências e Doença orientada pelo Professor Ramiro Almeida e pela Professora Ana Luísa Carvalho e apresentada ao Instituto de Investigação Interdisciplinar da Universidade de Coimbra (IIIUC)

Abril de 2015

· U C ·

Universidade de Coimbra

Presynaptic formation and function under the control of ubiquitin and the proteasome

Tese de Doutoramento em Biologia Experimental e Biomedicina,
Ramo de Neurociências e Doença

Maria Joana Guimarães Pinto
Abril 2015

Dissertação apresentada ao Instituto de Investigação Interdisciplinar da Universidade de Coimbra (III-UC) para prestação de provas de Doutoramento em Biologia Experimental e Biomedicina, Ramo de Neurociências e Doença.

Este trabalho foi realizado no Centro de Neurociências e Biologia Celular (Universidade de Coimbra) e no Departamento de Engenharia Biomédica da Universidade da Carolina do Norte em Chapel Hill, sob a supervisão do Professor Doutor Ramiro Almeida (Centro de Neurociências e Biologia Celular e Instituto de Investigação Interdisciplinar da Universidade de Coimbra) e co-supervisão da Professora Doutora Ana Luísa Monteiro de Carvalho (Departamento de Ciências da Vida, Faculdade de Ciências e Tecnologia da Universidade de Coimbra). Este trabalho foi financiado pela bolsa de Doutoramento individual SFRH/BD/51196/2010 da Fundação para a Ciência e Tecnologia (FCT, Portugal) e por fundos FEDER através do Programa Operacional Factores de Competitividade – COMPETE e por Fundos Nacionais através da FCT no âmbito dos projectos PTDC/SAU-NEU/104100/2008, EXPL/NEU-NMC/0541/2012, Pest-C/SAU/LA0001/2013-2014 e UID/NEU/04539/2013 e por Marie Curie Actions, International Reintegration Grant, 7th Framework Programme, EU.

In cover image, rat hippocampal neurons grow in a microfluidic device and extend their axons through microchannels into a separate, fluidically-isolated compartment.

Agradecimentos

Gostaria de agradecer ao meu orientador, Ramiro Almeida, por todo o conhecimento que me transmitiu durante estes anos, todos os conselhos e apoio, pela confiança que depositou em mim e acima de tudo pela liberdade que me deu no decorrer do trabalho laboratorial.

À Professora Ana Luísa Carvalho pela análise crítica, sugestões e ideias que ajudaram grandemente a definir um rumo a este trabalho.

Ao Professor Carlos Duarte por todo o acompanhamento intelectual no decorrer destes anos.

To Anne Taylor, for giving me the great opportunity of working in her lab and for all the help and support.

Ao Paulo Pinheiro pela ajuda na escrita da tese. Gostaria igualmente de agradecer à Célia pela ajuda na formatação. Muito obrigada à Luísa Cortes pela ajuda na microscopia. Gostaria igualmente de agradecer à Elisabete por toda a ajuda nas culturas e incansável organização do laboratório. Obrigada à D. Céu por toda a ajuda com o material, mas essencialmente pela extrema simpatia e pelo sorriso fortalecedor todas as manhãs.

Agradeço à Fundação para a Ciência e Tecnologia pelo financiamento, ao Programa Doutoral em Biologia Experimental e Biomedicina por me ter proporcionado esta oportunidade e ao Centro de Neurociências e Biologia Celular onde desenvolvi a maior parte do trabalho e que me possibilitou a entrada nesta vida científica.

A todos os membros do grupo do Ramiro Almeida com os quais partilhei bancada, pipetas, bebidas, noitadas ou madrugadas. Obrigada à Tânia Perestrelo, Luís Leitão, Inês Coelho, Sandra Rebelo, Ana Rita Pombo, Rui Costa, Pedro Alves, Helena Martins e Susana Sampaio. Um especial obrigado à Joana Pedro, o meu braço direito nesta longa caminhada, quero agradecer por todos os momentos partilhados, pela força que sempre me transmitiu, pelos desabafos (bons ou maus) e por todo o apoio. Ao meu fiel pupilo Luís Martins obrigada pela boa disposição e companheirismo, foi para mim um prazer trabalhar na atmosfera alegre que o rodeia.

Às muitas pessoas dos grupos do Carlos Duarte, Ana Luísa e João Peça, que pisaram ou que ainda pisam o laboratório e que, de variadíssimas formas e feitios, contribuíram para o ambiente fantástico onde trabalhamos o meu grandioso obrigado. Foi para mim um prazer "brincar" aos cientistas e às suas frustrações com todos vós (sem excepção).

Muito obrigada à Tatiana Catarino pelo carinho especial e a companhia que só uma namoradinha sabe dar! À Dominique pelos eventuais "miminhos" e pela companhia dentro e fora do laboratório. Uma vez chefinho, para sempre chefinho. Obrigada ao Graciano por ter começado isto comigo e por me ter dado a conhecer da melhor forma o mundo da investigação. Obrigada ao João Costa pela felicidade constante e contagiante. Ao Mário pelas conversas, por me espicaçar, por me fazer sentir burra e ignorante, por ser uma fonte de inspiração e admiração.

Aos meus 11 colegas do BEB com os quais partilhei tempos intensivos, mas agradáveis e muito estimulantes. Foi um óptimo equilíbrio entre trabalho e diversão e um excelente começo do doutoramento.

To everyone in Chapel Hill for making me feel welcome and belonged since the very beginning. Specially to my queen of the road Maria Abad, for all her positive and forceful vibrations, but mostly for sharing with me so much in such a little time. To Joyce Kamande for the wonderful time we spent together in the lab and for explaining me what a human hurricane really is.

A todos os meus amigos que mesmo não fazendo parte desta vida de ciência me enchem de felicidade e vontade de nunca parar.

Às minhas aulas de dança e à minha professora de ballet pelo escape maravilhoso que sempre foram para mim e pela energia com que delas sempre saía, mesmo que completamente estafada e suada.

À minha família pelo apoio, confiança e carinho. Um especial obrigado aos meus irmãos.

Ao Luís por me fazer sentir completa e feliz. Por ser uma excelente pessoa e investigador, pela sua coragem e pelo orgulho que nutro por ele, por tudo o que aprendi com ele e por tudo o que ainda aprenderei.

Ao meu pai, pela energia infindável.

À minha mãe, por ser o verdadeiro pilar da minha vida.

Table of contents

Abbreviations

2-AG	2-arachidonoyl glycerol
5-FDU	5-fluorodeoxyuridine
AKAP	A-kinase anchor protein
ALK	anaplastic lymphoma kinase
AMPA	α-amino-3-hydroxy-5-methyl-4-isoxazole propionic acid
APC	anaphase promoting complex
APP	amyloid precursor protein
ARL-8	arf-like small G protein
AS	Angelman syndrome
BCA	bicinchoninic acid
BDNF	brain-derived neurotrophic factor
BHK-1	baby hamster kidney 1
β-lactone	clasto-lactacystin β-lactone
BSA	bovine serum albumin
CamKII	calcium/calmodulin-dependent protein kinase II
CASK	calcium/calmodulin-dependent serine kinase
CAST/ERC	CAZ-associated structural protein/ELKS-Rab6-interacting protein-CAST
CAZ	cytomatrix of the active zone
Cbln	cerebellin
Cdk5	cyclin-dependent kinase 5
CLAP	chymostatin/ leupeptin/ antipain/ pepstatin
CNQX	6-cyano-7-nitroquinoxaline-2,3-dione
CNS	central nervous system
CP	catalytic core particle
CPE	carboxypeptidase E
CSPα	cysteine string protein α
D-AP5	D-2-amino-5-phosphonovalerate
DCC	deleted-in-colorectal cancer
DCV	dense-core vesicles
DIV	days *in vitro*
DLK	dual leucine-zipper-bearing kinase
DUB	deubiquitinating enzyme
ECF	enhanced chemifluorescence
eGFP	enhanced green fluorescence protein
Eps15	epidermal growth factor receptor substrate 15
ER	endoplasmic reticulum
ERAD	ER associated degradation
ERK	extracellular-signal-regulated kinase
F-actin	filamentous actin
Faf	fat facets
FBS	fetal bovine serum
FGF	fibroblast growth factor

FGFR	FGF receptor
FLRT3	fibronectin leucine-rich repeat transmembrane protein 3
FOVs	fields of view
GDNF	glial cell line–derived neurotrophic factor
GEF	guanine exchange factor
GFP	green fluorescence protein
GFRα1	glial cell line–derived neurotrophic factor receptor
GKAP	guanylate-kinase-associated protein
GluR	glutamate receptor
HBS	HEPES-buffered solution
HBSS	Hank´s balanced salt solution
HECT	homologous to E6-AP carboxy-terminus
HEK	human embryonic kidney
HEPES	N-(2-hydroxyethyl) piperazine-N'-(2-ethanesulfonic acid)
HSNL	hermaphrodite-specific motor neuron
Hsp	heat shock protein
Id2	inhibitor of DNA binding 2
IKK	inhibitor of κB kinase
IL-1RAcP	interleukin-1 receptor accessory protein
IL1RAPL1	interleukin-1-receptor accessory protein-like 1
IRES	ribosome entry site
JAMM	JAB1/MPN/Mov34 metallo enzyme
JNK	c-Jun N-terminal protein kinase
K	lysine
KIF	kinesin
KO	knockout
LAP	leucine-rich repeats and PDZ domain
LAR	leukocyte antigen-related
LIMK1	LIM kinase 1
LPA	L-α-Lysophosphatidic acid
Lqf	liquid facets
LRR	leucine-rich repeat
LRRTM	leucine-rich repeat transmembrane protein
Lys	lysine
MEM	minimum essential medium eagle
Met1	Methionine 1
MGL	monoaclyglycerol lipase
MJD	Machado-Joseph disease
MULAN	mitochondrial ubiquitin ligase activator of NF-κB
NA	numerical aperture
NaF	sodium fluoride
NF-κB	nuclear factor kappa enhancer binding protein
NGL	netrin-G ligand
NMDA	*N*-methyl-D-aspartate
NMJ	neuromuscular junction

NMNAT	nicotinamide mononucleotide adenyltransferase
NSF	N-ethylmaleimide sensitive factor
OTU	otubain proteases
PAP	proteasome activity probe
Par	portioning-defective proteins
PBS	phosphate buffered saline
PCT-1	cyclin-dependent Pctaire kinase
PDK1	protein kinase D1
PDL	poly-D-lysine
PDMS	poly-dimethylsiloxane
PDZ	PSD95/disc large/zonula occludens 1
PHR	human PAM, mouse Phr1, zebrafish Esrom, *Drosophila* Highwire and *C. elegans* RPM-1
PI3K	phosphatidylinositol-3-kinase
PIP_2	phosphatidylinositol 4,5-bisphosphate
PKA	protein kinase A
PMSF	phenylmethylsulfonyl fluoride
POI	protein of interest
PSD	postsynaptic density
PSD95	postsynaptic density protein 95
PTEN	phosphatase and tensin homolog
PTM	post-translational modification
PTP	protein tyrosine phosphatase
PTV	piccolo-bassoon transport vesicle
PVDF	polyvinylidene difluoride
RIM	rab3-interacting molecule
RING	really interesting new gene
RISC	RNA-induced silencing complex
RNF	RING finger protein
ROI	region of interest
RP	regulatory particle
Rpn	regulatory particle non-ATPase
Rpt	regulatory particle ATPse
RPTP	receptor type protein tyrosine phosphatase
RRP	readily-releasable pool
SCAMP1	secretory carrier-associated membrane protein 1
SDS	sodium dodecyl sulfate
SFC	skp1-Cullin-F-box
SIRP	signal regulatory protein
Slitrk	slit- and Trk-like family proteins
SM	sec1/Munc18-like
SMA	spinal muscular atrophy
SMN1	survival motor neuron 1
Smurf	smad ubiquitination regulatory factor
SNAP	soluble NSF-attachment protein
SNAP25	synaptosomal-associated protein 25

SNARE	soluble n-ethylmaleimide-sensitive factor attachment protein receptor
SPARC	secreted protein acidic and rich in cysteine
STV	synaptic vesicle protein transport vesicle
SUMO	small Ub-like modifier
SV	synaptic vesicle
SV2	synaptic vesicle protein 2
SynCAM	synaptic cell adhesion molecule
TAK1	TGFβ activated kinase 1
TBS	tris-buffered saline
TGS	tris-glycine-SDS
TNFR	TNF receptor
TNFα	tumor necrosis factor α
TrkB	tropomyosin-related kinase receptor B
TrkC	tyrosine kinase C
Ub	ubiquitin
UBD	ubiquitin-binding domain
UBL	ubiquitin-like domain
UBP	ubiquitin binding protein
UCH	ubiquitin C-terminal hydrolase
UCH-L1	ubiquitin C-terminal hydrolase L1
UiFC	ubiquitination-induced fluorescence complementation
UIM	ubiquitin interacting motif
UPS	ubiquitin proteasome system
USP	ubiquitin specific proteases
VAMP	vesicle-associated membrane protein
VGAT	vesicular GABA transporter
VGCC	voltage-gated calcium channels
Vglut1	vesicular glutamate transporter 1
Vit1a	vesicle transport through interaction with t-SNAREs homolog 1a
VSVG	vesicular stomatitis virus G
WB	western blot
WRC	WVE-WAVE regulatory complex
wt	wild-type
wtUb	wild-type form of ubiquitin
XL-SMA	X-linked infantile spinal-muscular atrophy

Keywords

Presynaptic differentiation

Neurotransmitter release

Ubiquitin

Proteasome

Polyubiquitination

FGF22

BDNF

Palavras-Chave

Diferenciação pré-sináptica

Libertação de neurotransmissores

Ubiquitina

Proteassoma

Poliubiquitinação

FGF22

BDNF

Resumo

O bom funcionamento da função cerebral no sistema nervoso depende do estabelecimento de contactos sinápticos precisos durante o desenvolvimento. O cérebro adulto é composto por um sem fim de sinapses as quais se estabelecem de forma ordenada. Em cada uma destas sinapses, um terminal pré-sináptico onde se acumulam vesículas contendo neurotransmissores encontra-se perfeitamente alinhado com uma série de receptores localizados na membrana pós-sináptica. O processo de formação de sinapses é um fenómeno de extrema importância que ocorre no cérebro em desenvolvimento, sendo que malformações durante este processo conduzem a graves doenças ao nível do desenvolvimento do sistema nervoso. Desta forma, o estudo em detalhe dos mecanismos que estão na base da diferenciação pré-sináptica assume um papel de extrema importância.

O estabelecimento de terminais pré-sinápticos ocorre ao longo do axónio em regiões afastadas do corpo celular. O material pré-sináptico chega a estes locais via transporte axonal na forma de complexos pré-fabricados, os quais são retidos em domínios específicos do axónio originando em última instância o terminal pré-sináptico. Uma das questões mais relevantes na área da biologia da formação de sinapses consiste em entender como o axónio consegue reter o material pré-sináptico e rapidamente organizá-lo numa estrutura pré-sináptica funcional. Até agora, vasta informação tem sido recolhida relativamente aos factores extracelulares ou factores transmembranares que comandam a diferenciação pré-sináptica; no entanto, poucos detalhes são ainda conhecidos sobre o que ocorre intracelularmente. A proteostase local, sobretudo através do sistema ubiquitina-proteassoma, tem sido apontada como essencial neste processo. A ubiquitina pode ligar-se às proteínas na sua forma monomérica ou na forma de cadeias de ubiquitina resultando em diferentes consequências na vida de uma proteína, incluindo o seu endereçamento para o proteassoma e posterior degradação.

Alterações na localização do proteassoma, a nível celular, ocorrem para satisfazer necessidades específicas. Neste trabalho, observámos que o proteassoma é redistribuído ao longo do axónio no decorrer da diferenciação pré-sináptica induzida por duas moléculas sinaptogénicas distintas: FGF22 e BDNF. Estas moléculas aumentam também o número de regiões de intensa actividade catalítica do proteassoma ao longo do axónio, e o seu efeito na formação de agregados pré-sinápticos depende da actividade do proteassoma. Um activador do proteassoma aumenta também o número de complexos pré-sinápticos de forma semelhante ao FGF22 e BDNF. Este primeiro conjunto de resultados sugere que a formação do terminal pré-sináptico requer degradação mediada pelo proteassoma e que simultaneamente ocorre redistribuição e acumulação do proteassoma activo.

De forma inesperada, inibidores do proteassoma apresentam um notável efeito sinaptogénico quando aplicados em axónios imaturos isolados. Na tentativa de entender esta dupla e aparente função antagónica do sistema ubiquitina proteassoma na montagem de complexos pré-sinápticos, usámos uma combinação de abordagens baseadas em microscopia em células vivas, marcação de terminais pré-sinápticos activos com sondas FM, diversos inibidores do sistema ubiquitina proteassoma, bem como formas mutantes da ubiquitina. Observámos que a montagem de um complexo pré-sináptico é acompanhada por uma diminuição localizada na actividade do proteassoma. Concluímos ainda que a acumulação de proteínas ubiquitinadas em resposta à inibição do proteassoma regula a pré-sinaptogénese, e que proteínas poliubiquitinadas através da lisina 48 acumulam-se localmente na sinapse em formação. Por último, observámos também que impedindo a formação de caudas de poliubiquitina, as quais se pensa direccionarem substratos para o proteassoma, o aumento na formação de complexos pré-sinápticos é

bloqueado. Desta forma, concluímos que uma paragem transitória na degradação ao nível do proteassoma promove a acumulação local de conjugados de poliubiquitina, o que funciona como um mecanismo desencadeador para a diferenciação pré-sináptica. No seu conjunto, os nossos resultados indicam que a ubiquitina e o proteassoma são capazes de promover diferenciação pré-sináptica através de dois processos idênticos, embora que opostos: aumento na degradação de proteínas ou acumulação transiente de conjugados poliubiquitinados.

No último grupo de resultados, focámos a nossa atenção no papel da ubiquitina ao nível da função pré-sináptica. Apesar de existirem algumas evidências de que sinalização através de ubiquitina influencia a libertação de neurotransmissores pré-sinapticamente, o envolvimento da poliubiquitinação neste fenómeno nunca tinha sido estudado. Observámos um aumento na taxa de libertação pré-sináptica após expressão de ubiquitina, o qual foi parcialmente bloqueado quando impedida a poliubiquitinação através das lisinas 11, 29 e 63. Desta forma, sugerimos que a ligação de cadeias de poliubiquitina aos seus substratos potencia a libertação de neurotransmissor pré-sinapticamente.

Em conclusão, estas observações destacam a importância da sinalização celular através de ubiquitina no terminal pré-sináptico, quer durante a sua formação, quer para a sua actividade. A natureza reversível e versátil das caudas de ubiquitina, particularmente ao nível das proteínas pré-sinápticas e/ou axonais, pode controlar múltiplas vias locais, e aparentemente antagónicas, que permitem modular o desenvolvimento e a função do terminal pré-sináptico.

Abstractet

Proper brain function in the nervous system relies on the accurate establishment of synaptic contacts during development. Countless synapses populate the adult brain in an orderly fashion. In each synapse, a presynaptic terminal loaded with neurotransmitters-containing synaptic vesicles is perfectly aligned to an array of receptors in the postsynaptic membrane. Synapse formation is a crucial event taking place in the young brain and abnormal synaptic wiring leads to severe neurodevelopmental diseases. It is therefore of the utmost importance to study in detail the mechanisms underlying presynaptic differentiation.

Building of presynaptic terminals occurs along the axon in regions that are distantly located from the cell body. Presynaptic material reaches these sites by axonal transport in the form of preassembled packets and will be retained in specific axonal domains ultimately giving rise to a presynaptic bouton. A major question in the field of synapse formation is to understand how the axon can capture presynaptic material and quickly arrange it into a functional presynaptic structure. So far, researchers have gathered a vast knowledge of extracellular or transmembrane factors that instruct presynaptic differentiation; however, what happens intracellularly is for the most part unresolved. Emerging evidence has attributed a role to local proteostasis, mainly through the ubiquitin-proteasome system. Ubiquitin can be attached to proteins either as a monomer or as a chain of ubiquitins with several different outcomes including targeting to the proteasome for degradation.

In cells, proteasome localization can undergo changes to fulfill specific needs. Herein, we observed that proteasomes redistribute along axons upon induction of presynaptic differentiation by two distinct synaptogenic factors, FGF22 and BDNF. These same molecules increase the number of catalytically active proteasome hot-spots along axons and their presynaptogenic effect is dependent on proteasome activity. Furthermore, a proteasome activator also increases the number of presynaptic clusters with the same magnitude as FGF22 and BDNF. Altogether, this first set of results indicates that FGF22 and BDNF-induced clustering of presynaptic material requires proteasome-mediated degradation and occurs alongside redistribution and accumulation of active proteasome.

Unexpectedly, proteasome inhibitors display a striking presynaptogenic activity when applied to immature isolated axons. In an attempt to understand this dual and antagonic role of the UPS in presynaptic assembly, we used a combination of live imaging approaches, labeling of active terminals with FM dye, distinct UPS inhibitors and site-directed mutants for the ubiquitin molecule. We observed that assembly of a presynaptic cluster is accompanied by an *on-site* decrease in proteasome activity. We further concluded that the accumulated pool of ubiquitinated proteins in response to proteasome inhibition is mediating the presynaptogenic effect and that lysine 48-linked polyubiquitinated proteins accumulate at the site of a nascent presynapse. Lastly, by preventing formation of polyubiquitin tags that are believed to target substrates for the proteasome, the enhanced formation of presynaptic clusters is abolished. We thus conclude that in response to a transient halt in proteasome degradation subsequent *on-site* accumulation of polyubiquitinated conjugates will function as the trigger for presynaptic differentiation. Altogether, our results indicate that ubiquitin and the proteasome are capable of promoting presynaptic assembly by two related, albeit opposite, routes: enhanced degradation of proteins or transient increased accumulation of a pool of polyubiquitinated conjugates.

On our last set of results, we extended our attention to the role of ubiquitin on presynaptic function. Despite some evidence that ubiquitin signaling affects presynaptic release, the involvement of

polyubiquitination has never been addressed. We observed an increased rate of presynaptic release following expression of ubiquitin that was partially reverted when polyubiquitination on lysines 11, 29 and 63 was prevented. We thus assume that attachment of polyubiquitin chains on substrates enhances the release properties of a presynaptic bouton.

Overall, these findings highlight the significance of ubiquitin signaling at the presynaptic terminal both during its formation and activity. Due to its reversible and versatile nature, ubiquitin tags on presynaptic and/or axonal proteins may engage on multiple, even antagonic, local pathways to modulate presynaptic development and function.

Chapter 1

General Introduction

Neurons are the basic working units of the nervous system that rely on synapses to execute their functions. Sypnapses represent points of contact between neurons, however their role is far wider than a merely structural bridge. Indeed, neurons talk to each other at synapses: an electrical signal travelling along an axon reaches the presynaptic terminal, is converted into a chemical message and transferred onto the apposed postsynaptic terminal. Synaptic activity is then generated in the form of an action potential that flows along the dendrite, thus guaranteeing information processing, exchange and continuity in a neuronal circuit. It is nowadays widely recognized that synapses are vital structures for learning, memory acquisition and storage. Rough estimates tell us that the human brain has 100 billion neurons, each one establishing thousands of synapses with other neurons. Remarkably, most of the synapses, let's say trillions of them, will be formed almost simultaneously early during development, in a time window as narrow as few weeks or few months in rats and humans, respectively. Moreover, integration of synapses will later define a successful or unsuccessful functionality of neuronal networks.

In broad terms, a growing axon is guided by extracellular cues to a precise spatial location where it encounters the receptive dendrites of its partner. Synapse formation is then triggered and specified by multiple factors including soluble molecules and cell adhesion complexes. Later, synapses will be strengthened and enlarged or pruned mostly depending on their activity status. Hence, multiple developmental events will together orchestrate the formation of functional synapses, and these include cell fate determination, neurite formation, axon outgrowth and guidance, dendritic growth, spine formation, synaptic target selection, presynaptic and postsynaptic differentiation, synaptic maturation and synapse elimination. In this work we focused our attention on the mechanisms leading to the differentiation of the presynaptic bouton. So, on the following sections, an overview of the current knowledge on presynaptic differentiation will be presented and discussed.

The presynaptic terminal

Synapses are highly specialized asymmetric structures in which a presynaptic and a postsynaptic compartment are perfectly juxtaposed. In the presynapse, neurotransmitter-filled synaptic vesicles (SVs) are packed together awaiting to be exocytosed, whilst the membrane of the postsynapse is decorated with a string of specific postsynaptic receptors responsive to the release of such neurotransmitters. Despite minor differences between organisms and synapse type, all presynaptic terminals share an identical structure. The plasma membrane region harboring the pool of SVs is highly specialized, and can be spotted in electron microscopy as an electron-dense thickening of the presynaptic membrane. This region is known as the active zone and within it several molecular components are orderly assembled into the cytomatrix of the active zone (CAZ). Because the main role of the presynaptic terminal is to guarantee rapid and controlled neurotransmitter release, its structure and the proteins involved are perfectly organized to meet this demand.

The general three-dimensional architecture of the presynaptic terminal of vertebrate central nervous system (CNS) synapses is well known[1–3]. Techniques like electron tomography and super resolution microscopy allowed a considerable advance of the detailed organization of this structure. Scattered on top of a relatively small active zone, with a surface area of 0.07 μm^2, a pool of 383 SVs is clustered together on a presynaptic volume of around 0.37 μm^3 [3]. Amazingly, despite their huge number, SVs account for no more than 4% of the total volume of the presynaptic bouton, which is actually densely populated by a meshwork

of presynaptic proteins[3]. One valuable piece of information was the observation that SVs are trapped by a dense network of linking filaments that tightly interconnect them between each other and to the active zone (figure 1.1A-D)[1,2]. Each SV is connected to neighboring ones by short (<40 nm) filaments, the connectors[1,2]. SVs that are closer to the active zone are also linked to this specialized portion of the plasma membrane by tethers, which can either occur through a single long one or multiple short tethers[2], the latter most probably constituting the readily releasable pool (RRP) of SVs[4]. In agreement with the idea that connectors and tethers prevent diffusion of SVs thus maintaining the SV cluster in a resting synapse, a large number of linking filaments is dissipated upon synaptic stimulation[2,4], thus allowing fusion of SVs and neurotransmitter release. It remains to be determined the molecular nature of these filaments and their role on the regulated release of SVs. They are believed to be mainly composed of synapsin, however they are not completely eliminated from boutons of a synapsin triple knockout (KO) mice[1], probably revealing a more complex molecular composition.

A comprehensive molecular description of SVs is also currently available. Each SV has a diameter of approximately 40 nm and is mainly composed of integral membrane proteins embedded in the lipid membrane surrounding an aqueous lumen filled with neurotransmitters (figure 1.1E)[5]. The amount of proteins adorning a typical SV is much higher than anticipated, representing a quarter of the entire membrane volume, and include: SV-specific proteins such as synapsin, synaptophysin, synaptogyrin and synaptic vesicle protein 2 (SV2), which are believed to assist in neurotransmitter release; the vesicular component of the soluble n-ethylmaleimide-sensitive factor attachment protein receptor (SNARE) complex, known as vesicle-associated membrane protein (VAMP)/synaptobrevin; small GTPases, like Rab proteins; neurotransmitters transporters, such as the vesicular glutamate transporter 1 (Vglut1) and vesicular GABA transporter (VGAT); channel proteins, such as the proton pump V-ATPase required for acidifying the SV interior; the calcium sensor synaptotagmin; proteins of the trafficking machinery like the secretory carrier-associated membrane protein 1 (SCAMP1) or the vesicle transport through interaction with t-SNAREs homolog 1a (Vit1a), among others[5].

On its turn, the active zone is a region of the presynaptic membrane highly specialized for the controlled docking and fusion of SVs and release of neurotransmitters. It is best characterized by its complex electron-dense meshwork of proteins, the CAZ, which can be viewed under the electron microscope as an electron-dense projection juxtaposed to the postsynaptic density (PSD), with varying structures depending on the organism or synapse type[6]. The first glimpse to the structure of the mammalian CNS active zone came from a study from Colman and colleagues, who succeeded in purifying the presynaptic "particle web" [7]. This fraction is able to self-assemble into its native structure after complete solubilization, and has the appearance of a grid-like structure in which pyramidally-shaped particles connected by fibrils create open slots for SVs to dock[7] (figure 1.1F,G). The great majority of CAZ proteins are scaffolding proteins, characterized by a multitude of domains for protein-protein interactions and relatively few catalytic domains. These include, but are not limited to, proteins such as Rab3-interacting molecules (RIMs), RIM-binding proteins, the high molecular weight proteins Bassoon and Piccolo, liprinα, the CAZ-associated structural protein/ELKS-Rab6-interacting protein-CAST (CAST/ERC) proteins, calcium/calmodulin-dependent serine kinase (CASK) and Munc13[8,9]. In addition to these elements, within the CAZ, concentration of docked vesicles, voltage-gated calcium channels (VGCC), proteins of the exocytotic machinery and cell adhesion molecules, as well as cytoskeleton elements, is also observed[8,9]. Altogether, these proteins organize exocytotic sites and their spatial distribution at the active zone is believed to be meticulously specified to guarantee an effective synaptic transmission[8] (figure 1.1H). For instance, Bassoon and CAST/ERC reside approximately 70 and 30 nm away from the active zone[1]. It is not entirely clear how the ultra-structural

organization of CAZ proteins is promoted, however evidence indicate a major role for protein-protein interactions between presynaptic proteins.

Researchers have now a clear picture of the presynaptic terminal. Recently, a high-throughput study made a significant step forward towards the understanding of the structural and molecular composition of presynaptic terminals. By combining information of the copy number of presynaptic proteins and their relative location within the presynaptic bouton, authors created the first 3D representation of the presynapse[3]. Further insights into the composition of the presynaptic protein network came from the identification of proteins from fractions highly enriched in docked SVs, in which only the proteins embedded in the active zone along with associated SVs are included[10,11]. Between 400 to 485 proteins from different functional categories compose the active zone, thus further emphasizing the complexity of this tiny structure. In the light of these recent advances, it is extremely likely that complete knowledge of the presynaptic terminal composition and structure will soon be available.

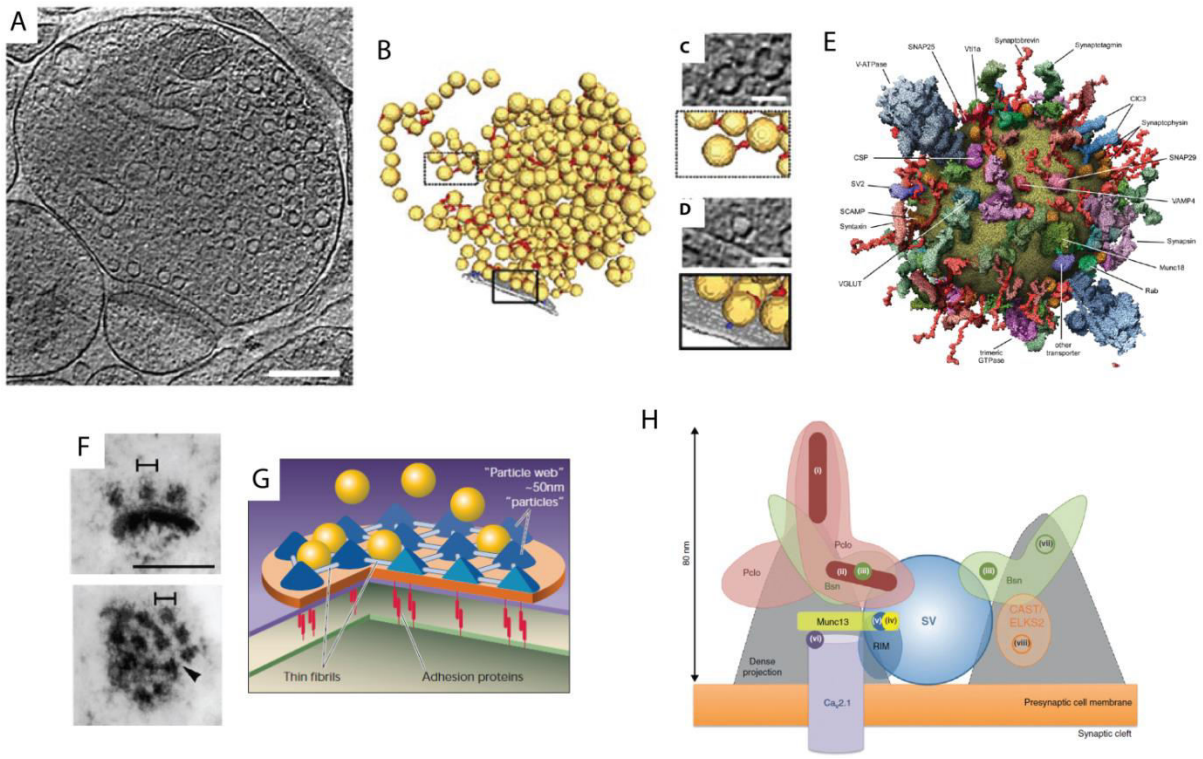

Fig. 1.1 - Structure of the presynaptic terminal in the CNS. (**A**) 2.7-nm-thick tomographic slice of a representative synaptosome. (**B**) 3D representation of SVs (yellow) and active zone (gray). Connectors and tethers are highlighted in red and blue, respectively. (**C**, **D**) Example of a (**C**) connector and (**D**) tether in a tomographic slice, with the corresponding 3D representations (**A**-**D**, adapted from [2]). (**E**) 3D-representation of an average SV (reproduced from [5]). (**F**) Lateral view (top) and view en face (bottom) of the active zone under electron microscopy (adapter from [7]). (**G**) Representation of the active zone in mammalian CNS synapses (adapted from [6]). (**H**) Scheme of the organization of the active zone in conventional brain synapses. Localization of key proteins like Bassoon (Bsn) and Piccolo (Pclo) is presented (adapted from [8]).

Presynaptic differentiation

Early in development, a navigating axon projects to distant target regions where it will establish synaptic connections. When conditions are favored, either at the tip of the axon (terminal synapse) or along its shaft (*en passant* synapse), changes will occur so that a presynaptic terminal will be formed. Presynaptic differentiation corresponds to the set of changes that transform an undifferentiated portion of the axoplasm into a presynaptic specialization, in which a stable pool of SVs faces the active zone. Despite the immense complexity of the presynaptic terminal, its formation occurs very rapidly. Imaging studies in living neurons reveal that a functional presynaptic terminal can be formed within minutes to a few hours[12–15]. So, what strategies do the axons employ to accomplish this? Remarkably, neurons have a smart and easy way of doing so. Very briefly, soma-derived pre-assembled packets containing presynaptic material are trafficked along the axon to sites of synapse formation. Upon instructive signals, these mobile precursors halt in specific axonal spots and assemble in the form of a presynaptic site. Even though neurons have devised an apparently easy system to form presynaptic boutons, it involves several and diverse proteins and intracellular mechanisms, most of them still debatable or unknown to the scientific community. In this work, we will focus our attention on presynaptic differentiation occurring at the mammalian CNS; however, insights from invertebrate organisms will be included whenever relevant for a better comprehension of the described events.

Origin and delivery of presynaptic material

Presynaptic material is delivered to nascent terminals in pre-assembled transport units. Long distance movement of cargo to axons is primarily mediated by microtubule-dependent axonal transport[16]. In accordance, delivery of soma-derived presynaptic material that will later be assembled into a proper presynaptic site also occurs through axonal transport[17,18]. Several studies indicate that presynaptic proteins rather than being transported individually to a nascent presynapse, are delivered simultaneously in the form of vesicular intermediates derived from the trans-Golgi network. Two main types of mobile packets crucial for presynaptic differentiation have been identified: synaptic vesicle protein transport vesicle (STV) and piccolo-bassoon transport vesicle (PTV). The former corresponds to the movement of SVs in bulk[19], later shown to contain several SV-associated proteins such as SV2, calcium channel subunit α1a, synapsin, amphiphysin and VAMP2[14]. These mobile packets of SVs undergo exocytosis upon depolarization at non-synaptic sites[19] and are recruited to and get stabilized in new axo-dendritic contact where they become activity competent in less than one hour[14]. Reasonably, authors proposed the 'prefabricated synapse' hypothesis, postulating that mobile units containing most of the presynaptic components would be freely mobile along the axon and would give rise to functional terminals once recruited to a specific axon spot[14]. Subsequently, PTVs were described as 80 nm-diameter dense core granulated vesicles containing mostly components of the active zone and devoid of SV proteins[20]. PTVs were shown to transport a handful of active zone proteins such as piccolo, bassoon, syntaxin, synaptosomal-associated protein 25 (SNAP25), N-cadherin, chromogranin B, and also the proteins of the SV exocytosis machinery, Munc18, Munc13, Rab3 and RIM, as well as subunits of calcium channels[20,21]. In a way of further reinforcing the 'prefabricated synapse' hypothesis, authors concluded that active zones would be formed in an unitary fashion by the incorporation of 2-3 PTVs into presynaptic membranes[21]. Overall, these observations led to the still prevailing active zone transport vesicle hypothesis, according to which modular units of pre-assembled

active zone material, PTVs, packed at the cell body and trafficked to nascent presynaptic sites, will fuse to the plasma membrane and create an active zone by local delivery of all the required components[9].

These presynaptic mobile units are believed to be generated in the Golgi complex and later selectively sorted to neurites. Bassoon and piccolo co-localize with the trans-Golgi network and remain accumulated at the soma level upon disruption of the Golgi complex[22]. Furthermore, many other active zone components associate with the Golgi prior to their trafficking[23]. Remarkably, at least two kinds of presynaptic vesicle precursors leave the Golgi towards the axon: a vesicle containing bassoon, piccolo and CAST/ERC and a distinct vesicle positive for Munc13[23]. These vesicle precursors can undergo additional maturation steps during their transport as evidenced by the association of RIMα- and bassoon-positive transporting vesicles[23]. Overall, these evidences indicate that the Golgi complex is instrumental for the generation of vesicle precursors containing presynaptic components. Accordingly, a conditional KO mice displaying defects in the trans-Golgi network have reduced number of presynaptic dense-core vesicles (DCVs) and SVs along with reduced synaptic transmission[24]. Few studies have tried to uncover the mechanisms underlying the sorting of presynaptic cargo specifically to axons. In *C. elegans*, polarized localization of synaptic components to the pre or postsynaptic compartments has been shown to occur in a manner dependent on phosphatidylinositol 4,5-bisphosphate (PIP_2) signaling[25,26] or through the activity of protein kinases[27]. The *C. elegans* protein kinase LRK-1 localizes to the Golgi apparatus and instructs sorting of SVs to axons most probably by preventing their association to dendrite-specific transport machinery[27]. Interestingly, in the mammalian brain, sorting of synaptic material from the Golgi is regulated by the protein kinase D1 (PDK1)[28], in whose absence dendritic membrane proteins are mispackaged into presynaptic material-containing vesicles and mistargeted to axons[28]. However, the signals controlling Golgi sorting of axon vesicular precursors remain elusive and further efforts should be made to address this issue.

In general, packets of synaptic material are actively trafficked to sites of nascent terminals by axonal transport. As previously mentioned, trafficking of STVs and PTVs to axonal synaptic regions is mediated by microtubule transport, which relies on the function of molecular motors that drive presynaptic cargo both anterogradely and retrogradely along the axon[17,18]. These motors are kinesins (KIFs) and dyneins, respectively. Several lines of evidence indicate that STVs and PTVs are independently trafficked towards the end of the axon by KIF1A/B[29–31] and KIF5B through the adaptor syntabulin[32–34], respectively. However, it is likely that transport of SVs and active zone material does not occur in such a straightforward and distinct manner. For instance, the scaffold active zone protein liprinα binds to KIF1A[35] (believed to be the specific KIF for STVs) and seems to act as a KIF1A partner required for linking cargo to this motor thus allowing their trafficking[35,36]. Actually, upon loss of liprinα, SVs aberrantly accumulate in non-presynaptic areas[36]. Very recently, an SV-associated protein, SAM-4, was identified in *C. elegans* has a regulator of SV transport in concerted action with liprinα[37]. Furthermore, it may even happen that some presynaptic components are delivered to nascent presynaptic sites by different modes of transport that do not involve STVs and PTVs. Indeed, synapsin, one of the major component of SVs[5], was shown to be transported in zebrafish axons independently of STVs and PTVs[38]. Recruitment of mobile synapsin1 puncta followed that of STVs and PTVs and was regulated by the cyclin-dependent kinase 5 (Cdk5), whose lack of activity does not alter the rate of STVs and PTVs recruitment[38]. Overall, this study predicts the existence of a third mobile packet of presynaptic material. In addition, some proteins reach the nascent synapse by cytosolic diffusion[39,40].

Surprinsingly, retrograde transport (towards the soma) of presynaptic vesicle precursors by dynein is also relevant for a correct distribution of cargo to nascent synapses. In *C. elegans* mutants for components of the cytoplasmic dynein complex, SV proteins misaccumulate along the axon[41,42]. Moreover, correct delivery

of presynaptic components to axons was shown to be governed by two different kinases through inhibition of dynein-mediated retrograde transport[43]. Cyclin-dependent Pctaire kinase (PCT-1) and Cdk5 prevent mislocalization of SVs and the active zone protein SYD-2 (*C. elegans* homolog of liprin-α) to dendrites by inhibiting the cytoplasmic dynein complex thus maintaining material in the axon by minimizing retrograde axonal transport[43]. Although we currently have a reasonably solid idea of the general mechanisms underlying the delivery of presynaptic material to axons, more work should be done to fully characterize this event.

Choosing where to create a presynaptic terminal

While on track to their destination, presynaptic mobile cargoes will need to know where to form a presynaptic bouton. At first sight, axons resemble thin and long highways, with no striking differences along the way. So, how STVs, PTVs or similar other packets know where to settle and organize into a terminal?

The axon has an intrinsic capacity to generate orphan presynaptic sites at specific locations. According to the simplest model of synaptogenesis, presynaptic material is recruited and clustered in sites of axo-dendritic contact, and is dependent on postsynaptically-derived presynaptic organizing proteins (see next subsection). Surprisingly, several lines of evidence have established that the axon has an intrinsic capacity to generate orphan presynaptic sites in selective locations prior to any contact with dendrites. During their transport to the distal part of the axon, STVs and PTVs pause frequently and move in both retrograde and anterograde directions[14,21]. Although their trafficking seems to be mutually independent, STVs and PTVs undergo extensive co-transport[44,45]. Moreover, they share the same axonal sites for pausing along the axon, and whenever together are more likely to pause simultaneously[44]. This coordinated transport might be indicative of multiple events occurring along their trafficking that readies precursors for presynapse formation. Moreover, it anticipates the existence of specialized regions of the axonal membrane for the building of presynaptic boutons. Indeed, many active presynaptic sites exist along the axon of a mature neuron that possess mature release properties, lacking however the postsynaptic partner[46]. These orphan presynaptic sites correspond to mobile presynaptic material that get transiently immobilized at non-synaptic regions along the axon upon evoked action potentials[47]. They are perfectly capable of performing SV fusion and recycling events, thus constituting extrasynaptic fusion sites[47]. Notably, during their transport, STVs pause preferentially in these specific sites within the axon, that actually perfectly match with sites in which an axodendritic synapse will later be formed[48]. Altogether, these studies indicate that there are predefined sites along the axon shaft in which *en passant* presynaptic terminals will selectively form.

So, which are the special features of these axonal subdomains that account for this intrinsic presynaptogenic property? In yeast, a multi-subunit complex named exocyst localizes to the tip of the bud, which is the predominant site of exocytosis of secretory vesicles, and is specifically involved in the recruitment of Golgi-derived vesicles to this site[49,50]. Along axons, subunits of the exocyst display a punctuate pattern and their accumulation in axonal sites precedes that of SV markers[51]. Notably, the exocyst subunit sec6 accumulates at STVs preferential pause sites[48], thus suggesting that exocyst components might define specific axonal domains for the deposition of presynaptic material and so localize presynaptogenesis in growing axons. In terms of postsynaptic differentiation, which is also known to rely on transport packets of synaptic material[52–54], the exocyst has a crucial role for the synaptic targeting and insertion of glutamate receptors[55] and for the growth of the postsynaptic membrane[56].

Another intriguing possibility is that lipid rafts may constitute platforms to which presynaptic material will be selectively recruited. Lipid rafts are small, heterogeneous and dynamic microdomains on the plasma membrane highly enriched in cholesterol and sphingolipids that normally compartmentalize cellular processes[57]. They are believed to act as platforms in which proteins can be functionally clustered. Indeed, clustering of sodium channels along axons perfectly coincides with these microdomains[58] and during axon guidance they function to localize signaling downstream of adhesion molecules and guidance receptors[59,60]. Interestingly, expression of flotilin, a protein that associates with the cytoplasmic side of lipid rafts[61], increases the number of synaptic sites[62]. Furthermore, higher concentration of cholesterol in lipid rafts is followed by increased levels of presynaptic proteins[63]. Although strong evidence is still lacking, it is plausible that presynaptic packets recognize lipid rafts as anchoring sites. Interestingly, the postsynaptic density is intimately associated with postsynaptic lipid rafts[64,65].

During transport, negative regulators of clustering avoid premature presynaptic assembly. Insights from studies in *C. elegans* help to further understand the molecular mechanisms coordinating spatial patterning of presynaptic assembly in axons. The Arf-like small G protein (ARL-8) associates with presynaptic cargoes and functions to suppress premature and extensive self-assembly of presynaptic precursors during transport[66]. In an *arl-8* mutant, presynaptic cargoes accumulate prematurely with a subsequent loss of distal presynapses[66]. The authors further concluded that AZ proteins within the moving particles, such as SYD2 (*C.elegans* homolog of liprinα), act as positive regulators of SV assembly and so counteract ARL-8 effect[66]. They also identified a c-Jun N-terminal protein kinase (JNK) pathway involved in the enhancement of aggregation of presynaptic precursors[45]. So, in moving packets of presynaptic material, factors that antagonistically control STV/PTV clustering co-exist. Hence, when STVs and PTVs encounter at an axonal pause site, the balance between positive and negative regulators of clustering will determine the extent of presynaptic assembly[45]. In conclusion, intrinsic regulators of aggregation vs. movement are present in presynaptic precursors moving particles. Hereafter, it would be instrumental to identify the local factors present at axonal pausing sites that govern this intricate balance, thereby determining spatial distribution of presynaptic sites along axons.

Interestingly, dendrites probably share with axons a similar intrinsic mechanism for the preferential localization of postsynaptic terminals in specific sites. Along dendrites, both stationary or mobile preformed complexes of postsynaptic proteins that lack the presynaptic counterpart can be found decorating an immature dendritic shaft[67]. They all contain postsynaptic density protein 95 (PSD95), guanylate-kinase-associated protein (GKAP) and Shank, however neuroligin can only be found on the stationary complexes[67]. Apposed to these latter complexes, a functional presynaptic terminal is readily formed in less than 2h[67], thus revealing the intrinsic propensity for originating postsynapses in predetermined dendritic sites.

In the light of these observations, it is foreseeable that synapse formation can be initiated in different ways (figure 1.2). Whenever at close proximity, axons and dendrites will eventually interact either by the extension of dendritic filopodia or by the growth of axonal branches, including the growth cone[68]. Synapse formation can be initiated at a random location as a direct consequence of an axodendritic contact and subsequent engagement of trans-synaptic adhesion (figure 1.2A). Alternatively, stabilization of a cell-cell contact into a nascent synaptic site will only occur at predefined axonal sites, which correspond to the preferential pausing sites of STVs and PTVs (figure 1.2B), or at dendritic spots adorned with a stable preformed postsynaptic scaffolding complex (figure 1.2C).

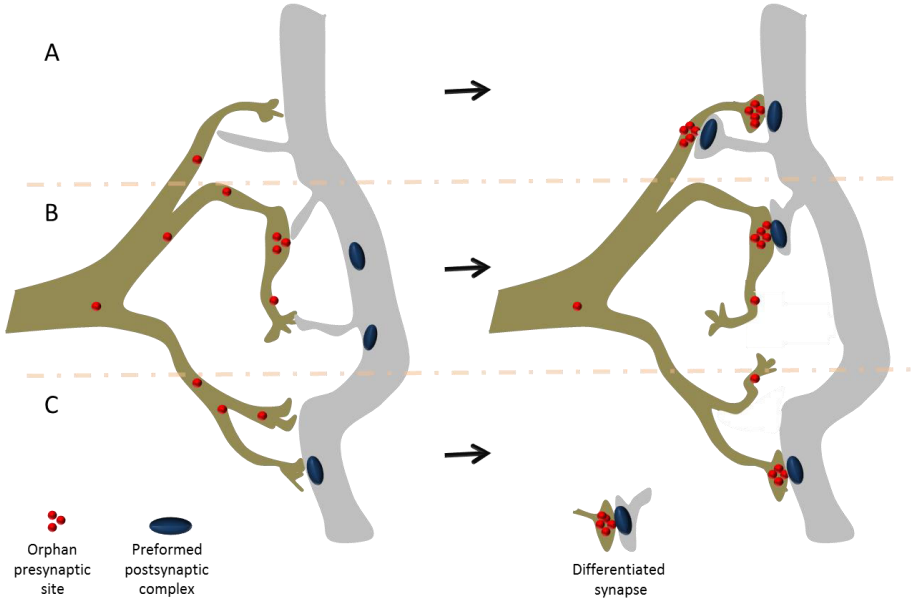

Fig. 1.2 – Models for the initiation of synapse development. When a growing axon (brown) and a nearby dendrite (grey) are in close proximity, synapse formation can be initiated by different ways. (**A**) In a first model, randomly extending dendritic filopodia or axons interact and establish a cell-cell adhesion contact that, whenever stable, will differentiate into functional synapses comprising presynaptic and postsynaptic terminals. (**B**) In a second model, *en passant* orphan presynaptic sites are formed in predefined axonal locations in young axons and constitute preferential sites for the establishment of an axodendritic synapse. Contacts between axon and dendrite that do not occur at these specific locations will not be further stabilized and differentiated into synapses. (**C**) In a third model, stationary preformed postsynaptic complexes are present in dendrites prior to contact with an axon and will dictate the location of new synapses. Formation of presynaptic terminals occurs when a navigating axon finds and establishes a physical contact with these postsynaptic specializations.

The cohort of presynaptic organizing proteins

Presynaptic differentiation is triggered by transsynaptic and soluble synaptogenic molecules. Regardless of the inherent capacity of axons to initialize the recruitment of presynaptic contents in a spatial specific manner, complete differentiation of a stable presynaptic terminal only occurs after contact with a postsynaptic partner. Hence, it has been intuitively proposed that signals coming from the postsynaptic neuron would trigger the assembly of presynaptic boutons. Indeed, axons and dendrites are capable of reciprocally inducing organization of pre- and postsynaptic terminals by the localized and coordinated action of synaptogenic molecules. These factors might either trigger the initiation of a synaptic domain by promoting intracellular synaptogenic machinery, which selectively and actively recruits material, or erect stable platforms along axons and dendrites in which mobile synaptic packets will become gradually trapped. Surprisingly, a recent work by Bury and Sabo[69] actually supports the latter hypothesis. This study shows that neither the movement of STVs and PTVs is altered by neuroligin (a well-known presynaptogenic molecule that will be described ahead), nor are they attracted to the protein. On the contrary, deposition of presynaptic material at synaptic spots happens as moving packets encounter these sites. Currently, we have a vast knowledge of the identity of synaptic organizers[70–72] that has continuously been updated at a fast rate.

In broad terms, two types of factors are able to instruct synaptic differentiation: transsynaptic adhesion complexes and secreted molecules. On table 1.1 a comprehensive list of these factors is presented, some of which will be discussed throughout this section. Because presynaptic and postsynaptic differentiation clearly share a great deal of synaptogenic cues, in this subsection the review will also be extended to postsynaptic-related findings.

Despite some previous vague evidence for the role of specific proteins in the initiation of synaptogenesis[73–76], the knowledge we gather today about synaptogenic factors has started by the pioneer study of Serafini and colleagues[77]. By analyzing the ability of neuronal adhesion molecules expressed in a non-neuronal cell to recruit presynaptic material on contacting axons, authors identified neuroligin as the first component of a machinery devised for the formation of CNS synapses[77]. Later, neuroligin was shown to be a postsynaptic transmembrane protein that interacts with presynaptically-located neurexins, triggers their clustering and, as a result, local recruitment and aggregation of presynaptic material creates a functional presynaptic terminal[78,79]. Furthermore, the neurexin/neuroligin transsynaptic complex is bi-directionally active and it can also trigger assembly of postsynaptic components[80,81]. The mystery had been disclosed, a pair of transmembrane proteins on either side of the nascent axo-dendrite synapse establishes an adhesive transsynaptic interaction that functions has a bi-directional potent inducer of synaptogenesis.

In the following years, a multitude of transsynaptic complexes displaying synaptogenic properties has been discovered (table 1.1). Whilst the great majority has an impact on pre- and postsynaptic differentiation simultaneously, others seem to specifically instruct clustering of material on only one side. For instance, synaptic cell adhesion molecules (SynCAMs) are synaptically localized adhesive proteins that can form homo- or heterophilic interactions[82]; when expressed on human embryonic kidney (HEK) cells they induce extensive clustering of SVs capable of KCl-induced release[83], however no evidence for its direct role on postsynaptic assembly has been reported. On the other hand, upon binding of the neurotrophin receptor tyrosine kinase C (TrkC) (postsynaptic) to the transmembrane protein tyrosine phosphatase σ (PTPσ) (presynaptic), robust clustering of pre- and postsynaptic markers is observed[84]. This synaptogenic effect is completely hampered in conditions in which aggregation of TrkC and PTPσ at the neuron surface is prevented[84], thus revealing a similar mode of action to that of the neuroligin/neurexin pair. The presynaptically-located protein PTPσ belongs to the family of type IIa receptor type protein tyrosine phosphatases (RPTPs), from which the leukocyte antigen-related (LAR) protein and PTPδ also belong. These presynaptic proteins can mediate presynaptic differentiation and trigger postsynaptic clustering by interacting with a wide range of postsynaptic partners, including netrin-G ligand (NGL), interleukin-1 receptor accessory protein (IL-1RAcP), interleukin-1-receptor accessory protein-like 1 (IL1RAPL1) and Slit- and Trk-like family proteins (Slitrk)[84–90]. This promiscuity is not restricted to the RPTP family. Neurexins, for instance, not only require neuroligins, but also instruct presynaptic assembly when binding to the brain specific transmembrane protein calsyntenin-3[91,92], to the leucine-rich repeat transmembrane protein 2 (LRRTM2)[93] or to members of the δ-type glutamate receptor (GluRδ)[94,95]. Formation of the latter transsynaptic complex, in opposition to the remaining interactions, has an interesting particularity. Neurexin does not bind directly to postsynaptic GluRδ receptors, but instead, the presynaptically-secreted protein cerebellin (Cbln) mediates this interaction[94–97]. We may speculate that formation of transsynaptic complexes as a triad may confer an additional layer of regulation to the process of synaptic differentiation. Lately, particular attention has been devoted to the involvement of synaptic leucine-rich repeat (LRR) proteins in the induction of presynaptic clustering. Notably, several presynaptogenic proteins, including LRRTMs, NGLs, Slitrks and the recently identified fibronectin leucine-rich repeat transmembrane protein 3 (FLRT3), contain LRRs in their extracellular domains, through which interaction with the correspondent synaptic partner occurs and as a

result presynaptogenesis is triggered[98]. Many other pairs of synaptic proteins promote clustering and organization of synaptic compartments as described in table 1.1; and in addition to these, it is predictable that many others are yet to be identified and studied. Indeed, novel candidates have been extracted from a pool of positive hits in different screens for synaptogenic proteins[99–102].

In parallel to the action of synaptic adhesion complexes, secreted molecules also promote selective formation of pre- and postsynaptic sites[70]. Secretion can either occur from the presynaptic neuron, the postsynaptic neuron or from glia cells (as evidenced in green, orange or blue boxes, respectively, in table 1.1). Due to their soluble nature and consequently longer reach, one can surmise a scenario in which their effect precedes that of adhesion complexes, eventually priming axonal and/or dendritic domains for later establishment of adhesive contacts and stabilization of synaptic sites. Moreover, the spatial specificity of their effect is somewhat questionable, being highly likely that they instruct synaptogenesis in a less constricted manner. Expression and location of their receptors might constitute a strategy devised by cells to spatially limit secreted factors-induced synaptogenesis.

In contrast to transsynaptic complexes, most of the axon- or dendrite-derived soluble factors function unidirectionally, exerting their effect on the opposite partner. This is the case of fibroblast growth factors (FGFs), which are presynaptic differentiation factors secreted from dendrites and whose receptors are located at the axon membrane. In the cerebellum, for instance, its secretion from the postsynaptic cerebellar granule cells coincides with axonal innervation; then the FGF receptor 2b (FGFR2b) expressed on mossy fibers of pontine and vestibular neurons will be activated and clustering of SVs promoted[99]. In the hippocampus, FGF22 and FGF7 were proposed to be secreted from CA3 pyramidal neurons thus instructing presynaptic assembly by activating receptors in projecting mossy fibers from the dentate gyrus[103]. Vice-versa, pentraxins are axonally-secreted and act on the postsynaptic membrane to cluster α-amino-3-hydroxy-5-methyl-4-isoxazole propionic acid (AMPA) receptors[104]. Interestingly, they exert this effect by binding to extracellular domains of GluR4 subunits, and so no endogenous intermediates or signaling cascades are required, but rather direct interaction with postsynaptic components.

Glia cells are of paramount importance to synapse formation. The role of glia cells as producers and secretors of synaptogenic factors was early anticipated by the observation that fewer synaptic connections were established in neurons cultured in an astrocyte-free environment[105–107]. Thrombospondins and cholesterol were subsequently identified as glia-derived factors capable of bidirectional induction of synaptogenesis[108–110]. Currently, the postsynaptic receptors responsible for thrombospondins outcome on synaptic clustering were identified as neuroligin1 and the gabapentin receptor α2δ-1[111,112], however there is no clue for its presynaptic target. An interesting breakthrough in glia control of synaptogenesis was the finding that astrocytes not only secrete synaptogenic molecules, but also tune their activity by the release of antagonic factors[113]. Hevin and secreted protein acidic and rich in cysteine (SPARC) were identified as the main players and behave as the inducer and the inhibitor, respectively, of glia-modulated synapse formation[113].

On the control of synaptogenesis, glia cells have many faces. For instance, they secrete glial cell line–derived neurotrophic factor (GDNF), a soluble factor that, similarly to Cbln, acts as a ligand-induced cell adhesion molecule that enables indirect binding of pre- and postsynaptic glial cell line–derived neurotrophic factor receptor (GFRα1)[114]. As a consequence of this interaction, presynaptic clustering will be triggered in axonal regions perfectly juxtaposed to postsynaptic terminals[114]. On the other hand, glial cells also express transmembrane γ-protocadherin through which synaptogenesis is induced in a contact-dependent

mechanism[115]. This finding indicates that close proximity of astrocytic processes to the site of synapse formation, at least in a transitory manner, is instrumental for its differentiation.

Table 1.1 - Synaptic organizing proteins of CNS excitatory and inhibitory synapses. The establishment of transsynaptic complexes and/or secretion of soluble factors has been shown to trigger structural and functional changes in both axon and dendrite subdomains. Formation of presynaptic and postsynaptic sites is thus induced. This table summarizes the current knowledge of synaptogenic factors functioning at the CNS, their interaction partners/receptors, effects at pre- and postsynaptic differentiation and the *in vivo* consequence of their loss. The information within this table is in accordance to the current literature, and so, susceptible to changes as new research unmasks the complete set of synaptogenic factors.

Transsynaptic adhesion complexes								
Pre-synaptic differ.	**Presynaptic partner**	**Mediator of interaction**	**Postsynaptic partner**		**Post-synaptic differ.**	**Synapse type**	***In vivo* phenotype**	**Ref.**
x	Neurexins α	?	Calsyntenin-3			ex/in	*Clstn3*$^{-/-}$ mice: reduced synaptic density and transmission	91,92
x	Neurexins α,β	↔	Neuroligins	2	√	in	*Neuroligin1*$^{-/-}$,*2*$^{-/-}$,*3*$^{-/-}$ mice: unchanged synapse density; Neuroligin1 and neuroligin2 transgenic mice: increased excitatory and inhibitory transmission, respectively	80,81,116,117
x x	Neurexins β	↔	Neuroligins	1/3	√	ex		77,78,80, 81,117–120
x x	Neurexins β	Cbln1	GluRδ2		√	ex	*Cbln1*$^{-/-}$ mice: mismatched synapses (also *GluD2*$^{-/-}$) and reduced transmission	94,96,97,121–123
x x	Neurexins α,β	Cbln1,2	GluRδ1			in		95
x x	Neurexins α	↔	LRRTMs	1,2	√	ex	*LRRTM1*$^{-/-}$ mice: altered Vglut1 clustering	93,100,124
x x	Glypican 4	↔	LRRTMs	4	√	ex	*LRRTM4*$^{-/-}$ mice: altered Vglut1 clustering	125,126
x x	SynCAM1,2	↔	SynCAM1,2			ex	SynCAM1 transgenic mice: increased functional excitatory synapses	82,83,118,127
x x	Netrin-G2	↔	NGLs	2	√	ex	*Ngl-2*$^{-/-}$ mice: low synapse density and reduced presynaptic clustering	128,129
x x	RPTPs LAR	↔	NGLs	3	√	ex		85,86
	RPTPs PTPσ	↔	NGLs	3	√	ex		86
x x	RPTPs PTPσ	↔	TrkC		√	ex		84
x x	RPTPs PTPδ	↔	IL1RAPL1		√	ex	*PTPδ*$^{-/-}$ mice: unchanged synapse density but not responsive to IL1RAPL1; *IL1RAPL1*$^{-/-}$ mice: decreased spine density	87,130
x x	RPTPs PTPδ	↔	IL-1RAcP		√	ex	*PTPδ*$^{-/-}$ mice: not responsive to IL-1RAcP; *IL-1RAcP*$^{-/-}$ mice: decreased spine density	88
x x	RPTPs PTPδ	↔	Slitrks	3	√	in	*Slitrk3*$^{-/-}$ mice: reduced inhibitory synapse density and transmission	89
x	?		Slitrks	1,2,4-6		ex/in		89

x x	Ephrin-B1,2	↔	EphB2		√	ex	*EphB1*$^{-/-}$,*2*$^{-/-}$,*3*$^{-/-}$ mice: reduced synapse density	131,132
x	EphB2	↔	Ephrin-B3		√	ex	*EphB3*$^{-/-}$ mice: reduced shaft synapses density and transmission	133–135
x x	N-cadherin	↔	N-cadherin		√	ex/in		102,136,137
x x	?	?	SALMs	3	√	ex/in		138
x x	?	?		5		ex/in		138
x x	Latrophilin 3	↔	FLRT3		√	ex		139
x	APP	?	APP					140
x	γ-protocadherin	γ-protocadherin #	γ-protocadherin		√	ex/in	*Pcdh*$^{fcon3/fcon3}$ mice: reduced synapse density	115
x x	GFRα1	GDNF	GFRα1			ex/in	*Gdnf*$^{+/-}$ mutant mice: reduced SV clustering	114

Soluble factors

Pre-synaptic differ.	Presynaptic receptor	Soluble factor		Postsynaptic receptor	Post-synaptic differ.	Synapse type	*In vivo* phenotype	Ref.
x	DCC	Netrin-1		DCC	√	ex	*Netrin-1*$^{-/+}$ and *DCC*$^{-/+}$ mice : reduced synaptic transmission	141,142
x	PlexinB1	Semaphorin 4D &		PlexinB1	√	in	*PlexinB1*$^{-/-}$ mice: unchanged synapse density and transmission but not responsive to semaphorin4D	143,144
x	FGFR2b	FGFs	FGF22			ex	*FGFR2*$^{flox/flox}$ mice: reduced density of SV clusters; *FGF22*$^{-/-}$ mice: reduced Vglut1 clustering and excitatory transmission; *FGFR2*$^{-/-}$ mice: reduced SV clustering	99,103,145
x	FGFR2b		FGF7			in	*FGF7*$^{-/-}$ mice: reduced VGAT clustering and inhibitory transmission; *FGFR2*$^{-/-}$ mice: reduced SV clustering	103
x	?	Wnts	Wnt-3					146
x x	Frizzled-5		Wnt-7a	?	√	ex	*Wnt-7a*$^{-/-}$ mice: reduced SV clustering	147–149
x	LRP6		Wnt-8	LRP6	√	ex		101
			Wnt-5a	?	√	in		150
		Pentraxins	Narp	?	√	ex	Triple pentraxin KO: decreased number of GluR4 synapses and transmission	76,151
			NP1	GluR4	√	ex		104
			NPR		√	ex		104
x x	TrkB	BDNF *		TrkB	√	ex/in	*BDNF*$^{+/- \text{ and } -/-}$ mice: impaired transmission and reduced pool of docked SVs; *BDNF*$^{+/-}$ mice: defective formation of synapses upon sensory input; *TrkB*$^{-/-}$ mice and *TrkB*$^{flox/flox}$ mice: decreased synapse density; Wnt1::Cre;*TrkB*$^{fl/fl}$ mice: reduced number of inhibitory synapses	75,152–160
x x	?	TSPs	1	Neuroligin 1 α2δ-1	√	ex	*TSP1*$^{-/-}$,*2*$^{-/-}$ mice: reduced synapse density	108,111,112
x	?		2,3,4,5	α2δ-1	√	ex		108,112
x x	?	TGF-β1		?	√	ex		161
x	?	cholesterol		?	√	ex		109,110

x x	?	Hevin	?	√	ex	*Hevin*$^{-/-}$ mice: reduced synapse density and defects in synapse morphology	[113]
		Glypican 4,6	?	√	ex	*Glypican4*$^{-/-}$ mice: reduced synapse density and activity	[162]

x, SV clustering; x, active zone formation; **√**, induction of postsynaptic differentiation; ↔ , direct interaction; **ex**, excitatory synapse; **in**, inhibitory synapse; green box, axon-secreted; blue box, glia-secreted (except for γ-protocadherin$^{\#}$, which is an astrocyte adhesion molecule); orange box, dendrite-secreted.

***** - Microglia-secreted BDNF also promotes synapse formation[156].

$^{\&}$ - Semaphorin is proteolytically cleaved from the surface of neurons. However, it is still debatable whether it acts as a cleaved extracellular domain or as a membrane-bound protein[143,144].

Abbreviations: APP, amyloid precursor protein; **BDNF**, brain-derived neurotrophic factor; **Cbln**, cerebellin; **DCC**, deleted-in-colorectal cancer; **differ.**, differentiation; **FGF**, fibroblast growth factor; **FGFR**, fibroblast growth factor receptor; **FLRT**, fibronectin leucine-rich repeat transmembrane protein; **GDNF**, glial cell line–derived neurotrophic factor; **GFRα1**, glial cell line–derived neurotrophic factor receptor; **GluRδ2**, orphan δ2 glutamate receptor; **IL-1RAcP,** interleukin-1 receptor accessory protein; **IL1RAPL1,** interleukin-1-receptor accessory protein-like 1; **LAR**, leukocyte antigen-related; **LRRTM**, leucine-rich repeat transmembrane protein; **Narp,** neuronal activity–regulated pentraxin; **NGL**, netrin-G ligand; **NP1**, neuronal pentraxin 1; **NPR**, neuronal pentraxin receptor; **Pcdh**, protocadherin; **PTP**, protein tyrosine phosphatases; **Ref.**, references; **RPTP**, type IIa receptor type protein tyrosine phosphatases; **SALM,** synaptic adhesion-like molecule; **SIRP,** Signal Regulatory Protein; **Slitrk**, Slit- and Trk-like family proteins; **SynCAM**, synaptic cell adhesion molecule; **TGF-β**, transforming growth factor β; **Trk**, tropomyosin-related kinase receptor; **TSP**, thrombospondin; **α2δ-1**, gabapentin receptor α2δ-1.

A crucial issue in synapse formation is the correct differentiation of excitatory vs. inhibitory terminals. How can axons or dendrites decide on which type of terminal to form? Apparently, this question may be partially resolved by synaptic organizers. Whereas some trigger formation of both excitatory and inhibitory terminals, others are specialized for only one type of synapse. A nice example of synaptic organizers that allow for such specification is the transsynaptic triad Neurexin-Cbln-GluRδ. Remarkably, GluRδ2 through Cbln1 mediates specifically excitatory synaptic differentiation, while GluRδ1 through Cbln1 or Cbln2 can only cluster inhibitory synaptic material[94,95]. Also within the FGF family, FGF22 and FGF7 are specifically assigned to instruct glutamatergic and GABAergic differentiation, respectively[103]. Puzzlingly, they both act through activation of the same type of receptors, making it difficult to perceive how the developing axon can distinguish between both. The answer may lie in the differential targeting of FGF22 and FGF7 to distinct secretion sites along the dendrite corresponding to excitatory and inhibitory domains[163]. Actually, FGF22 and FGF7 anterograde trafficking is mediated by different motors and it occurs in association with either excitatory or inhibitory PSD proteins, respectively[163]. Astrocytes also have the ability of selectively boosting inhibitory synaptogenesis, although the molecular factors involved have not yet been identified[164].

Negative factors maintain synapse formation within reasonable levels. As a way of maintaining synaptogenesis under control, negative regulators other than the astrocyte-secreted SPARC must exist. In the hippocampus, secreted semaphorins also seem to play a role in keeping a balanced level of synapses. Whilst semaphorin 4D signals differentiation of synaptic regions by activation of the receptor PlexinB1[143,144], semaphorin5A and semaphorin3A function as inhibitors of postsynaptic differentiation through activation of PlexinA2 and PlexinA3, respectively[165,166]. Further research will be needed to discover additional ways of negatively controlling synaptogenesis.

So far, a considerable panoply of presynaptic organizing proteins has been identified and their effect on presynaptic assembly studied in detail (table 1.1). They may function in concert with each other, eventually leading to differentiation of presynaptic boutons by paralleled and cooperative pathways. On the

other hand, they may "work" separately at different brain regions and different types of neurons, or even at distinct domains within the same cell. It is also conceivable that the action of synaptic organizers is associated with a high degree of redundancy, so that absence of one player does not hinder brain development. The fact that *in vivo* deletion of synaptogenic proteins does not greatly perturb synapse formation argues in favor of this idea.

Intracellular mediators of presynaptic assembly

Despite the wealth of knowledge on presynaptic organizers, the understanding of the downstream intra-axonal mechanisms is still crude and vague. What happens inside the axon that attracts and holds presynaptic material to a yet undifferentiated site? What stratagem do the axons use to “deceive” STVs and PTVs? Theoretically, the intra-axonal cascade of events leading to recruitment and clustering of presynaptic material should rely, at least initially, on the intracellular domains of the presynaptic transmembrane proteins that are activated either by interaction with the correspondent adhesive partner or by secreted factors. The set of presynaptogenic factors known up to now bear in their intracelular portion either domains for protein-protein interactions, mostly PSD95/disc large/zonula occludens 1 (PDZ) domains (such as neurexins, SynCAMs or ephrinBs), or domains conferring kinase or phosphatase activity [like FGFRs, tropomyosin-related kinase receptor B (TrkB) or RPTPs]. It is thus predictable that, following engagement of synaptic organizers, the series of intracellular changes are initiated by (de)phosphorylation events or via protein-protein interactions.

Presynaptic scaffolding proteins are believed to play a crucial role in presynaptic assembly through their protein-protein interaction domains. For instance, ephrinB1 and ephrinB2 are key regulators of EphB-induced presynaptic differentiation, likely through PDZ domain-dependent interaction with syntenin-1[132], an active zone protein containing tandemly repeated PDZ domains. Similarly, amyloid precursor protein (APP) requires its intracellular domain to induce SV clustering, which was later proved to form a complex with Mint1 and CASK[140]. These proteins, like syntenin-1, are abundant scaffolding proteins present at the active zone that participate in multiple protein-protein interactions[167]. They share the particularity of indirectly linking presynaptogenic transmembrane proteins to other active zone proteins with which they also interact. Due to this behavior, it has been proposed that key scaffold proteins create a network of protein-protein interactions at the base of activated receptors that dynamically nucleate several presynaptic components[71,167].

Although this idea is still a working model, several evidence point to its validity. In *C. elegans*, the active zone scaffolding proteins SYD-1 and SYD-2 (homolog of liprin-α) are crucial for the correct accumulation of numerous presynaptic proteins, and so, their loss compromises development of presynaptic sites[168–170]. Mechanistically, establishment of the transsynaptic complex SYG-2/SYG-1 induces accumulation of SYD-1 at immature synapses, which in turn facilitates recruitment of SYD-2[170]. This scaffold protein then serves as an anchor for several presynaptic proteins, including UNC10/RIM and ELKS[171,172], thus allowing for active zone assembly. Later, regulator of synaptogenesis-1 (RSY-1) was identified as a local antagonist of SYD-2[173], thus further reinforcing its prime role as a master organizer of the presynaptic terminal. The role of SYD-1 and SYD-2 is likely to be conserved in mammals. The intracellular protein mouse SYD-1 ortholog (mSYD1A) interacts with liprinα and Munc18, and its knockdown in cerebellar granule neurons decreases SV clustering[174]. Moreover, liprin-α (SYD-2 homolog) promotes dynamic scaffolding of two crucial active zone proteins, RIM1 and CASK, and was shown to be important for protein dynamics within a functional active

zone[175]. Importantly, liprin-α interacts with all members of the RPTP family[176], which have been widely recognized as mediators of presynaptic differentiation[90] (see table 1.1).

In addition to mSYD1A and liprin-α, other scaffolding proteins may also act as recruiters of presynaptic components. Presynaptic localization of calcium channels is mediated by interaction with RIM[177], which in turn interacts with several active zone and SV proteins[178,179]. CASK, for instance, interacts with SynCAM[83], neurexins[180], liprin-α[181] and rabphilin3a[182], and is likely to recruit via protein-protein interactions calcium channels to presynaptic locations[183,184], as well as the cytoskeleton-associated protein 4.1[185], which promotes formation of actin/spectrin microfilaments. Despite its obvious role in scaffolding the active zone, CASK deletion does not compromise synapse formation[186], which may be interpret as the overlap of redundant scaffolding roles in the presynapse. Indeed, mice lacking piccolo have apparently normal and functional synapses, however, upon co-deletion with bassoon, a decrease in the propensity of presynaptic sites to cluster SVs is observed[187]. Furthermore, mice engineered to lack Bassoon, one of the first proteins accumulating in nascent presynapses[12,188], display only mild clustering defects at immature stages, which are later corrected in older mice[189]. In the light of these observations, we may hypothesize that presynaptic recruitment is initiated at the tip of surface receptors by the establishment of an ordered and sequential chain of high affinity protein-protein interactions, promoted by the concerted action of multiple presynaptic scaffolds, rather than a sole master anchor (as it seems to be the case in worms).

Formation of an actin-based cytoskeleton is currently believed to allow for the development of presynaptic sites. It may not be easy for a protein jammed in a moving particle, clearly with restricted access, to be recruited in a manner dependent on protein-protein interactions. It is thus foreseeable that the axon employs a different strategy to capture STVs and PTVs. Remarkably, several studies have highlighted the possible role of actin cytoskeleton as a local trap. The actin depolymerizing agent, latrunculin A, almost completely erases clusters of the presynaptic marker synaptophysin when applied at a culture stage in which synaptogenesis is at its peak[190]. Later during development, synaptic dependence on filamentous actin (F-actin) is lost[190], suggesting a specific role for actin in the initial building of a synapse. Moreover, nascent synapses are associated with localized accumulation of F-actin[191]. On poly-D-lysine (PDL)-coated beads, an alternative system for the induction of presynaptic assembly, clustering of SVs occurs alongside localized accumulation of actin and is abruptly diminished upon actin depolymerization[192]. Because clustering on beads was proposed to occur by a mechanism dependent on a cell surface transmembrane proteoglycan, this study highlights that induction of presynaptic clustering requires dynamic cytoskeleton rearrangements downstream activation of synaptogenic adhesion complexes[192].

Actually, the actin cytoskeleton has been shown to be the link between synaptic partner recognition and assembly of presynaptic boutons. In *C. elegans*, for instance, recruitment of the aforementioned active zone organizers, SYD-1 and SYD-2, to nascent sites occurs via F-actin[193,194]. Activation of the axon surface receptor SYG-1 leads to its interaction with a key regulator of actin cytoskeleton, the WVE-WAVE regulatory complex (WRC), which in turn promotes formation of a local F-actin network[194]. Next, the actin binding protein NAB-1/neurabin binds to F-actin and recruits SYD-1 and SYD-2, thus serving as an adaptor between synaptogenic adhesion molecules and CAZ proteins[193]. Interestingly, NAB-1 is transiently enriched in the nascent presynaptic site and it is only required early during synaptogenesis, being completely unnecessary in later stages[193]. This finding gives further support to the idea of a transitory actin nest that recruits presynaptic proteins which are then permanently incorporated via high affinity protein-protein interactions into the growing active zone. A similar mechanism of instructing presynaptic assembly also occurs in *Drosophila* upon activation of the netrin receptor UNC-40/deleted-in-colorectal cancer (DCC)[195]. Through

CED-5/DOCK180, a protein that directly binds to UNC-40/DCC, regulators of actin polymerization are localized to presynaptic regions in which they give rise to F-actin accumulation and SV clustering[195]. Furthermore, local enrichment of F-actin downstream netrin-1 stimulation was also reported in rat cortical cells, in which SV clustering is, once again, sensitive to actin depolymerization[142].

In mammals, the best described intracellular cascade of events preceding SV clustering begins with surface cadherins and, amazingly, is also F-actin-mediated. Upon engagement of a cadherin-cadherin transsynaptic pair, β-catenin is recruited by direct interaction and will promote SV clustering in a manner dependent on its PDZ domain[196]. Scribble, a member of the leucine-rich repeats and PDZ domain (LAP) protein family, is one of the proteins interacting with β-catenin[197]. Then, the fourth element, β-pix, is brought to the complex in a manner dependent on scribble[198]. β-pix is a Rac/Cdc42 guanine exchange factor (GEF), which promotes localized actin polymerization at synapses via regulation of Rac/Cdc42 by its GEF activity[198]. Polymerized actin, in turn, recruits SVs to discrete sites along the axon[198]. Surprisingly, the cadherin/β-catenin/scribble/β-pix complex is not able to assemble active zone proteins, thus showing the need for co-functioning of different intracellular events instructing different steps of presynapse assembly. Nevertheless, the active zone protein piccolo was characterized as a key regulator of presynaptic F-actin[199], thus revealing a possible coordination between active zone formation and SVs clustering through F-actin. One might now wonder how F-actin can recruit and retain SVs. To date, this question cannot be answered clearly. Although the possibility of a physical barrier looks like a plausible explanation, it is possible that other events are also taking place. The finding that SVs contain a transmembrane form of carboxypeptidase E (CPE) whose cytoplasmic tail interacts with λ-adducin that binds actin enriched at the nerve terminal[200], indicates that localization of SVs can occur through direct interaction with F-actin.

Brain-derived neurotrophic factor (BDNF) is likely to be the most promiscuous synaptogenic factor. It does not only promote presynaptic differentiation after being secreted from different sources[156,157], but it might also be able to affect local actin polymerization with a subsequent influence on SV clustering in different ways. On one hand, it seems to generate new synaptic sites by splitting of existing ones following disruption of cadherin-β-catenin interaction[201] and possibly dynamic changes in the synaptic pool of F-actin. On the other hand, it inhibits the actin capping protein Esp8, which was shown to negatively regulate the number of axonal filopodia[202], structures that contain VAMP clusters and are believed to play a decisive role in the initial stages of synaptogenesis[203].

One last compelling piece of the final puzzle is the likelihood that presynaptic clustering is an activity-driven process. In culture, KCl-induced depolarization triggers F-actin polymerization and increased sites of SV clustering[190]. In mice deficient for Munc18, which lack both evoked and spontaneous release, the number of synapses is decreased three to fivefold[204]. Furthermore, mice engineered to release less glutamate from bipolar cells in the retina display reduced synapse density and fewer presynaptic active zones[205], clearly demonstrating that activity regulates synapse formation. More recently, two studies have given hints that *N*-methyl-D-aspartate (NMDA) receptor activation is the trigger for presynaptic clustering: treatment with the selective NMDA receptor antagonist APV reduces accumulation of multiple proteins, including SV and active zone proteins, at developing presynaptic terminals[206]; and the astrocyte-secreted factor TGF-β1 induces synaptogenesis in a manner dependent on NMDA receptor activity[161]. Furthermore, in presynaptic terminals being formed on non-neuronal cells in the absence of the postsynaptic cell or glia, clustering of presynaptic material was also diminished upon inhibition of NMDA receptor activity[206]. This indicates a possible role for the activation of presynaptic, and not postsynaptic, NMDA receptors. One can speculate that glutamate release from immature boutons activates autocrine presynaptic NMDA receptors and corresponding

downstream cascades that further enhance recruitment of material and stabilization of those immature sites. Although still in its infancy, synaptic activity in presynaptic differentiation is an appealing concept mostly due to its ability of fine-tuning the neuronal network as a whole.

Putting all the pieces together, we may conceive a blurred preliminary idea of what happens inside the axon downstream presynaptic organizers. Either simultaneously or sequentially, the combination of a local trap in the form of actin filaments and a complex grid of proteins bound together through their interaction domains will eventually halt and retain passing packets. Once at their destination, it is predictable that PTVs will easily and rapidly self-assemble into an active zone, as suggested by the quick reconstitution of a presynaptic "particle web" after its complete disassembly[7]. Nevertheless, a complete understanding of the basic mechanism governing presynapse assembly is still inaccessible.

Neurotransmitter release

Neurotransmitter release is a calcium-driven process that is triggered in less than one millisecond. Following arrival of the action potential at the presynaptic terminal, VGCC will open and the inflow of Ca^{2+} triggers fusion of neurotransmitter-containing SVs primed at the active zone (figure 1.3B, C). After exocytosis, SVs will be recycled back at the endocytic or periactive zone, an area surrounding the active zone where the required endocytotic material is located (figure 1.3D). Most, if not all, SVs are recovered by clathrin-mediated endocytosis (reviewed in [207–209]), in which a clathrin coat will sequentially be assembled on the intracellular side of the SV membrane forcing it to curve until a basket like structure is formed, allowing a dynamin ring to pinch off the coated vesicle. An alternative event in which SVs do not fully collapse and are quickly recovered after neurotransmitters are released through a transient pore has also been described and is known as kiss-and-run (reviewed in [210,211]). Following membrane retrieval, SVs are refilled with neurotransmitters (figure 1.3E, F) and positioned back for fusion (figure 1.3A). The same SV can undergo several cycles of regulated exocytosis and endocytosis to sustain prolonged release upon physiological stimulation. In this section, a brief description of neurotransmitter release, mostly focused on SV exocytosis at the active zone, will be described.

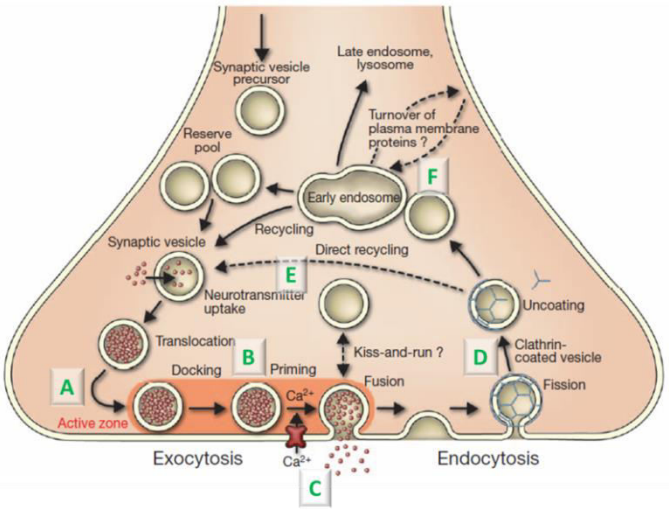

Fig. 1.3 – The SV cycle. Within the presynaptic terminal, (**A**) SVs are filled with neurotransmitters and positioned for release at the active zone. (**B**) Docking and priming grant SVs the readiness for (**C**) fusion

following arrival of an action potential and Ca^{2+} uptake. (**D**) SVs that are exocytosed can be recycled back by clathrin-mediated endocytosis, (**E**) directly refilled with neurotransmitters or (**F**) incorporated into an endosomal intermediate before delivered back to the pool of recycling vesicles (adapted from [212]).

Within the presynaptic terminal, SVs are organized into three distinct pools: the RRP, the recycling pool and the reserve pool[213]. The RRP is morphologically characterized by their physical contact with the active zone membrane, it includes SVs that are immediately available for fusion mainly because they are already docked at the active zone and primed for release. This pool comprises no more than 1% of the total SV pool and so it is rapidly depleted following Ca^{2+} entrance. Continued neurotransmitter release during moderate stimulation is guaranteed by the recycling pool, which comprises 5-20% of all SVs that are continuously recycled during neurotransmission. Accordingly, presynaptic release is mainly supported by the RRP together with the recycling pool. Lastly, the reserve pool constitutes a SV reservoir in which the remaining vesicles are clustered awaiting for periods of intense stimulation. It was previously believed that these SVs were rarely recruited under physiological activity[213]; however, recent studies indicate that recruitment of vesicles from the reserve pool may actually underlie important activity-dependent changes in presynaptic efficacy[214].

Presynaptic release is initiated by SV docking, defined as the attachment of vesicles to the active zone at the synapse, and followed by priming, which accounts for all the molecular steps that confer a SV readiness for fusion. Exocytosis of SVs is promoted by SNARE proteins which assemble into a trans-complex holding the SV to the active zone membrane. Full zippering of the SNARE complex and subsequent opening of the fusion pore requires the participation of additional proteins and is triggered by Ca^{2+} (figure 1.4)[215,216]. There are three synaptic SNAREs: VAMP (also known as synaptobrevin) in the SV membrane and the SNARE proteins syntaxin and SNAP25 located in the plasma membrane (figure 1.4A)[217]. They are characterized by a SNARE motif of 60-70 residues forming a coiled-coil stretch. Interaction between SNAREs occurs through the SNARE motifs that assemble into a tight bundle of four parallel α-helices, one from each VAMP and syntaxin and two motifs from SNAP25[218,219]. Progressive zippering of the SNARE complex will bring SV and active zone membranes into close proximity which is crucial for Ca^{2+}-triggered pore opening (figure 1.4B)[220,221]. SNARE zippering is absolutely dependent on Sec1/Munc18-like (SM) proteins, mainly on the binding of Munc18 to syntaxin (figure 1.4B). The latter acquires a closed conformation when disassembled in the membrane, in which the SNARE motif is hidden. Munc18 binds to this closed conformation[222], and remains associated with syntaxin (albeit in a different binding mode) after it changes into an open conformation and formation of the SNARE complex occurs[223]. Although the function of Munc18 is still not totally clear, its binding to syntaxin's closed conformation is an essential intermediate step in exocytosis[222,224]; and moreover, its binding to assembling SNAREs via interaction with syntaxin mediates SV priming thus disposing the vesicle ready for fusion[225,226]. Another determinant player in SV priming is the presynaptic protein Munc13[227], which has recently been proposed to mediate syntaxin opening and to orchestrate, together with Munc18, SNARE complex assembly[228].

Once SNARE/SM protein complex is established, complexin binds to a groove on the surface of the SNARE complex in order to further increase SV priming[229] (figure 1.4C). On one hand, complexins may act as co-factors of the Ca^{2+} sensor synaptotagmin by sensitizing and modelling the SNARE complex to its activation; on the other hand complexins have been proposed to clamp progression of SNARE zippering, thus preventing spontaneous release in the absence of Ca^{2+} entry[212,216]. Synaptotagmins are SV transmembrane

proteins harboring two cytoplasmic C2-domains that can bind Ca^{2+} and syntaxin. Mice with a point mutation on synaptotagmin that reduces Ca^{2+} binding results in a reduction in neurotransmitter release[230], thus firmly demonstrating that Ca^{2+} binding to synaptotagmin triggers SV fusion. However, this is probably dependent on complexins because mice lacking the protein have decreased Ca^{2+}-dependent neurotransmitter release efficiency[231]. Furthermore, structural analysis show that complexin binding stabilizes the SNARE complex by minimizing the repulsive forces between the apposed membranes[229]. Overall, complexins are important players in SV priming by further preparing the release complex for Ca^{2+} entry and binding to synaptotagmin domains.

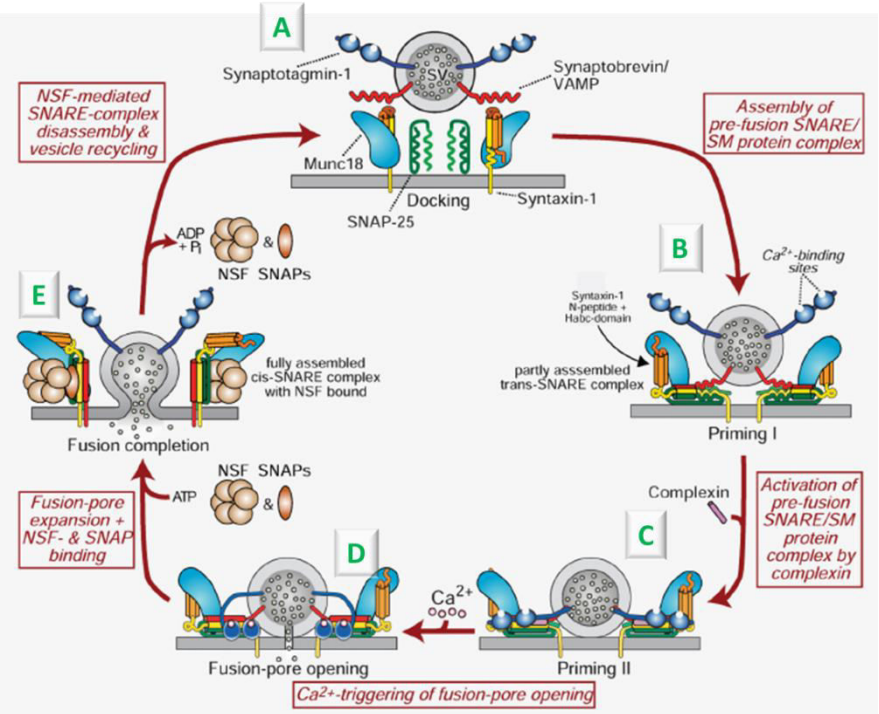

Fig. 1.4 – The steps of neurotransmitter release: docking, priming, fusion and recycle. (**A**) A SV first approaches and docks at the active zone membrane. (**B**) The SV-located SNARE, VAMP, assembles with syntaxin and SNAP25 at the plasma membrane forming a trans-SNARE complex. Binding of Munc18 to syntaxin and Munc13 to Munc18 is crucial for the assembly of the SNARE complex and for priming vesicle for fusion. (**C**) Binding of complexin to the SNARE complex will further increase SV priming and readiness for Ca^{2+} triggered fusion. (**D**) Ca^{2+} entry and binding to synaptotagmin promotes opening of the fusion pore with subsequent neurotransmitter release. (**E**) The ATPase NSF and its adaptors SNAPs then disassemble the resulting cis-SNARE complex and prepare them for being reused. See text for further details (adapted from [216]).

The "superprimed" SNARE/SM/complexin complex is then ready to rapidly respond to rises in intracellular Ca^{2+}. Binding of Ca^{2+} to synaptotagmin will probably change the release complex into a fusion-competent conformation that destabilizes the two opposing membranes so that fusion is favored with the ultimate formation of a pore through which neurotransmitters are released (figure 1.4D)[212]. After membranes merge completely, SNARE components are converted into cis-SNARE complexes that will be disassembled by the ATPase N-ethylmaleimide sensitive factor (NSF) and its adaptors soluble NSF-attachment proteins (SNAPs), which utilize the energy of ATP hydrolysis to dissociate the complex and make individual SNAREs available for subsequent rounds of fusion (figure 1.4E)[232]. Proper and functional SNARE

assembly is maintained by chaperone systems, including the cysteine string protein α (CSPα) and synucleins, which prevent aggregation or accumulation of abnormal SNARE proteins[233,234]. Lastly, the rapidity of neurotransmitter release is attained by the integration of all components at a short distance, thereby enabling a fast and synchronous SV release. This is at least partially accomplished by the multi-domain active zone protein RIM, which binds and tethers Ca^{2+} channels[177,235] and also SVs through its interaction with the vesicular protein Rab3[236–238]. RIM also interacts with the active zone proteins Munc13 and liprinα to form a protein scaffold at the terminal[178]. Thereby, RIM connects channels to SVs in the active zone and keeps them at close proximity to allow for a tight coupling of Ca^{2+} influx to fusion triggering. Moreover, RIM activates the priming factor Munc13 by releasing it from an autoinhibitory homodimerization state[239]. So, not surprisingly, RIM deletion abrogates neurotransmitter release by simultaneously impairing SV priming and presynaptic concentration of Ca^{2+} channels[177].

In order to achieve an effective synaptic transmission, the SV fusion machinery should be able to complete the task at lightning speed with no flaws. Previous positioning of all the components into rapidly-geared devices comes as a great advantage. Notwithstanding, one can easily imagine that several modulatory and regulatory mechanisms at the backstage of SV fusion guarantee its flawless occurrence. In chapter 5 results supporting a role for polyubiquitination in the modulation of presynaptic release are presented.

Ubiquitination and proteasome-mediated degradation

In the brain, not only synapse-related, but also basic cellular mechanisms work together to give rise to functional synapses perfectly integrated in a neuronal network. One of such basic mechanism is the ubiquitin proteasome system (UPS), the major proteolytic machinery in cells. Wide expression of UPS components in the synapse[240,241], a diverse brain ubiquitome[242,243] and UPS-related neurodevelopmental diseases[244], constitute prime clues for a fundamental role of UPS in the developing and mature brain. In the present work, we set out to study the involvement of ubiquitination and proteasome-mediated degradation in the formation of presynaptic sites. Accordingly, in the following sections a brief description of UPS mode of function and an extensive review of its participation in axon development will be included.

Ubiquitin signaling

Ubiquitin (Ub) is a highly conserved small protein with 76 amino acids and has the unusual property of being covalently attached to other proteins. The attachment of ubiquitin to a protein, event known as ubiquitination, constitutes a type of posttranslational modification that can alter several properties of the target protein such as its structure, function, localization and interaction with other proteins[245,246]. It is a highly stable protein that adopts a compact β-grasp fold with an exposed carboxy terminal tail containing a diglycine motif that forms an isopeptide bond with the ε-amino group of lysine (K or Lys) residues of a substrate protein (figure 1.5A)[245]. In addition to its flexible C-terminal tail, signaling through ubiquitin is mostly attributed to two other special features within its structure: the presence of a flexible hydrophobic region that is often the site of recognition for ubiquitin binding proteins (UBPs); and seven lysine residues covering all surfaces of ubiquitin and pointing into distinct directions that can all serve as attachment sites for another ubiquitin molecule (figure 1.5A)[245]. As a consequence, proteins can be found in cells in a

monoubiquitinated or in a polyubiquitinated form, the latter resulting from the polymerization of Ub chains on the first substrate-conjugated Ub. Because all seven lysine residues in the Ub molecule are prone to accept another Ub, different chain types linked via K6, K11, K27, K29, K33, K48 and K63 can be attached to substrates[245,247,248] (figure 1.5). Ubiquitin signaling is further diversified by the attachment of single Ub molecules to multiple sites of a protein (multi-monoubiquitination); addition of Ub moieties to the previous Ub amino terminal methionine residue (generation of linear chains); or formation of heterotypic chains containing mixed linkage types (figure 1.5B)[245,247,248].

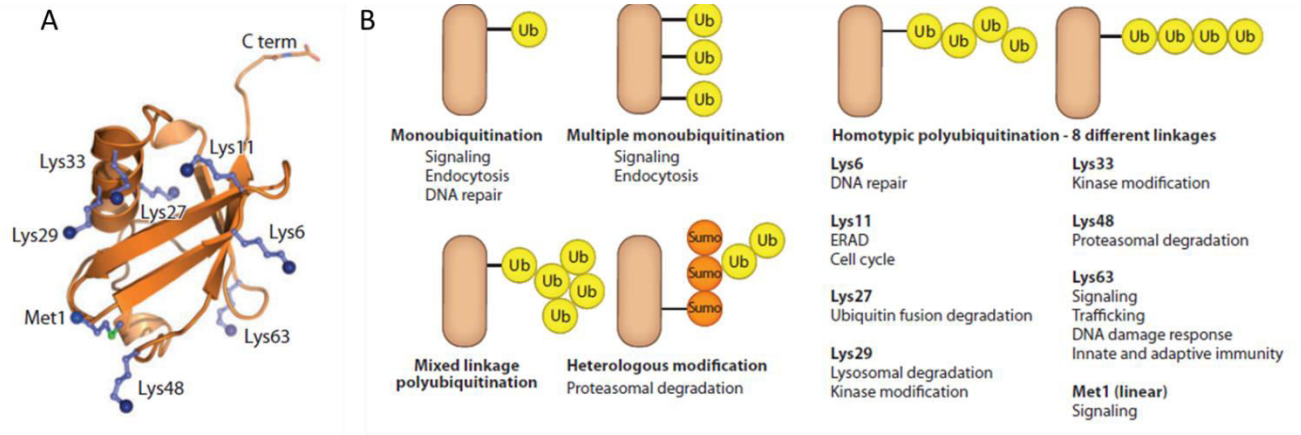

Fig. 1.5 – The many faces of ubiquitin signaling. (**A**) Structure of ubiquitin indicating the C-terminal tail, the seven lysine residues (K6, K11, K27, K29, K33, K48 and K63) and methionine 1 (Met1) (adapted from[245]). (**B**) Different Ub tags and their involvement in cellular processes (adapted from [249]). ERAD, endoplasmic reticulum-associated degradation; SUMO, small ubiquitin-like modifier.

Assembly of Ub chains is performed by a three-step enzymatic cascade involving an E1 ubiquitin-activating enzyme, an E2 ubiquitin-conjugating enzyme and an E3 ubiquitin-ligase. The first step comprises activation of Ub for conjugation by acyl-adenylation of its C-terminal glycine by the E1 ubiquitin-activating enzyme in an ATP-dependent manner[250]. This unstable and high-energy intermediate is subject to rapid nucleophilic attack by the catalytic cysteine of E1, resulting in a thiol-ester bond between the E1 cysteine and the C-terminal glycine (G76) of Ub. Then, activated Ub is transferred to the E2 enzyme, which also forms a thiol-ester bond between E2 cysteine and Ub G76. Lastly, the E2 enzyme forms a complex with an E3 ligase that carries the substrate and the Ub is added to the lysine residue of the target protein[251]. Formation of Ub chains is accomplished by the same cascade of reactions, by which another Ub is attached to an internal lysine residue or the N-terminal methionine in the first Ub (figure 1.6). The diversity of Ub signals is generated by a complex and highly regulated combination of E2s and E3s[245,247].

E3 ligases are the key specifiers of protein ubiquitination mostly due to their high number in cells (more than 500 in mammals) and to their recognition of substrates by specific protein-protein interactions. E3 ligases can be divided in two main groups based on the presence of a really interesting new gene (RING) finger domain or a homologous to E6-AP carboxy-terminus (HECT) domain. RING E3 ligases bind the substrate and the E2 enzyme and promote direct transfer of the Ub from the E2 to the substrate. In HECT E3 ligases an additional thiol-ester linked HECT~Ub intermediate is formed in the HECT catalytic cysteine and later transferred to the lysine residue of the target protein[252]. RING E3 ligases can either function as a single protein or as a multisubunit complex, which is composed of a scaffold, an adaptor and a substrate-binding

protein. Two important examples of multisubunit RING E3s that will be mentioned ahead are Skp1-Cullin-F-box (SFC) complex and the anaphase promoting complex (APC). In an SCF complex, an F-box protein that recognizes the substrate is linked to the RING finger domain-containing protein Rbx1/Roc1 through a linker and a scaffold, Skp1 and Cullin, respectively[253]. There are many possible F-box proteins that will determine substrate specificity of the SCF complex. Within the APC complex, the substrate recognition protein can be either Cdh1 or Cdc20 (Cdh1-APC or Cdc20-APC), multiple adaptors will link it to the scaffold APC2 and to the RING finger protein APC11[254].

The reversibility nature of the ubiquitin signaling is accomplished by enzymes capable of removing Ub molecules from substrates, generally termed deubiquitinating enzymes (DUBs). DUBs are divided into five categories based on their catalytic domain. The ubiquitin C-terminal hydrolases (UCH), ubiquitin specific proteases (USP), Machado-Joseph disease (MJD) proteases and otubain proteases (OTU) are cysteine proteases, while JAB1/MPN/Mov34 metallo enzyme (JAMM) proteases are zinc-dependent mettalo-proteases[255]. They can either fully deubiquitinate a substrate or edit polyubiquitin chains, thus redirecting a substrate fate following ubiquitination. They also have a prime role in disassembling unanchored Ub chains and removing Ub from substrates destined to proteasomal degradation (described in the following section)[255]. Accordingly, in addition to their role in ensuring correct ubiquitination of substrates, they are believed to be essential for the maintenance of the cellular pool of free Ub, known to be a prerequisite for proper cell function and viability[256], and in particular for the development of the nervous system[257]. For instance, mice with a loss-of-function mutation in the proteasome-associated deubiquitinating enzyme USP14 exhibit severe malformation of the neuromuscular junction (NMJ)[258–260]. Furthermore, inhibition of ubiquitin C-terminal hydrolase L1 (UCH-L1), which is selectively and abundantly expressed in neurons, alters synaptic density and structure that are rescued by Ub overexpression[261]. Concomitantly, both USP14 and UCH-L1 loss are associated with decreased levels of free monomeric Ub[258,262], thus further reinforcing their role in sequestering Ub and preventing its degradation. A great breakthrough in the Ub field came from a very recent study in which authors suggest a new mode of restraining ubiquitination. Ub itself is acetylated at lysines 6 or 48 thus preventing chain elongation[263]. Therefore, DUBs might not be alone in their negative control of Ub chains.

Lastly, what is the decoding system used by cells to decipher the diverse Ub messages on proteins? This is accomplished by proteins that recognize ubiquitin signals on substrates, are able to read and interpret these signals and then generate different biochemical outputs in the cell. These proteins are generally termed ubiquitin-binding proteins (UBPs) and contain specialized ubiquitin-binding domains (UBDs) that bind transiently and noncovalently to either mono- or polyubiquitin[249,264]. Importantly, UBDs fold into secondary structural elements like α-helices, zinc fingers or plekstrin homology folds, which bind preferentially to a hydrophobic patch on Ub surface, and exhibit relative or absolute selectivity for different types of Ub chains[249,265]. A quick and self-explanatory example are proteasome shuttle factors, such as Rad23, Dsk2 and Ddi1, that predominantly bind to proteins bearing a K48-linked ubiquitin chain and deliver them to the proteasome for degradation[179,180]. Overall, cells possess all the required material for a coordinated assembly and editing of Ub signals on proteins, as well as their decoding and translation into different cell responses that support a multitude of biological processes.

The ubiquitin proteasome system: basic mechanism

Proteasome-mediated degradation is the most well-known outcome of Ub signaling, classically associated to K48 polyubiquitin chains, more precisely to the controlled degradation of substrates harboring an Ub chain with four or more Ub moieties linked together through their lysine 48[267]. The UPS is the major degradative pathway of soluble short-lived proteins in cells and, as a result, it is involved in essentially every cellular event. In neurons, it is of utmost importance for neuronal development, function, plasticity and aging[268–270]. The macromolecular structure that degrades polyubiquitinated proteins is referred to as the 26S proteasome that is formed by the assembly of a 20S catalytic core particle (CP) and 19S regulatory particles (RP) at one or both ends (figure 1.6). The 19S RP is responsible for the selective recognition of substrates, their deubiquitination, unfolding and translocation towards the catalytic subunits of the 20S CP, which will then cleave proteins into small peptides of 3-22 amino acids[271].

The 20S CP is a barrel-shaped structure composed of four rings each with seven subunits. The outer rings contain seven identical α subunits and the inner ones seven identical β subunits ($\alpha_7\beta_7\beta_7\alpha_7$). In a way of restricting degradation to tagged proteins, the proteolytically active sites are directed towards the inner core of the cylinder. There are three catalytically active subunits, β1, β2 and β5, which possess caspase, trypsin and chymotrypsin-like activities, respectively. The two β rings form the catalytic chamber whose access is limited by two axial pores of about 13Å diameter formed by the flanking α subunits. As a result, only unfolded substrates can reach the proteasome catalytic center[271,272].

The 19S RP is composed of nineteen subunits organized into two subcomplexes, the base and the lid. The lid is composed of nine regulatory particle non-ATPase (Rpn) subunits (Rpn3, 5-9, 11, 12 and 15) [271,272]. One of the major functions of the lid is to detach Ub chains from trapped substrates, primarily mediated by the lid integral deubiquitinating enzyme Rpn11, which removes the entire Ub chain en bloc only after proteasome has been committed to degradation[273]. The activity of this enzyme is aided by two DUBs, USP14 and UCH37, that are physically associated with subunits of the 19S RP. Together, they guarantee removal of Ub from substrates thus sparing it from degradation, which is critical for the maintenance of the free Ub pool. Recently, it was proposed that USP14 function limits proteasome degradation by removal of the Ub tag earlier than the cascade of events leading to substrate degradation[274]. The base subcomplex comprises a heterohexameric ring of six ATPase subunits [regulatory particle ATPse 1-6 (Rpt1-6)], which lay on the outermost α rings of the 20S core, and four non-ATPase subunits: Rpn1 and Rpn2 which are the largest subunits, and Rpn10 and Rpn13 that function as integral Ub receptors due to their ability of binding and thus trapping polyubiquitinated substrates[271,272]. Following substrate recognition, the ATP generated by the Rpt ring is utilized to unfold the target protein and the subunits Rpt2 and Rpt5 give access to the catalytic chamber by opening the pore in the α ring[275].

Instrumental to an effective function of the UPS are adaptor proteins, also known as proteasome shuttle factors, such as Rad23, Dsk2 and Ddi1. These proteins contain both an UBD and an ubiquitin-like domain (UBL), and so, they can simultaneously bind polyubiquitinated targets and be recognized by the Ub receptors on the 19S RP[266]. Due to these features, their prime role is to collect ubiquitinated substrates and deliver them to the proteasome. To sum up, proteins that need to be removed from the system are tagged for degradation by the attachment of a K48 polyubiquitin chain by the coordinated action of E1, E2 and E3 enzymes. Through diffusion or assistance by shuttle factors, ubiquitinated proteins reach the proteasome, their polyubiquitin tag is removed; the substrate is then unfolded and ultimately driven into the 20S for catalytic processing (figure 1.6).

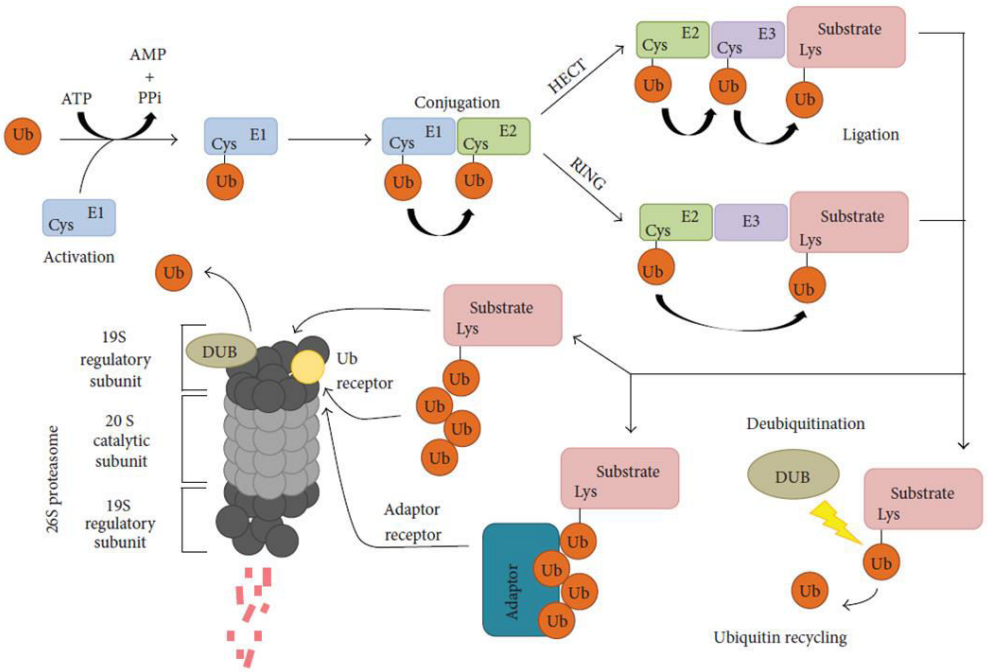

Fig 1.6 – Steps of the ubiquitin proteasome system. Attachment of Ub moieties to naked substrates is promoted by a cascade of enzymes (E1 ubiquitin-activating enzyme, E2 ubiquitin-conjugating enzyme and E3 ubiquitin-ligase). Proteins harboring a degradation tag are directed to the proteasome, deubiquitinated, unfolded and degraded within the 20S catalytic core. Proteasome-associated DUBs prevent degradation of Ub by removing it from substrates prior to their degradation (taken from [276]).

Recently, substantial data has been gathered demonstrating that other types of Ub chains also tag proteins for proteasome degradation. Remarkably, all except for K63 polyubiquitin chains accumulate in cells shortly after proteasome inhibition[277,278] or in the brain of a 26S conditional KO mice[279], thus indirectly suggesting their involvement in targeting proteins for the proteasome. Indeed, the E3 complex APC, which governs cell cycle transition, in combination with a specific E2 enzyme assembles K11-linked Ub chains to mitotic regulators and their subsequent proteasome degradation[280–282]. In line with these observations, loss of APC completely prevents formation of K11 Ub chains in response to proteasome inhibitors[282], thus suggesting its master role as a supplier of K11-linked chains to substrates. However, it was also demonstrated that attachment of K11 Ub chains to β-catenin by an SCF-like complex also induces proteasomal degradation[283]. Furthermore, this type of linkage also instructs clearance of defective or misfolded polypeptides from the endoplasmic reticulum (ER), a quality control pathway known as ER associated degradation (ERAD)[277,284]. So far, it seems that the ER integral membrane E2 enzyme, Ubc6, primarily synthesizes K11 linked chains on targets[277], which then interact with the ATPase p97 promoting their dislocation to the cytosol proteasome[284].

Despite the fact that K63 ubiquitin chains are not upregulated by proteasome inhibition, some studies suggest their recognition as a degradation tag for the proteasome. *In vitro*, specific substrates bearing K63 Ub chains are prone to be degraded by the proteasome[280,285]; *in vivo*, an Ub ligase in yeast was shown to assemble K63-linked chains to substrates whose levels are then reduced in a proteasome-dependent manner[286]. These discrepancies might be explained by the fact that in mammals K63 Ub linked chains have decreased proteasome accessibility due to: soluble factors that selectively bind to K63 linkages and block

their binding to the proteasome, selective recognition of K48 chains by the proteasome shuttle protein Rad23 or faster deubiquitination rates of proteasome-bound K63 chains in comparison to K48 Ub linkages[287,288]. Surprisingly, combined linkages of the small Ub-like modifier (SUMO) with Ub moieties have also been shown to drive specific substrates for proteasome-mediated degradation[289–291]. In addition, the repertoire of Ub signals for proteolysis is further diversified by substrates harboring a single Ub, multiple single ubiquitins or even non-ubiquitinated[292] and also branched chains[293]. These studies highlight the role of non-canonical Ub chains in targeting substrates for the proteasome. This broader range of degradation tags may confer the UPS higher specificity and plasticity in its selection of targets to eliminate. It is conceivable that K48 tags, and eventually K11, function in cells as constitutive signals for degradation, whilst non-canonical Ub signals are exploited in order to fulfill specific cellular needs. It is also likely that specific subsets of E2-E3s pair, UBDs and DUBs independently control distinct Ub chain types on their way to the proteasome.

Proteasome unrelated outcomes of the ubiquitin code

Ubiquitin signaling is often initiated after thiol-ester conjugation to substrates, comprising the pool of conjugated Ub. In the mouse brain, 35% and 5% of total Ub are present as monoubiquitin and polyubiquitin modifications on substrates, respectively[294]. In terms of polyubiquitin chains, they are expressed in the rat brain in the following ascending order: K29, K27, K33, K6, K11, K63 and K48 (approximately 0.05%, 0.5%, 8%, 9%, 15%, 29% and 37%, respectively)[243]. Although the physiological significance of K48 and K63 polyubiquitin chains is well understood, much remains to be unmasked about the roles of the remaining types of Ub linkages (figure 1.5B). A great deal of research has demonstrated that K63 polyubiquitin chains are instrumental in events such as the endocytic pathway and intracellular trafficking[295], DNA repair[296–298] and in the nuclear factor kappa enhancer binding protein (NF-κB) regulatory pathway[248,299]. Interestingly, K63 Ub chains share their function with other types of Ub signals. For instance, endocytosis of surface receptors into endosomes is triggered not only by K63 polyubiquitin chains[295], but also by single or multiple monoubiquitin signals[300–303]. On the contrary, later sorting of endocytic vesicles to lysosomes for degradation is believed to be mostly driven by K63 polyubiquitination[304,305], and in exceptional cases by K29 polyubiquitin signals[306]. For instance, signaling of one member of the FGFR family is regulated by ubiquitination-induced endocytosis and lysosome targeting[307,308]. Upon activation of the receptor, the E3 ligase Nedd4 binds directly to and ubiquitinates its intracellular domain resulting in endocytosis[308]; then, the duration of FGFR signaling is limited by lysosomal sorting as a result of a second round of ubiquitination[307]. Besides their co-function in the endocytic pathway, K63 ubiquitin tags and monoubiquitination both ensure an effective DNA damage response[296,298]. In general, DNA lesions are first detected by proteins that, in part through K63 or monoubiquitination, recruit and activate additional components of the DNA repair machinery[296,298].

Ubiquitin signaling also plays a crucial role in the activation of the NF-κB pathway that in turn evokes different responses in cells including immunity, inflammation and apoptosis. The canonical pathway leading to NF-κB activation is initiated by binding of the cytokine tumor necrosis factor α (TNFα) to its receptor (TNFR). Downstream activation of TNFR signaling proteins will be recruited including E2s and E3s that catalyze synthesis of K63, K11 and linear polyubiquitin chains on TNFR complexes or even unanchored Ub chains. These ubiquitinated chains function as scaffolds for the ultimate recruitment of the protein kinases TGFβ activated kinase 1 (TAK1) and inhibitor of κB kinase (IKK) that contain multiple UBDs[248,299]. This is a highly complex cascade in which linkage specific E3s and UBPs are involved, thus allowing for the

coordinated assembly of an Ub rich platform and sequential recruitment of signaling kinases downstream TNFR activation.

The functional significance of the remaining types of Ub signals is mostly unknown; however, data has been recently collected that suggest a wider broad of action than ever expected (figure 1.5B). K29 and K33 Ub chains are predicted to modulate the activity of kinases, anticipated by their non-degradative outcome following ubiquitination of residues normally submitted to phosphorylation[309]. K27 linkages might be essential for the selective recognition and clearance of damaged mitochondria[310], however the precise mechanism is far from being understood. Ubiquitination can also alter several properties of a protein, either directly or indirectly, including its activity, location or propensity to interact with partners[245,246]. A good example of the latter is the K29 ubiquitination of axin by the E3 Smad ubiquitination regulatory factor 1 (Smurf1)[311]. Axin interacts with the coreceptor LRP5/6 of the synaptogenic protein Wnt, however upon addition of the K29 Ub tag the interaction is disrupted and Wnt signaling repressed[311]. Overall, the diverse world of possible Ub tags, along with the ever-broadening list of possible outcomes, suggests that Ub is involved in a horde of cellular events that have so far not been addressed, thus highlighting the unexplored potential of Ub signaling.

Ubiquitin and the proteasome in axons

Formation of a functional presynaptic terminal requires the execution of several tasks by the growing axon. After differentiation of a neuronal branch into an axon, it first extends and follows the correct route to reach its dendritic target, then axon growth halts and presynaptic differentiation takes place. So far, data has revealed that axon development and presynaptic function are regulated by ubiquitin pathways in a spatial and temporal specific manner[312]. Despite the fact that this work is mainly focused on the mechanisms supporting presynaptic formation, this section will present an overview of ubiquitin-related mechanisms governing all stages of axon development (summarized in table 1.2). This will provide an idea of the UPS machinery working locally within the developing axon, as well as deeper understanding of how ubiquitin and the proteasome can govern axonal events. Moreover, due to lack of knowledge in vertebrates, information from studies in invertebrates will also be included and discussed.

Neuronal polarity

Probably the best example for the requirement of spatially coordinated proteasomal degradation is in the establishment of neuronal polarity. Apparently, neurons have devised a strategy to differentiate a single axon from the multitude of primordial neuronal branches that depends on asymmetric degradation of specific proteins[313–316]. Briefly, axon growth promoting and disrupting proteins will be selectively enriched and eliminated, respectively, in nascent axons by differential proteasome degradation; and in addition, proteasomal removal of axon-promoting proteins in nascent dendrites guarantees formation of a single axon. Axon differentiation is initiated by phosphatidylinositol-3-kinase (PI3K) activation of Akt/PKB (Akt) [317–319], and so, in order to prevent it from happening in dendrites both Akt[313] and the PI3K downstream effector Rap1B[314] are degraded by the proteasome only in dendrites. For the latter, ubiquitination and subsequent degradation was shown to depend on the activity of the E3 ligase Smurf2[314]. Although the machinery responsible for Akt ubiquitination and dendritic elimination was not identified, a later study demonstrated

that it can be, in fact, negatively regulated in an UPS manner by the E3 ligase mitochondrial ubiquitin ligase activator of NF-κB (MULAN)[320]. In concert with PI3K, neuronal polarity is also specified by localized accumulation of portioning-defective proteins (Par)[317]. Interestingly, Smurf1 can degrade both Par6 and the growth-disrupting RhoA depending on its phosphorylated status[315]. BDNF stimulates Smurf1 phosphorylation, which then loses affinity for Par6 while preferentially ubiquitinating RhoA, thus resulting in an increased spatial ratio of Par6 versus RhoA that is required for axon formation[315]. Smurf1 itself is regulated by an additional round of proteasome-mediated degradation elicited by the E3 complex Cdh1-APC[321]. This specific spatiotemporal axonal-inducing pattern, created by asymmetric degradation of specific proteins, is further reinforced by axonal degradation of the RhoA activator RhoGEF mediated by the KLHL20-based E3 ligase complex[316].

Axon outgrowth

After a neuronal branch has been chosen for axon, it must grow until it reaches the neuronal partner. Growing evidence suggest that intrinsic mechanisms involving the UPS also control this process. Perhaps the wider effect is that of the E3 complex Cdh1-APC that acts in the nucleus to alter transcription of genes involved in axon growth and patterning, thus ultimately functioning as a negative regulator of this event[322]. Indeed, mice lacking Cdh1 have longer axons[323]. Currently, researchers have unraveled at least part of the cascade of events responsible for this phenotype: activation of Cdh1-APC in the nucleus[324–327] enhances ubiquitination and proteasome degradation of the transcription factors SnoN[328] and inhibitor of DNA binding 2 (Id2)[329]. SnoN and Id2 either up or downregulate transcription of genes enriched at the axon that increase and decrease its growth, such as the signaling scaffold protein Cdc1[330] and the Nogo receptor[329], respectively. Altogether, Cdh1-APC acts in the nucleus as an inhibitor of axonal growth.

On the other hand, the UPS may act locally to regulate axon growth, for instance by interfering with the cytoskeleton, both actin microfilaments and tubulin microtubule. LIM kinase 1 (LIMK1) enhances polymerization of F-actin and by doing so accelerates axon extension[331]. Its levels in the growth cone were shown to be negatively regulated by the E3 ligase RING finger protein 6 (RNF6) with a clear shortening of axon length[332]. Furthermore, the axonal actin cytoskeleton is indirectly regulated by the UPS through the control of phosphatase and tensin homolog (PTEN) levels, which is a negative regulator of PI3K that acts to regulate cytoskeleton dynamics[333]. Both in rat and *Xenopus*, PTEN is targeted for proteasome degradation by the E3 ligase Nedd4 with clear outcomes in the capacity of axons to grow and branch[332,334].

Growing evidence indicate that E3 ligases also affect axonal outgrowth by altering the dynamics of microtubules within the extending axon. PHR (human PAM, mouse Phr1, zebrafish Esrom, *Drosophila* Highwire and *C. elegans* RPM-1) proteins contain an E3 RING-finger domain and have a widely described role in both axon and synapse development[335]. Deletion of PHR has deleterious effects in the normal axon navigation pattern with a striking failure to reach the correct destination[336–338]. Interestingly, authors concluded that these phenotypes were due to aberrant microtubule dynamics that could be corrected by pharmacological manipulation of microtubule assembly[337,338]. However, the mechanism of PHR regulation of microtubules awaits further study. Contributions from works in *C. elegans* and *Drosophila* may give us hints of what might be happening in the axoplasm. PLR-1 and HUWE1 are E3 ligases that work in the control of axon outgrowth and branching in *C. elegans* and *Drosophila*, respectively[339,340]. In both, disruption of the Wnt/β-catenin pathway was proposed to be the link between E3s activity and axonal defects[339,340]; moreover, dishevelled levels are upregulated by overexpression of HUWE1[340]. Importantly, Wnt signaling

induces changes in microtubule organization[147,341] and can modulate axonal outgrowth vs. growth cone enlargement by regulating microtubule dynamics[342]. Furthermore, dishevelled, a key component of the Wnt pathway, is required for Wnt-mediated microtubule reorganization and changes in axon behavior[342,343]. Interestingly, growth cones from *phr* mutant axons[337,338] are strikingly similar to those obtained after Wnt stimulation or dishevelled expression[342], thus emphasizing the possible involvement of Wnt/β-catenin signaling in PHR-mediated axon navigation. Altogether, these studies highlight a potential role for the UPS in modulating axon development primarily through dynamic changes in microtubule organization.

Table 1.2 – Ubiquitin and/or proteasome-dependent mechanisms regulating axon development and presynaptic function.

E3	Target	Ub chain	Outcome	Neuronal compartment	Role in axon	model	Ref.
	AKT	polyUb	Prot. deg.	dendrites	Neuronal polarity/ Formation of single axon	Rat	313
Smurf2	Rap1B	polyUb	Prot. deg.	dendrites		Rat	314
Smurf1	RhoA	polyUb	Prot. deg.	axon		Rat	315
	Par6	polyUb					
KLHL20-Cullin3-Roc1	RhoGEF	polyUb	Prot. deg./ RhoA inactivation	axon		Rat	316
RNF6	LIMK1		Prot. deg./ reduced actin dynamics	Growth cone	Inhibition of axonal growth	mice	332
HUWE1	Dishevelled		Prot. deg.? Disruption of Wnt/β-catenin pathway ?	axon	Regulation of axonal branching	Dro.	340
PLR-1				axon	Control of axon extension and guidance	C.el.	339
EBAX-type CRL	SAX-3/Robo receptor		Degradation of misfolded protein	axon	Accuracy of guidance signaling	Dro.	344
	PTEN		Prot. deg.	Growth cones	Axonal branching/ Axonal outgrowth	Xen/ Rat	334,345
Nedd4 sh	Commissureless	monoUb	Endocytosis	Muscle membrane	Neuronal innervation and synaptogenesis	Dro. NMJ	346
Nedd4 lo				Muscle	Negative regulator of synaptogenesis	Dro. NMJ	347
Cdh1-APC	SnoN	polyUb	Prot. deg.	nucleus	Inhibition of axonal growth	Rat	323,328, 330
	Id2	polyUb	Prot. deg.	nucleus		Rat	329
	Liprin α			Presynaptic boutons	Control of synaptic size	Dro. NMJ	348
Cdc20-APC	NEUROD2	polyUb	Prot. deg.	nucleus	Promotion of presynaptic differentiation by inhibiting complexin II expression	Rat	349
PHR	ALK		Prot. deg. ?	Presynaptic boutons	Promotion of presynaptic differentiation	C.el.	350
	DLK-1/ Wallenda	polyUb	Prot. deg. ?	Axon tip/ Presynaptic boutons	Regulation of axon guidance, axon termination and presynaptic differentiation	C.el. Dro.	351–355
			Altered microtubule dynamics	axons	Axon outgrowth/ pathfinding	Zeb. mice	336–338
	NMNAT		Prot. deg. ?	axons	Promotion of axonal degeneration	Dro. mice	356,357

SCF^{SEL-10}				axons	Promotion of synapse elimination	C.el.	[358]
$SCF^{SCRAPPER}$	RIM1	polyUb	Prot. deg.	Presynaptic sites	Presynaptic release	mice	[359]
RNF13	snapin	K29 polyUb	Higher association with SNAP25	Presynaptic sites	SNARE complex assembly	mice	[360]
SCF^{Fbxo45}	Munc13		Prot. deg.	Presynaptic sites	Presynaptic release	mice	[361]
SCF^{MEC-15}	VAMP		Synaptic abundance	axons	Regulation of inhibitory activity	C.el.	[362]
DUBs	**Target**	**Role in axon**				**mo.**	**Ref.**
Faf	Lqf (epsin 1 homolog)	Promotion of presynaptic differentiation				Dro.	[363,364]
USP33		Axon guidance				mice	[365]
USP4/20		Axon outgrowth				rat	[366]
USP14		Presynaptic formation and function				mice	[258,259,367]
E2	**Target**	**Role in axon**				**mo.**	**Ref.**
Bendless		Initial stages of presynaptic differentiation/ Transition from axon to synaptic growth				Dro.	[368]
UEV-3	PMK-3 ?	Suppression of RPM-1/DLK-1 role in axon termination and presynaptic differentiation				C.el.	[369]

Abbreviations: ALK, anaplastic lymphoma kinase; **C.el.**, *C. elegans*; **CRL**, Elongin BC-containing Cullin-RING ubiquitin ligase ; **Dro**., *Drosophila*; **EBAX-1**, Elongin BC-Binding AXon regulator; **Faf**, Fat facets; **FSN**, F-box/SPRY domain-containing protein 1; **HUWE1**, HECT, UBA and WWE domain containing 1; **Id2,** inhibitor of DNA binding 2; **LIMK1**, LIM kinase 1; **lo**, long isoform; **Lqf**, Liquid of facets; **Nedd4**, neuronal precursor cell expressed developmentally downregulated 4; **NeuroD2**, neurogenic differentiation factor 2; **NMJ**, neuromuscular junction; **PHR**, human PAM, mouse Phr1, zebrafish Esrom, *Drosophila* Highwire and *C. elegans* RPM-1; **Prot. deg.**, proteasomal degradation; **PTEN**, phosphatase and tensin homolog deleted on chromosome 10; **RIM1**, Rab3-interacting molecule; **RNF13**, RING finger protein 13; **sh**, short isoform; **Smurf**, Smad ubiquitination regulatory factor; **USP**, ubiquitin-specific proteases; **Xen.**, *Xenopus*; **Zeb.**, zebrafish.

Axon guidance

Ubiquitin and the proteasome also have a great deal to offer to the events guiding an axon towards the correct partner. Loss of *Drosophila* PHR incapacitates segregation of axons to different lobes[354], and in mice, retinal innervation is abolished in the absence of this E3 ligase[336]. In cultures, netrin-1-induced attractive turning and L-α-Lysophosphatidic acid (LPA)-induced growth cone collapse are dependent on proteasome activity and both cues elicit rises in ubiquitinated conjugates in growth cones[370]. Interestingly, levels of the netrin receptor DCC are decreased by netrin itself through the UPS[371], thus revealing that the proteasome might be crucial for controlling the expression of receptors and so responsiveness to external cues. Indeed, in *Drosophila* the surface levels of the Robo receptor for the repulsive cue Slit[372], are controlled by the E3 Nedd4 to prevent recrossing of the midline and so ensure accurate pathfinding[373]. Furthermore, the UPS maintains accuracy of axon guidance by performing protein quality control and degrading misfolded Robo proteins[344]. Briefly, the EBAX-type Cullin-RING E3 ligase interacts with the cytosolic heat shock protein 90 (Hsp90) and is capable of regulating axon guidance by removing through proteasome degradation damaged Robo receptors that accumulate upon temperature variations[344]. Notably, not only ubiquitination but also deubiquitination of Robo are required for correct axon guidance. The deubiquitinase USP33 interacts with and deubiquinates Robo, thus maintaining its stability in the axon; this proccess is required for axon responsiveness to Slits and, more importantly, for accurate midline crossing[365]. Overall, presently it seems that ubiquitin signaling is instrumental for the maintenance of axon pathfinding mostly by tuning levels and quality of surface receptors.

Presynaptic formation

If the axon succeeds in finding its target, the next step is formation of the presynaptic terminal juxtaposed to the postsynaptic specialization. It was early demonstrated that precise balance between ubiquitination and deubiquitination is crucial for synapse development[363]. In the *Drosophila* NMJ, overexpression of the deubiquitinase fat facets (Faf) and loss-of-function mutations in Highwire, the PHR *Drosophila* homolog, both result in synaptic overgrowth[363,374], thus showing that ubiquitination-dependent mechanisms act to restrict presynaptic differentiation. Moreover, the phenotype of *Drosophila* PHR loss is suppressed in the absence of Faf, which highlights the role of endogenous deubiquitination in the enhancement of synapse development[363]. Later, efforts to identify ubiquitin-modified downstream targets revealed that Highwire forms an SCF-like complex with SkpA[375] and the F-box protein DFsn[353] and together downregulate Wallenda, the *Drosophila* homolog of dual leucine-zipper-bearing kinase (DLK)[352,353]. This kinase activates a signaling pathway involving JNK kinase activity and Fos-mediated transcription that confers synaptogenic capacity, and accordingly, Highwire restrains synaptic development by promoting Wallenda elimination[352]. Faf-induced synaptic overgrowth also converges on wallenda[352], thus emphasizing the idea that wallenda is a key substrate whose ubiquitinated status determines the propensity to form presynaptic specializations. Against all odds, Faf-induced synaptic overgrowth requires another substrate, the epsin 1 *Drosophila* homolog Liquid facets (Lqf), whose levels are not altered by Highwire[364]. It is so predictable that different candidate substrates for deubiquitination regulate presynaptic development by different routes initiated by the same UPS enzyme.

E3-mediated downreguation of synaptic kinases and scaffold proteins controls presynapse formation. Although the molecular players are conserved between *Drosophila* and *C. elegans*, complete opposite outcomes in presynaptic formation are observed. In the latter, RPM-1, the PHR *C.elegans* homolog, rather than restricting presynaptic development, promotes it by negatively targeting DLK-1 (wallenda homolog), which initiates a kinase cascade that functions cell-autonomously in the suppression of presynaptic development[351]. The UPS is believed to be in charge of DLK-1 downregulation due to its direct ubiquitination by RPM-1 and elevated levels upon loss of this E3 enzyme[351]. Additional studies reveal that Ub signaling coordinates RPM-1/DLK-1 pathway in more than one step. The E2 Ub-conjugated enzyme UEV-3 acts downstream of DLK-1 and aids in the activation of the kinase cascade by a mechanism not yet understood, probably involving activation of a specific kinase via ubiquitination as the authors thereby propose[369]. The effect of RPM-1 in presynaptic differentiation is not restricted to DLK-1 downregulation, but also depends on targeting the receptor tyrosine kinase anaplastic lymphoma kinase (ALK)[350]. Formation of an SCF-like complex comprising the F-box protein FSN-1 and RPM-1 in the periactive zone can control the extent and position of presynaptic development by locally modulating levels of ALK[350]. Another good example for the requirement of *on-site* Ub-related mechanisms is the control of the dimensions of the presynaptic site by Cdh1-APC[348,376]. Presynaptically located Cdh1-APC downregulates the active zone scaffolding protein liprinα, with a resulting limitative effect in synaptic size[348]. Altogether, these studies in invertebrates emphasize the local role of axonal E3s ligases in modulating the triggering cascades that steer presynaptic assembly. Although no studies in vertebrates have so far revealed a localized role of UPS, the fact that the F-box protein Fbxo45 associates with PAM (human PHR homolog) and that mice lacking both Phr1 and Fbxo45 display severe synaptic defects[377,378], makes it likely that similar modes of regulation underlie synapse formation in more complex organisms.

Surprisingly, the UPS does not only control synapse formation by acting at the site of nascent terminals. It can, as a matter of fact, instruct presynaptic differentiation from far distances such as the nuclei

or the postsynaptic cell. The E3 complex Cdc20-APC ubiquitinates the transcription factor NeuroD2 with subsequent proteasomal degradation[349]. By removing NeuroD2, Cdc20-APC precludes expression of complexin, which normally acts in the axon to obstruct formation of presynaptic sites[349]. Accordingly, at the stage of synaptogenesis Cdc20-APC is upregulated, as observed by decreasing levels of NeuroD2 throughout development, thus alleviating the constrain on presynaptic formation[349]. Interestingly, a similar mode of action, however involving SUMOylation rather than ubiquitination, coordinately orchestrates maturation vs. elimination of newborn presynaptic terminals[379]. Perhaps the most puzzling way by which Ub supports formation of nascent presynaptic sites is by promoting endocytosis of the transmembrane protein Commissureless in the postsynaptic muscle cell in the *Drosophila* NMJ[346,347,380]. During the period of motoneuron-muscle interaction, Commissureless is highly expressed in the muscle cell and its endocytosis is mandatory for synaptogenesis to initiate[380]. This is promoted by monoubiquitination via the postsynaptically located short isoform of E3 Nedd4, which by promoting Commissureless internalization guarantees proper muscle innervation by motoneuron branches[346]. This event is counteracted by the long isoform of Nedd4 whose levels transiently decrease during synaptogenesis[347]. Importantly, in Nedd4 mutant mice axons project to the muscle but are unable to innervate it and establish synaptic contacts[381]. This example demonstrates how Ub signaling can exploit nondestructive roles in the modulation of presynaptic development. The relevance of Ub in presynaptic development is further reinforced by studies in mice mutated for the deubiquitinase USP14[258,259]. In these mice, loss of USP14 and concomitant decrease in synaptic levels of monomeric and conjugated Ub result in severe structural and functional defects in the NMJ[258,259], thus revealing how vital the Ub pool is for the presynaptic terminal undergoing development.

Synapse elimination

In parallel to the wide role of the UPS during axon development, it also adjusts mechanisms to govern events in the more mature axon, such as synapse elimination. Following the initial boost in synapse formation, elimination of unwanted or unnecessary terminals will refine the neuronal network. In *C. elegans*, elimination of extra presynaptic clusters in the hermaphrodite-specific motor neuron (HSNL) is mediated by an SCF complex[358]. Terminals stabilized by the establishment of the SYG-SYG transsynaptic pair will be spared due to inhibition of SCF assembly following interaction with SYG[358]. Interestingly, in the postsynaptic terminal the proteasome itself can interact with the transmembrane protein protocadherin and promote synapse elimination thereafter[382]. So it seems that UPS machinery can be anchored to the membrane and activated by direct interaction with adhesive transmembrane proteins, what might be particularly advantageous in terms of response promptness and spatial specificity. Control of self-destructive events can also be mediated in neurons by the broad-spectrum PHR E3s through depletion of the axon survival molecule nicotinamide mononucleotide adenyltransferase (NMNAT), which will result in axonal degeneration[356,357]. NMNAT normally protects synapses from destruction by shielding the active zone structural protein Bruchpilot (CAST/ERC *Drosophila* homolog) from UPS degradation[383]. These studies emphasize the versatility of UPS machinery in regulating axon events as opposite as growth and destruction.

Presynaptic function

Ubiquitin-related events control presynaptic function. And what about presynaptic function is concerned? Can Ub regulate presynaptic release? Two main findings clearly tell us that a strong link between

synaptic activity and UPS is determinant. First, proteasome inhibition boosts neurotransmitter release[384–386] and secondly depolarization-induced calcium elevation alters the ubiquitinated pool towards a decrease of Ub conjugates[387]. Together, these observations point to a fundamental role for a dynamic pool of polyubiquitinated proteins in the events launching neurotransmitter release. In order to maintain synaptic activity within reasonable boundaries thus avoiding excessive release, activity of the E3 ligases SCRAPPER and the Fbxo45-PAM complex[377] reduce levels of the active zone proteins RIM1 and Munc13, respectively[359,361], which function in the presynaptic terminal as coordinators of SV fusion. Apart from proteasome-mediated removal of SV recycling machinery, Ub may be capable of affecting presynaptic release through multiple other ways. The RNF13 ligase adds a K29 polyubiquitin chain to snapin which fortifies its association with the SNARE protein SNAP25[360]. Snapin was previously shown to enhance SV fusion by binding to SNAP25 and potentiating its interaction with synaptotagmin[388–390]. This example beautifully emphasizes Ub skillfulness in rapidly converting dormant presynaptic proteins into active release machinery. E3s may even function in a synapse-type specific manner concomitantly regulating excitation/inhibition balance; for instance, in *C. elegans* the F-box protein MEC-15 maintains levels of presynaptic proteins at GABAergic terminals by a mechanism still not fully understood and, accordingly, its loss impairs inhibitory transmission[362].

Concluding remarks

Overall, mounting data demonstrate that Ub signals, in most of the cases culminating in proteasome degradation, function in axons right from the beginning of their differentiation to proper presynaptic transmission. In addition to the list of possible Ub and/or proteasome targets summarized on table 1.2 that have direct roles in axonal events, many other presynaptic proteins, including SV and active zone proteins, are known to be posttranslationally regulated in such fashion (table 1.3). Conceivably, it is predictable that Ub may influence axon-related events in countless other ways. Interestingly, ubiquitination machinery can be regulated by presynaptic proteins, as evidenced for the E3 ligase Siah whose activity is molded by Bassoon and Piccolo[391]. This finding tells us that protein ubiquitination in axons occurs in a controlled manner as opposed to a constitutive and reckless way; and that this control is executed by presynaptic proteins themselves, most probably as a way of guaranteeing that Ub is utilized wisely to meet axon's demands. Importantly, some neuronal diseases arise from deficiencies in the UPS system thus further reinforcing the need to fully elucidate Ub signaling in neurons[244]. In Parkinson's disease, Angelman syndrome, Gracile axonal dystrophy and ataxia, the genes involved codify proteins belonging to the ubiquitination machinery that are present in axons or whose deletion affect axonal events, namely the E3s Parkin[392,393] and UBE3A[394], and the deubiquitinases UCHL1[395] and USP14[258,259], respectively.

Table 1.3 - Additional axonal proteins regulated by ubiquitin.

E3		Target	Function	Ub chain	Outcome	Ref.
EDD		β-catenin	Presynapse assembly and release	K11/29 polyUb	Enhanced stability and activity	396
				K11 polyUb	Prot. deg.	283
Siah*	1	Synaptophysin	SV membrane protein/ Role in presynaptic release	polyUb	Prot. deg.	397
		Synphilin-1	SV associated protein	polyUb	Prot. deg.	398,399
		DCC	Netrin receptor	polyUb	Prot. deg.	371,400
	2	α-synuclein	SV clustering and exo/endocytosis	monoUb	Prot. deg.	399,401
Staring		Syntaxin	SNARE complex component SV fusion	polyUb	Prot. deg.	402
		Syntenin	Active zone scaffolding protein	polyUb		403
Parkin		Synaptotagmin	Calcium sensor/ SV fusion	polyUb		404
		CDCrel-1	SV membrane GTPase/ SV exocytosis	polyUb	Prot. deg.	405
		Eps15	Endocytic adaptor protein/ SV endocytosis	monoUb	Decreased interaction with EGFR; Repression of endocytosis	406
		$Ca_v2.2$	Presynaptic release	polyUb	Prot. deg.	407–409
		Liprin α	Active zone scaffolding protein		Prot. deg.	175
		CASK	Active zone scaffolding protein/ kinase	polyUb	Prot. deg.	410
		Bruchpilot (CAST/ERC homolog)	Active zone scaffolding protein	polyUb	Prot. deg.	383
Nedd4		FGFR1	Signaling		Endocytosis and sorting to lysosomes	307,308
Smurf1		axin	Component of the Wnt signaling	K29 polyUb	Decreased interaction with Wnt coreceptor; Repression of Wnt/β-catenin signaling	311
Bassoon; NSF, vesicle fusion ATPase; SNAP25; synapsin; SV2; VAMP; Vglut; APP; neurexin [#]						

*****, Siah activity was proposed to be regulated by Bassoon and Piccolo[391].

#, Presynaptic proteins identified in the rat brain ubiquitome by Peng and colleagues[243].

Abbreviations: APP, amyloid precursor protein; **CASK,** calcium/calmodulin-dependent serine kinase; **CAST/ERC**, CAZ-associated structural protein/ELKS-Rab6-interacting protein-CAST; **DCC**, deleted in colorectal cancer; **EDD**, E3 ubiquitin ligase identifi ed by differential display; **EGFR**, epidermal growth factor receptor; **Eps15**, endocytic adaptor epidermal growth factor receptor substrate 15; **FGFR1**, fibroblast growth factor receptor; **monoUb**, monoubiquitination; **Nedd4**, neuronal precursor cell developmentally downregulated 4; ***NSF,*** N-ethylmaleimide-sensitive *fusion* protein; **polyUb**, polyubiquitination; **Prot. deg.**, proteasomal degradation; **Siah**, seven in absentia homolog; **Smurf**, Smad ubiquitination regulatory factor; **SNAP25**, synaptosomal-associated protein 25; **SV2**, synaptic vesicle glycoprotein; **VAMP**, vesicle-associated membrane protein; **Vglut**, vesicular glutamate transporter.

Objectives

The main objective of this work was to uncover the role of the UPS in presynaptic differentiation. This structure is a highly specialized axonal compartment for the coordinated release of synaptic vesicles. Although reduced in size, it combines all the required presynaptic material perfectly assembled. Its main function is to rapidly react to a propagating action potential and to guarantee the flow of information from one neuron to another through the release of neurotransmitters. Remarkably, a functional terminal is formed in approximately one hour, therefore we hypothesized that intra-axonal events play an important role in this process.

The axon is extremely long and most of its terminals will be formed at considerable distances from the soma. A great deal of research has been focused on the events occurring at the site of a nascent nerve terminal, which bring about coordinated recruitment and clustering of presynaptic material. Evidence indicates that local turnover of proteins is likely to play a major role.

Studies in *C. elegans* and *Drosophila* have identified proteins whose local downregulation in a manner dependent on UPS machinery governs formation of presynaptic boutons[350,352]. Moreover, the proteasome itself can redistribute in dendrites[411]. However, local proteasome dynamics and requirement during presynaptic assembly in the vertebrate CNS remains to be studied. On chapter 3, we aimed to understand whether and how the proteasome redistributes along axons upon induction of presynaptic differentiation. To accomplish this goal we analyzed the effects of two presynaptogenic molecules, FGF22 and BDNF, on proteasome localization and activity. Given that proteasome activity is a requisite in axon outgrowth and guidance[370], we further explored the requirement of proteasome-mediated degradation on FGF22 and BDNF-induced presynaptic clustering.

Puzzlingly, we and others[384–386,412] have observed that proteasome inhibitors have a potentiating effect on both presynaptic function and formation. However, the role of UPS-mediated synaptic development as well as the molecules and signaling pathways activated are still elusive. On chapter 4, we aimed to investigate the mechanism underlying the presynaptogenic effect of proteasome inhibitors in isolated axons. Herein, we extensively characterized the pattern of presynaptic clustering in response to axonal proteasome inhibition. By using a live-imaging approach, we monitored local changes in proteasomal degradation in an axon undergoing synapse formation. Furthermore, the use of distinct UPS inhibitors and ubiquitin mutants allowed us to investigate the role of the pool of presynaptic ubiquitinated conjugates in the formation of functional presynaptic terminals.

As a follow up to the described enhancement of presynaptic release by proteasome inhibitors, we aimed to explore the role of ubiquitin. Dynamic protein ubiquitination has been proposed to regulate presynaptic release[384]. Because part of the ubiquitin signaling occurs in the form of polyubiquitin chains, on chapter 5 we analyzed the role of polyubiquitination on the rate of presynaptic release.

Our findings provide clear evidence that ubiquitination can control the formation of presynaptic boutons using distinct pathways, either by promoting proteasome-mediated protein degradation or by building a dynamic pool of polyubiquitinated presynaptic proteins.

Chapter 2

Experimental Procedures

Materials

Antibodies and reagents

Table 2.1 - List of reagents (including factors, inhibitors and antibodies) in use throughout this work, their concentration of use and respective commercial source.

Factors	Concentration	Source (catalog #) (company)
BDNF	100 ng/ml	Peprotech (#450-02) (Rocky Hill, USA)
FGF22	2 nM (pseudo-explants); 10 nM (microfluidic devices)	R&D Systems (#3867-FG-025) (Minneapolis, USA)
Inhibitors/ Reagents	**Concentration**	**Source (catalog #) (company)**
Advasep-7	1 mM	Biotium (#70029) (Hayward, USA)
Aliphatic amine latex beads, 2% w/v 4.5µm	2 drops to 500 ul medium	Life Technologies (#A37370) (Carlsbad, USA)
Anisomycin	10 µM	Calbiochem (#176880) (Darmstadt, Germany)
B27 supplement	2% v/v	GIBCO (#17504) (Carlsbad, USA)
clasto-lactacystin β-lactone	10 µM	Calbiochem (#426102) (Darmstadt, Germany)
6-cyano-7-nitroquinoxaline-2,3-dione (CNQX)	20 µM	TOCRIS biosciences (#1045) (Bristol, UK)
D-2-amino-5-phosphonovalerate (D-AP5)	50 µM	TOCRIS biosciences (#0106) (Bristol, UK)
Emetine	10 µM	Sigma Aldrich (#E2375) (Saint Louis, USA)
FM 5-95 dye	10 µM	Life Technologies (#T23360) (Carlsbad, USA)
IU1	75 µM	TOCRIS biosciences (#4088) (Bristol, UK)
Me4BodipyFL-Ahx3Leu3VS - Proteasome activity probe (PAP)	500 nM	BostonBiochem (#I-190) (Cambridge, USA)
MG132	1 µM	Calbiochem (#474790) (Darmstadt, Germany)
Mouse laminin I	2 µg/ml	Cultrex (#3400-010-01) (Helgerman Court, USA)
Poly-D-lysine (PDL) hydrobromide	0.1 mg/ml	Sigma Aldrich (#P7280) (Saint Louis, USA)
PR619	1 µM	Sigma Aldrich (#SML0430-1MG) (Saint Louis, USA)
Sylgard 184 Silicone elastomer kit	Two part, 10:1 mix	Dow Corning (Midland, USA)
Ziram	1 µM	Sigma Aldrich (#45708-250MG) (Saint Louis, USA)
Primary antibodies	**Dilution (application)**	**Source (catalog #) (company)**
Bassoon	1:400 (ICC); 1:1000 (WB)	Enzo Life Sciences (#ADI-VAM-PS003) (Ann Arbor, USA)
FGFR2	1:2000 (ICC)	Abcam (#ab52246) (Cambridge, UK)
GFP	1:2000 (ICC)	Abcam (#ab290) (Cambridge, UK)
GFP	1:1000 (WB)	Invitrogen (#A6455) (Carlsbad, USA)
K48 ubiquitin (Apu2)	1:500 (ICC); 1:1000 (WB)	Millipore (#05-1307) (Temecula, USA)
MAP2	1:5000 (ICC)	Chemicon (#AB5543) (Billerica, USA)
Rpt3	1:500 (ICC); 1:1000 (WB)	Enzo Life Sciences (#BML-PW8175) (Lausen, Switzerland)
SNAP25	1:1000 (ICC); 1:20000 (WB)	Sigma Aldrich (#55187) (Saint Louis, USA)
SV2a	1:1000 (ICC); 1:1000 (SV2)	Hybridoma bank (#10ea) (Iowa, USA)

Synapsin I	1:2000 (ICC)	Millipore (#AB1543P) (Temecula, USA)
Tau	1:1000 (ICC)	Abcam (#ab75714) (Cambridge, UK)
TrkB	1:200 (ICC)	Promega (#G1561) (Madison, USA)
Tubulin	1:300000 (WB)	Sigma Aldrich (#T7816) (Saint Louis, USA)
Tuj1	1:1000 (ICC)	Covance (# MMS-435P) (Princeton, USA)
Ubiquitin	1:200 (ICC); 1:1000 (WB)	Dako Denmark (#Z0458) (Glostrup, Denmark)
Vglut1	1:1500 (ICC)	Millipore (#AB5905) (Temecula, USA)
Vglut1	1:5000 (WB)	Synaptic systems (#135503) (Goettingen, Germany)
Secondary antibodies	**Dilution (application)**	**Source (catalog #) (company)**
Alexa 350-conjugated anti-mouse	1:1000 (ICC)	Life Technologies (#A11045) (Carlsbad, USA)
Alexa 350-conjugated anti-rabbit	1:1000 (ICC)	Life Technologies (#A21068) (Carlsbad, USA)
Alexa 488-conjugated anti-chicken	1:1000 (ICC)	Life Technologies (#A11039) (Carlsbad, USA)
Alexa 488-conjugated anti-mouse	1:1000 (ICC)	Life Technologies (#A11059) (Carlsbad, USA)
Alexa 488-conjugated anti-rabbit	1:1000 (ICC)	Life Technologies (#A11034) (Carlsbad, USA)
Alexa 568-conjugated anti-chicken	1:1000 (ICC)	Life Technologies (#A11041) (Carlsbad, USA)
Alexa 568-conjugated anti-mouse	1:1000 (ICC)	Life Technologies (#A11004) (Carlsbad, USA)
Alexa 568-conjugated anti-rabbit	1:1000 (ICC)	Life Technologies (#A11036) (Carlsbad, USA)
Alexa 647-conjugated anti-chicken	1:1000 (ICC)	Life Technologies (#A21449) (Carlsbad, USA)
Alexa 647-conjugated anti-guinea pig	1:1000 (ICC)	Life Technologies (#A21450) (Carlsbad, USA)
Alexa 647-conjugated anti-mouse	1:1000 (ICC)	Life Technologies (#A21235) (Carlsbad, USA)
Alexa 647-conjugated anti-rabbit	1:1000 (ICC)	Life Technologies (#A21245) (Carlsbad, USA)
Alkaline phosphatase-conjugated anti-mouse	1:10000 (WB)	Jackson ImmunoResearch (#115-055-003) (West Grove, USA)
Alkaline phosphatase-conjugated anti-rabbit	1:20000 (WB)	Jackson ImmunoResearch (#305-055-003) (West Grove, USA)
AMCA-conjugated anti-chicken	1:200 (ICC)	Jackson ImmunoResearch (#103-155-155) (West Grove, USA)

Abbreviations: ICC- Immunocytochemistry; **WB** - Western blot

Constructs

F(syn)WRBN-Vglut1mCherry, a vector for lentiviral expression of a fusion version of the Vglut1 to mCherry, was kindly offered by Prof. Etienne Herzog[413] (Interdisciplinary Institute for Neuroscience, Bordeaux, France). Vglut1mCherry coding sequence was amplified by PCR and cloned into pSinRep5 vector (Invitrogen) through ApaI and MluI sites by the In-Fusion HD Cloning Kit (Clontech, #639648, Mountain View, USA), so that a Sindbis viral expression version of this fusion protein was generated. The degradation reporter Ub^{G76V}-GFP[414] (addgene plasmid #11941) and the correspondent vector backbone pEGFP-N1 (Clontech, #6085-1), as well as GFP-Ub (addgene plasmid #11928) were kindly offered by Prof. Carlos Duarte (Center for Neuroscience and Cell Biology, University of Coimbra, Coimbra, Portugal). To generate a plasmid for Sindbis viral-mediated expression of the degradation reporter, Ub^{G76V}-GFP coding sequence was amplified by PCR and cloned into pSinRep5 vector (Invitrogen) through ApaI and MluI sites by the In-Fusion HD Cloning Kit (Clontech, #639648). The constructs for ubiquitination-induced fluorescence complementation (UiFC), pcDNA3-UiFC-C (UiFC-C) and pcDNA3-UiFC-N (UiFC-N), were kindly offered by Prof. Shengyun Fang[415] (Department of Biochemistry and Molecular Biology, University of Maryland, Baltimore, Maryland, USA). In order to generate a sindbis viral construct for the expression of ubiquitin (Ub), the coding

sequence of the wild-type form of Ub (wtUb) was amplified from GFP-Ub by PCR and cloned into pSinRep-IRES-eGFP vector[416] [kindly offered by Ulrich Hengst (Department of Pathology and Cell Biology, Columbia University, New York, USA)] through XbaI site by the In-Fusion HD Cloning Kit (Clontech, #639648). In the resulting plasmid, pSinRep-wtUb-IRES-eGFP, the expression of Ub is under control of the subgenomic promoter, whilst eGFP expression is controlled by a ribosome entry site (IRES). The empty vector pSinRep-IRES-eGFP was used as the control. Site-directed mutagenesis to the coding sequence of Ub inserted into the pSinRep-wtUb-IRES-eGFP plasmid was performed by QuickChange II XL Site-Directed Mutagenesis Kit (Agilent Technologies, #200521). Lysines in the positions 11, 29, 48 and 63 of Ub sequence were mutated to arginine to generate the Ub mutant forms UbK11R, UbK29R, UbK48R and UbK63R respectively.

Methods

Microfluidic devices for neuron culture

Microfluidic devices consist of a molded poly-dimethylsiloxane (PDMS) chamber assembled in a glass coverslip[417]. The molds for the PDMS devices used in this study were kindly fabricated and offered by Noo Li Jeon (School of Mechanical & Aerospace Engineering, Seoul National University, Seoul 151-472, Korea).

PDMS was prepared from the Sylgard 184 Silicone elastomer kit (Dow Corning) and poured onto the microfluidic molds and cured for 4-6 h at 60^{o}C. PDMS devices were peeled off from the molds, individually cleaned with 3M Scotch Brand 471 tape to lift off debris, rinsed once in filtered 75% ethanol for sterilization and air-dried in the culture hood. Glass coverslips (Marienfeld #0101060) were cleaned in nitric acid 65% for 24 h, washed 5 times (30 min each wash) with mQH_2O, rinsed twice in 100% ethanol, dried at 50^{o}C for approximately 20 min and sterilized under ultraviolet radiation for 15 min. For live imaging experiments, glass coverslips from Assistent (#01012229) were used, sonicated in 100% ethanol for 45 min, air-dried and rinsed in water twice. Both types of coverslips were coated overnight with PDL and the excess removed by 3 washes with sterile mQH_2O. Coverslips were completely air-dried before assembling the devices. The following steps were carried out under sterile conditions. Each PDMS device was assembled on a glass coverslip, reservoirs filled with plain neurobasal medium containing 2 µg/ml laminin and incubated for 2 h at 37^{o}C. Before plating cells, neurobasal medium with laminin was replaced by plating medium [minimum essential medium eagle (MEM) supplemented with 0.026 M $NaHCO_3$, 0.025 M glucose, 1 mM sodium pyruvate and 10% fetal bovine serum (FBS)].

Primary culture of hippocampal neurons

Primary cultures of rat hippocampal neurons were prepared from E18 Wistar rat embryos. After dissection, hippocampi were dissociated in 0.045% trypsin/ 0.01% v/v deoxyribonuclease in Hank´s balanced salt solution (HBSS) [5.36 mM KCl, 0.44 mM KH_2PO_4, 137 mM NaCl, 4.16 mM $NaHCO_3$, 0.34 mM $Na_2HPO_4.2H_2O$, 5 mM glucose, 1 mM sodium pyruvate, 10 mM N-(2-hydroxyethyl)piperazine-N'-(2-ethanesulfonic acid) (HEPES) and 0,001% phenol red] for 15 min at 37^{o}C. Hippocampi were then washed once in plating medium containing 10% FBS thus stopping trypsin activity, mechanically dissociated in fresh plating medium and cell density determined. Cells were plated in plating medium to PDL-coated surfaces as follows: in 6-well plates for biochemical purposes at a density of 9 x 10^3 cells/cm^2; to create pseudo-explants

for the isolation of axons 1 x 10^4 cells were plated inside a cylinder (6 mm diameter) placed at the middle of a coverslip-containing well of a 24-well plate; in 450 µm-microfluidic devices 7 x 10^4 cells were plated in the somal compartment; in synapse formation chambers 7 x 10^4 and 1 x 10^5 cells were plated in the presynaptic and postsynaptic compartment, respectively. Neurons were allowed to attach for 2-4 h and then plating medium was replaced for culture medium (neurobasal medium supplemented with 2% B27, 25 µM glutamate, 0.5 mM glutamine and 1:400 penicillin-streptomycin). In microfluidic devices, as a way of reducing glutamate excitotoxicity in growing axons, glutamate-free culture medium was added to the axonal compartment of 450 µm-microfluidic devices and to the synaptic compartment of synapse formation chambers. Cells were maintained in a humidified incubator with 5% CO_2/ 95% air at 37^{o}C. At days *in vitro* (DIV) 3/4, the mitotic inhibitor 5-fluorodeoxyuridine (5-FDU) (10 µM final concentration) was added to reduce contamination with glia cells. Cells were allowed to grow and, unless otherwise indicated, experiments were performed at DIV 7/8.

Synaptosome preparation

Purification of synaptosomes was performed as previously described[418]. Hippocampi from Wistar rats (P3, P7 and adult) were dissected and homogenized in a motor driven glass Teflon homogenizer (30 stokes, 900 rpm, at 4^{o}C) in HEPES-buffered sucrose buffer [0.32 M sucrose, 4 mM HEPES (pH 7.4)] supplemented with protease and phosphatase inhibitors [0.2 mM phenylmethylsulfonyl fluoride (PMSF), 1 µg/ml chymostatin/ leupeptin/ antipain/ pepstatin (CLAP), 0.1 mM sodium ortovanadate (Na_3VO_4) and 50 mM sodium fluoride (NaF)]. The homogenate was then centrifuged at 900 x g for 15 min at 4^{o}C, the supernatant collected and centrifuged at 18000 x g for 15 min at 4^{o}C, to yield the synaptosomal fraction. It was further washed by ressuspension in HEPES-buffered sucrose buffer and centrifugation at 18000 x g for 15 min at 4^{o}C. Quantification of protein was performed by the bicinchoninic acid (BCA) assay, and samples (40 µg) were denatured with denaturating buffer [62.5 mM tris-HCl (pH 6.8), 10% v/v glicerol, 2% v/v sodium dodecyl sulfate (SDS), 0.01% w/v bromophenol blue and 5% v/v β-mercaptoethanol (added fresh)], and boiled at 95^{o}C for 5 min before running the western blot (WB).

Generation of Sindbis and Lentivirus

For the generation of Sindbis virus, the pSinRep construct expressing the desired gene of interest and the helper plasmid DH26S were linearized with either XhoI, PacI or NotI and properly treated for the removal of RNAse contamination. Synthesis of RNA from linearized DNAs was performed by in vitro transcription using the mMESSAGE mMACHINE SP6 kit (Ambion, #1340). Baby hamster kidney 1 (BHK-1) cells were electroporated with 12 µg DH26S RNA and 12 µg of the desired pSinRep RNA, and production of virus was allowed to occur for 24-36 h. Supernatant was then collected and virus particles were purified by centrifugation at 60000 x g for 2 h 20 min at 15^{o}C. The viral pellet was then ressuspended in phosphate buffered saline (PBS) (137 mM NaCl, 2.7 mM KCl, 10 mM Na_2HPO_4, 1.8 mM KH_2PO_4, pH 7.4) with 0.1% bovine serum albumin (BSA) and stored at -80^{0}C. The virus titer was determined in BHK-1 cells and the volume of virus for infection was adjusted so that more than 85% of neurons were transduced. For expression of Ub and its mutant forms in microfluidic devices, expression was allowed to occur for 18-20 h before fixation. For live-imaging experiments, cells were incubated with virus for 6-8 h before imaging.

For the generation of Lentivirus, HEK293T cells were transfected using calcium phosphate transfection with the lentiviral expression vector [F(syn)WRBN-Vglut1mCherry] and three lentiviral packaging vectors: pLP1, pLP2 and pLP-VSVG, for the expression of gag/pol genes, rev gene and vesicular stomatitis virus G (VSVG) envelope glycoprotein gene, respectively. The supernatant containing virus particles was collected 48-60h after transfection and concentrated by centrifugation at 60000 x g for 2 h at 22^{o}C. The viral pellet was then ressuspended in PBS with 0.1% BSA and stored at -80^{0}C. After infection, expression of protein occurred for 48-60 h.

Neuron transfection

The degradation reporter Ub^{G76V}-GFP (addgene plasmid #11941), the correspondent vector backbone pEGFP-N1 (Clontech, #6085-1) and the constructs for UiFC expression (UiFC-C and UiFC-N) were recombinantly expressed in primary neurons using calcium phosphate transfection. The DNA (2 µg of each DNA per well of a 24-well plate or 1.5 µg per each DNA per microfluidic device) was diluted in Tris-EDTA transfection buffer (10 mM Tris-HCl and 1 mM EDTA, pH 7.3), then $CaCl_2$ solution (2.5 M in 10 mM HEPES) was added dropwise to yield a final concentration of 250 mM. This solution was then added dropwise to an equivalent volume of HEPES-buffered transfection solution (274 mM NaCl, 10 mM KCl, 1.4 mM Na_2HPO_4, 11 mM dextrose, 42 mM HEPES, pH 7), and phosphate calcium DNA precipitates allowed to form for 30min protected from light (vortex every 5 min). Transfection solution was then added to cells in a medium containing 2 mM of kynurenic acid and incubated for 1 h. At the end of transfection, DNA precipitates were destroyed by incubating cells in a slightly HCl-acidified neurobasal medium with 2 mM kynurenic acid for 15 min, then washed once and returned to the incubator in conditioned culture medium. Expression was allowed to occur for 48-72 h. For live-imaging experiments, UiFC plasmids were expressed for 16-18 h before imaging.

PDL-coated beads

Aliphatic amine latex beads were incubated with PDL for 30 min at 37^{o}C, centrifuged to remove supernatant, washed twice in sterile mQH_2O and diluted in culture medium. Bead suspension was added to the axonal compartment of microfluidic devices and incubated at 37^{o}C for the indicated period of time. For live-imaging experiments, beads were diluted in HEPES-buffered solution (HBS) (119 mM NaCl, 5 mM KCl, 2 mM $CaCl_2$, 2 mM $MgCl_2$, 30 mM glucose, 10 mM HEPES, pH 7.4).

Drug treatment

Treatment of cells with UPS inhibitors or protein synthesis inhibitors was performed in conditioned medium. The concentrations used are listed on table 2.1. For proteasome inhibitors a pre-incubation of 30 min and 15 min was performed with clasto-lactacystin β-lactone (β-lactone) and MG132, respectively. When cells were co-treated with proteasome inhibitors and protein synthesis inhibitors, PR619 or ziram, both inhibitors were added simultaneously. All inhibitors were diluted in conditioned medium from a 1000x stock in DMSO and added to cells, except for the protein synthesis inhibitors, emetine and anisomycin, that were diluted in mQH_2O. Equal amounts of DMSO or water were added to the control conditions.

FGF22 and BDNF were also diluted in conditioned medium from a stock in PBS with 0.1% BSA and added to cells. Equal amounts of BSA were added to control conditions.

Biochemistry

To perform WB, cells were first washed twice in cold PBS. Protein extracts were then prepared by scrapping cells in RIPA lysis buffer [150 mM NaCl, 50 mM Tris-HCl (pH 7.4), 5 mM EGTA, 1% Triton, 0.5% deoxycholate and 0.1% SDS, pH 7.5, freshly supplemented with 50 mM NaF, 1.5 mM Na3VO4, 0.1mM PMSF and 1 µg/ml CLAP]. Lysates were sonicated, centrifuged at 16100 x g for 10 min at 4°C and the supernatant collected. Quantification of protein was performed by the BCA assay, and samples (40 µg in 40 µl) were denatured with denaturating buffer and boiled at 95°C for 5 min. Protein extracts were electrophoresed in a tris-glycine-SDS (TGS) buffer (25 mM Tris, 192 mM glycine, 0.1% w/v SDS, pH 8.3) in 7.5%, 12%, 15% or 4-15% gradient polyacrylamide gel 1.5 mm thick. Electrotransfer onto a polyvinylidene difluoride (PVDF) membrane was performed either overnight at 40 V at 4°C or by using an equivalent protocol for rapid transfer (250 mAmp for 4 h or 250 mAmp for 6 h at 4°C depending on the weight of the protein of interest). Membranes were washed once with tris-buffered saline (TBS) (20mM Tris, 137mM NaCl) with 0.1% v/v Tween 20 (TBS-T), and then blocked for 1 h at room temperature in TBS-T with 5% non-fat dry milk or 3% BSA. Membranes were again washed for three times with TBS-T and incubated with the primary antibody diluted in TBS-T containing 5% or 0.5% w/v non-fat dry milk or 3% BSA. Incubation was performed either overnight at 4°C or at room temperature for 1h. After three washes, membranes were incubated for 1h with alkaline phosphatase conjugated secondary antibodies (anti-mouse or anti-rabbit, depending on the primary antibody host species) at room temperature, washed again for three times and resolved with enhanced chemifluorescence (ECF) substrate for a maximum of 5 min. Membranes were scanned with the Storm 860 Gel and Blot Imaging system (Amersham Biosciences) and quantification was performed using ImageQuant software under linear exposure conditions. Whenever necessary, membranes were stripped with NaOH 0.2 M for 20 min and reprobed. Dilutions of primary and secondary antibodies used are listed in table 2.1.

Live-cell imaging

Live imaging experiments were all performed using a spinning disk confocal imaging system (CSU-X1-M1N-E, Yokogawa) configured for an Olympus IX81 motorized inverted microscope driven by Andor iQ 3.1 software. Images were collected with a 60x water objective [1.2 numerical aperture (NA)] and an Andor IXON-X3 EMCCD camera.

For the time-lapse imaging experiments, culture medium was replaced for the imaging medium HBS at least 30 min before. The device was mounted on the microscope stage and positions of interest (in which dually infected, Ub^{G76V}-GFP^{+} and $Vglut1mCherry^{+}$, or UiFC-expressing axons have crossed the microgrooves into the axonal compartment) were selected. To increase experimental throughput, data were collected sequentially from several defined positions (a maximum of 15 per device). Focal drift during the experiment was corrected automatically using the autofocus feature of the Olympus system. Lasers intensities were kept as low as possible to avoid photobleaching and laser-induced toxicity. We used 2 x 2 binning to improve the signal to noise ratio, thus allowing us to reduce the laser power and acquisition time. In the experiments involving beads, 3 frames were captured to the selected positions on the axonal compartment before the

addition of beads, then beads were added to both compartments (the same volume was added to both sides to prevent focus drift due to unbalanced preparation). Time-lapse was resumed 5 min after addition of beads. The frames were acquired as z-stacks (35-40 slides, 8-10 µm range) every 5 or 10 min.

For the FM 5-95 dye experiments, culture medium was replaced with pre-warmed HBS and cells were allowed to recover for 30 min at 37°C. Each cycle of FM dye loading/ unloading comprised the following steps: FM 5-95 dye loading solution containing high KCl concentration (HBS with 90 mM KCl supplemented with 10 µM FM 5-95 dye, 20 µM CNQX and 50 µM D-AP5) to promote depolarization was added to microfluidic devices for 1 min and washed once with 10 µM FM 5-95 dye in HBS for 1 min. Additional three washes with 1 mM Advasep-7 in HBS, 1 min each, were performed for optimal removal of FM dye excess. This medium was then replaced by HBS containing 20 µM CNQX and 50 µM D-AP5 and the device was placed on the microscope stage. CNQX and D-AP5, which are AMPA/kainate and NMDA receptors antagonists respectively, were added to the medium to block recurrent excitation. Positive and negative electrodes were placed on each well of either the somal or axonal compartment and the unloading of the FM dye was induced by electrical stimulation, which was performed by a two-channel stimulus generator (multichannel systems, #STG4002) in current mode with an asymmetric waveform (-480 µA for 1 ms and +1600 µA for 300 µs) at 20 Hz for 1200 pulses for 1 min. At least 4 frames were acquired before stimulation. The frames were acquired as z-stacks (35-40 slides, 8-10 µm range) every 15 s for 5 min in a 2 x 2 binning mode.

For the experiments in which we were interested in monitoring the appearance of new FM puncta on beads (figure 4.2A), beads were first added to the axonal compartment of microfluidic devices and incubated for 3 h. Then, a first cycle of FM 5-95 dye was performed, followed by complete destaining with high KCl HBS solution for 1 min and two washes with HBS containing 20 µM CNQX and 50 µM D-AP5. An image after FM dye destaining was acquired for later subtraction from the initial image of the second FM dye cycle. Cultures were then treated with proteasome inhibitors, PR619 or DMSO for 1 h. A second cycle of FM dye with live-monitored unloading at exactly the same position was then performed, to look for the formation of new functional FM puncta. The position of the beads and the microgrooves were instrumental for localizing the imaging position between the first and second FM dye cycles. All experiments were done at room temperature (~20°C).

Immunocytochemistry

Cells were fixed in pre-warmed 4% paraformaldehyde (in PBS with 4% sucrose) for 10 min at room temperature. For cultures in microfluidic devices, a pre-fixation of 5 min in 1% paraformaldehyde was performed to prevent damaging the population of isolated axons. Cultures were washed 3 times in PBS, then permeabilized in PBS with 0.25% triton X-100 for 5 min at room temperature and washed once in PBS before blocking for 30 min in PBS with 3% BSA. Preparations were incubated with the mix of primary antibodies in 3% BSA either overnight at 4°C or for 2 h at 37°C, washed three times in PBS and incubated with the mix of secondary antibodies for 1 h at room temperature in 3% BSA. Cultures were again washed, this time twice in PBS with 0.1% Triton X-100 and once in PBS, the coverslip was rinsed in mQH2O and mounted in prolong mounting media with or without DAPI. For microfluidic chambers, the PDMS device was disassembled from the coverslip only before mounting on the microscope glass. Dilutions of primary and secondary antibodies used are listed in table 1.

Microscopy of antibody-labeled cultures

Fixed preparations were imaged using a Zeiss Observer Z.1 microscope equipped with a Plan-NeoFluar 63x oil objective (1.4 NA), an AxioCam HRm camera and Zen Blue 2011 software. In microfluidic devices, unless otherwise indicated, images were taken to the axonal compartment. In pseudo-explants, images were taken to regions surrounding the central bulk of neurons, where growing axons could be found isolated. For the proteasome activity probe, due to its weak signal along axons, z-stacks (7 slices with a 2 µm range) were captured, deconvoluted using Hyugens software and maximum z-projected in ImageJ software.

XY reconstructions of microfluidic devices (with both somal and axonal compartments) were performed either in a Zeiss LSM 510 Meta confocal microscope with an ECPlanNeofluar 40× objective (1.3 NA) and SM 510 software or a spinning disk confocal imaging system (CSU-X1-M1N-E, Yokogawa) configured for an Olympus IX81 microscope with a 60x water objective (1.2 NA) and Andor iQ 3.1 software. Post-hoc immunocytochemistry following live experiments was performed using the spinning disk system above mentioned. In these preparations, the device was not disassembled after immunocytochemistry and retrospective imaging was performed in PBS using a 60x water objective. This allowed us to easily locate the multiple positions where live data was collected by using the microgrooves as coordinates. Briefly, microgrooves were numbered according to the orientation of the device on the microscope stage, and at the end of acquisition, to each position the microgroove nearer to its center was marked down. The position was then corrected manually by comparing the DIC image acquired at the end of the live experiment with that of the fixed preparation. Moreover, the plug-in 'Align images by line ROI' in ImageJ was further used to guarantee perfect alignment.

Quantitative imaging analysis

Quantification of fluorescence images was performed using ImageJ software. For fixed cells, samples within an experiment were simultaneously stained and imaged with identical settings (exposure time and fluorescence light intensity kept constant throughout acquisition). Images to random fields of view (FOVs) to either isolated axons or cell bodies were taken. Selection of regions of interest to acquire fluorescent images was carried out either on the axonal or somal marker to avoid bias acquisition. All images were converted to 8-bit for quantification purposes. For quantifying differences in signal intensity in different neuronal structures, raw intensity values of the protein of interest (POI) within a region of interest (ROI) were divided by area of the selected marker.

To quantify the number of presynaptic puncta along axons, the axonal marker image was used to select populations of axons to quantify. Axonal length was determined by performing analysis (ImageJ plugin “Analyze skeleton”) of a “skeletonized” version of the axonal marker. The sum of the length of all the axonal branches identified in an image was used as the axonal length. Correspondent images of synaptic markers (also proteasome markers) were thresholded (threshold values conserved in individual experiments) and particle analyzes was performed to calculate number and area of puncta. To quantify the number of presynaptic clusters (Bassoon-Vglut1 clusters), the presence or absence of Vglut1 puncta within Bassoon puncta ROIs was determined, and the total number of Bassoon ROIs containing Vglut1 puncta divided by the axonal length. Analysis was limited to Bassoon puncta bigger than the smaller quantifiable object (0.05 μm^2) in accordance to our imaging settings.

For quantification of live experiments, confocal slices were sum projected in ImageJ, alignment of frames within each movie performed by 'TurboReg' or 'StackReg' plugins and converted to 8-bit. In experiments involving accumulation of synaptic material on beads, analysis was performed similarly to a study by Colman and colleagues[192]. The brightfield image was used to locate beads in contact with axons, ROIs for individual beads and adjacent sites along the axon were created (on-bead and off-bead, respectively). Change in signal was quantified by measuring the fluorescence intensity at each bead and correspondent off-bead site in each individual frame of the time-lapse video. Individual values were then normalized to the fluorescence intensity in that site at the frame preceding addition of beads (t0, 0 min) both for on-bead and off-bead sites.

For the experiment in which formation of presynaptic clusters on dendrites was monitored, digital movies of the time-lapse sequence for each position were prepared and carefully analyzed to detect formation of stable Vglut1mCherry clusters in sites not detected at prior time points ("new") or clusters stable at approximately the same location throughout the entire time-lapse ("old"). After identification of "new" and "old" puncta, their locations were overlaid on the corresponding post-hoc MAP2 immunostained images (see section on microscopy of antibody-labeled culture for further details on acquisition of images after retrospective labeling). Alignment of Vglut1mCherry and Ub^{G76V}-GFP videos with MAP2 retrospective ones was done according to the brightfield images of the same region taken at the end of the time-lapse and the one after immunostaining, by the ImageJ plug-in 'Align images by line ROI'. The alignment correction used for DIC images was applied to Vglut1mCherry and Ub^{G76V}-GFP, and "new" and "old" Vglut1mCherry clusters formed onto dendrites were considered. ROIs encompassing the whole Vglut1mCherry cluster were created at the site of clustering (on-site) and equal sized ROIs at adjacent axonal sites (off-site). Change in signal was quantified by measuring the fluorescence intensity at each ROI in each individual frame of both Vglut1mCherry and Ub^{G76V}-GFP time-lapse videos. For Vglut1mCherry, individual values were normalized to the fluorescence intensity in that site at t0. For "new" and "old" puncta, t0 is considered to be the frame before clustering is initiated or the first frame of the time-lapse, respectively. For "new" puncta, we considered beginning of clustering as the frame at which the stable puncta first appeared, recognized as a high increase in fluorescent signal (at least a 30% increase in signal intensity in relation to the previous frame). For Ub^{G76V}-GFP, the ratio of its intensities between on and off site was calculated.

For the FM dye experiments, the brightfield image was used to create ROIs encompassing beads or dendrites that contact with axons. Then, the number of FM puncta on each bead or along each dendritic segment was quantified by performing particle analysis in ImageJ. To evaluate the unloading capacity of FM puncta, quantification was adapted from previous work[419]. Each puncta intensity is measured throughout the registered sequence of images (frames every 15 s for 5 min), normalized to the frame before stimulation and corrected for the baseline slope (calculated from the change in intensity in the 3 frames preceding stimulation). Puncta that unloaded more than 5% of their FM dye content after 1min of stimulation were considered as functional. For the experiment with a double FM dye cycle, the net gain in functional and total FM puncta was calculated by subtracting the number of puncta after and before treatment. The theoretical time constant, τ, was estimated by curve-fitting the data corresponding to the stimulation time-points for each individual FM puncta to a one-phase exponential decay function (plateau considered equal to 0) in Graph Pad Prism 5 software. Puncta with time constants higher than 360 s (longer period than the experimental run time) were considered non-releasing puncta and not included in the analysis.

Kymograph analysis was performed in ICY software. Kymographs were extracted from axonal segments from a 1h time-lapse (frames every 1min). The kymograph tracking tool was used to trace the path

of UiFC puncta on kymographs and for each puncta the net displacement and mean speed were quantified. Puncta with mean speed values greater than 0.05µm/min and net displacements greater than twice their width were considered as mobile. Per each axonal segment, the number of mobile and stable puncta per length was calculated.

All images were processed and prepared for presentation using Photoshop (Adobe).

Statistical analysis

Results are presented as averaged values ± s.e.m. Graphs and statistical analysis were performed in Graph Pad Prism 5 software. Statistical significance was assessed by non-parametric tests. Mann-Whitney test or Wilcoxon paired t-test were performed for comparisons of changes between two groups. For comparisons between multiple groups we used Kruskal-Wallis test followed by the Dunn's multiple comparison test. For the live imaging data, we performed 2-way ANOVA with time as the repeated measure, to assess changes between two groups throughout time.

Chapter 3

Proteasome Dynamics and Requirement in FGF22 and BDNF-induced Presynaptic Assembly

Maria Joana Pinto, Ramiro Almeida

An on-going study

Summary

The proteasome is responsible for the controlled proteolysis of most soluble and short-lived proteins within the cell. It is thus plausible that cells require a dynamic proteasome so that their specific needs (spatially and temporally speaking) are fulfilled. A growing body of evidence supports the idea that the proteasome is a crucial player for the formation of the presynaptic site. To further explore this idea, axonal proteasome distribution, activity and requirement were studied at the context of presynaptic assembly induced by two soluble presynaptogenic factors, FGF22 and BDNF. We concluded that the endogenous proteasome is transiently redistributed along axons and its activity upregulated during FGF22 and BDNF-induced clustering of synaptic vesicles. Distinct hot-spots of proteasome activity populate an axon undergoing presynaptic assembly. Moreover, the effect of FGF22 and BDNF is dependent on the degradation of proteins by the proteasome. Overall, this study suggests that presynaptic organizing molecules operate in parallel with proteasome distribution and require its activity.

Introduction

Neurons are highly complex and polarized cells with a remarkable network of functionally active processes that extend outwards the cell body. Within the brain, each neuron's axon establishes thousands of synaptic contacts with either neighboring or fairly distantly located neurons. The cascade of events leading to the formation of a functional presynaptic terminal, in which a pool of SVs is clustered on specialized electron-dense portions of the plasma membrane known as the active zone, is designated presynaptic differentiation. This event occurs early in development, roughly during the first three postnatal weeks[167,420], and it comprises recruitment and coordinated local clustering of presynaptic material that can be found along the axon in the form of cell body-derived mobile units[68,421]. As a way of preventing ectopic formation of presynaptic boutons thus conferring specificity to this phenomenon, axons rely on cues derived from their postsynaptic partner that by activating axonal receptors will act as presynaptic organizers[70–72]. Several classes of proteins have already been shown to play a role in this process, such as secreted soluble factors, including Wnts, FGFs, neurotrophins, thrombospondins, netrins, signal regulatory proteins (SIRPs); and also cell adhesion molecules like neuroligins, SynCAMs, LRRTMs or the NGL family of adhesion proteins[70–72]. These factors might orchestrate together the formation of presynaptic terminals, through compensatory, cumulative or even opposite mechanisms, or act independently in different synapse types, brain regions or be involved in different steps of the presynaptic differentiation sequence of events.

For instance, BDNF can be secreted in a regulated or constitutive manner from either sides of the synapse[422] and also from astrocytes[423] or even microglia[156]. It has long been shown to increase the density of functional presynaptic clusters[152,201,424] by activation of TrkB receptors[75,155]. More recently, the striking potential of FGF22 as an excitatory presynaptic organizer was discovered. So far, it has already been reported to induce formation of nerve terminals on motoneurons[425], cerebellum[99], hippocampus[103] and retina[145]. In the cerebellum, for instance, it is secreted from the postsynaptic cell, the cerebellar granule cells, at the moment of axonal innervation and acts on presynaptically expressed receptors, FGFR2b, located on mossy fibers of pontine and vestibular neurons[99]. Notably, this trans-synaptic FGF22 signaling seems to be shared among brain regions[103,145,426].

Despite the huge number of proteins implicated in presynaptic differentiation, this is a highly rapid event that occurs in a time-scale of minutes to few hours[12,13]. Furthermore, axons are extremely long and presynaptic terminals are to be formed in remote sites. On top of this, each presynaptic site is an individual micro-domain, meaning that changes in one do not necessarily affect adjacent axonal segments. Under these circumstances, it is reasonable to believe that axons rely on intra-axonal mechanisms to support and sustain their prompt response to cues, which will then lead to a site-specific clustering of presynaptic components. In line with this idea, local control of protein turnover is rapidly gaining acceptance as an axonal event involved in synapse formation, and in fact, local downregulation of synaptically localized proteins has been shown to regulate differentiation of presynaptic sites. In the *Drosophila* NMJ, the mitotic ubiquitin ligase APC/C regulates presynaptic bouton number by modulating the levels of the presynaptic scaffold liprin-α[348]. The PHR ubiquitin ligases (comprising the human PAM, mouse Phr1, *Drosophila* Highwire and *C. elegans* RPM-1) are localized in the periactive zone[427], which is the region surrounding the active zone. Control of presynaptic development by these ubiquitin ligases is mediated by fine-tuning the levels of the presynaptic kinase DLK-1 (or its *Drosophila* homolog Wallenda)[337,351,352]. Moreover, RPM-1 and the F-box protein FSN-1, which mediates substrate recognition[428], are within an SCF-like ubiquitin ligase complex that controls the extent of presynaptic development by probably targeting ALK[350]. Interestingly, the activity of PHRs might either restrict[352,374] or promote presynaptic clustering[350,351,429,430], thus revealing opposite modes of

regulation of presynaptic terminal organization by E3 ligases between different organisms. It remains to be proven whether local downregulation of these presynaptic targets occurs in a manner dependent on ubiquitination and proteasome degradation. Actually, the proteasome, a multi-subunit complex by which controlled proteolysis occurs in cells, is highly active locally in presynaptic terminals[385,431] and has been shown to play crucial roles in neuronal development, function and plasticity[268–270].

An important aspect is how proteasome-mediated degradation is regulated so that proteins will be degraded according to cellular needs, in opposition to a non-controlled constitutive proteolysis. Indeed, neurons have developed ways of guaranteeing spatial and temporal regulation of proteasome degradation[432]. For instance, in spines, the RNA-induced silencing complex (RISC) protein MOV10 is degraded in an activity-dependent manner upon activation of NMDA receptors[433], thus relieving repression of translation in a precise temporal fashion. Moreover, formation of ectopic and aberrant excitatory postsynaptic terminals is in part prevented by ephexin5, which is degraded by the proteasome only after synaptic contact is initiated and trans-synaptic interactions are established[434]. In the developing axon, for instance, proteasome degradation of monoaclyglycerol lipase (MGL) is spatially confined to the growth cone thus creating a micro-domain sensitive to signaling for growth cone turning[435]. Differential proteolysis of MGL along the axon will later be lost so that the growth cone halts and synaptogenesis is initiated[435]. Alternatively, dynamic changes in the subcellular localization of the proteasome may represent a regulatory mechanism underlying controlled intracellular degradation of proteins. For example, during mitosis proteasomes redistribute in the cell and get transiently enriched at the microtubule organizing center[436,437]; lens differentiation is accompanied by a redistribution from the cytoplasm to the nucleus[438] and following DNA damage proteasome is relocated to the nucleus[439]. At a neuronal level, synaptic activity induces entry and (long-term) sequestration of proteasomes in dendritic spines[411] in a manner dependent on calcium/calmodulin-dependent protein kinase II α (CamKIIα) autophosphorylation[440], thus locally modeling protein turnover.

Although we can easily surmise that regulated UPS activity influence differentiation of presynaptic terminals, the potential role of presynaptogenic molecules on modulating proteasome activity or its redistribution throughout presynaptic differentiation is entirely unknown. In the present work, we studied FGF22 and BDNF-induced presynaptogenesis to evaluate axonal changes in proteasome redistribution, activity and requirement. We observed that the endogenous proteasome is redistributed along axons in a way temporally correlated with SV clustering. Both BDNF and FGF22 enhance proteasome degradation and new hot-spots of proteasome activity along the axon can be found. Moreover, activation of proteasome degradation triggers SV clustering, probably through the same mechanism as FGF22 and BDNF. Lastly, the capacity of FGF22 or BDNF to generate SV clusters is dependent on proteasome activity. Altogether, these results predict a role for proteasome activity and redistribution during the assembly of SV clusters.

Results

Proteasome redistribution during FGF22 and BDNF-induced presynaptic differentiation

Taking into consideration the emerging role of the proteasome in presynaptic differentiation[432,441], and the fact that its availability in neuronal compartments can be altered in response to activity[411], we hypothesize that formation of presynaptic sites might occur alongside redistribution of the proteasome in axons. To evaluate whether presynaptic clustering alters proteasome localization in axons, we stained hippocampal primary neurons with an antibody specific for the Rpt3/S6b subunit of the proteasome 19S regulatory complex, previously used to monitor changes in the location of the proteasome in dendrites[411]. In order to easily find isolated axons in culture to perform imaging, neurons were plated in the form of a pseudo-explant. To accomplish so, at the moment of plating, neurons were placed inside a cylinder, which was only later removed after cells have adhered. Randomly growing axons extended outwards the central bulk of cells and at DIV 7 (time at which all the experiments within this study were performed) a considerable population of axons could be found at the periphery of the pseudo-explant. Rpt3 staining revealed that the 19S proteasome was present in axons and was evenly and diffusely distributed in the axon (figure 3.1A). We further observed that it accumulated in discrete puncta homogeneously scattered in the axonal shaft (figure 3.1A). These Rpt3 puncta may represent sites along the axon at which the proteasome is preferentially accumulated or may correspond to mobile units of proteasome transport. Indeed, it was very recently described the movement of assembled and functional 26S proteasome complexes coordinated with the movement of membranous organelles, like mitochondria and lysosomes, by fast axonal transport[442].

To induce presynaptic differentiation we stimulated cultures with FGF22, a postsynaptic secreted factor that acts as an excitatory presynaptic organizer in the hippocampus[103]. FGF22 is a high affinity ligand for FGFR2b[443], it can also bind to FGFR1b however with a much lesser affinity[443]. In terms of presynaptic differentiation, the effect of FGF22 is most likely mediated by activation of FGFR2b[99]. In accordance, we confirmed the presence of FGFR2 on axons of hippocampal neurons at DIV 7 (figure S3.1A, B, left panels). The receptor was present throughout the axon and was highly enriched in the growth cones. Cultures were stimulated for different periods with 2 nM FGF22, concentration already proven to elicit near-maximal effects on SV clustering[99]. Staining was performed for two SV markers, SV2 and Vglut1 (the latter only stains excitatory presynaptic sites), along with the proteasome subunit Rpt3. The effect of FGF22 on presynaptic clustering was assessed by measuring the number of SV clusters along axons, a hallmark of presynaptic differentiation. FGF22 induced a robust and rapid increase in the number of SV2 and Vglut1 puncta, with maximal effects after 1h, which were maintained at approximately the same level until 24h of stimulation (figure 3.1B, C). On the contrary, the average size of SV puncta did not differ greatly; we only detected a small increase in Vglut1 puncta area following a 14h-stimulation that did not persist in longer FGF22 applications (figure 3.1D). Interestingly, the distribution pattern of the endogenous proteasome, Rpt3 staining, was transiently altered at the moment of FGF22 maximum presynaptogenic effect (figure 3.1B, C). A clear increase in the number of Rpt3 puncta along the axon was observed at 1h followed by a decrease to basal levels in prolonged stimulations (figure 3.1B, C). This transient accumulation of the 19S proteasome that is coincident with FGF22-induced SV clustering (figure 3.1C), led us to hypothesize that the proteasome was being dynamically recruited to nascent presynaptic clusters in order to locally modulate protein composition and assist in presynaptic assembly. To address this biological question, we quantified the fraction of SV puncta containing Rpt3 puncta and also the intensity of Rpt3 puncta within SV clusters or along the axonal shaft (figure 3.1F and G, respectively). Unfortunately, the fraction of presynaptic clusters co-localizing with Rpt3 puncta was kept relatively constant throughout the time-course, thus indicating that

Rpt3 puncta did not preferentially appear on sites of nascent SV clusters in response to FGF22 (figure 3.1E,F). On the other hand, although not significantly different, a higher intensity of Rpt3 puncta within SV clusters was observed at 1h, with no changes in the amount of Rpt3 intensity along the axon, thus suggesting that a higher amount of proteasome might be found at presynapses (figure 3.1E, G). Together, these data suggest that there was not an increased proportion of presynaptic clusters containing proteasome, however its availability might be increased in the population of SV clusters in which it accumulates. We should further emphasize that the fraction of SV clusters colocalizing with Rpt3 puncta was fairly low (ranging from 6.8% to 8.3% for SV2 puncta and from 8.3% to 10.5% for Vglut1 puncta) (figure 3.1F), meaning that in the great majority of sites of SV clustering the proteasome did not accumulate in the form of discrete puncta. Based on previous findings[12,46,48,411], it is entirely likely that proteasome redistribution and SV clustering are highly dynamic events and so difficult to conceive in fixed axons.

(image on next page)

Fig. 3.1 - FGF22 induces clustering of SVs and redistributes endogenous proteasome along axons. (**A**) Rpt3 proteasome subunit distribution in axons. Dissociated rat embryonic hippocampal neurons were plated inside cylinders as a way of obtaining pseudo-explants for the isolation of axons. After 7 days, cultures were stained for the Rpt3/S6b subunit of the proteasome 19S regulatory complex (green) and for tau (blue) as the axonal marker. Proteasomes were distributed evenly throughout the axonal shaft (left) and accumulated occasionally in distinct Rpt3 puncta (right). The scale bar is 5 µm. (**B**) Time-course of SV and Rpt3 puncta number upon FGF22 stimulation. Cultures were treated with 2 nM FGF22 for the indicated periods of time and clustering of presynaptic material was assessed by immunostaining for two SV markers, SV2 (white) and Vglut1 (red). Co-staining for the 19S proteasome subunit Rpt3 (green) was performed to analyze changes in axonal proteasome distribution. FGF22 induced clustering of SVs and transiently altered the distribution pattern of endogenous proteasome in a time point at which SV clustering reached its maximum level (1h stimulation). The scale bar is 5 µm. (**C**) Quantitative summary data of number of SV2, Vglut1 and Rpt3 puncta per axonal length upon treatment with FGF22 for the indicated period of time. Results are expressed as % of control cells. (**D**) Averaged raw values of SV2, Vglut1 and Rpt3 individual puncta area (left, middle and right graphs, respectively). (**E**) Colocalization of SV and Rpt3 puncta in response to FGF22. Representative merged images of SV puncta [SV2 (red) and Vglut1 (red) in left and right images, respectively] and Rpt3 (green) puncta along axons upon bath application of FGF22 for the indicated period of time. Transient Rpt3 puncta did not preferentially colocalize with nascent SV puncta. The scale bar is 5 µm. (**F**) Quantitative data presented as the fraction of SV puncta containing Rpt3 puncta. (**G**) Quantitative values for the intensity of Rpt3 puncta within SV puncta or present in the total axon (normalized for area of SV marker or tau area, respectively). (**C**, **D**, **F**, **G**) n represents the total number of analyzed microscope FOVs from 6 independent experiments. Statistical significance was assessed by the Kruskal-Wallis test followed by the Dunn´s multiple comparison test (***p<0.001, **p<0.01 and *p<0.05 when compared to 0min time-point). Error bars indicate s.e.m.

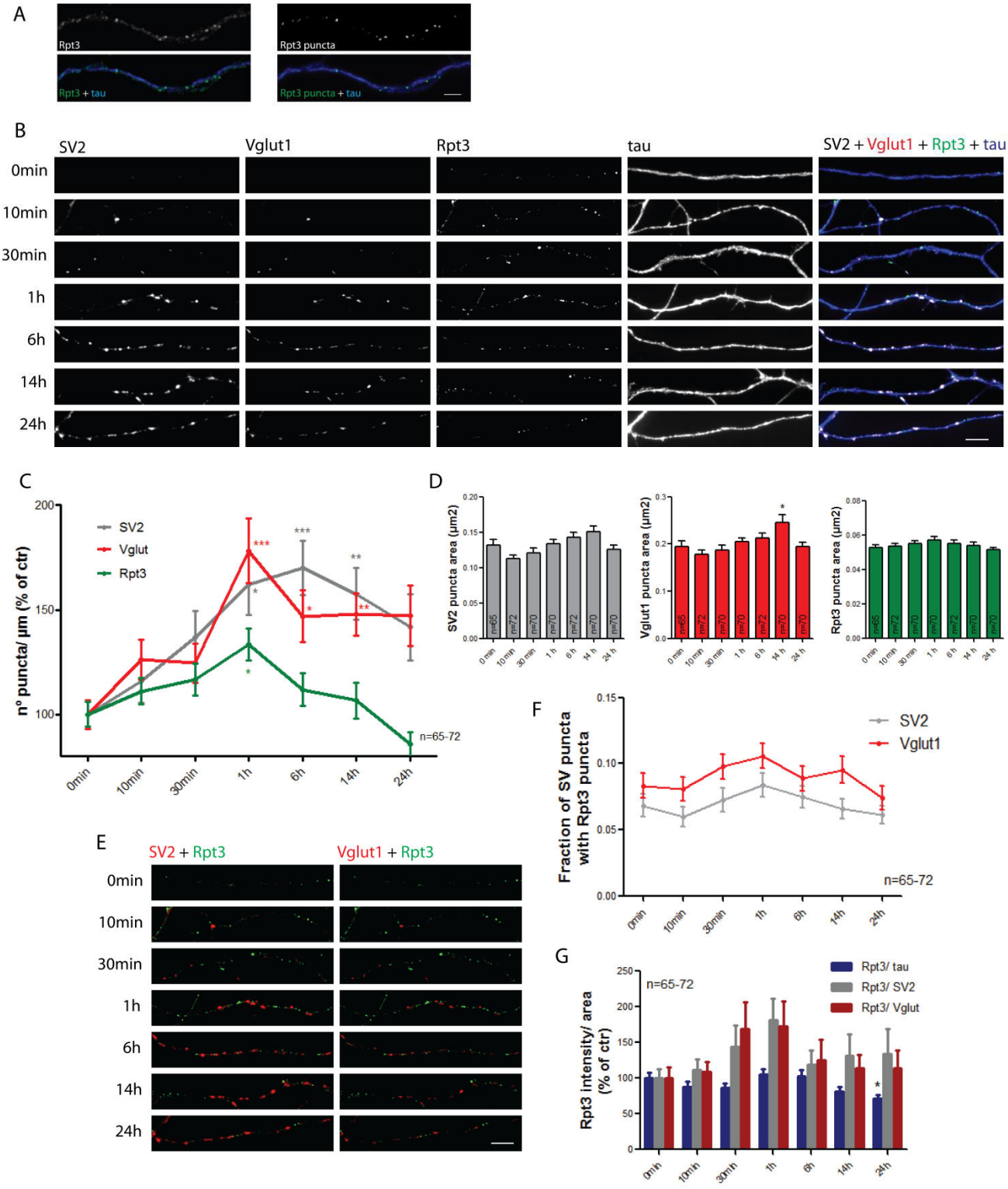

(**Fig. 3.1** – Legend on previous page)

Simultaneously, we evaluated proteasome redistribution along axons upon stimulation with BDNF, another secreted presynaptic organizing molecule. Similarly to FGF22, BDNF also upregulates the number of presynaptic terminals in hippocampal neurons[152], however through activation of the non-related receptor, TrkB[75,155]. This receptor is highly expressed in the hippocampus[444,445], and was abundantly present along the

axon until its tip (figure S3.1A, B, right panels). 1h-stimulation with BDNF also resulted in a strong SV clustering with an increased number of SV puncta along axons and also an increased average size of individual puncta, for both SV2 and Vglut1 (figure 3.2A-C). Interestingly, BDNF also increased the number of Rpt3 puncta (figure 3.2A, B), however the fraction of presynaptic clusters containing those proteasome accumulations did not increase (figure 3.2D, E). Furthermore, we evaluated total levels of the markers used in these experiments (SV2, Vglut1 and Rpt3) and concluded that FGF22 and BDNF treatment did not alter their total expression, thus showing that their clustering effect was not reminiscent of a higher amount of proteins along axons (figure S3.2). Altogether, this first set of results show us that the 19S proteasome is redistributed along axons upon induction of presynaptic clustering by FGF22 and BDNF, two distinct synaptogenic molecules.

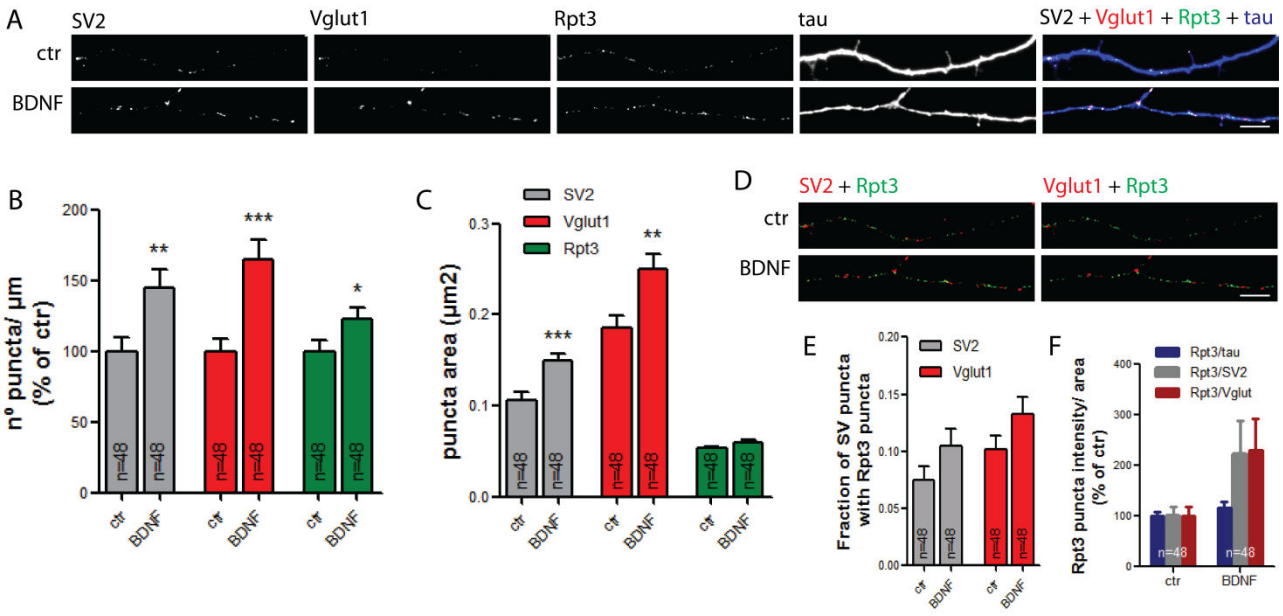

Fig. 3.2 - BDNF, another presynaptogenic molecule, alters proteasome redistribution along axons. (**A**) Effect of BDNF on SV and Rpt3 puncta number. Hippocampal neurons in pseudo-explants were stimulated with BDNF (100 ng/ml) for 1 h and stained for two distinct SV markers, SV2 (white) and Vglut1 (red), and for the 19S proteasome subunit Rpt3 (green). BDNF enhanced formation of clusters of SVs along axons and also increased the number of 19S proteasome puncta. The scale bar is 5 µm. (**B**) Quantitative values of number of SV2, Vglut1 and Rpt3 puncta per axonal length upon 1 h BDNF treatment. Results are expressed as % of control cells. (**C**) Averaged raw values of SV2, Vglut1 and Rpt3 individual puncta area. (**D**) Colocalization of SV and Rpt3 puncta in response to BDNF. Representative merged images of SV puncta [SV2 (red) and Vglut1 (red) in left and right images, respectively] and Rpt3 (green) puncta along axons upon BDNF stimulation. 19S proteasome was not preferentially accumulated in nascent SV puncta. The scale bar is 5 µm. (**E**) Quantitative data presented as the fraction of SV puncta containing Rpt3 puncta. (**F**) Quantitative values for the intensity of Rpt3 puncta within SV puncta or present in the total axon (normalized for area of SV marker or tau area, respectively). (**B**, **C**, **E**, **F**) n represents the total number of analyzed microscope FOVs from 4 independent experiments. Statistical analysis by Mann Whitney test (***p<0.001, **p<0.01 and *p<0.05 between pairs of bars)**.** Error bars indicate s.e.m.

Enhanced proteasome degradation in presynaptic assembly

Despite the fact that some proteins need to be downregulated to allow for presynaptic differentiaton to occur[350,351], until now no presynaptic organizer has been shown to enhance proteasome-mediated degradation. So, can presynaptogenic stimuli activate the proteasome? We asked whether FGF22 and BDNF, in addition to redistribute the proteasome, could affect the rate of protein degradation. To accomplish this aim, we expressed in neurons the proteasomal degradation reporter Ub^{G76V}GFP, which consists of a mutated uncleavable Ub moiety (Ub^{G76V}) in frame with GFP[414]. The G76V substitution prevents removal of the N-terminal linked ubiquitin by deubiquitinating enzymes, and so it will serve as an acceptor for polyubiquitin K48-linked chains. This signal renders GFP highly unstable and rapidly targeted for degradation by the cellular UPS. Accordingly, its signal intensity is inversely proportional to the rate of proteasome-mediated degradation[414] (figure 3.3A). Cells were treated with the proteasome activator IU1 (75 μM) or proteasome inhibitor MG132 (1 μM) for 1 h to serve as positive and negative controls and validate the degradation reporter. MG132 is a peptide aldehyde that reversibly inhibits the proteasome by covalently binding to the active site of all three primary catalytic subunits[446–448]. IU1 is a selective small-molecule inhibitor of the deubiquitinating activity of Usp14[274]. This proteasome-associated deubiquitinase limits proteasome degradation by trimming ubiquitin chains from substrates, and so, its inhibition by IU1 stimulates proteasome-mediated protein degradation[274]. As expected, by WB analysis, IU1 decreased accumulation of the degradation reporter, whilst MG132 increased its signal in neurons, in accordance with their enhancement and inhibition of proteasome activity, respectively (figure 3.3B, C). After stimulation with FGF22 (for the indicated periods of time) or BDNF (1 h), a decrease in Ub^{G76V}GFP intensity was observed (figure 3.3B, C), thus meaning that these factors enhance protein degradation by the proteasome.

We further validated this finding by using a recently developed and characterized active site-directed fluorescent probe specific for the proteasome, Me4BodipyFL-Ahx3Leu3VS (proteasome activity probe, PAP)[446,447,449]. This probe is cell-permeable and can be applied to living cells; it consists of a Bodipy-based fluorophore (Me4BodipyFL) fused to a proteasome targeting moiety (Ahx3Leu3VS), which contains an α,β-unsaturated sulfone part (VS) that reacts with the N-terminal threonine of all catalytic proteasome subunits (β1,β2,β5)[447]. In accordance, it has the ability to bind irreversibly to activated proteasome catalytic subunits thus fluorescently labeling only active proteasomes inside the cell. The proteolytic activity of the 20S complex resides in the inner β rings, with three distinct catalytic activities, caspase-like, trypsin-like and chymotrypsin-like, as a result of the action of individual catalytic β subunits, β1, β2 and β5, respectively[275,450]. By running cell extracts previously incubated with PAP in a 15% acrylamide gel, separation of the three distinct catalytic subunits can be achieved due to different migration profiles and their relative activity quantified[447]. IU1 and MG132 increased and decreased, respectively, band intensities of all catalytic proteasome subunits (figure 3.3D, E), which is in agreement with the expected action of these inhibitors on proteasome activity. Indeed, MG132 had already been shown to inhibit all catalytic β subunits[446,447]. When cells were stimulated for 1 h with FGF22 and BDNF, an increased intensity of the β1 band was observed, which corresponds to caspase-like activity (figure 3.3D, E). Additional individual experiments will be performed to fully prove the validity of this observation. The versatility of PAP allowed us to also look for proteasome activity in fixed neurons, thus giving further insights of the subcellular location of proteasome activation. At the somatodendritic level, a clear increased PAP intensity was induced by FGF22 or BDNF stimulation, which resembled the effect of the proteasome activator IU1 (figure 3.3F, G). We thus conclude that both FGF22 and BDNF activate proteasome degradation.

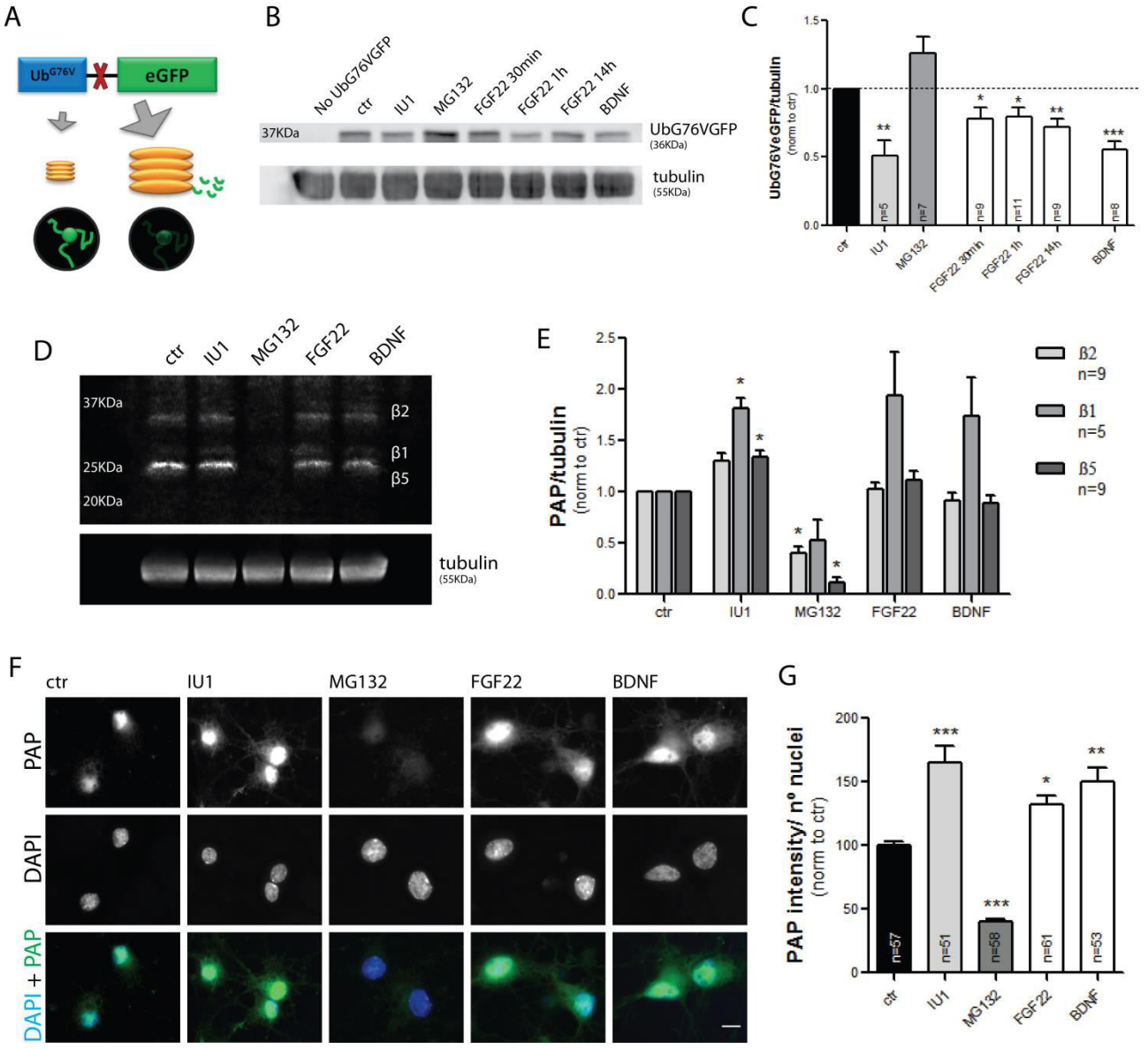

Fig. 3.3 - FGF22 and BDNF increase proteasome activity. (**A**) Assessment of proteasome activity by a degradation reporter. The degradation reporter $Ub^{G76V}GFP^{414}$ consists of a GFP fused to an Ub moiety that cannot be removed and so will function as a signal for proteasomal degradation. Reduced proteasome activity in cells allows for accumulation of the reporter and higher signal intensity, whereas highly active proteasomes will have the opposite effect. (**B**) Proteasome-mediated protein degradation rate upon FGF22 and BDNF treatment. The degradation reporter $Ub^{G76V}GFP^{414}$ was expressed in hippocampal neurons and WB for GFP was performed after treatment. Cultures were treated with either the proteasome activator IU1[274], the proteasome inhibitor MG132, or the soluble factors FGF22 or BDNF for 1 h, unless otherwise indicated. IU1 and MG132 were used as positive and negative control, respectively. Tubulin was used as the loading control. Similarly to IU1, both FGF22 and BDNF decreased the levels of $Ub^{G76V}GFP$, thus meaning that proteasome-dependent degradation was enhanced. (**C**) Quantitative levels of $Ub^{G76V}GFP$ relative to the loading control. Results were normalized to control values. Statistical analyses was performed by the Kruskal-Wallis test followed by the Dunn´s multiple comparison test (***p<0.001, **p<0.01 and *p<0.05 when compared to control). n represents the number of individual experiments. Error bars indicate s.e.m. (**D**) Activity of catalytic proteasome subunits upon FGF22 and BDNF. After treatment for 1 h with IU1, MG132, FGF22 or BDNF cells were

incubated for 30 min with PAP, which can efficiently bind to all catalytically active proteasome subunits in living cells[447]. Cell extracts were obtained and WB was performed in a 15% gel so that the bands corresponding to β1, β2 and β5 proteasome catalytic subunits could be distinguished (β1, β2 and β5 are responsible for caspase-like, trypsin-like and chymotrypsin-like proteolytic activities, respectively). Membrane was then scanned and direct fluorescence of the probe was detected. Tubulin was used as the loading control. Although not statistically significant, FGF22 and BDNF induced an increase in caspase-like proteasome activity. (**E**) Quantitative levels of β1, β2 and β5 relative to the loading control. Statistical significance between conditions for each proteasome catalytic subunit was assessed by Kruskal-Wallis test followed by the Dunn´s multiple comparison test (*p<0.05 when compared to control). n represents the number of individual experiments. Error bars indicate s.e.m. (**F**) Cell body staining of the endogenous active proteasome. Cells were treated with UPS inhibitors, FGF22 or BDNF, and incubated with PAP (green) before being fixed. Increased intensity of the probe was observed upon activation of the proteasome with IU1 and after FGF22 and BDNF application. (**G**) Change in PAP intensity per number of nuclei analyzed. Results are normalized to control values. Statistical analyses was performed by the Kruskal-Wallis test followed by the Dunn´s multiple comparison test (***p<0.001, **p<0.01 and *p<0.05 when compared to control). n represents the number of FOVs from 5 independent experiments. Error bars indicate s.e.m.

In this work, we are mainly interested in identifying the mechanisms leading to the formation of presynaptic sites, and accordingly we looked closely to the pattern of proteasome degradation and activity along axons during induction of SV clustering. We first measured the rate of protein degradation along axons by means of the degradation reporter Ub^{G76V}GFP. Both FGF22 and BDNF enhanced degradation of the aforementioned reporter in axons, but did not alter axonal expression levels of the control GFP vector (figure 3.4A, B). We then analyzed proteasome activity along axons by incubating cells with PAP. Based on our previous results depicting proteasome redistribution in axons and its accumulation in puncta (figure 3.1 and 3.2), we wondered whether activation of the proteasome upon presynaptogenic stimuli would occur in a site-specific manner. IU1-induced proteasome activation in fact increased PAP signal per tau area (figure 3.4C, D). On the other hand, following FGF22 and BDNF stimulation, the proteasome became more proteolytically active in specific spots along the axon, hereby named as hot-spots of proteasome activity (figure 3.4C, E, F). We observed an increased number of these proteasome activity hot-spots, whose size was unchanged, upon FGF22 and BDNF, but not IU1 treatment (figure 3.4C-F). So, it looks that IU1 increased proteasome activity ubiquitously in axons, whilst FGF22 and BDNF aggregated active proteasomes in concrete locations along the axon. We then asked whether formation of SV clusters would occur at sites of increased proteasome activity, and for that we quantified the fraction of SV puncta containing these hot-spots. Similarly to what was described in the previous results section, SV puncta did not preferentially co-localize with proteasome activity hot-spots (figure 3.4G, H).

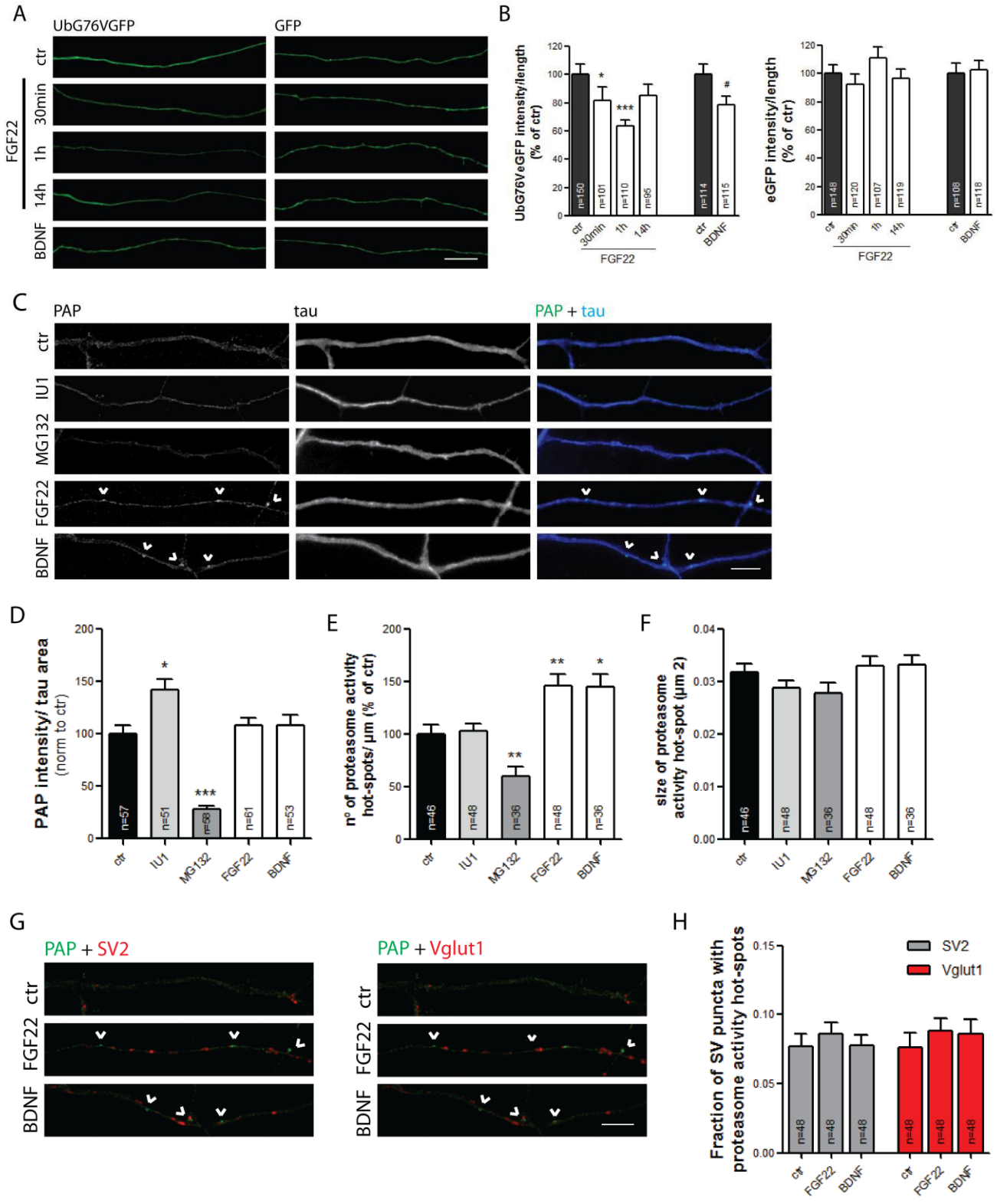

Fig. 3.4 - Appearance of hot-spots of proteasome activity along axons upon FGF22 and BDNF stimulation. (**A**) Staining of the degradation reporter along axons following FGF22 and BDNF treatment. The degradation reporter $Ub^{G76V}GFP$ or its respective control empty vector pEGFP-N1 were expressed in hippocampal neurons and their intensity along axons analyzed following incubation with FGF22 (for the indicated period of time) and BDNF (1 h). Both synaptogenic factors increased proteasome-mediated degradation along axons as observed by a decrease in the intensity of $Ub^{G76V}GFP$, but not the eGFP control. The scale bar is 5 µm. (**B**) Quantitative data expressed as $Ub^{G76V}GFP$ (left) or eGFP (right)

intensity per length of $eGFP^+$ axons. Results are expressed as % of control cells. Statistical analyses was assessed by the Kruskal-Wallis test followed by the Dunn´s multiple comparison test for the FGF22 conditions (***p<0.001, **p<0.01 and *p<0.05 when compared to control) and by Mann Whitney test between control and BDNF ($^{\#}$p<0.05). n represents the number of FOVs analyzed from 4 independent experiments. Error bars indicate s.e.m. (**C**) Expression pattern of the endogenous active proteasome along axons. Representative images of axonal segments labeled with PAP (green) after treatment with IU1, MG132, FGF22 or BDNF for 1 h. Tau (blue) was used as the axonal marker. In response to 1 h incubation with FGF22 and BDNF, bright puncta of PAP appeared along the axon, hereby recognized as hot-spots of proteasome activity (arrowheads). The scale bar is 5 µm. (**D**-**F**) Quantitative data of (**D**) PAP intensity per axonal area, (**E**) number of hot-spots of proteasome activity per axonal length and (**F**) their average size. (**G**) Colocalization of SV and PAP hot-spots upon FGF22 and BDNF. Representative merged images of SV puncta [SV2 (red) and Vglut1 (red) in left and right images, respectively] and PAP (green) puncta along axons upon bath application of FGF22 or BDNF. Hot-spots of proteasome activity did not preferentially colocalize with nascent SV clusters. The scale bar is 5 µm. (**H**) Quantitative data presented as the fraction of SV puncta containing a hot-spot of proteasome activity. (**D**-**F**, **H**) Statistical analyses was performed by the Kruskal-Wallis test followed by the Dunn´s multiple comparison test (**p<0.01 and *p<0.05 when compared to control). n represents the number of FOVs from 6 independent experiments. Error bars indicate s.e.m.

Taken into consideration that both FGF22 and BDNF trigger formation of SV clusters (figure 3.1 and 3.2) and that both enhance proteasome degradation (figure 3.3 and 3.4), we hypothesized that presynaptic differentiation would be induced by activation of the proteasome. Indeed, a 1h IU1 treatment increased the number of SV puncta, both SV2 and Vglut1, equally to the effect of FGF22 or BDNF and when applied together similar rates of SV clustering were obtained (figure 3.5A-C). Moreover, co-stimulation of FGF22 and BDNF produced SV clustering with the same magnitude as FGF22 or BDNF alone (figure 3.5D-F). Because no cumulative effect was observed neither when both presynaptogenic factors were co-applied nor when each one of them was combined to IU1 treatment, we predict that they are all acting through the same mechanism. Furthermore, we anticipate, based on the fact that IU1 accelerates degradation of tagged proteins, that the predicted shared mechanism involves enhanced proteasome degradation of specific substrates.

Altogether, these data suggest that FGF22 and BDNF induce presynaptic differentiation by enhancing proteasome activity and degradation of proteins in concrete spots along the axon.

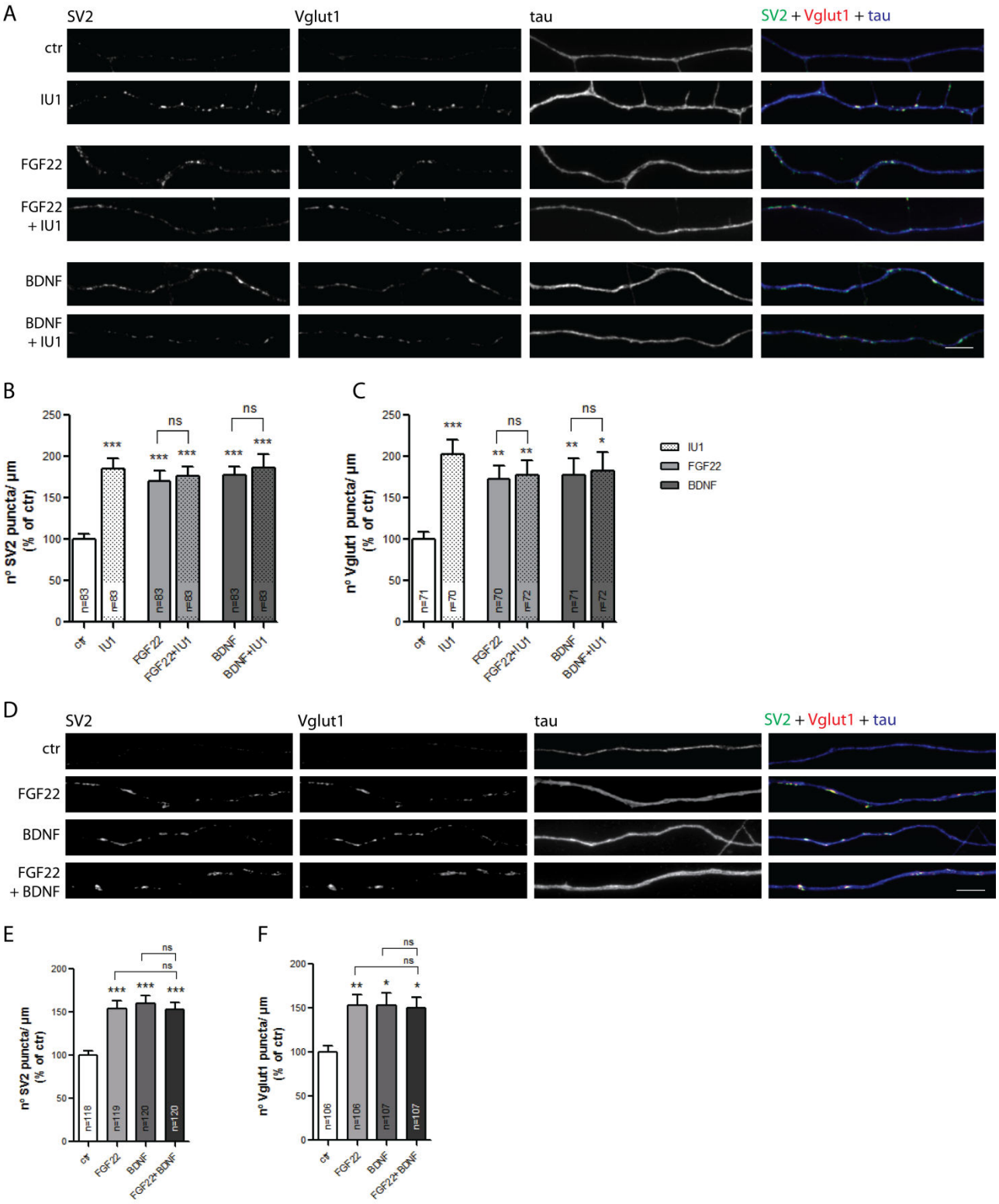

Fig. 3.5 - Activation of proteasome degradation triggers, *per se*, presynaptic clustering, probably through a shared mechanism with FGF22 and BDNF. (**A**) Effect of proteasome activation on basal and FGF22 and BDNF-induced SV clustering. Hippocampal neurons were incubated with the proteasome activator IU1 alone or in combination with FGF22 or BDNF and stained for SV2 (green), Vglut1 (red) and tau (blue). Enhancement of proteasome-mediated protein degradation induced SV clustering with the same magnitude as FGF22 or BDNF; however combination of IU1 with each of the soluble factors did not further enhance the number of SV clusters along axons. The scale bar is 5 µm. (**D**) The same

experiment was performed to evaluate the combined effect of FGF22 and BDNF on presynaptic clustering. When both soluble factors were applied, also no cumulative effect was observed. The scale bar is 5 µm. (**B**, **C**, **E**, **F**) Quantitative values of number of (**B**, **E**) SV2 and (**C**, **F**) Vglut1 puncta per axonal length. Results are expressed as % of control. Statistical analyses was performed by the Kruskal-Wallis test followed by the Dunn´s multiple comparison test (***p<0.001, **p<0.01 and *p<0.05 when compared to control). n represents the number of FOVs from 6-9 independent experiments. Error bars indicate s.e.m.

Proteasome activity requirement for FGF22 and BDNF-induced presynaptic clustering

So far, we have demonstrated that FGF22 and BDNF probably share a common mechanism for triggering presynaptic differentiation that involves activation of proteasome degradation. Yet, it remains to be known whether their presynaptogenic effect is actually dependent on proteasome activity. For instance, netrin-1-induced growth cone turning[370] or EphB2 ectodomain-triggered growth cone collapse [451] are dependent on proteasome function. To assess requirement of UPS function in FGF22 and BDNF-induced SV clustering, these factors were applied to cells alone or in combination with proteasome inhibitors. We used two unrelated proteasome inhibitors, MG132 (1 µM) and (β-lactone) (10 µM) (β-lactone), widely known to inhibit the 20S proteasome. The latter is a highly selective inhibitor that irreversibly modifies all three catalytic subunits by acylation[452,453]. The synaptogenic effect of both FGF22 and BDNF was abolished when the proteasome was inhibited (figure 3.6). We observed a clear reversion of SV clustering phenotype, not only for FGF22 or BDNF-triggered increase in the density of SV clusters (figure 3.6A, B, D), but also for BDNF-induced increase in the size of SV puncta (figure 3.6A, C, E).

(image on next page)

Fig. 3.6 - FGF22 and BDNF-induced presynaptic differentiation is proteasome-activity dependent. (**A**) Effect of proteasome inhibition on FGF22 and BDNF-induced SV clustering. Hippocampal neurons were incubated with FGF22 or BDNF in the presence or absence of the proteasome inhibitors, β-lactone and MG132 and stained for SV2 (green), Vglut1 (red) and tau (blue). Proteasome inhibition reverted the presynaptogenic effect of both FGF22 and BDNF. The scale bar is 5 µm. (**B**-**E**) Quantitative values of number of (**B**) SV2 and (**D**) Vglut1 puncta per axonal length expressed as % of control and average area of (**C**) SV2 and (**E**) Vglut1 punta. Statistical significance was assessed by the Kruskal-Wallis test followed by the Dunn´s multiple comparison test (***p<0.001, **p<0.01 and *p<0.05 when compared to control and $^{###}$p<0.001, $^{##}$p<0.01 and $^{#}$p<0.05 between indicated bars). n represents the number of FOVs from 5 independent experiments. Error bars indicate s.e.m.

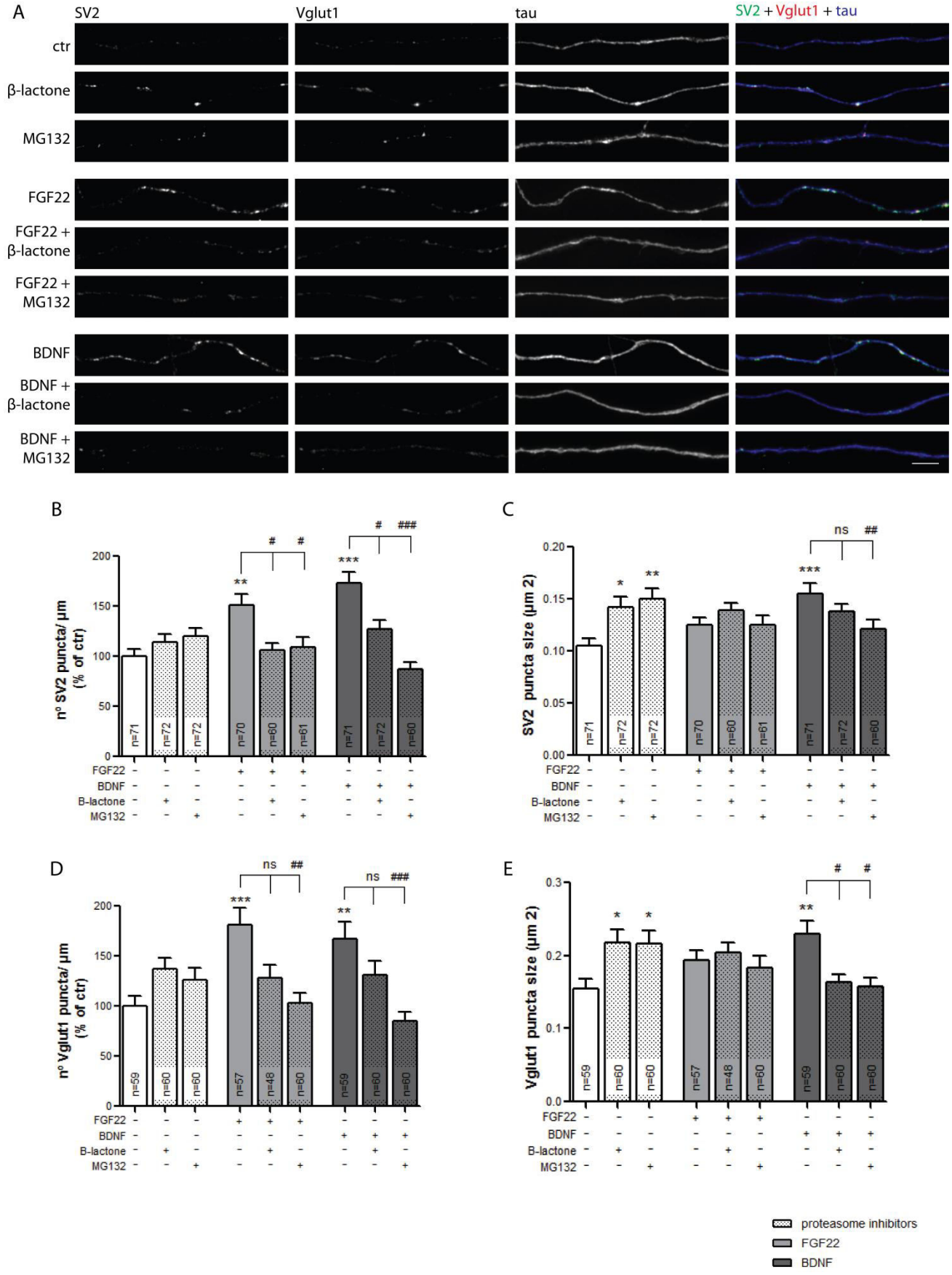

(**Fig. 3.6** – Legend on previous page)

Lastly, we wondered whether this observation would be a local effect, meaning being solely dependent on axonal proteasome degradation. Due to the rapidity of the clustering effect (1 h) and the fact that analyzed axons were mostly isolated, it is extremely likely that proteasome activity is required at the axon rather than at the somatodendritic level. To address this issue we cultured neurons in microfluidic devices, in which two compartments are connected by a set of microgrooves (450 µm length) (figure 3.7A, also see chapter 4, figure 4.1A and S4.1). Neurons were plated in only one compartment and on the opposite side a pure population of fluidically isolated axons was obtained[454] (see chapter 4, figure 4.1A and S4.1). Previously in our lab, we had observed that fluidically isolated axons show a different responsiveness to FGF22 concentration. We believe this might be the result of either non-specific adsorption of proteins by PDMS[455], which is the main component of microfluidic devices, thus trapping FGF22; or a different level of axonal maturity between axons in culture and fluidically isolated ones. Accordingly, we stimulated the axonal compartment of microfluidic devices with increasing doses of FGF22 and stained for the SV markers synapsin I and Vglut1. We concluded that, in this context, a minimal concentration of 10 nM was required for FGF22 to exert its effect (figure S3.3). By inhibiting the proteasome specifically in axons (figure 3.7A), FGF22 clustering phenotype was partially (synapsin puncta) or completely (Vglut1 puncta) reverted (figure 3.7B-D), with no changes in average puncta size (figure 3.7E, F), thus validating the requirement of intra-axonal proteasome degradation for FGF22-induced SV clustering. Puzzlingly, proteasome inhibitors alone had a striking and completely unexpected effect on SV clustering in isolated axons. Actually, their effect closely resembled that of FGF22, however when applied together they canceled each other out (figure 3.7B-D). This observation may seem contradictory at first, however it also indicates us that the UPS may contribute to presynaptic assembly through multiple and antagonistic routes. The presynaptogenic effect of proteasome inhibitors was investigated in detail and will be discussed in chapter 4.

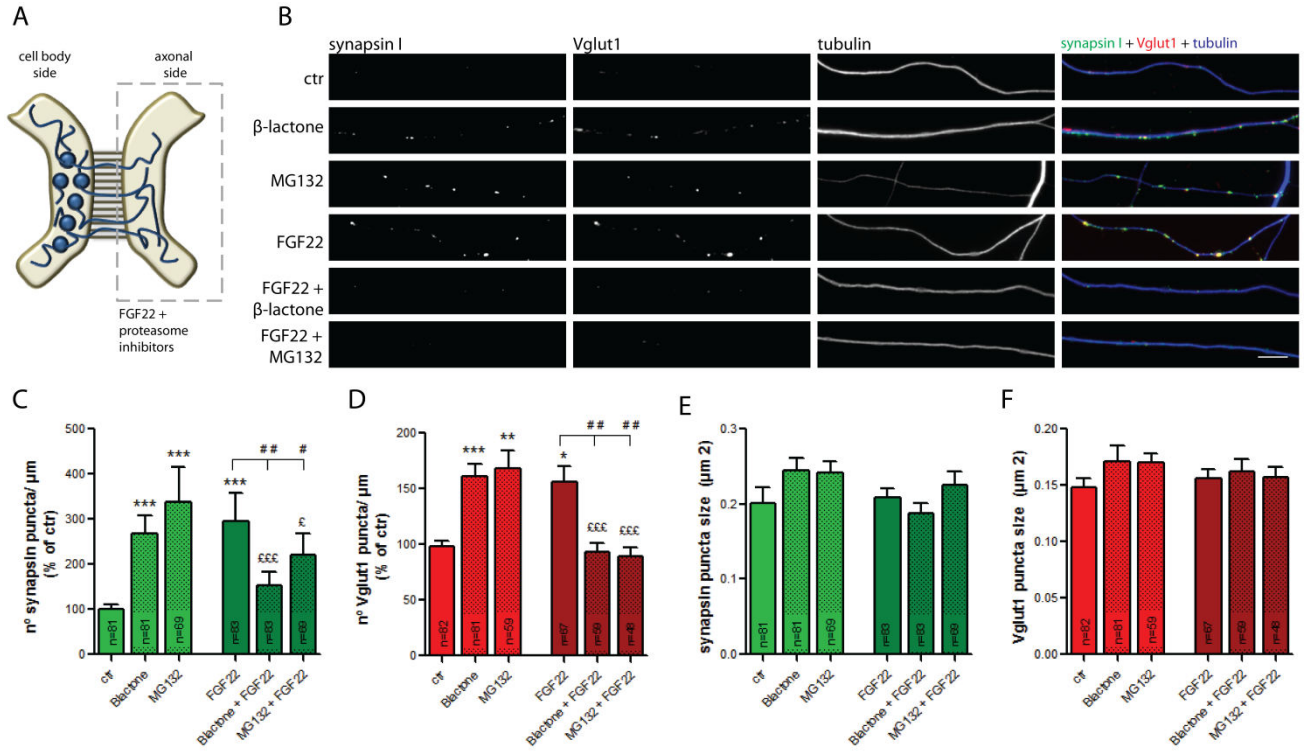

Fig. 3.7 - FGF22 synaptogenic effect requires intra-axonal proteasome activity. (**A**) Microfluidic devices for the isolation of axons. Hippocampal neurons were plated in microfluidic devices (see chapter 4,

figure 4.1A and S4.1) in which compartmentalized axons are fluidically isolated from somatodendritic structures[454]. (**B**) Local inhibition of proteasome activity blocks FGF22-induced synaptogenic effect. FGF22 (10 nM) was added to the axonal compartment for 1 h with or without the proteasome inhibitors, β-lactone and MG132, and cultures were stained for synapsin I (green), Vglut1 (red) and tubulin (blue). Inhibition of the proteasome specifically in axons abolished the effect of FGF22 on presynaptic differentiation. Note that a boost in the number of SV clusters was also observed when proteasome was inhibited in isolated axons (discussed in chapter 4). The scale bar is 5 µm. (**C**-**F**) Quantitative values of number of (**C**) synapsin I and (**D**) Vglut1 puncta per axonal length expressed as % of control and average area of (**E**) synapsin I and (**F**) Vglut1 puncta. Statistical analysis was performed by the Kruskal-Wallis test followed by the Dunn´s multiple comparison test (***$p<0.001$, **$p<0.01$ and *$p<0.05$ when compared to control; $^{\#\#}p<0.01$ and $^{\#}p<0.05$ between indicated bars and $^{\&\&\&}p<0.001$ and $^{\&}p<0.05$ when compared to the respective inhibitor applied alone). n represents the number of FOVs from 6-7 independent experiments. Error bars indicate s.e.m.

Discussion

The current knowledge on presynapse formation is still extremely incomplete, for instance, the intracellular link between cue-induced activation of presynaptic surface receptors and clustering of synaptic material is for the most part unresolved. Here, we show that presynaptogenic signals are capable of altering proteasome redistribution and rates of protein degradation. This is particularly relevant at the context of an axon, a thin and long structure in which functional and individual microdomains, such as presynaptic boutons, are present. We show that FGF22 and BDNF redistribute the proteasome in axons in the course of presynaptic differentiation. They also enhance proteasome activity and generate hot-spots of protein degradation along axons. Moreover, IU1, a proteasome activator, triggers SV clustering likely through the same pathway as FGF22 and BDNF. In agreement, proteasome inhibition is a requisite for FGF22 and BDNF-induced SV clustering. Finally, we demonstrate that presynaptic assembly is dependent on intra-axonal proteasome activity. Together these results highlight the significance of axonal UPS dynamics and function in cue-induced presynaptic differentiation.

Subcellular localization of a protein indicates where its function takes place. Indeed, degradation of MOV10 in individual spines is proportional to local proteasome availability[433] and proteasomes can redistribute in dendrites and be inserted into spines upon synaptic activity[411]. In this work, our initial hypothesis predicted that during the process of formation of a presynaptic cluster, proteasomes would be locally recruited to presynaptic sites. By analyzing the immunostaining of Rpt3, a 19S proteasome subunit, upon induction of SV clustering by presynaptogenic cues (FGF22 and BDNF), we concluded that proteasome redistributes along axons and clusters in specific locations (figure 3.1 and 3.2). However, it seems that it does not accumulate specifically in nascent presynapses (figure 3.1 and 3.2). On the other hand, it may happen that accumulation of proteasomes on clustering sites precedes the actual SV clustering or that their co-existence happens in a narrow time window, thus not possible to observe in fixed preparations. Thereby, it would be interesting to set up a live-imaging approach to address these ideas. Contrariwise, appearance of proteasome puncta may occur at axonal sites adjacent to newly-formed SV clusters, with the transient creation of a hot-spot of protein turnover at the periphery of nascent presynaptic boutons. For instance, in *C. elegans*, UPS components including FSN-1 and RPM-1 are present in regions surrounding the active zone from which they control the extent of presynaptic differentiaton[350]. Furthermore, the 26S proteasome is trafficked by fast axonal transport in moving particles[442], and so, Rpt3 puncta may correspond to transport units. If this is the case, we can speculate that a presynaptogenic factor might upregulate their anterograde trafficking and/or upon formation of an SV cluster, mobile proteasome units might pause at or near nascent presynaptic sites. Future attempts will be made to fully comprehend and describe proteasome redistribution during presynaptic assembly.

In this study, we demonstrated that FGF22 and BDNF enhance proteasome activity in hippocampal neurons in culture. We observed an enhanced rate of protein degradation and found that the proteasome is more proteolytically active (figure 3.3 and 3.4). BDNF likely functions in the synapse as a master regulator of protein composition through the UPS. In rat cortical neurons, BDNF-TrkB signaling upregulates ubiquitination of synaptic proteins[456]. Moreover, wide changes in postsynaptic composition upon synaptic activity as a result of degradation by the UPS[457] may in part be mediated by BDNF[456]. Indeed, the BDNF scavenger TrkB-IgG or the TrkB inhibitor K252a completely reverted activity-dependent changes in the expression of a subset of synaptic proteins[456]. Furthermore, BDNF itself bidirectionally alters expression of synaptic proteins in a manner dependent on proteasome activity[456]. In contrast to our results, this same study observed no changes in the intensity of a degradation reporter following BDNF stimulation and accordingly they conclude

that it does not affect proteasome activity[456]. Two possible explanations for this different phenotype can be pointed out. On one hand, authors used a different type of neuronal culture, cortical vs. hippocampal (in our case) neurons, thus possibly accounting for different intracellular machineries activated in response to BDNF. On the other hand, the degradation reporter used in this study, GFPu[458,459], is substantially different from the one expressed in our cells, $Ub^{G76V}GFP$[414]. GFPu relies on a 16 aminoacid degradation signal (CL1) fused to the carboxyl terminus of GFP. Whereas CL1 degron is a sequence that signals proteins for UPS degradation via the E2 conjugating enzymes Ubc6 and/or Ubc7[459], Ub^{G76V} consists of a mutated uncleavable ubiquitin moiety[414] that works as an acceptor for additional Ub molecules. Accordingly, ubiquitination and degradation of $Ub^{G76V}GFP$ may theoretically occur ubiquitously in cells by the activity of a wide range of E2s and E3s, whilst degradation of GFPu is probably constrained to the function of Ubc6/7[460]. We thus predict that GFPu might not be affected by the enhanced rate of proteasome degradation induced by BDNF. Our results are also in direct disagreement with a very recent paper that observes a biphasic BDNF effect on caspase-like and trypsin-like proteasome activity on cultured hippocampal neurons[461]. In this study, 30min and 1h-BDNF treatment decreased proteasome activity, whilst stimulation for 3h enhanced it[461], in contrast to our results in which proteasome activation was observed following a 1h-treatment. The difference in the kinetics of proteasome activity in response to BDNF may be due to the different experimental approaches used or to a different degree of culture maturity at the moment of stimulation. Together, these data demonstrate that BDNF is capable of bidirectionally alter proteasome function in the hippocampus.

Unlike BDNF, evidence that FGF systems act through the UPS are scarce. It was described that FGF2 induces degradation via the proteasome system of the non-catalytic region of tyrosine kinase adaptor Nck to prevent apoptosis in cancer cells[462] and also degradation of the tyrosine phosphatase HD-PTP to modulate angiogenesis[463]. Moreover, FGFR2 activation triggers ubiquitination and degradation of α5 integrin and PI3K for the control of skeletogenesis[464,465]. However, no role has been attributed to the FGF system in regulating the UPS at the context of neuronal development. To our knowledge, this work highlights an involvement of proteasome degradation in FGF22 signaling for the first time.

An immediate question that arises from our results is how FGF22 and BDNF redistribute and activate the proteasome in axons. In dendrites, it is now known that synaptic activity recruits proteasomes to dendritic spines[411] and enhances its activity[466] in a manner dependent on CamKIIα[440,466]. The proteasome is associated with CamKIIα, which stimulates its activity by phosphorylation of the proteasome subunit Rpt6[440,466,467]. Although there are no evidence for a link between FGF signaling and CamKII, in the brain BDNF might in fact function through its activation[468,469]. Briefly, in sympathetic cholinergic transmission, inhibition of presynaptic CamKII prevents the BDNF-dependent shift to inhibitory neurotransmission[468]. Moreover, BDNF was shown to stimulate phosphorylation of δCamKII[468]. Interestingly, activation of CamKII by BDNF also leads to the ultimate activation of the cyclic AMP response element-binding protein (CREB)[440]. From the work done in dendrites, it is known that redistribution of CamKII is required for activity-dependent proteasome insertion into spines[440], and amazingly, at the presynaptic level, CamKII is also prone to suffer changes in its localization[470]. In this study, the translocation of CamKII from the periphery of SV clusters to their center following KCl depolarization is thoroughly described[470]. It is thus conceivable that a conserved mechanism of proteasome regulation (redistribution and activity) through CamKII occurs in both dendrites and axons. Directed research to address this hypothesis would be crucial for the complete understanding of proteasome dynamics in FGF22 and BDNF-induced presynaptic clustering.

A novel finding in this study was that synaptogenic factors upregulate the number of 19S proteasome puncta (figure 3.1 and 3.2) and, more importantly, the number of catalytically active proteasome hot-spots

(figure 3.4) along axons. We may straightaway ask whether the accumulated proteasome is in a catalytic active state. A study using Rpt6 phopho mutants that mimic activation of the proteasome by CamKII show that phosphorylated Rpt6 (active proteasome) has a higher association with scaffolds and/or cytoskeletal components and that inability to phosphorylate Rpt6 decreases its accumulation in synapses[467]. So, it seems that the active proteasome is more prone to accumulate and tether in synaptic compartments. However, the biological significance of these hot-spots of proteasome activity is far from being understood.

One of the main conclusions from this study is that FGF22 and BDNF-induced presynaptic differentiation requires proteasome-mediated degradation of specific substrates. We further predict that they may act on the same candidates due to their non-cumulative effect when co-applied. Several presynaptic and postsynaptic proteins have already been identified as targets for proteasome degradation[241,270]. In addition, the brain ubiquitome comprises synaptic proteins and other proteins with direct roles in synaptogenesis[242,243], thus further emphasizing the potential role of protein degradation during neuronal development. The next step would be to identify the proteins being downregulated upon presynaptogenic stimulation and the requirement of their degradation for the formation of functional presynaptic terminals.

Supplementary figures

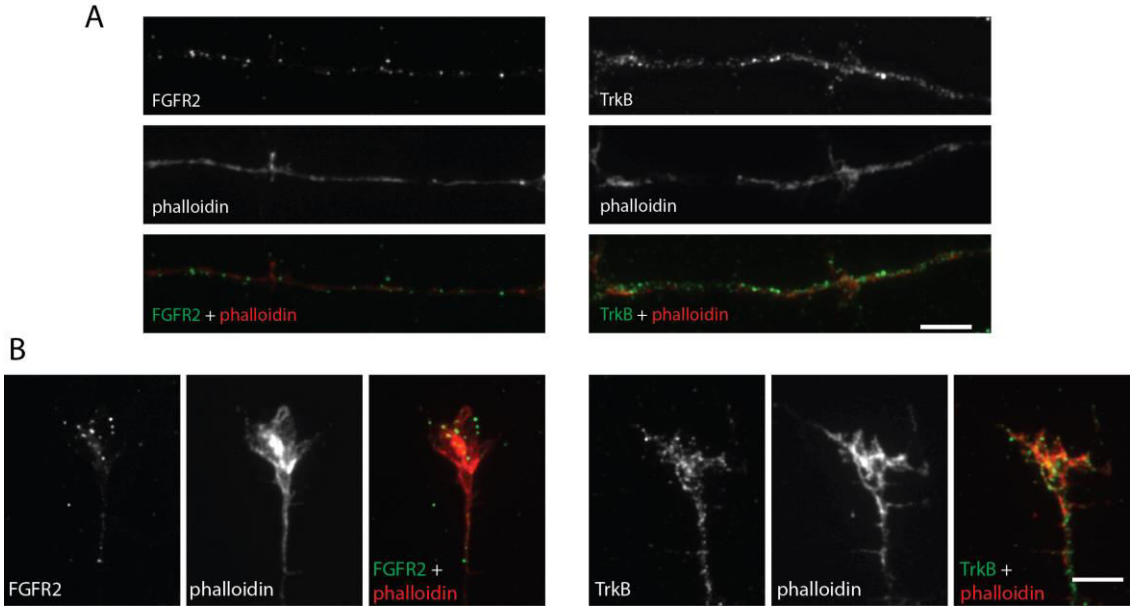

Fig. S3.1 - Expression pattern of FGFR2 and TrkB in axons of hippocampal neurons. (**A**, **B**) FGFR2 and TrkB staining in axons and growth cones. Hippocampal cultures were stained for the FGFR2 (green) and TrkB (green), which are the specific binding receptors for FGF22 and BDNF, respectively[443,471]. Particular attention was given to their expression pattern (**A**) along axons and in (**B**) growth cones. Phalloidin (red) was used as a marker for growth cones. FGFR2 was homogeneously distributed in a punctuate pattern all along the axon until its most distal region, the growth cone, where it was highly enriched. TrkB receptor was also greatly expressed in both the axonal shaft and growth cone. Scale bars are 5 µm.

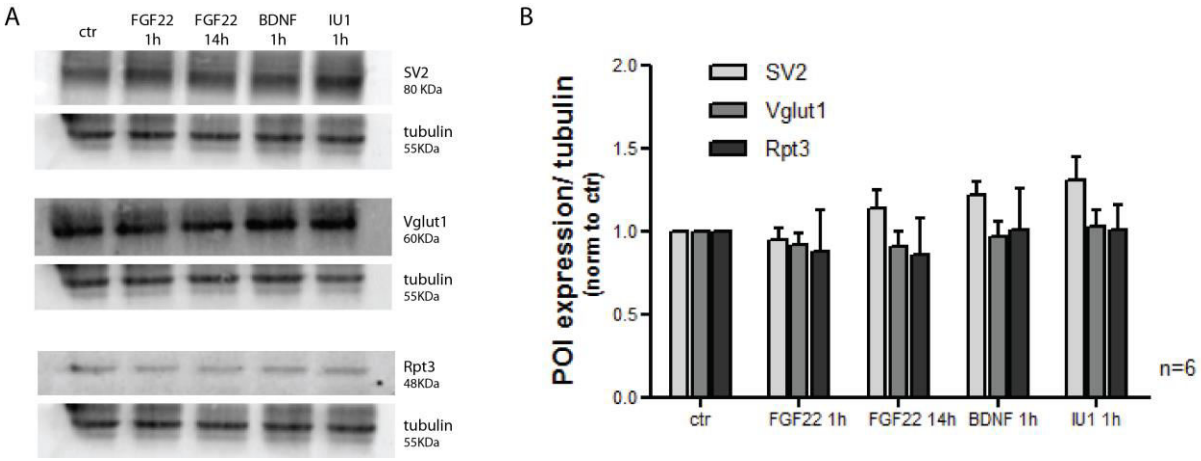

Fig. S3.2 - Total protein levels of the presynaptic and proteasome markers are unchanged. (**A**) Total expression levels of markers analyzed. Total cell lysates were obtained from DIV 7 hippocampal neurons after treatment with FGF22, BDNF or the proteasome activator IU1 for the indicated period of time. WB

for SV2, Vglut1 and Rpt3 was performed. Tubulin was used as the loading control. Expression levels of the presynaptic markers (SV2 and Vglut1) and proteasome marker (Rpt3) were unchanged following the aforementioned treatments. (**B**) Quantitative levels of protein of interest (POI) relative to the loading control. Statistical significance was assessed by the Kruskal-Wallis test followed by the Dunn´s multiple comparison test. n represents the number of individual experiments. Error bars indicate s.e.m.

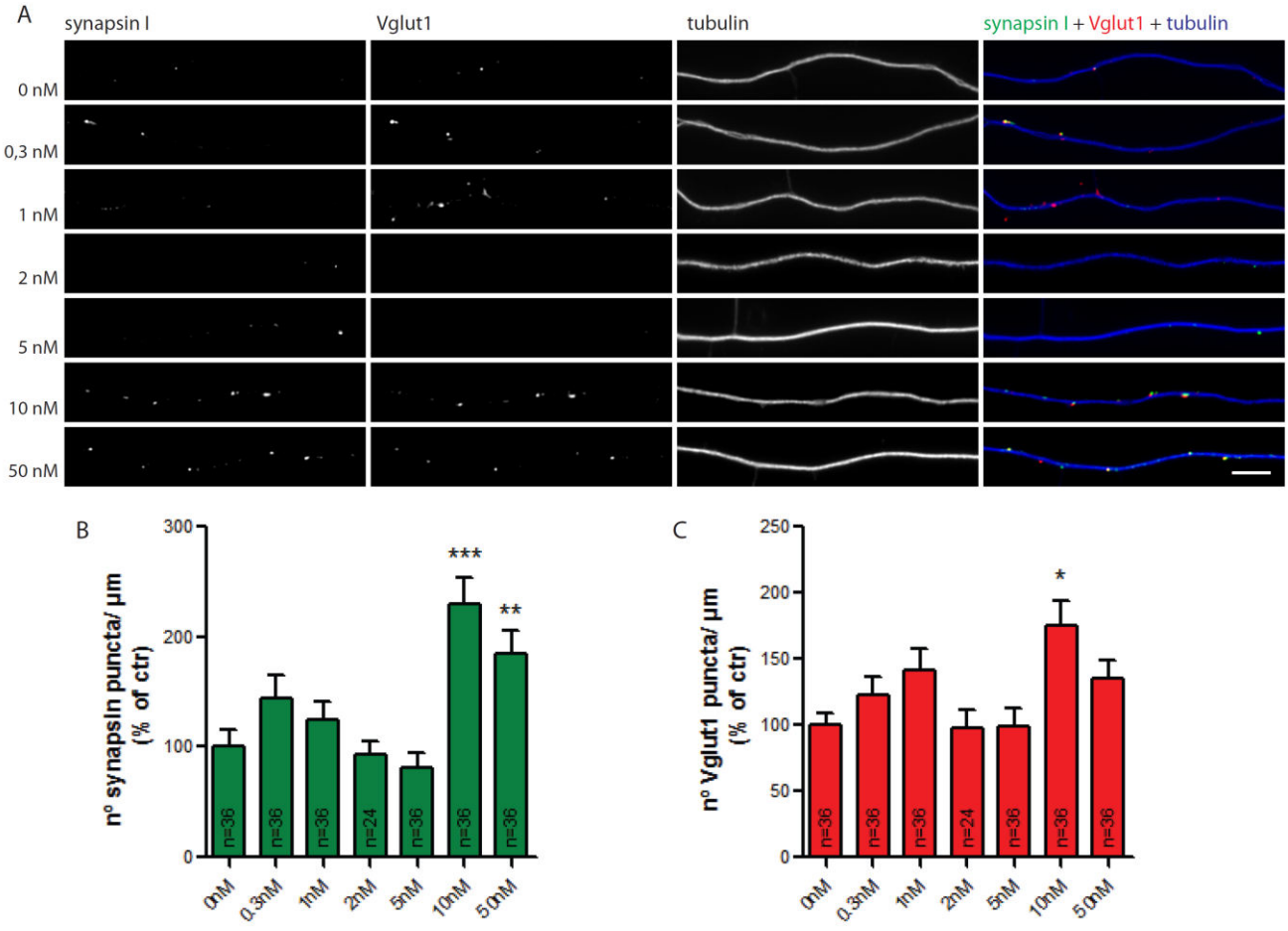

Fig. S3.3 - Dose-response curve for FGF22-induced presynaptic clustering in isolated axons cultured in microfluidic devices. (**A**) FGF22 stimulation in the axonal compartment. Isolated axons in microfluidic devices were incubated with different concentrations of FGF22 for 14 h and stained for the presynaptic markers synapsin I (green) and Vglut1 (red). Tubulin (blue) was used as an axonal marker. A concentration of 10 nM was required for FGF22 to exert its effect on the formation of SV clusters in isolated axons. The scale bar is 5 µm. (**B**, **C**) Quantitative values of number of (**B**) synapsin I and (**C**) Vglut1 puncta per axonal length expressed as % of control. Statistical significance was assessed by the Kruskal-Wallis test followed by the Dunn´s multiple comparison test (***p<0.001, **p<0.01 and *p<0.05 when compared to 0 nM). n represents the number of FOVs from 3 independent experiments. Error bars indicate s.e.m.

Chapter 4

Proteasome Governs Presynaptic Differentiation Through Modulating an *On-site* Pool of Polyubiquitinated Conjugates

Maria Joana Pinto, Pedro Alves, Luís Martins,
Joana Reis Pedro, Anne Taylor, Ramiro Almeida

In preparation for publication

Summary

Differentiation of the presynaptic terminal is a highly complex and rapid event that normally occurs in axonal regions far distant from the cell body. It is thus believed to be dependent on intra-axonal mechanisms that are activated by cues derived from the postsynaptic partner. Here we investigated the involvement of the UPS, which is the major degradative pathway within the cell, in the local modulation of presynaptic differentiation. We found that proteasome inhibition has a presynaptogenic effect on isolated axons. Formation of a stable SV cluster onto a postsynaptic partner occurs in parallel to a localized decrease in the activity of the proteasome. We also observed that a pool of accumulated polyubiquitinated proteins is the local trigger for presynaptic clustering. In accordance, K48 polyubiquitinated proteins concentrate at nascent presynaptic sites. Finally, we uncover a role for proteolyitc-related ubiquitin chains (K11, K48) as local signals for the assembly of the presynaptic terminal. Overall, these findings unravel a new UPS-mediated axon-intrinsic mechanism leading to presynaptic differentation and support a new model in which a localized pool of polyubiquitinated proteins triggers the initial recruitment and clustering of presynaptic material.

Introduction

Throughout development, the establishment of functional synaptic contacts is pivotal for the correct wiring of neurons and ultimately proper brain function in the adult life. Therefore, it is of utmost importance to fully comprehend the cascade of events comprising synapse formation. One such event, presynaptic differentiation, corresponds to the organized clustering of presynaptic material in specific spots along the axon[68,421]. Briefly, soma-derived presynaptic proteins are transported along axons in the form of mobile packets. STVs contain not only SVs, but also SV-associated proteins and SV fusion and recycling machinery; and PTVs, which consist of preassembled units of active zone components[14,20,21]. These packets cluster spontaneously and preferentially at predefined *en passant* sites along the axons, that will later be stabilized if contact with postsynaptic elements occurs[48]. Then, differentiation of these primitive boutons into mature presynaptic terminals will be induced by a cohort of presynaptogenic proteins including trans-synaptic adhesion complexes or secreted signaling factors[70–72]. Less is known about the intracellular downstream effectors of these presynaptic organizers that link their activation to the recruitment of STVs and PTVs. Growing evidence supports the idea that trans-synaptic complexes interact with key active zone scaffolds that in turn bring together several presynaptic proteins via high-affinity protein-protein interactions; and secreted factors depend on the activation of signaling transduction cascades involving kinases and GTPases[71,167]. However, the question of what are the intra-axonal *on-site* events triggering the clustering of presynaptic material at spots of axodendritic contact is still poorly understood.

The UPS, which is best known for its role in the degradation of ubiquitin-tagged proteins, has been shown to act locally at synapses[432,441]. Prior to degradation, proteins are ubiquitinated by a cascade of enzymes: E1 ubiquitin-activating enzymes, E2 ubiquitin conjugating enzymes and E3 ubiquitin ligases. Ubiquitinated conjugates bearing a lysine 48-linked ubiquitin chain are driven to the proteasome, unfolded and degraded within its catalytic core[271]. For instance, in axons, local proteasome-mediated degradation of RhoA and PTEN are crucial for neuronal polarity and axon branching, respectively[315,345]. Moreover, downregulation of ubiquitinated proteins within the presynaptic compartment is also crucial for synapse formation[351] and neurotransmiter release[359]. Recently, Bassoon and Piccolo, large scaffolding proteins of the active zone, were identified as master regulators of protein ubiquitination and degradation at the presynaptic terminal by negatively regulating the E3 ligase Siah1[391]. These and other studies substantially support a prominent localized role for UPS-dependent protein degradation at axonal structures.

Interestingly, accumulating evidence show that constitutive activity of the proteasome in the presynaptic compartment might act as an inhibitory constraint on its formation and function, thus possibly exerting a homeostatic role. For instance, proteasome inhibitors rapidly strengthen neurotransmitter release[384,385], increase the size of the recycling vesicle pool[412] and boost the number of axonal synaptic inputs in an *Aplysia* sensory and motor neuron co-culture system[386]. Taking these studies in consideration, one can speculate that selective (both temporal and spatial) proteasome inhibition throughout the development and lifetime of an axon is prone to function as a way of controlling presynaptic events.

However, the role of the UPS in the developing axon seems to be far more complex than the straightforward ubiquitination-degradation mode of action. The ataxia mice Ups14^{axJ}, with a loss-of-function mutation in the proteasome-associated deubiquitinating enzyme Usp14, display severe structural and functional dysfunctions at the NMJ[258,259]. These synaptic defects are completely rescued by restoration of neuronal ubiquitin levels[258,259]. Intriguingly, the synaptic compartment was shown to be highly susceptible to fluctuations in the levels of ubiquitin, with an interesting correlation between synaptic restoration of free

and conjugated ubiquitin and amelioration of the mutant mice synaptic defects[258]. Moreover, abnormal synaptic structures in the deubiquitinase UCH-L1-inhibited neurons are restored by expression of Ub[261], further reinforcing the requirement of steady-state levels of monomeric Ub in the synapse. A pioneer study in the *Drosophila* NMJ highlights the involvement of ubiquitin-dependent mechanisms during synapse development[363]. Authors concluded that a balance between ubiquitination and deubiquitination is crucial for proper synapse structure and function, thus revealing a role for the pool of synaptic ubiquitinated proteins. In fact, ubiquitinated proteins are highly enriched at the *Drosophila* NMJ, with aggregates of Ub conjugates surrounding the active zone[472]. Notably, UPS components and Ub-related proteins are upregulated in the brain at developmental stages coincident with the peak of synapse formation (at the first postnatal week), as well as higher accumulation of K48 ubiquitinated proteins[259]. Also, several neuronal Ub carriers are active during synaptogenesis[242], thus revealing that UPS is highly industrious and dynamic at this stage.

Further information arises from proteomic screenings that succeed in identifying neuronal ubiquitinated proteins. For instance, in *Drosophila* embryos undergoing synaptogenesis several proteins with known roles in synaptogenesis are ubiquitinated under physiological conditions[242]. These include both structural and signaling proteins, such as adhesion molecules, presynaptic scaffolds, kinases and cytoskeleton proteins[242]. Furthermore, several presynaptic proteins, mainly SV-associated or active zone proteins, are present in their ubiquitinated form in the adult rat brain[243]. Despite the wealth of knowledge on synaptic proteasome-mediated degradation of specific proteins, the physiological significance of such a complex presynaptic ubiquitinated proteome is far from being understood.

In the present study, we have discovered that accumulation of an *on-site* pool of polyubiquitinated proteins in response to localized proteasome inhibition plays a critical role in the assembly of presynaptic components. By using a microfluidic system, we observed that specific inhibition of the proteasome in axons boosts formation of presynaptic clusters. Strikingly, assembly of presynaptic clusters upon contact with a postsynaptic partner occurs under site-specific decrease in proteasome activity. The effect of proteasome inhibitors is independent on protein synthesis but requires ubiquitination. Moreover, only modest increases in the total amount of polyubiquitinated conjugates mediated by an inhibitor of deubiquitination significantly increase the number of presynaptic clusters. We also observed presynaptic accumulation of K48 ubiquitinated conjugates at sites of newly-formed clusters. Lastly, we identify a role for different proteolytic-related ubiquitin chains in the differentiation of presynaptic terminals. Together, these findings attribute a modulatory role for the UPS at sites of newly-formed presynapses.

Results

Inhibition of the proteasome in isolated axons has a presynaptogenic effect

To understand the axonal intrinsic processes underlying formation of presynaptic clusters, we used throughout this work microfluidic devices. This system has extensively been used in a variety of studies to look deep into axon-related mechanisms[419,473–477]. Hippocampal neurons plated in the cell body compartment extended their axons through a set of 450 µm-microgrooves into the axonal compartment (figure 4.1A and S4.1A), in which no cell bodies or dendrites were detected. We used this platform to specifically inhibit the proteasome in axons (figure S4.1), from here onwards referred to as local or axonal proteasome inhibition. To accomplish so, two distinct proteasome inhibitors were applied to the axonal compartment, MG132 (1 µM) and β-lactone (10 µM) for 10 min, 30 min, 1 h and 14 h. To guarantee that cultures were not compromised upon axonal proteasome inhibition, neuron viability and axonal degeneration were assessed (figure S4.1B-E). Moreover, to validate this fluidic system and firmly confirm that locally applied proteasome inhibitors do not affect proteasome activity at the cell body level, we made use of Ub^{G76V}GFP, a GFP-based reporter substrate for proteasome degradation[414]. This reporter consists of an uncleavable N-terminal Ub mutant (Ub^{G76V}) in frame with GFP. The Ub moiety is recognized as a degradation signal, thus potentiating its further polyubiquitination and degradation by the proteasome[414]. Accordingly, the reporter is constitutively degraded within the cell and will accumulate if UPS degradation halts, resulting in an increased signal intensity, or vice-versa. As expected, when expressed in the cell body side of microfluidic devices, Ub^{G76V}GFP only suffered changes to its intensity when proteasome inhibitors were added to the soma side (figure S4.1F, G). Therefore, microfluidic devices allow for the specific inhibition of the proteasome in axons, and so, constitute a useful tool for the study of proteasome involvement in axon-intrinsic mechanisms governing its differentiation.

Having characterized our system, we then looked closely to the clustering of presynaptic material along isolated axons upon treatment with proteasome inhibitors. All experiments throughout this study were performed at DIV 7, which corresponds to the peak of synaptogenesis in primary hippocampal cultures[478]. To visualize the formation of new presynaptic sites we analyzed the pattern of Vglut1 and Bassoon puncta, markers of excitatory SVs and the active zone, respectively. Both MG132 and β-lactone caused a robust increase in the number, but not the size, of Vglut1 puncta along axons (figure 4.1B-D), that peaked at 1h-inhibition with a slight decrease afterwards. To guarantee that we were actually looking to nascent presynaptic sites, we quantified the clusters in which a Vglut1 puncta and a Bassoon puncta colocalize, hereafter referred as presynaptic clusters. Bassoon puncta smaller than 0.05µm^2 were discarded to exclude mobile PTVs (figure S4.2A, B). Active zone material is pre-assembled in PTVs that are freely mobile along the axon. At the sites of presynaptic terminal formation, recruitment and fusion of PTVs to the plasma membrane gives rise to the active zone[20,21]. To exclude the possible contribution of mobile PTVs (0.02µm^2) and to ensure that Bassoon puncta are presynaptic, analysis was limited to Bassoon puncta bigger than the smaller quantifiable object (0.05µm^2) according to the imaging resolution limit[479]. Once again, proteasome inhibitors strongly increased the number of Bassoon puncta >0.05 µm^2 (figure S4.2A, B) and the number of presynaptic clusters (figure 4.1B, E) per axonal length. In terms of the latter, maximum effect was again observed at 1h inhibition followed by a decrease to almost basal levels. We hypothesize that this reduction is due to the unstable nature of the newly-generated presynaptic clusters that will eventually disassemble if no contact with a postsynaptic partner occurs. In fact, coordinated elimination of presynaptic sites that exist along the axon and do not contact with postsynaptic elements have already been reported[379,480]. On the other hand, the time line of Bassoon clustering showed a different pattern, with an unexpected rapid

increase in the number of puncta only after 10 min of proteasome inhibition (figure S4.2A, B). It is reasonable to assume that later clustering of Vglut1 will occur on these previously assembled Bassoon puncta. This idea correlates quite well with findings showing that recruitment of Bassoon precedes clustering of SVs in the sequence of events leading to the assembly of a nascent glutamatergic presynaptic site[12,188]. Furthermore, the rapid assembly of presynaptic clusters upon proteasome inhibition (1 h) is in perfect agreement with the proposed time line[12]. Taken these observations into consideration the subsequent experiments were performed using the 1 h time point.

Additionally, we also demonstrated that another active zone protein, SNAP25, was selectively enriched in newly-formed SV clusters upon local proteasome inhibition (figure S4.2D-F), indicating that SVs and active zone proteins are assembled together upon proteasome inhibition. To address the possibility that the observed presynaptic phenotype is due to a random increase in the total levels of presynaptic proteins that will no longer be degraded upon proteasome inhibition, we analyzed by WB the levels of these proteins when the proteasome was inhibited. Hippocampal neurons were incubated with MG132 and β-lactone for 1 h and the endogenous levels of Bassoon, Vglut1 and SNAP25 determined in whole cell lysates (figure S4.3). There was no alteration in the expression of these proteins demonstrating the specificity of our results (figure S4.3). Taken together, these results demonstrate that proteasome inhibition in isolated axons results in the formation of new presynaptic sites, and strongly suggest that the proteasome could have a synaptogenic role.

(image on next page)

Fig. 4.1 - Local proteasome inhibition leads to the formation of presynaptic sites in immature isolated axons. (**A**) Microfluidic devices for the isolation of axons. Dissociated rat embryonic hippocampal neurons were plated in the cell body side of microfluidic devices, allowed to grow until DIV 7 and then immunostained for MAP2 (red) and Tuj1 (green). A pure population of axons was observed on the axonal side. (**B**) Effect of axonal proteasome inhibition on presynaptic clustering. Isolated axons were treated with two distinct proteasome inhibitors, β-lactone (10 μM) and MG132 (1 μM), for the indicated periods and clustering of presynaptic material was assessed by immunostaining for the SV marker Vglut1 (red) and the active zone marker Bassoon (green). Tau (blue) was used as the axonal marker. Local proteasome inhibition induced an extensive clustering of presynaptic material. White arrowheads show presynaptic clusters along the axon. Scale bar is 5 μm. (**C**-**E**) Quantitative summary data of (**C**) number of Vglut1 puncta per axonal length, (**D**) Vglut1 puncta area and (**E**) number of presynaptic clusters per axonal length, hereby considered as a Bassoon punctum with an area bigger than 0.05μm^2 that colocalizes with Vglut1 puncta. (**F**-**H**) Developmental profile for the effect of proteasome inhibition. The same presynaptic parameters were analyzed at different developmental time-points in response to 1h inhibition of the proteasome in the axonal compartment and plotted together. Responsiveness to proteasome inhibitors was lost in aged axons. (**C**, **E**, **F**, **H**) Results are expressed as % of control cells or (**D**, **G**) raw value of puncta area and are averaged from 4-11 independent experiments. (**C**-**H**) A minimum of 12 microscope FOVs to the axonal side were analyzed per individual experiment in each condition. Statistical significance was assessed by the Kruskal-Wallis test followed by the Dunn´s multiple comparison test (***p<0.001 and **p<0.01 when compared to 0min time-point or control condition and $^{###}$p<0.001 when compared to 1h time-point). Error bars indicate s.e.m.

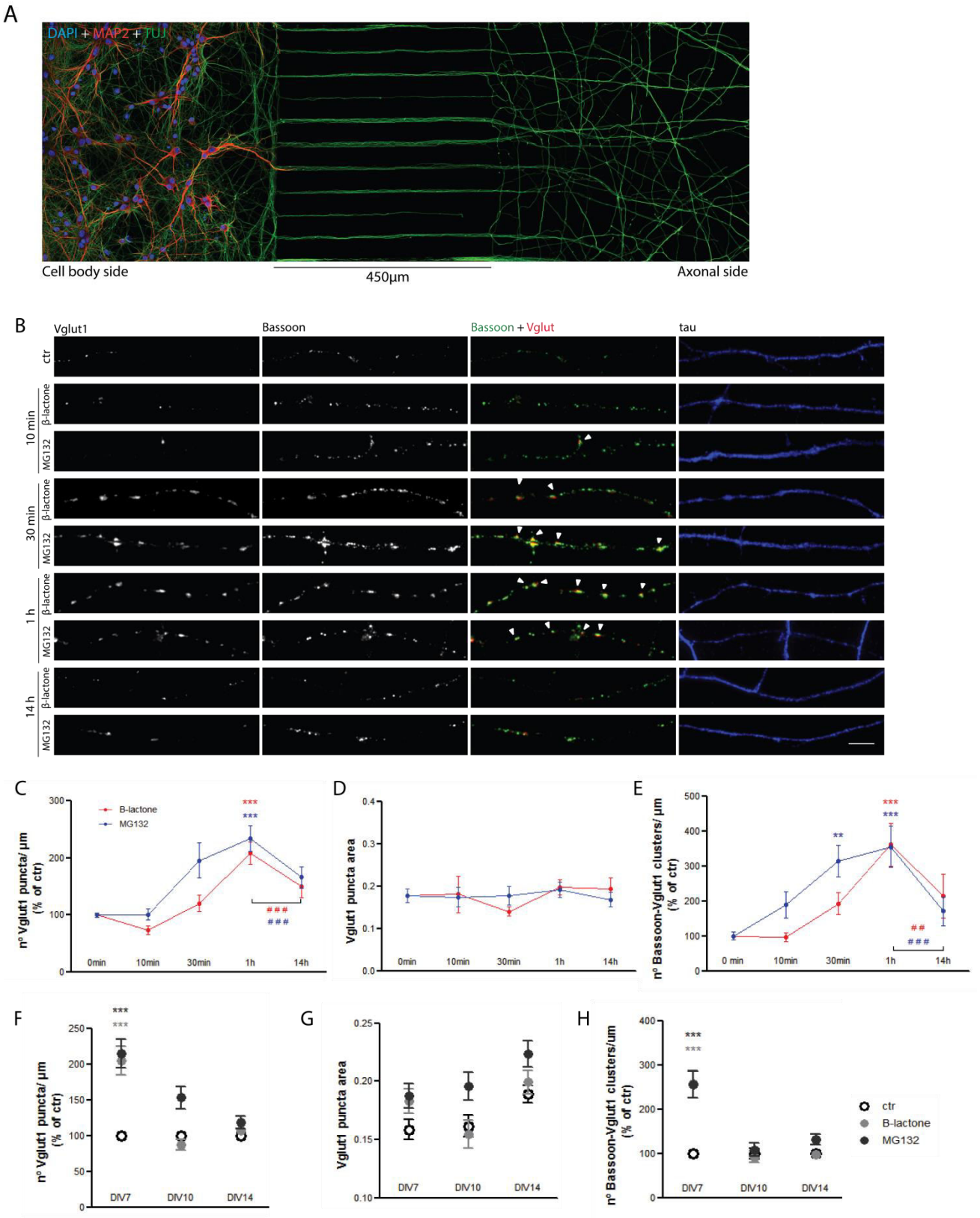

(**Fig. 4.1** – Legend on previous page)

We then evaluated the responsiveness of older axons to proteasome inhibition. By plotting the density of presynaptic puncta against different developmental stages, we observed that proteasome inhibitors could

no longer exert their presynaptogenic effect in 10-day old cultures (figure 4.1F-H and S4.2C). This indicates us that modulation of presynaptic clustering by the proteasome is probably of higher importance in younger neurons. As opposed to the reported effect of proteasome inhibitors on the size of the recycling vesicle pool, in which a mature neuronal state is required[412]. Thus, proteasome inhibition might modulate both number and size of presynaptic sites according to the axon developmental stage.

To detect the appearance of newly-formed functional presynaptic terminals upon local proteasome inhibition, we used PDL-coated beads, a synapse-inducing system which spatially restricts sites of presynaptic differentiation. These beads have previously been shown to induce formation of presynaptic boutons on contacting axons[192]. In fact, when added to the axonal compartment they are capable of clustering presynaptic material[419], which was enhanced by local treatment with proteasome inhibitors (figure S4.4). After adding beads to the axonal compartment (3h), recurrent labeling of active presynaptic sites with FMdye was performed flanking a 1h-treatment with proteasome inhibitors or vehicle (figure 4.2A). Monitoring of live formation of new presynaptic boutons with repeated cycles of FMdye staining has been extensively described[12,13,481]. Loading of the dye was performed by KCl-mediated depolarization, followed by a live-monitored unloading mediated by electrical stimulation. FM puncta that unloaded more than 5% of their dye content after 1min of stimulation were considered as functional presynaptic sites[419]. Proteasome inhibitors significantly increased the number of new FM puncta on beads in comparison to vehicle-treated axons (figure 4.2B, C). Approximately half of these new puncta were capable of releasing the dye upon stimulation, thus showing that local proteasome inhibition leads to the formation of new functional presynaptic terminals within 1h.

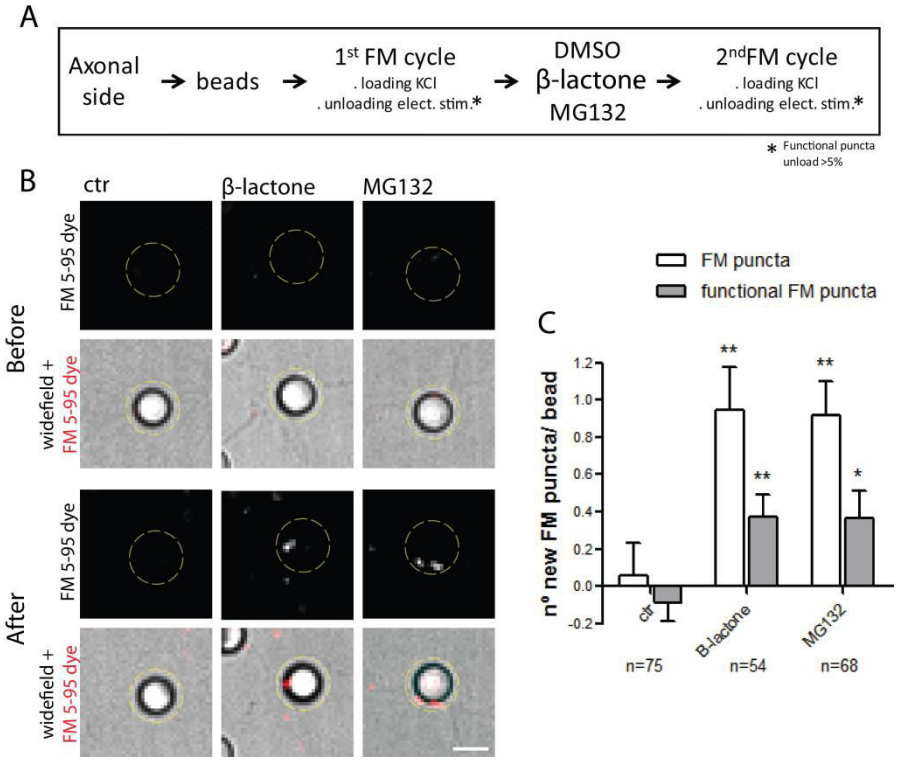

Fig. 4.2 - New functional presynaptic terminals are formed upon inhibition of the proteasome. (**A**) Live FM dye protocol to assess formation of functional presynaptic sites. Schematic representation illustrating the protocol used to examine the formation of new functional presynaptic clusters by means of the lipophilic styryl dye FM 5-95 dye. Briefly, PDL-coated beads were added to the axonal compartment for 3 h and then two cycles of FM 5-95 dye loading and unloading were interspersed with

proteasome inhibitors or DMSO treatment. FM puncta that unloaded more than 5% of their content after 1 min of electrical stimulation were considered functional presynaptic clusters. For further details see Live-imaging section on Chapter 2. (**B**) Outcome of proteasome inhibition on the formation of new functional terminals. The live FM dye protocol was performed on DIV7 hippocampal cultures and the appearance of new FM dye (red) puncta on beads after treatment (DMSO, β-lactone or MG132 for 1 h) was monitored. Axonal proteasome inhibition gave rise to new functional FM puncta on beads. The scale bar is 5 μm. (**C**) Quantitative data presented as the number of new FM puncta per bead obtained by subtracting the number of FM puncta before and after treatment, both for total and active puncta. Statistical significance was assessed by the Kruskal-Wallis test followed by the Dunn´s multiple comparison test (**p<0.01 and *p<0 .05 when compared to control). n represents the number of beads analyzed from 3 independent experiments. Error bars indicate s.e.m.

To evaluate the physiological relevance of localized proteasome inhibition for presynaptic differentiation in an axodendritic synapse, we used a novel type of microfluidic chambers specialized for the compartmentalization of synapses[482], hereby referred as synapse formation chambers (figure 4.3). In these devices, axons coming from the presynaptic side contact with dendrites originated from the postsynaptic side in a middle compartment known as the synaptic compartment (figure 4.3A). The excitatory SV marker, Vglut1-mCherry, was presynaptically expressed using a lentiviral system and axons from transduced neurons cross to the synaptic compartment (figure 4.3B). Post-staining for MAP2 and Bassoon showed that, in fact, Vglut1-mCherry-expressing axons contacted with dendrites in the synaptic compartment and that Vglut1-mCherry puncta were formed and scattered along dendrites (figure 4.3C). Specific inhibition of the proteasome in the synaptic compartment increased the number of these presynaptic clusters formed on dendrites (figure 4.3D-F). Because analysis was specific to Vglut1-mCherry-containing presynaptic clusters, whose somatodendritic elements were not exposed to the inhibitors, this system demonstrates that inhibition of the proteasome in distal axons enhances their capability of establishing synapses with a postsynaptic partner. Taken together, this first set of results indicates that local proteasome inhibition has a synaptogenic effect, increasing the number of presynaptic terminals in immature axons and the number of axodendritic synapses.

(image on next page)

Fig. 4.3 (continued) (**C**) Top, post-staining for MAP2 (blue) and Bassoon (green). Several dendrites crossed the short set of microgrooves reaching the synaptic compartment. The scale bar is 50 μm. Bottom, enlarged image of box in the top image. Vglut1mCherry puncta formed along dendrites on the synaptic compartment. The scale bar is 5 μm. (**D**) Effect of local proteasome inhibition in the formation of presynaptic clusters on dendrites. Treatment with proteasome inhibitors for 1 h was performed on the synaptic compartment and cultures were immunostained for MAP2 (blue) and Bassoon (green). An increased number of Vglut1mCherry puncta along dendrites was observed after local proteasome inhibition. The scale bar is 5 μm. (**E**, **F**) Quantitative data presented as (**E**) number of Vglut1mCherry puncta (**F**) and Bassoon-Vglut1mCherry clusters along dendrites per length of transduced axons overlapping each dendritic segment. Statistical significance was assessed by the Kruskal-Wallis test followed by the Dunn´s multiple comparison test (***p<0.001 and **p<0.01 when compared to control). n represents the number of dendritic segments analyzed from 3 independent experiments. Error bars indicate s.e.m.

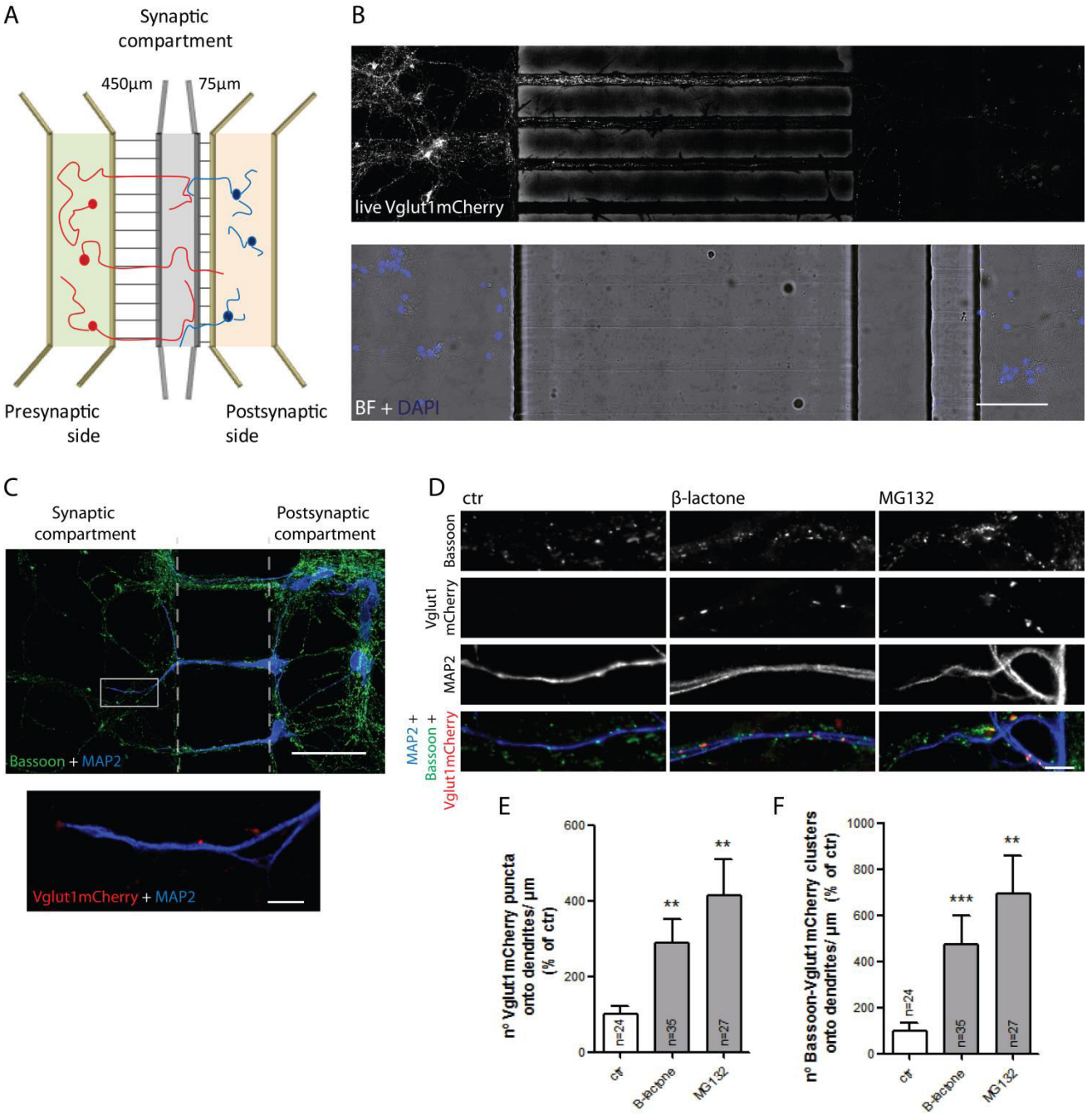

Fig. 4.3 - Increased number of axodendritic presynaptic clusters induced by local proteasome inhibition. (**A**) Tripartide microfluidic devices for compartmentalizing axodendritic synapses. In synapse formation chambers, three compartments are separated by two sets of microgrooves of different length[482]. The presynaptic compartment and the postsynaptic compartment are connected to the middle synaptic compartment by 450 µm and 75 µm microgrooves, respectively. Due to the short length of the second set of microgrooves, dendrites coming from the postsynaptic compartment reach the synaptic compartment in which they will contact with axons derived from the presynaptic compartment. (**B**) Top, expression of the presynaptic marker Vglut1mCherry by a lentiviral system on the presynaptic compartment with several growing axons extending into the synaptic compartment. Bottom, correspondent brightfield image and DAPI (blue) staining to locate neurons. The scale bar is 100 µM.

(legend continues on previous page)

Presynaptic assembly is accompanied by an *on-site* decrease in proteasome activity

Regardless some evidence that the axon and dendrite have an intrinsic capability for initiating synaptic clustering[48,67,483], the current model of synapse formation implies that contact between an axon and a dendrite is fundamental for triggering the cascade of events leading to differentiation on both sides of the synapse[167,484]. Therefore, we wondered whether contact with a postsynaptic partner would induce changes in the rate of proteasome-mediated protein degradation along the axon. To address this question, formation of stable presynaptic clusters on beads (figure 4.4) and dendrites (figure 4.5) was monitored using live-cell imaging. Neurons in microfluidic devices co-expressing Vglut1-mCherry (presynaptic reporter) and Ub^{G76V}GFP (degradation reporter) extended their axons into the axonal compartment, to which subsequent addition of beads will trigger formation of presynaptic boutons (figure 4.4A, B). Upon contact with a bead, axons responded very rapidly (20 min) with an on-bead increased intensity of the degradation reporter that remained elevated until the end of the time-lapse imaging (170 min) and was not observed in adjacent (off-bead) axonal segments (figure 4.4C, D), indicative of an *on-site* decreased proteasome activity. Because no changes in signal intensity were observed in off-bead sites throughout the experiment, we can discard the possibility of diffusion of the reporter from adjacent regions to on-bead sites. In parallel with these changes in the degradation rate, clustering of Vglut1-mCherry on-bead was also observed, however only statistically significant at later times (formation of stable clusters is observed at around 150 min of bead contact). Interestingly, post-staining for the active zone marker bassoon revealed that its clustering is enhanced on beads that were capable of rapidly decreasing local proteasome activity (figure 4.4F, G). In summary, presynaptic differentiation induced on beads is preceded by a local decrease in proteasome degradation.

We then evaluated axonal changes in proteasome activity during the formation of presynaptic clusters in axon-dendrite contacts. Cells were plated on either sides of a microfluidic chamber and presynaptic clustering was monitored on axons doubly infected with the reporters aforementioned when in contact with $MAP2^{+}$ structures (figure S4.5A, B). Imaging was performed on the compartment opposite to infection in a way of guaranteeing that the quantified signal is axon-specific, without contribution from the postsynaptic cell. We were mainly interested in quantifying changes in the axonal degradation rate occurring at the site of a newly-formed Vglut1-mCherry cluster ("new") in comparison to a pre-existing cluster ("old") on dendrites (figure S4.5C). Only clusters that after appearance remained stable at approximately the same location until the end of the time-lapse for at least 30min were considered as "new". During formation of a new stable Vglut1-mCherry cluster in an axodendritic synapse, the intensity of Ub^{G76V}GFP increased locally (figure 4.5A) with a significant increase in the ratio of its intensity between the site of clustering and a non-synaptic site (Ub^{G76V}GFP intensity on/off site ratio) (figure 4.5B, C). This response occurred simultaneously to Vglut1-mCherry clustering (t0), with a significant difference between timepoints before and after clustering was initiated (figure 4.5C). On the contrary, no local changes in the degradation reporter signal intensity were observed throughout the lifetime of an "old" puncta (figure 4.5D, E). In conclusion, assembly of an excitatory presynaptic terminal onto a postsynaptic partner is preceded and accompanied by a localized reduction in the activity of the proteasome.

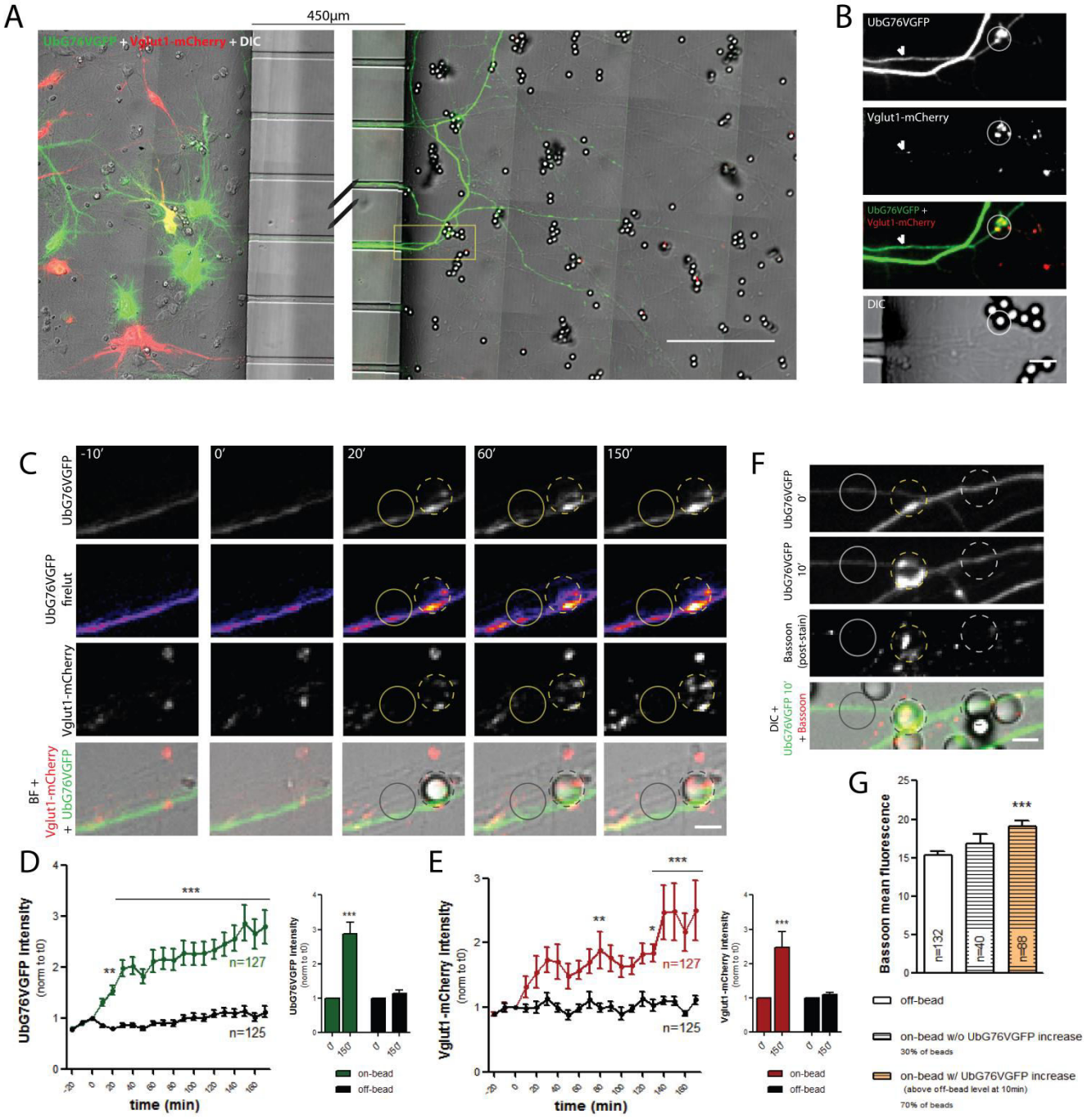

Fig. 4.4 - Rapid increase in the intensity of a degradation reporter on beads precedes clustering of presynaptic material. (**A**) Experimental set-up to monitor axonal changes upon bead contact. Dual sindbis viral expression for the presynaptic reporter Vglut1mCherry (red) and the degradation reporter $Ub^{G76V}GFP$ (green) on the somal side of microfluidic devices. Infected axons reached the axonal compartment, and subsequently beads were added and their effect on the contacting axon monitored using live-cell imaging. The signal for $Ub^{G76V}GFP$ and Vglut1mCherry was differently adjusted between right and left image to prevent over-saturation of signal at the soma level. The scale bar is 100 µm. (**B**) Enlarged image of yellow box in (**A**) showing a dually infected axon (GFP^+ and $mCherry^+$, arrowhead) extending into the axonal compartment and establishing a contact with a bead (white circle). The scale bar is 10 µm. (**C**) Profile of proteasome activity rate and presynaptic clustering on bead. Individual frames of a time-lapse series showing the initial contact of a bead (dashed circle) with a dually infected

axon and its *on-site* effect on the reporters aforementioned. Bead contact resulted in a rapid decrease in proteasome activity, as evidenced by an increase in the local intensity of the degradation reporter, and later clustering of Vglut1mCherry, which were not observed in an off-bead axonal site (solid circle). The scale bar is 5 µm. (**D**, **E**) Left, quantification of (**D**) Ub^{G76V}GFP intensity and (**E**) Vglut1mCherry intensity on beads (on-bead) and adjacent sites (off-bead) throughout time. Results are normalized to the reporter intensity at t0 (0min), which corresponds to the frame before addition of beads. Statistical significance was assessed by 2-way ANOVA (***p<0.001 , **p<0.01 and *p<0.05 between on and off-bead at each time point). n represents the number of beads analyzed and equivalent off-sites from 3 independent experiments. Right, comparison of intensity values at t0 and 150min after beads were added for both on and off-bead sites. Statistical analysis was performed by Wilcoxon paired t-test (***p<0.001 when compared to the correspondent t0 value). (**F**) Post-hoc clustering of active zone material on beads that reduced axonal proteasome activity. Following the time-lapse (4-5 h after addition of beads), cultures were fixed and stained for Bassoon (red). Clustering of Bassoon was more pronounced on beads at which increased intensity of Ub^{G76V}GFP at 10 min was detected (yellow vs. white dashed circle). Solid circle indicates an off-bead site. Scale bar is 5 µm. (**G**) Quantitative Bassoon intensity values in off and on-bead sites. Beads were divided according to their capacity to increase Ub^{G76V}GFP intensity in the contacting axon above off-bead levels at 10 min (approximately 70% and 30% of beads with and without increases in Ub^{G76V}GFP intensity, respectively). Results are expressed as raw intensity values and averaged from 3 independent experiments. Statistical significance was assessed by the Kruskal-Wallis test followed by the Dunn´s multiple comparison test (***p<0.001 when compared to off-bead). n represents the number of beads analyzed and equivalent off-sites. Error bars indicate s.e.m.

(image on next page)

Fig. 4.5 (continued) (**A**) Simultaneously to the formation of a Vglut1 cluster, a localized increased intensity of the degradation reporter was observed at the site of clustering (white dashed box) as opposed to adjacent axonal sites (yellow dashed box). Scale bar is 5 µm. (**D**) No local changes in Ub^{G76V}GFP intensity were observed throughout the lifetime of an "old" Vglut1 cluster or in regions adjacent to the cluster site (white and yellow dashed boxes, respectively). Scale bar is 5 µm. (**B**, **E**) Time courses of the changes in: Vglut1mCherry intensity on sites of clustering (on-site, red line) and adjacent sites (off-site, brown line) normalized to t0; and the on/off site ratio of Ub^{G76V}GFP intensities (green line). For (**B**) and (**E**) t0 corresponds to the frame right before clustering was initiated and the beginning of the time-lapse, respectively. Statistical significance was assessed by 2-way ANOVA for Vglut1mCherry ($^{\#}$p<0.05 on vs. off-site at each time point) and by Kruskal-Wallis test for Ub^{G76V}GFP ratio. (**C**) Comparison of on/off site Ub^{G76V}GFP ratio at -40, 0, 10 and 60 min. Statistical analysis was performed by Kruskal-Wallis test followed by the Dunn´s multiple comparison test (*p<0.05 in comparison to -40 min). (**B**, **C**, **E**) Results are averaged from 3 independent experiments. n represents the number of Vglut1mCherry clusters analyzed. Error bars indicate s.e.m

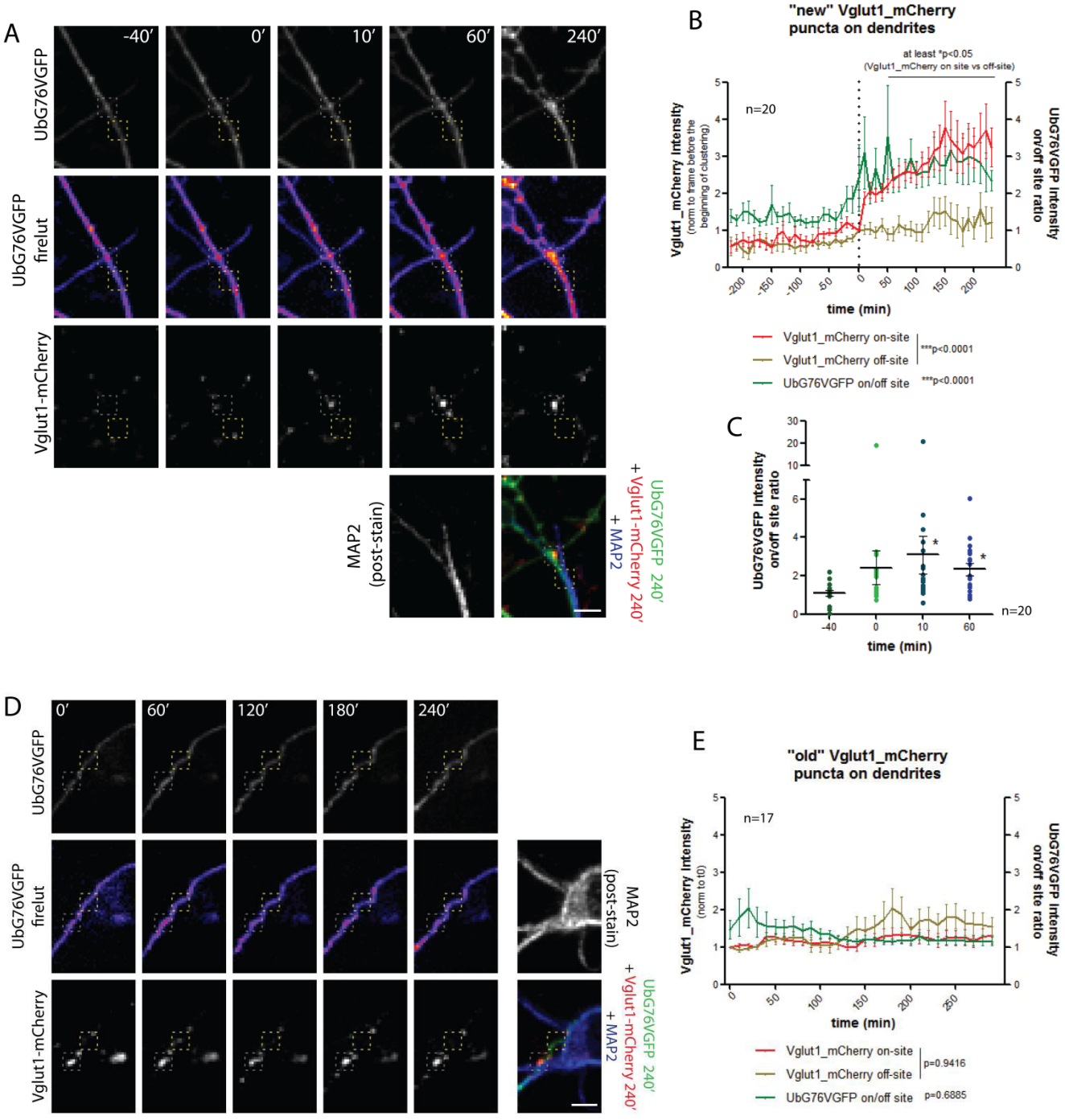

Fig. 4.5 - Axonal *on-site* decreased proteasome activity during formation of a stable Vglut1 cluster on dendrites. (**A**, **D**) Changes in the axonal rate of proteasome activity upon SV clustering on dendrites. Dually infected axons expressing both Ub^{G76V}GFP and Vglut1mCherry were imaged every 10 min for at least 5 h in the microfluidic devices' compartment opposite to viral infection. See figure S4.5 for further details of the live-imaging experimental set-up. Close attention was given to (**A**) newly-formed Vglut1mCherry clusters on MAP^+ somatodendritic structures that remained stable until the end of the time-lapse (for at least 30 min), designated "new Vglut1-mCherry puncta on dendrites"; and to (**D**) Vglut1-mCherry clusters on dendrites that were present at the beginning and persisted throughout the entire time-lapse at the same location, designated "old Vglut1-mCherry puncta on dendrites".

(legend continues on previous page)

Presynaptic accumulation of ubiquitinated conjugates as the trigger for presynaptic differentiation

Evidence indicates that proteasome inhibitors have a great impact on the normal function of the presynaptic terminal[384–386,412,485]. However, a full comprehension of the mechanism underlying the effect of proteasome inhibitors at this neuronal compartment is still lacking. While some studies argue that their effect is dependent on increased levels of active zone proteins that are UPS targets[385,485], others attribute a role for altered ubiquitination dynamics[384]. In fact, blocking the proteasome triggered an extensive accumulation of ubiquitinated proteins that are no longer degraded (figure S4.6). To begin to unmask the local mechanism whereby axonal inhibition of the proteasome generates new presynaptic clusters, we asked whether such an accumulation of proteins would be dependent on additional synthesis. Indeed, not only the requirement of local protein synthesis for the formation of the presynapse[486,487], but also a strict interplay between local synthesis and degradation in neuritic compartments[433,435,488], have already been demonstrated. However, when the proteasome was inhibited along with protein synthesis inhibitors (10 µM emetine and 10 µM anisomycin) on the axonal compartment, formation of presynaptic clusters was still elicited (figure 4.6A, B and S4.7A). Therefore, we concluded that the presynaptogenic effect of proteasome inhibitors is not dependent on newly-synthesized proteins.

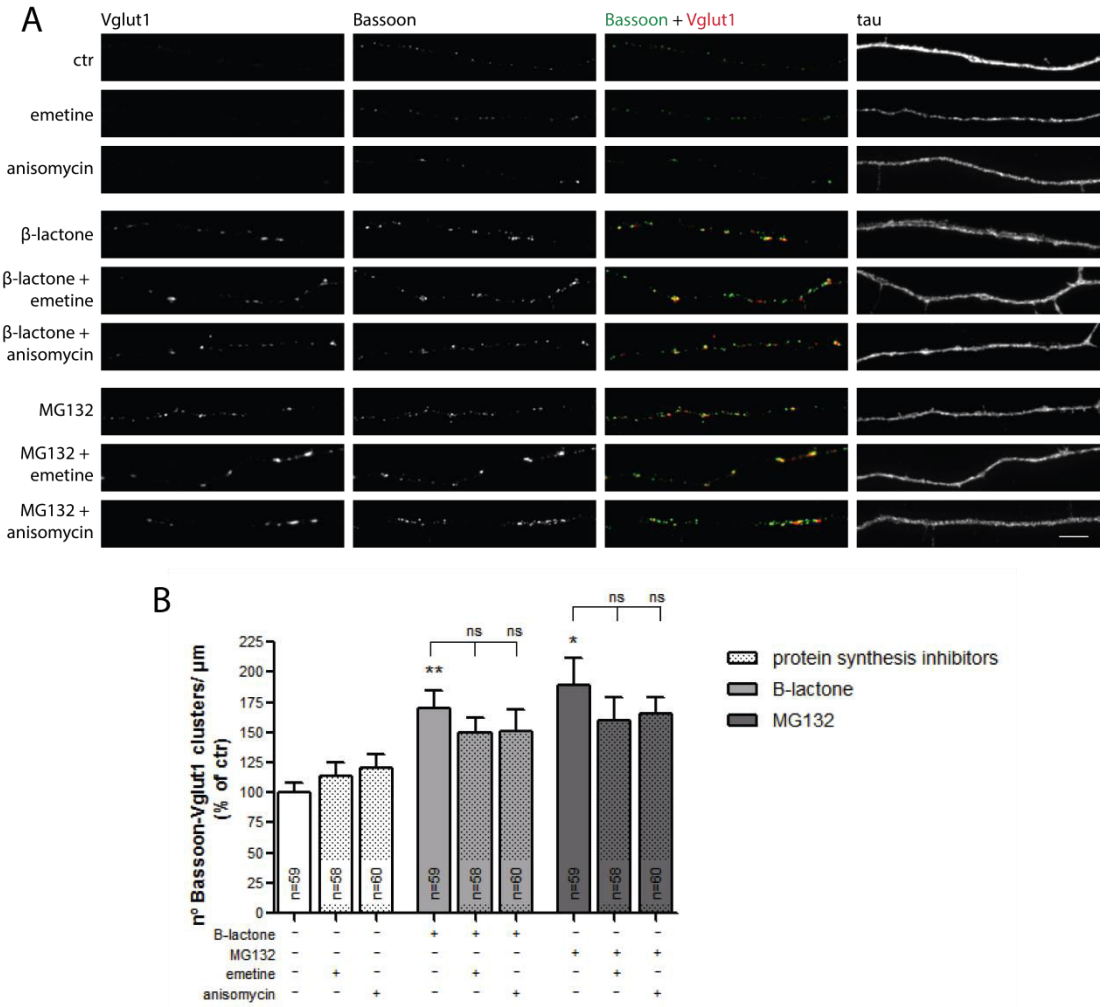

Fig. 4.6 - The presynaptogenic effect of proteasome inhibition is protein synthesis independent. (**A**) Dependence of proteasome inhibitors-induced presynaptic assembly on newly-synthesized proteins. At

DIV 7, the axonal compartment of microfluidic devices was treated with protein synthesis inhibitors [emetine (10 µM) or anisomycin (10 µM)] or proteasome inhibitors alone or in combination for 1 h, then fixed and immunostained for the presynaptic markers Bassoon (green) and Vglut1 (red). Inhibition of protein synthesis did not revert the proteasome inhibition-induced increase in the number of presynaptic clusters. The scale bar is 5 µm. (**B**) Quantitative summary data of the number of presynaptic clusters (Bassoon-Vglut1) per axonal length. Results are expressed as % of control and are averaged from 5 independent experiments. Statistical significance was assessed by the Kruskal-Wallis test followed by the Dunn´s multiple comparison test (**p<0.01 and *p<0.05 when compared to the control). n represents the total number of analyzed microscope FOVs to the axonal side. Error bars indicate s.e.m.

Next, we wondered whether the effect would be dependent on *de novo* ubiquitination of proteins. To accomplish so, we used an inhibitor of the E1 ubiquitin-activating enzyme, ziram. This UPS inhibitor reduces E1 activity by preventing formation of E1-ubiquitin conjugates, thus compromising the subsequent steps of ubiquitination[384,489]. However, this inhibitor does not affect proteasome 20S proteolytic activity[384,489]. Ziram inhibited degradation of the Ub^{G76V}GFP reporter (data not shown) that is required to be ubiquitinated before being targeted to the proteasome, as elsewhere reported[489]. Accordingly, in a ziram-treated condition preubiquitinated proteins are still degraded, but degradation of non-ubiquitinated conjugates, still in need of the addition of the first ubiquitin, does not occur. Treatment of isolated axons with ziram alone (1 µM) had no effect on the number of presynaptic clusters (figure 4.7A, B and S4.7B, C). Because E1 inhibition also results in accumulation of non-degraded proteins, the lack of effect of ziram is indicative of a role for the pool of ubiquitinated conjugates that accumulate after proteasome inhibition. Moreover, when proteasome inhibitors were applied in combination with ziram, a complete reversion of their presynaptic assembly effect was observed (figure 4.7A, B and S4.7B, C). This clearly demonstrated us that ubiquitination, and most probably accumulation of proteins in their ubiquitinated state, is required for local proteasome inhibition-induced presynaptogenesis. To further validate this hypothesis, we used a broad-range inhibitor of DUBs, PR619[490], which inhibits removal of Ub chains. Similarly to proteasome inhibitors but without interfering with its activity, PR619 (1 µM) incubation led to an accumulation of ubiquitinated conjugates[491] (figure S4.6C, D). Notably, it also increased the number of presynaptic clusters along axons (figure 4.7C, D and figure S4.7D, E). This increase had the same magnitude as the increase induced by proteasome inhibition, yet the combined treatment did not further enhance the effect (figure 4.7C, D and figure S4.7D, E). Most probably because both inhibitors act through the same mechanism, which might be already saturated. This last set of data showed that accumulation of ubiquitinated conjugates is sufficient to induce presynaptic clustering. We further evaluated the capacity of PR619 to give rise to new functional presynaptic sites by using the live FM dye protocol (figure 4.2A). Local inhibition of deubiquitination resulted in a significant increase in the number of new functional FM puncta on beads (figure 4.7E, F). Altogether, we conclude that the pool of ubiquitinated proteins that accumulates after localized proteasome blocking works as the trigger for presynaptic assembly.

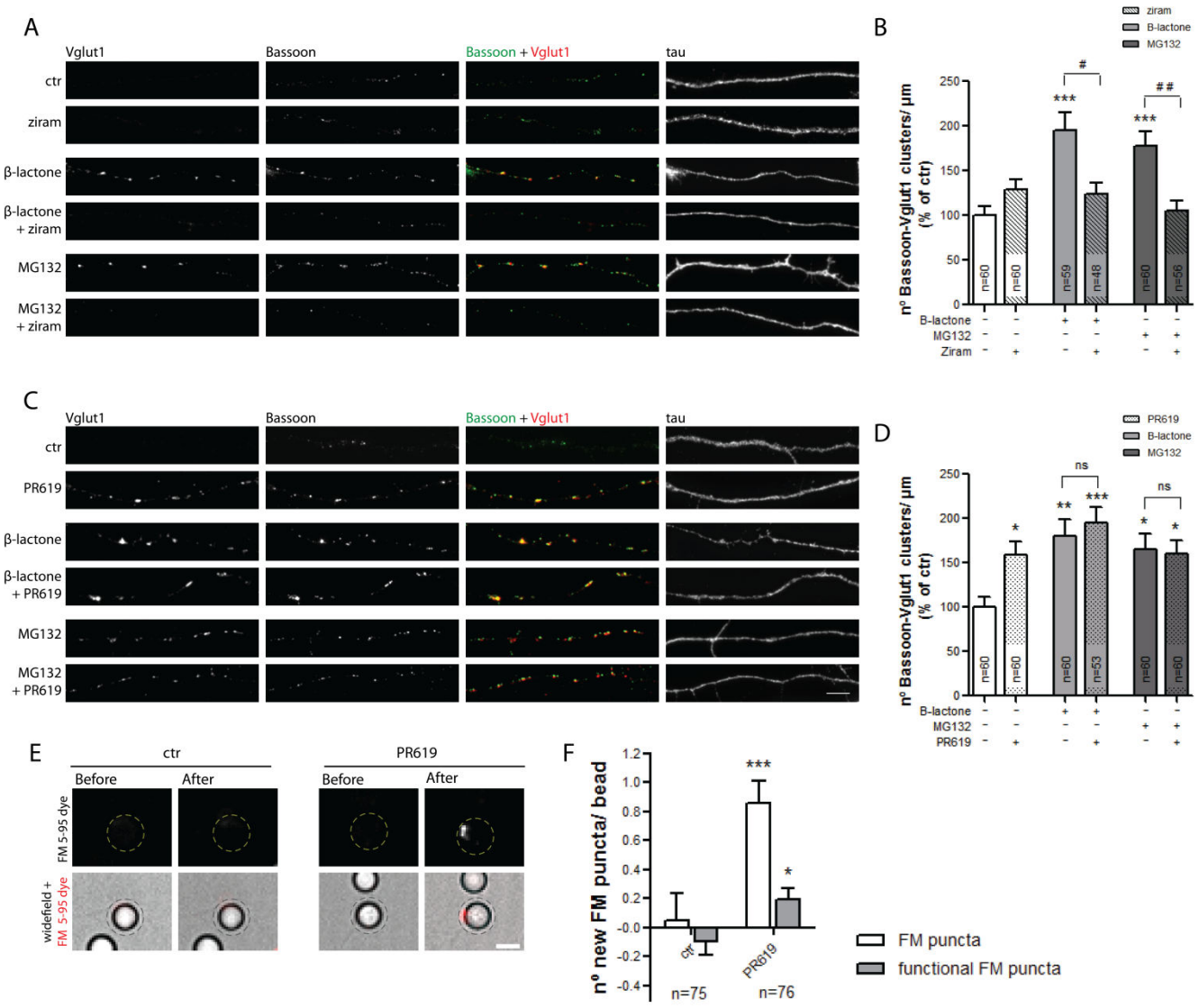

Fig. 4.7 - Accumulation of ubiquitinated conjugates is required and sufficient to induce formation of presynaptic clusters. (**A**, **C**) Effect of E1 and DUBs inhibition on basal and proteasome inhibitors-induced presynaptic clustering. At DIV 7, the axonal compartment of microfluidic devices was treated with (**A**) ziram (1 µM), an E1 inhibitor, or with (**C**) PR619 (1 µM), an inhibitor of DUBs. In addition, these inhibitors were applied in combination with proteasome inhibitors. Cultures were stained for Bassoon (green), Vglut1 (red) and tau (white). (**A**) The presynaptogenic effect of proteasome inhibition was completely abolished when E1-mediated ubiquitination was prevented. (**C**) PR619, which upregulated accumulation of ubiquitinated conjugates (figure S4.6), locally boosted formation of presynaptic clusters in a way similar to proteasome inhibitors. The scale bars are 5 µm. (**B**, **D**) Quantitative summary data of the number of presynaptic clusters (Bassoon-Vglut1) per axonal length. Results are expressed as % of control and are averaged from 5 independent experiments. Statistical significance was assessed by the Kruskal-Wallis test followed by the Dunn´s multiple comparison test (***p<0.001, **p<0.01 and *p<0.05 when compared to the control and $^{\#\#}$p<0.01 and $^{\#}$p<0.05 between indicated bars). n represents the total number of analyzed microscope FOVs from the axonal side. Error bars indicate s.e.m. (**E**) Outcome of PR619 on the formation of active terminals. Formation of new functional presynaptic clusters on beads by PR619 was assessed using the live FM dye protocol (see figure 4.2). PR619 led to an increase in the formation of total and functional FM puncta on beads. The scale bar is 5 µm. (**F**) Quantitative data presented as the number of new FM puncta per bead obtained by subtracting the number of FM puncta before and after treatment, both for total and active puncta. Statistical

significance was assessed by the Kruskal-Wallis test followed by the Dunn´s multiple comparison test (***p<0.001 and *p<0 .05 when compared to control). n represents the number of beads analyzed from 3 independent experiments. Error bars indicate s.e.m.

Considering that contact with a postsynaptic partner induced an *on-site* decreased activity of the proteasome coincident with the moment of presynaptic assembly (figure 4.4 and 4.5), we asked whether ubiquitinated conjugates accumulate at sites of newly-formed presynaptic clusters. It is widely known that lysine 48 (K48)-linked polyubiquitin chains function as a tag, targeting substrates for proteasomal degradation. In accordance, we and others[277] observed a robust upregulation of K48 polyubiquitinated proteins upon proteasome inhibition (figure S4.6E, F). To detect accumulation of polyubiquitinated conjugates bearing this type of Ub chain, cultures were stained with an antibody specific for polyubiquitin chains linked through K48 (Apu2)[492]. In control conditions, K48 polyubiquitin staining had a diffuse pattern along the axon shaft, however, upon treatment with both proteasome inhibitors and PR619, but not ziram, a pronounced concentration of K48 ubiquitin signal was observed in presynaptic clusters (figure 4.8A, B). This revealed that at sites of clustering of presynaptic material, intense accumulation of polyubiquitinated conjugates occurs. Interestingly, immunoblot analysis of synaptosomal preparations showed that synaptic expression of K48 Ub chains is higher at developmental stages coincident with the peak of synaptogenesis in the hippocampus[493] (figure 4.8C). This result is in agreement with data from whole brain extracts, in which a similar pattern is observed[259]. We next asked whether contact with a postsynaptic partner induces accumulation of K48 polyubiquitinated proteins in the contacting axon. To address this issue, we made use of presynaptic differentiation-inducing beads added to the axonal compartment of microfluidic devices. A higher intensity of K48 polyubiquitin signal on beads in comparison to an off-bead adjacent site was observed (figure 4.8D, E). Altogether, these data demonstrate that polyubiquitinated conjugates bearing the tag for proteasome degradation accumulate at nascent presynaptic sites.

To study the dynamics of K48 polyubiquitin accumulation on beads, the constructs for ubiquitination-induced fluorescence complementation (UiFC)[415], which allow for its live detection, were expressed and validated in neurons (figure S4.8). UiFC consists of two constructs (UiFC-C and UiFC-N) each bearing ubiquitin interacting motifs (UIMs) fused to either the N- or C-terminal non-fluorescent fragments of venus. Upon polyubiquitination, interaction of UIMs with growing chains reconstitutes venus fluorescence. It was shown to preferentially detect K48 ubiquitin chains[415]. Under basal conditions, puncta of UiFC were present both in the cell body and axons (figure S4.8B). Further analysis indicated that these aggregates were relatively stable in the axonal shaft (figure S4.8E, F), possibly corresponding to hot-spots of accumulation of polyubiquitinated conjugates. Bead contact induced in isolated axons a rapid (10 min) local increase in the intensity of our polyubiquitination reporter, UiFC, as opposed to adjacent sites (figure 4.9A, B). The dynamics of accumulation of K48 polyubiquitin conjugates on beads correlated remarkably with the local decrease in the activity of the proteasome previously discussed (figure 4.4). Furthermore, the proportion of beads with an increased intensity of Ub^{G76V}GFP and UiFC in contacting axons was equal, 70% for both (figure 4.4G and figure 4.9D). We thus propose that accumulation of K48 ubiquitin signal on beads is the result of a halt in local degradation of proteins. In line with this, clustering of Bassoon was enhanced on beads that were capable of rapidly increasing UiFC signal (figure 4.9C, D), thus revealing an association between presynaptic clustering and accumulation of polyubiquitinated conjugates.

Altogether, these data suggest that an accumulation of polyubiquitinated conjugates at sites of nascent presynases, in response to a local halt in proteasome degradation, functions as the trigger for presynaptic clustering.

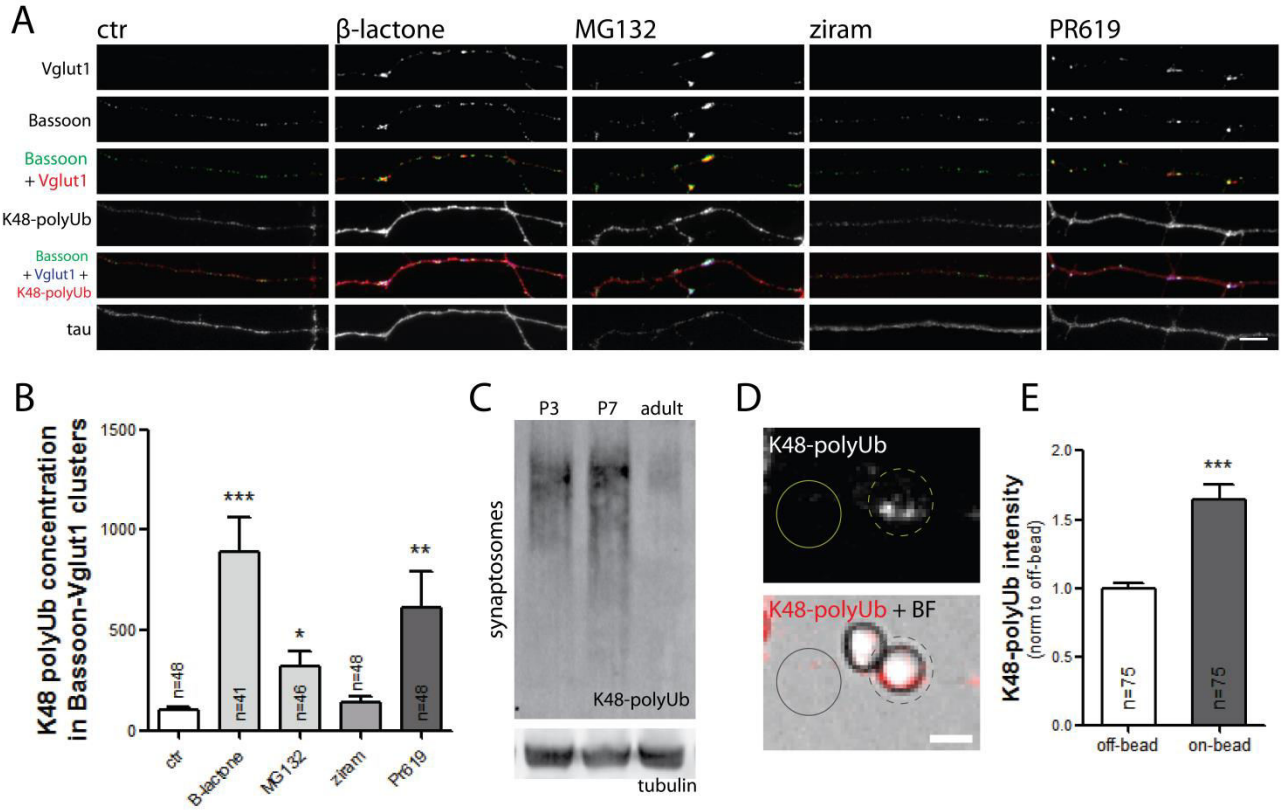

Fig. 4.8 - Presynaptic accumulation of K48 ubiquitinated conjugates correlates with presynaptic assembly. (**A**) Assessment of K48 polyubiquitin concentration on presynaptic clusters upon proteasome, E1 and DUBs inhibition. Isolated axons in microfluidic devices were treated for 1 h with β-lactone, MG132, ziram, PR619 or vehicle, and immunocytochemistry was performed for the presynaptic markers Bassoon (green) and Vglut1 (red and blue) and for K48 polyubiquitin chains (Apu2 antibody) (red). Proteasome inhibitors and PR619 induced an accumulation of K48 polyubiquitin signal on newly-formed presynaptic clusters. The scale bar is 5 µm. (**B**) Quantification of K48 polyubiquitin signal intensity in presynaptic clusters (Bassoon-Vglut1). Results are expressed as % of control and are averaged from 4 independent experiments. Statistical significance was assessed by the Kruskal-Wallis test followed by the Dunn´s multiple comparison test (***p<0.001, **p<0.01 and *p<0.05 when compared to the control). n represents the total number of analyzed microscope FOVs from the axonal side. Error bars indicate s.e.m. (**C**) Developmental profile for the expression of K48 polyubiquitinated conjugates in synaptosomes. Representative immunoblot of K48 ubiquitin chains from synaptosomal preparations of P3, P7 and adult rats in a 4-15% gradient gel. Tubulin was used as loading control. The expression of K48 ubiquitinated conjugates in the presynaptic compartment is upregulated at early postnatal development in comparison to adult. (**D**) Effect of beads on the accumulation of K48 polyubiquitin conjugates along axons. Addition of beads to the axonal compartment for 4-5 h resulted in an accumulation of K48 ubiquitinated conjugates on-bead as opposed to an off-bead site. The scale bar is 5 µm. (**E**) Quantitative values of K48 ubiquitin signal intensity on vs. off-bead. Results are normalized to off-bead values and are averaged from 3 independent experiments. Statistical significance was assessed by Wilcoxon paired t-test (***p<0.001).

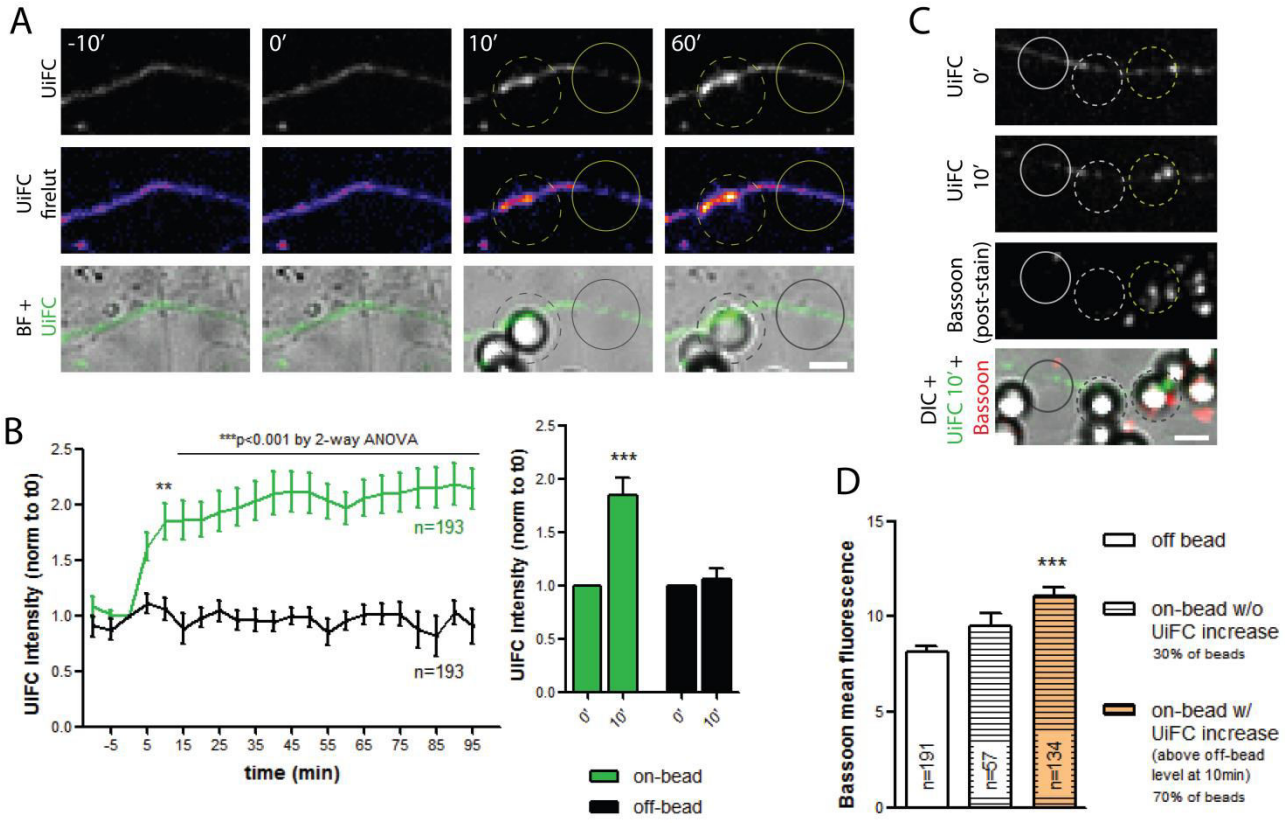

Fig. 4.9 - **Live accumulation of K48 ubiquitin chains on beads.** (**A**) Profile of polyubiquitin accumulation and presynaptic clustering on beads. UiFC plasmids[415] (see figure S4.8) were transfected in neurons grown in microfluidic chambers in order to later monitor live accumulation of K48 ubiquitin chains on beads. Individual frames of a time-lapse series showing the initial contact of a bead (dashed circle) with a UiFC-expressing axon (green). Bead contact resulted in a rapid and strong increase in the local intensity of UiFC signal, as opposed to an off-bead site (solid circle). Scale bar is 5 µm. (**B**) Left, quantification of UiFC intensity at bead (on-bead) and adjacent sites (off-bead) throughout time. Results are normalized to the reporter intensity at t0 (0 min), which corresponds to the frame before addition of beads, and are averaged from 2 independent experiments. Statistical significance was assessed by 2-way ANOVA (***p<0.001 , **p<0.01 between on and off-bead at each time point). Right, comparison of intensity values at t0 and 10min after beads were added for both on and off-bead sites. Statistical analysis was performed by Wilcoxon paired t-test (***p<0.001 when compared to the correspondent t0 value). (**C**) Post-hoc clustering of active zone material. Similarly to figure 3F,G, retrospective immunostaining for Bassoon (red) was performed. Clustering of Bassoon was higher on beads that displayed increased intensity of UiFC at 10 min (yellow vs. white dashed circle). Solid circle indicates an off-bead site. Scale bar is 5 µm. (**D**) Quantitative Bassoon intensity values in off and on-bead sites. Results are expressed as raw intensity values and averaged from 2 independent experiments. Statistical significance was analyzed by the Kruskal-Wallis test followed by the Dunn´s multiple comparison test (***p<0.001). (**E**, **G**, **I**) n represents the number of beads analyzed and equivalent off-sites. Error bars indicate s.e.m.

A role for proteolytic-related polyubiquitin chains in presynaptic assembly

Considering the results gathered so far, we hypothesized that an accumulated pool of polyubiquitinated proteins functions as a signal for presynaptic differentiation. Accordingly, we predicted a role for polyubiquitin chains (mostly K48-linked) in the assembly of presynaptic sites. Ubiquitination can occur in cells in a variety of different forms (mono, multi or polyubiquitination) that control distinct biological events[247]. The formation of polyubiquitin chains on substrates, in which ubiquitin molecules are attached to each other, can occur at any of the lysines present in Ub, K6, K11, K27, K29, K33, K48 and K63[494]. Whilst K48 polyubiquitination has widely been recognized as a target for proteasome degradation, K63 ubiquitin chains have a role in non-degradative pathways in cells such as DNA repair, kinase activation, signal transduction and endocytosis[247]. Less is known about the remaining types of chains, however recent data reveal that degradation of substrates can also be triggered by assembling of K11-linked Ub chains[277,281,293,495]. Furthermore, all non K63 polyubiquitin chains accumulate upon proteasome inhibition, thus suggesting their involvement in the targeting of proteins to the proteasome[277,496,497]. We generated Sindbis virus expressing wtUb and mutant forms of Ub that prevent polyubiquitination onto different lysines, by their mutation into arginine (UbK11R, UbK29R, UbK48R and UbK63R). As expected, all constructs elevated ubiquitin levels in neurons both in somas and axons in comparison to the eGFP control (figure S4.9A, B). Expression of Ub constructs also induced accumulation of conjugated Ub in cells that was prevented if the specific Ub mutant was expressed (figure S4.9C, D). This validation was performed by staining for K48 polyubiquitin, nevertheless we assume that the same holds true for all the other mutants. Expression of wtUb in neurons residing in microfluidic devices strongly increased the number of presynaptic clusters (figure 4.10A, B and figure S4.10A, B). Surprisingly, prevention of K11, K29 and K48 polyubiquitination completely suppressed presynaptic clustering, as opposed to the K63 mutant (figure 4.10A, B and figure S4.10A, B). We thus concluded that upregulation of polyubiquitinated conjugates upon expression of Ub triggers presynaptic assembly. Interestingly, all ubiquitin chains with expected roles in proteasome degradation (K11, K29 and K48), but not the non-proteolytic K63, were required. Both proteasome inhibition and prevention of protein polyubiquitination reduce global protein degradation. The difference resides in the state of the substrates being accumulated in cells: polyubiquitinated vs. mono or non-ubiquitinated. Accordingly, the lack of presynaptogenic effect of UbK48R (or UbK11R) further supports the hypothesis that the effect of proteasome inhibitors is attributed to the remaining pool of polyubiquitinated substrates. We hereby demonstrate that K11, K29 and K48 polyubiquitinated proteins in this pool are the triggers for formation of presynaptic clusters.

Lastly, we evaluated the formation of functional presynaptic sites upon expression of Ub mutants on beads (figure 4.10C, D) and dendrites (figure 4.10E, F). In axons expressing wtUb or its mutant forms, beads were added and the FM dye loading/unloading protocol was performed. Although not statistically significant, the formation of active terminals on beads upon expression of wtUb and its mutant forms showed a similar trend to the clustering observed in isolated axons (figure 4.10C, D and S4.10C). We finally analyzed the density of functional presynaptic sites along dendrites. Amazingly, elevation of Ub levels in cultures increased the number of functional FM puncta per dendritic length, which was completely reverted when K48 and K11 polyubiquitination were prevented, but not K29 and K63 (figure 4.10E, F). Changes in the number of FM functional sites were accompanied by equal changes in the number of total FM puncta along dendrites (figure S4.10D). In contrast to isolated axons, K29 ubiquitination was not relevant in the context of presynaptic formation on an axodendritic synapse. Taken together, this last set of results underscores a role for proteasome-related polyubiquitin chains (mostly K11 and K48) in presynaptic differentiation.

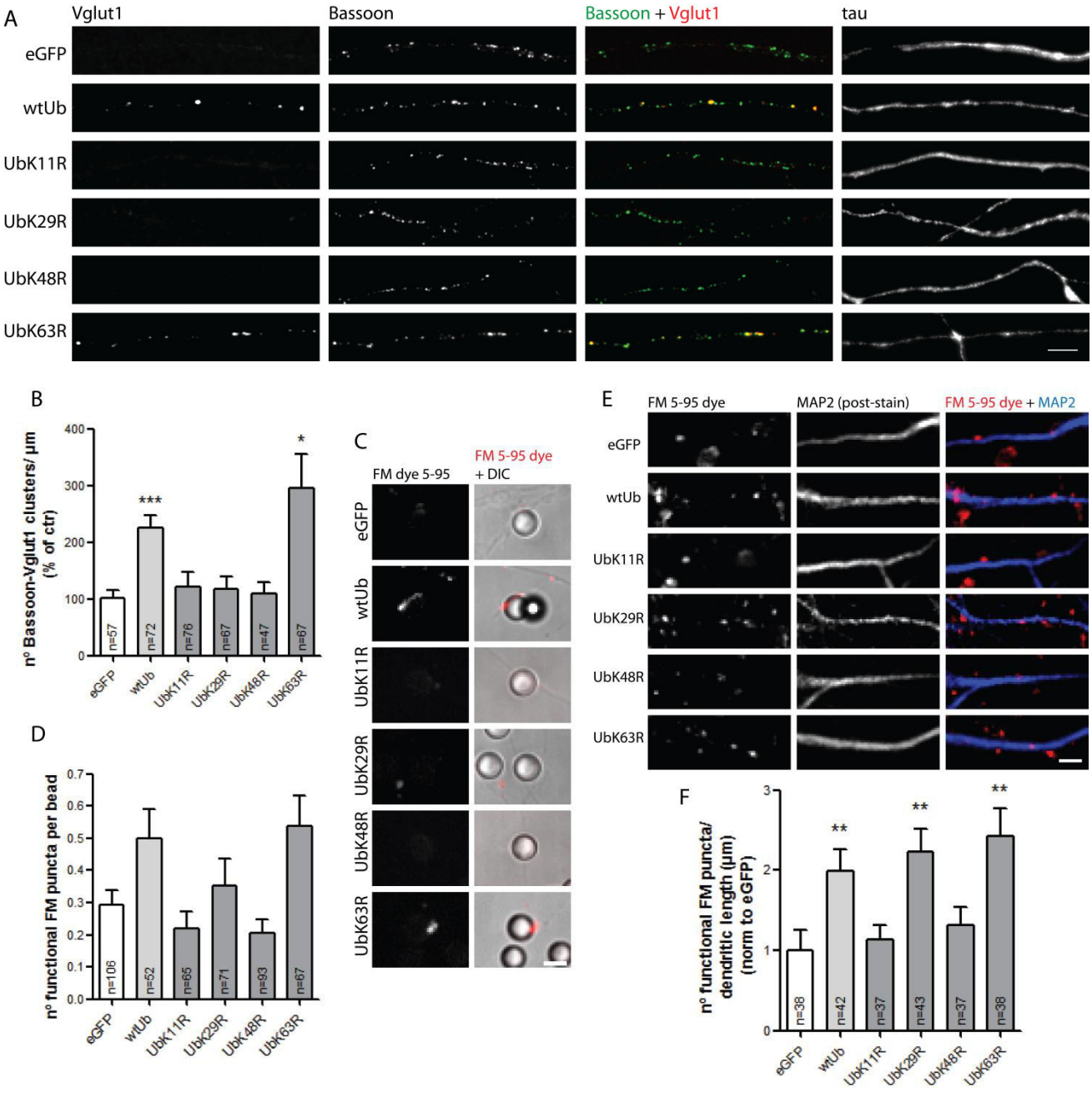

Fig. 4.10 - K48 and K11 polyubiquitination trigger formation of presynaptic clusters. (**A**) Contribution of polyubiquitin chains of different topologies to presynaptic assembly. Neurons in microfluidic devices were infected with Sindbis virus expressing wtUb and mutant forms of ubiquitin that prevent polyubiquitination on specific lysines (UbK11R, UbK29R, UbK48R, UbK63R). The empty vector expressing eGFP was used as control. Overexpression of wtUb led to the formation of presynaptic clusters along the axon, which was abolished when K11, K29 and K48 polyubiquitination was compromised. The scale bar is 5 µm. (**B**) Quantitative data of the number of presynaptic clusters (Bassoon-Vglut1) per axonal length. Results are expressed as % of control and are averaged from 5 independent experiments. Statistical significance was assessed by the Kruskal-Wallis test followed by the Dunn´s multiple comparison test (***p<0.001 and *p<0.05 when compared to eGFP). n represents the total number of analyzed microscope FOVs from the axonal side. Error bars indicate s.e.m. (**C**) Effect of lysine-specific polyubiquitination on the number of active terminals. To look for the formation of functional presynaptic terminals, beads were added to the axonal compartment for 4-6 h and an FMdye loading/unloading protocol was performed. The scale bar is 5 µm. (**D**) Quantitative data presented as

the number of functional FM puncta per bead. Statistical significance was assessed by the Kruskal-Wallis test. n represents the number of beads analyzed from 4 independent experiments. Error bars indicate s.e.m. (**E**) Contribution of polyubiquitin chains of different topologies to the formation of functional presynaptic sites onto dendrites. The FM dye loading/unloading protocol was performed on the somal side of microfluidic devices at DIV 7 after viral infection with the Ub constructs. Under the brightfield light, positions to image were carefully chosen to include nearly the same number of cell bodies. Dendrites were detected by retrospective immunocytochemistry for MAP2 (blue). By increasing neuronal Ub levels, an increase in the number of FM puncta along dendrites is observed, which does not occur for UbK11R and UbK48R mutants. (**F**) Quantification of the number of functional FM puncta (capable of unloading 5% of their content after 1 min of electrical stimulation) per dendritic length. Results are normalized to eGFP and averaged from 2 individual experiments. Statistical significance was assessed by the Kruskal-Wallis test followed by the Dunn´s multiple comparison test (**$p<0.01$ when compared to eGFP). n represents the total number of dendrites. Error bars indicate s.e.m.

Discussion

In this study we unmask a new *on-site* UPS-related mechanism controlling the formation of presynaptic sites. Our results show that local inhibition of the proteasome increases the density of presynaptic clusters along the axon. Due to the nature of our experimental system (compartmentalized axons), we believe that this is an axon specific and intrinsic response, and so, it will allow us to disclose the axonal intracellular signaling pathways triggering recruitment and clustering of presynaptic material. Remarkably, formation of a presynaptic cluster onto a postsynaptic partner is accompanied by a local decrease in protein degradation by the proteasome. In an attempt to understand the mechanism underlying this phenomenon, we identified the resultant pool of polyubiquitinated proteins as a novel trigger of presynaptic differentiation. Indeed, polyubiquitinated conjugates bearing the tag for proteasome degradation (K48 ubiquitin chains) concentrate at nascent presynaptic sites. Finally, we have identified proteolytic-related ubiquitin chains (mostly K11 and K48) as important players. Taken together, we propose a model where local reduction of proteasome activity leads to a localized increase in polyubiquitinated proteins, which triggers clustering of presynaptic material and subsequently presynaptic formation (figure 4.11).

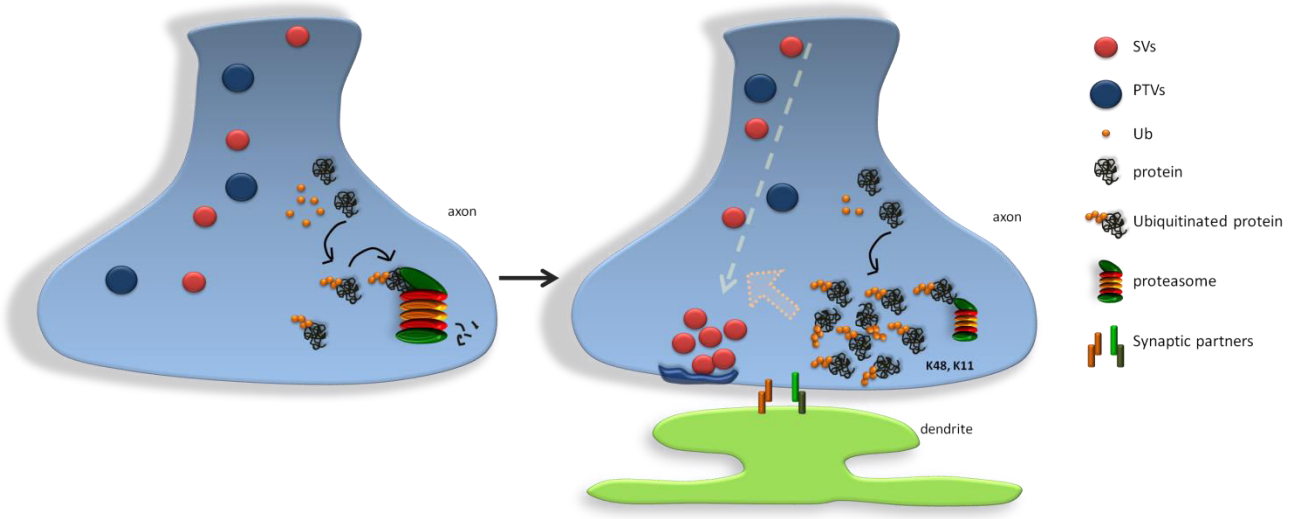

Fig. 4.11 - Proteasome inhibition triggers presynaptic assembly by *on-site* accumulation of polyubiquitinated conjugates. According to our current model, upon contact with a postsynaptic partner, transitory and *on-site* inhibition of the proteasome results in a localized accumulation of polyubiquitinated conjugates that will trigger recruitment and clustering of presynaptic material and their proper organization into a functional presynaptic terminal.

An interesting fact lies on the developmentally-regulated nature of proteasome activity. In the rat brain, all three proteasome proteolytic peptidases are highly active during the first postnatal week with subsequent loss of function observed in the young rat (2-4 months)[498]. Also, UPS components are upregulated at this development time-point and high concentrations of K48 tagged proteins are observed in brain extracts[259]. Moreover, in the *Drosophila* embryo, K48 and K11 ubiquitin chains represent 57% and 11%, respectively, of the neuronal ubiquitome[242]. Altogether, these studies demonstrate that at stages

corresponding to synaptogenesis the UPS is highly active in the brain. Our results show a clear and robust increase in the density of presynaptic clusters along axons in response to proteasome inhibition (figure 4.1, 4.2 and 4.3). Accordingly, we hypothesize that in the young brain a high proteasome activity might be functioning as a constraint on the formation of presynaptic sites, that will be relieved upon spatially and temporally controlled inhibition of the proteasome. In line with this hypothesis, the Wnt signaling pathway, known to induce clustering of SVs[147], acts by preventing constitutive degradation of proteins. Without directly affecting the proteasome, activation of Frizzled-Lrp5/6 complex by Wnt proteins inactivates the kinase responsible for β-catenin phosphorylation and subsequent proteasome-degradation[499–502]. It was also previously suggested by Martin and colleagues that in *Aplysia* proteasome activity restrains synaptic strength in mature neurons[386]. In this same study, authors observed an increase in the number of presynaptic boutons on motor neurons upon 24h-treatment with β-lactone[386], which correlates with the synaptogenic effect of proteasome inhibitors in our model system. The different biological organisms and the fact that in our study axons were deprived from soma-derived synaptogenic stimuli, may account for the difference in the time of proteasome inhibition required to generate new presynaptic sites (24h vs. 1h). We thus conclude that a transient and local brake in proteasome activity during brain development may trigger the initial cascade of events culminating in the differentiation of the presynaptic terminal.

The idea that local decreased proteasome activity dictates the onset of presynaptogenesis, implies that the developing axon has ways of promoting endogenous inhibition of the proteasome. Although we do not approach this issue throughout this work, several studies indicate that proteasome function can be regulated. Dynamic modifications of the proteasome such as phosphorylation, o-glycosilation, cleavage by caspases or disassembly of the 20S and 19S subcomplexes can alter proteasome activity[503]. In neurons, activation of the NMDA receptor causes disassembly of the 26S proteasome with a decline in its activity[504,505]. Moreover, the proteasome can be negatively regulated by cleavage of the Rpn10 subunit in response to mitochondrial dysfunction[506]. At the postsynaptic level, proteasome function is upregulated by phosphorylation of one of its subunits, Rpt6, by CaMKII in an activity-dependent manner[440,466]. Although the phosphatase responsible for its dephosphorylation and consequent downregulation of proteasome activity has not yet been identified, it is highly plausible to predict its existence. Catalytic activity of the presynaptic proteasome was also shown to be both positively and negatively regulated by other kinases such as PKC, MAPK and protein kinase A (PKA)[431]. Altogether, these studies clearly indicate that neurons have diverse strategies of regulating proteasome activity in response to external cues or intracellular changes, however, it remains to be determined whether presynaptogenic factors can actually downregulate proteasome activity. To our knowledge, no evidence for a direct regulation of proteasome by cues that instruct formation of the presynaptic terminal has been reported.

In this study, we demonstrated that *on-site* accumulation of polyubiquitinated proteins triggers formation of presynaptic sites. To begin with, local proteasome inhibition results in the accumulation of polyubiquitinated conjugates that concentrate at nascent presynaptic clusters (figure S4.6, figure 4.8 and 4.9). Secondly, incubation of isolated axons with ziram, which blocks the UPS at the first step of ubiquitination thus preventing degradation of non-ubiquitinated proteins, has no effect on presynaptic clustering. Moreover, it abolishes proteasome inhibitors-mediated formation of presynaptic clusters, which indicates that proteasome inhibitors rely on *de novo* ubiquitination of proteins to exert their effect (figure 4.7). Thirdly, inhibition of deubiquitination by PR619 as well as expression of wtUb, which elevate intracellular levels of polyubiquitinated conjugates, have an effect on presynaptic clustering similar to proteasome inhibitors (figure 4.7 and 4.10). Lastly, when formation of specific polyubiquitin chains (proteolytic-related) is compromised thus preventing accumulation of proteins bearing a polyubiquitin tag,

there is no increase in the formation of new presynaptic sites (figure 4.10). Taken together, our results strongly suggest that accumulation of proteins in their polyubiquitinated state functions as a local trigger for presynaptic assembly. Interestingly, the three types of chains known to target proteins for degradation (K11,K29,K48)[277], were shown to be involved. So, we reason that a brake in proteasome degradation will increase the lifetime of proteins in their polyubiquitinated state, thus allowing them to act at a different level of regulation (in this particular case, in triggering presynaptic clustering). We thus propose that ubiquitin signals constitutively recognized as targets for proteasome-degradation are transiently accumulated to signal a different event within the cell.

In fact, several proteins with important roles for axon development and even presynaptic specific proteins have been reported to be ubiquitinated. A great deal of research has focused on proteins being ubiquitinated and downregulated in axons in an E3-dependent manner[270,441]. These include, but are not exclusive to, kinases like LIMK, DLK1 and ALK, and active zone proteins like RIM, DUNC-13 and the scaffold liprinα[270,441]. Further contributions on identifying synaptic ubiquitinated proteins came from proteomic screens. For instance, proteins with known roles in synaptogenesis were identified in *Drosophila* embryos [for example scaffolds like flotilins and 14-3-3 proteins, or the endocytic adaptor epidermal growth factor receptor substrate 15 (Eps15)][242]. Another study using whole rat brain extracts identified several SV-associated and active zone proteins (for example SNAP25, synapsin and Bassoon)[243]. In most of the cases, it is unknown the type of Ub chain with which presynaptic proteins are decorated. The ones downregulated in a proteasome-dependent manner are speculated to bear K48 chains, however, firm validation is needed. Interestingly, recent data show that the Wnt signaling pathway, which induces presynaptic clustering as we already mentioned[147], is regulated by unconventional polyubiquitin chains in a nonproteolytic manner[311,396]. For instance, β-catenin protein stability is enhanced by ubiquitination through K29 and K11[396] and K29 ubiquitinated axin negatively regulates Wnt pathway[311]. Overall, these studies predict a crucial role for polyubiquitination on different lysines in the control of presynaptic events.

In what our work is concerned, it is possible that a pool of polyubiquitinated proteins rather than a single protein is exerting this presynaptogenic effect. Several lines of evidence indicate so: i) upon proteasome inhibition several proteins will remain accumulated in cells; ii) PR619 treatment will also increase the amount of several proteins in their polyubiquitinated state; iii) axons respond equally to both inhibitors and the combined effect is not cumulative; iv) accumulation of K48 ubiquitinated conjugates at sites of nascent terminals is too strong to account for only a single protein; v) and different types of Ub chains are required for presynaptic assembly. We thus hypothesize that this site-specific pool of polyubiquitinated proteins might act as a "hub" for the recruitment of presynaptic material. Interesting insight comes from other cellular events, for instance, one of the strategies for DNA repair involves extensive ubiquitination of histones and other chromatin-associated proteins at the site of DNA damage. Several E3s and checkpoint proteins that recognize these Ub chains will then be recruited to the site of lesion[296,297]. A similar mode of action is also observed for the NF-κB signaling, which regulates several biological processes like immunity and apoptosis. Activation of NF-κB pathway relies on activation of surface receptors like TNFR by specific ligands. Subsequently, several downstream intracellular substrates will be differently polyubiquitinated and will serve as a local platform for the recruitment of kinase complexes, thus guaranteeing the normal progression of the signaling pathway[248,299]. Analogously, we may have recruitment of STVs and PTVs to sites along the axon at which a transient increase in the pool of polyubiquitinated proteins had occurred.

Ubiquitin signals in the form of polyubiquitin chains are normally decoded in cells by proteins containing UBDs. Apart from UBDs identified on E3 ligases, DUBs and proteasome shuttle factors, several other proteins were shown to contain these Ub recognition domains[249,265]. So far, to our knowledge, only four presynaptic proteins bearing UBDs were identified: the SV-associated protein amphiphysin[507], the active zone scaffolding protein syntenin[403,508] and the endocytic adaptor proteins epsin-1[509,510] and Eps15[510], which have important roles in SV endocytosis[511–513]. It is plausible that one or more of the previous proteins, or even additional candidates whose UBDs have not yet been identified, act downstream of proteasome inhibitors in the recognition of the enriched sites of polyubiquitinated conjugates as recruiting locations for presynaptic clustering. Scaffolding proteins of the active zone, like syntenin, are potential candidates due to their role in tethering several proteins in the presynaptic terminal. Accordingly, their recognition of Ub chains would in turn recruit interaction partners to the same site and promote formation of a new terminal.

In conclusion, this study provides new mechanistic insights on how UPS locally triggers formation of presynaptic sites. According to our model, a transient *on-site* decrease in proteasome activity will result in the accumulation of a pool of polyubiquitinated proteins that in turn triggers recruitment of presynaptic material. Further investigation will be needed to identify strategies by which the axon can locally control proteasome function. Our results also open the question of how a pool of polyubiquitinated conjugates function as an intracellular signal to presynaptic clustering. Furthermore, we anticipate the need to identify the axonal machinery responsible for the recognition and decoding of these polyubiquitin signals.

Supplementary figures

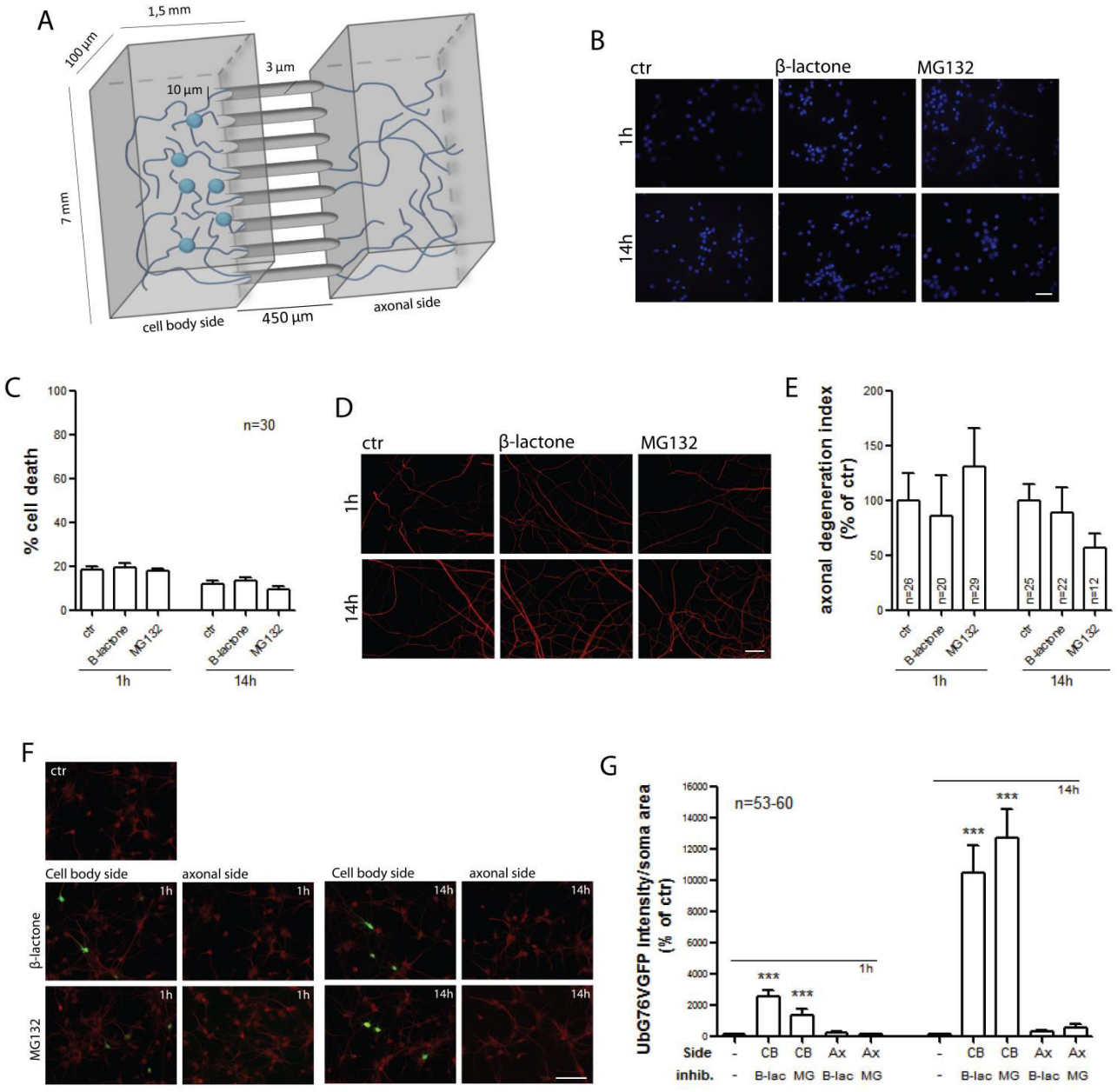

Fig. S4.1 - Specific inhibition of the proteasome in fluidically isolated axons. (**A**) Microfluidic devices for the study of axon-intrinsic mechanisms. In order to study developing axons without influences from the somatodendritic compartment, neurons were plated in microfluidic devices. In these chambers, two compartments are connected by a set of microgrooves, which allow axons to cross to the opposite compartment but not somas and dendrites due to their narrow and long structure. In addition to this physical separation, microfluidic devices also grant fluidical isolation between compartments[454]. (**B**) Assessment of neuronal viability in the cell body side and (**D**) axonal degeneration in the axonal side after axonal proteasome inhibition with β-lactone or MG132 for the indicated time. Up to 14 h, proteasome inhibitors applied to the axonal side did not affect neuronal viability. Scale bars are 50 and 20 µm, respectively. (**C**) Cell death percentage measured by counting the number of apoptotic nuclei

(DAPI staining) and (**E**) axonal degeneration index was calculated as the ratio between circular fragmented axonal area and total axonal area [tubulin was used as an axonal marker (red)]. (**F**) Specific proteasome inhibition in isolated axons. To validate inhibition of the proteasome specifically in axons, the degradation reporter $Ub^{G76V}GFP^{414}$ was expressed and its intensity in the soma [MAP2 staining (red)] analyzed after inhibition of the proteasome on either side of the compartment. Axonal inhibition of proteasome activity did not affect protein degradation at the soma level. Scale bar is 50 µm. (**G**) Change in reporter intensity in somas per MAP2 area. Increased reporter intensity was observed when proteasome inhibitors were added to the cell body side (CB), but not when added to the axonal side (Ax), indicating that proteasome activity is specifically inhibited in axons and no cross-inhibition is observed in the cell bodies. When indicated, results are expressed as % of control cells and are averaged from 3 independent experiments. Statistical significance was assessed by the Kruskal-Wallis test followed by the Dunn´s multiple comparison test (***p<0.001 when compared to the control condition). n represents the total number of analyzed microscope FOVs. Error bars indicate s.e.m.

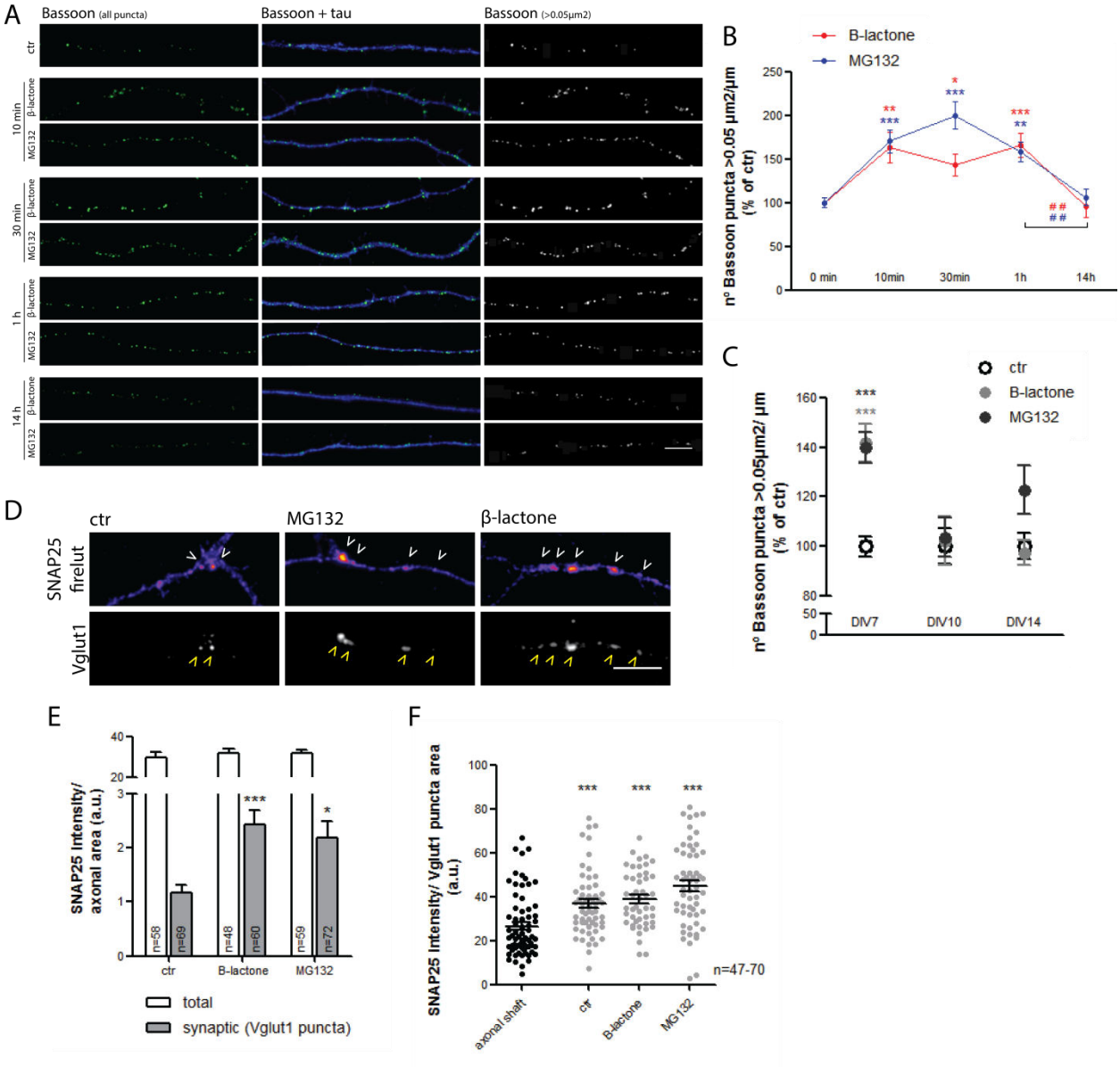

Fig. S4.2 - Inhibition of the proteasome in isolated axons enhances clustering of the active zone markers, Bassoon and SNAP25. (**A**) Effect of axonal proteasome inhibition on Bassoon clustering.

Following axonal proteasome inhibition for different periods of time in microfluidic devices, immunostaining for the active zone marker Bassoon (green) was performed. Specific inhibition of the proteasome in isolated axons resulted in the rapid formation of Bassoon puncta bigger than 0.05µm^2. Scale bar is 5 µm. (**B**) Quantitative summary data of the number of Bassoon puncta bigger than the designated threshold per axonal length. (**C**) Effect of proteasome inhibitors on Bassoon clustering according to culture age. The same presynaptic parameter was analyzed at different culture developmental time-points in response to 1 h inhibition of the proteasome. In aged axons proteasome inhibitors did not upregulate the number of Basson puncta. (**B**, **C**) Results are expressed as % of control cells and are averaged from at least 4 independent experiments. A minimum of 12 microscope FOVs from the axonal side were analyzed per individual experiment in each condition. Statistical significance was assessed by the Kruskal-Wallis test followed by the Dunn´s multiple comparison test (***p<0.001, **p<0.01 and *p<0.05 when compared to 0min time-point or control condition and $^{\#\#}$p<0.01 when compared to 1 h time-point). Error bars indicate s.e.m. (**D**) Intensity of SNAP25 on SV puncta. In addition to Bassoon, clustering of another active zone marker, SNAP25 (firelut), was analyzed. SNAP25 was selectively enriched at sites of newly-formed SV puncta upon 1 h local proteasome inhibition. White arrowheads indicate spots of higher SNAP25 intensity along the axon that are coincident with Vglut1 puncta (yellow arrowheads). The scale bar is 5 µm. (**E**) Quantification of total and synaptic SNAP25 intensity per axonal area revealed specific increases in synaptic SNAP25 levels while total levels remained constant. (**F**) Quantification of SNAP25 intensity per Vglut1 puncta area showed that newly-generated Vglut1 puncta after proteasome inhibition contained similar levels of SNAP25 as control Vglut1 puncta. The values for SNAP25 intensity along the axonal shaft were included for reference. (**E**, **F**) Results are averaged from at least 5-6 independent experiments. Statistical significance was assessed by the Kruskal-Wallis test followed by the Dunn´s multiple comparison test (***p<0.001 and *p<0.05 when compared to the control or the axonal shaft value). n represents the total number of analyzed microscope FOVs to the axonal side. Error bars indicate s.e.m.

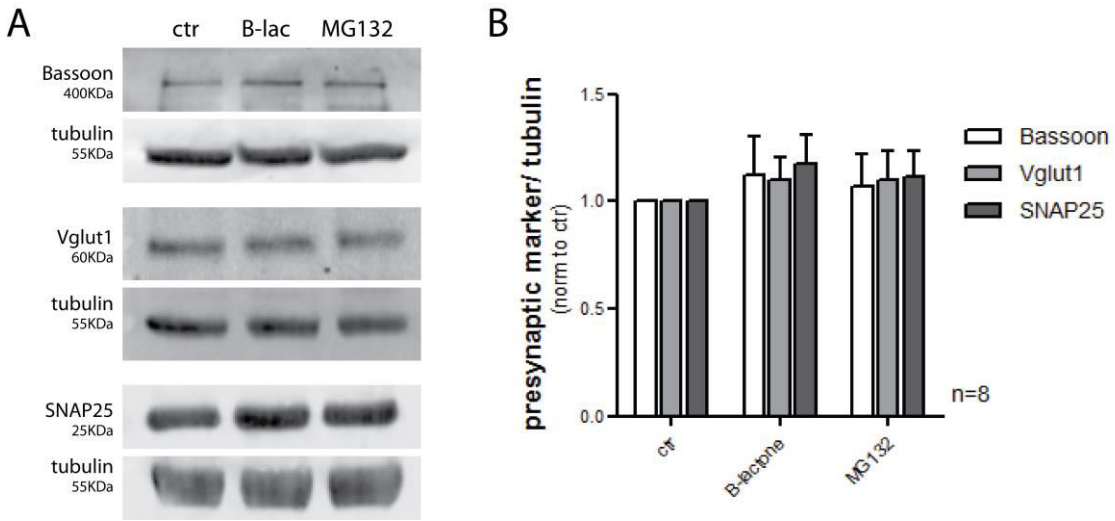

Fig. S4.3 - Proteasome inhibitors do not alter total levels of the presynaptic markers. (**A**) Analysis of presynaptic markers expression levels upon proteasome inhibition. Total cell lysates were obtained from DIV 7 hippocampal neurons after treatment with proteasome inhibitors or vehicle for 1 h. The levels of expression of the presynaptic markers used throughout this study were determined by WB. Tubulin was used as loading control. Total levels of presynaptic proteins did not differ, thus discarding the possibility that proteasome inhibition-induced clustering would be an artifact of a random increased amount of presynaptic POI along the axon. (**B**) Quantitative levels of presynaptic POI relative to the loading control. Results were normalized to the control condition. Statistical significance was assessed

by the Kruskal-Wallis test followed by the Dunn´s multiple comparison test. n represents the number of individual experiments. Error bars indicate s.e.m.

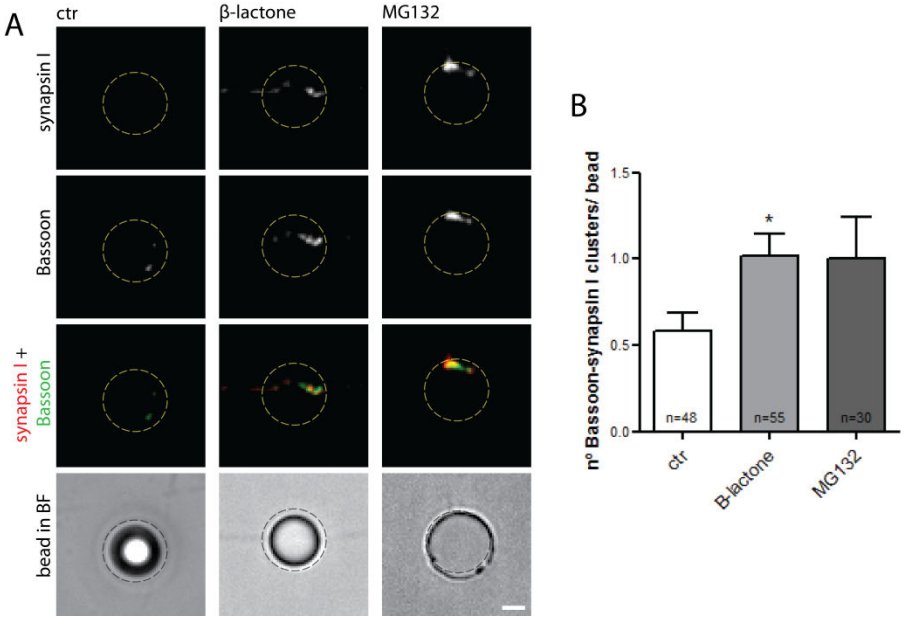

Fig. S4.4 - Axonal proteasome inhibition further induces formation of presynaptic clusters on beads. (**A**) Formation of presynaptic clusters on beads following proteasome inhibition. Beads were added to the axonal compartment for 3 h, then axons were treated with proteasome inhibitors or vehicle for 1 h and immunostained for Bassoon (green) and synapsin I (red). Axonal proteasome inhibition enhanced formation of presynaptic clusters on beads. The scale bar is 5 µm. (**B**) Quantitative data of the number of Bassoon puncta colocalizing with a synapsin puncta per bead. Results are expressed as the average from 1 independent experiment. Statistical significance was analyzed by the Kruskal-Wallis test followed by the Dunn´s multiple comparison test (*$p<0.05$ when compared to the control). n represents the number of beads. Error bars indicate s.e.m.

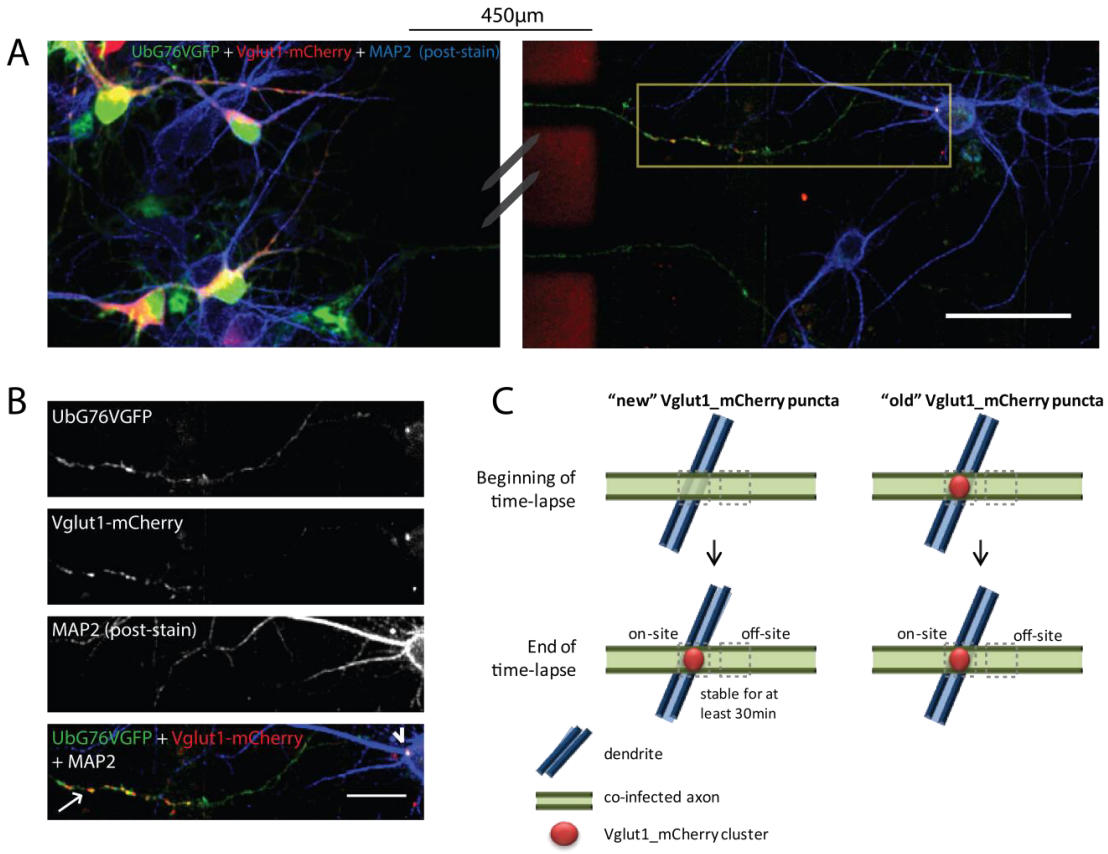

Fig. S4.5 - Live-imaging approach to visualize formation of presynaptic clusters in axodendritic synapses. (**A**) Experimental set-up to monitor changes in the axonal domain undergoing presynaptic differentiation onto dendrites. Neurons were plated on either sides of microfluidic devices and dually infected with Sindbis virus expressing Ub^{G76V}GFP and Vglut1-mCherry on only one side. Infected axons reached the opposite compartment, in which they establish synaptic contacts with resident neurons. Cultures were later fixed and stained for MAP2 (blue) and retrospective imaging of the same region was performed to detect dendrites. The signal for Ub^{G76V}GFP and Vglut1-mCherry was differently adjusted between right and left image to prevent over-saturation of signal at the soma level. The scale bar is 50 µm. (**B**) Enlarged image of yellow box in (**A**) showing a co-infected axon (GFP^+ and $mCherry^+$) (arrow) extending into the opposite compartment and forming a presynaptic clusters (arrowhead) on a $MAP2^+$ cell body. The scale bar is 20 µm. (**C**) Quantification strategy used for the live-imaging approach in which we monitored *on-site* axonal changes in proteasome degradation rate during formation of presynaptic clusters in an axon-dendrite synapse (see figure 4.5). Vglut1mCherry puncta on dendrites were grouped as "old" or "new" if they persisted throughout the whole experiment or they were newly-formed and stable until the end (at least in 3 consecutive frames, 30 min), respectively. Regions of interest (ROIs) were created at the site of clustering (on-site) and at adjacent axonal regions (off-site) for both "new" and "old" puncta. Intensity values of Vglut1-mCherry and Ub^{G76V}GFP signals within these ROIs were extracted from the time-lapse sequence of images and used to generate the dataset presented on figure 4.5.

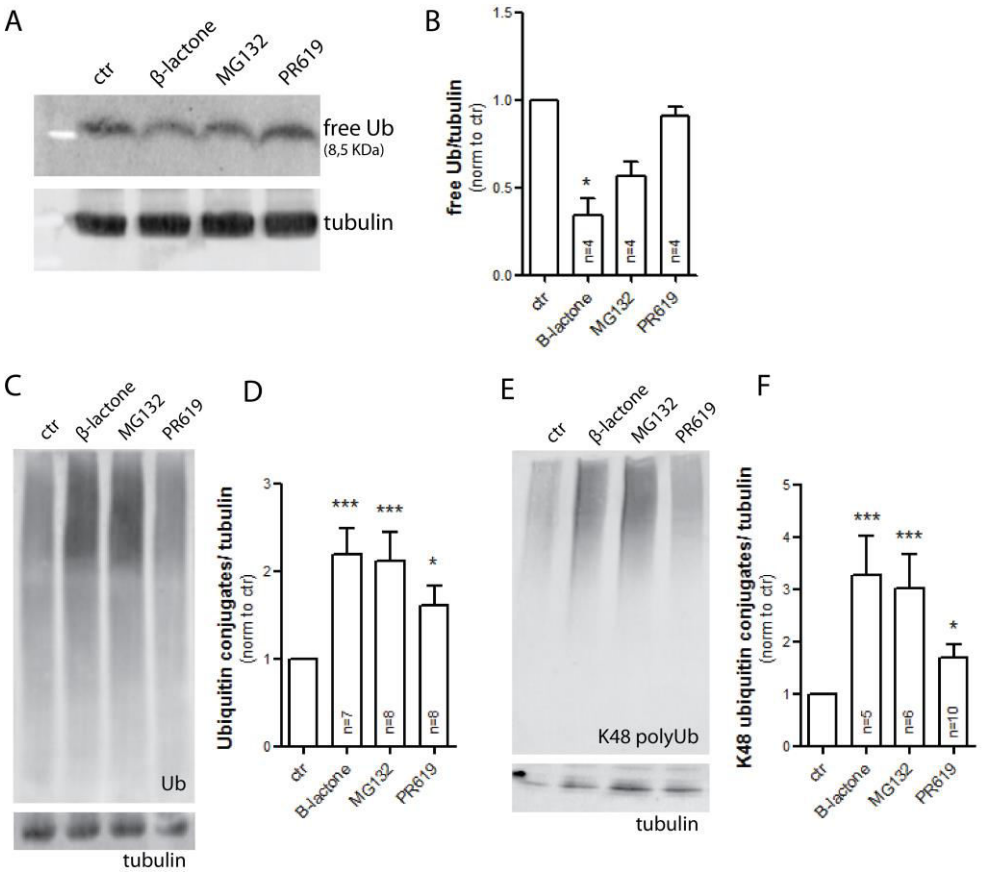

Fig. S4.6 - Changes in the pool of ubiquitinated proteins upon proteasome and DUBs inhibition. (**A**, **C**, **E**) Effect of proteasome inhibitors and PR619 on the levels of free and conjugated Ub. Total cell lysates were obtained from DIV 7 neurons after 1 h treatment with β-lactone, MG132, PR619 or vehicle. Analysed by WB for ubiquitin to examine levels of free Ub (**A**, in a 15% gel), ubiquitinated conjugates (**C**, in a 4-15% gradient gel) and for K48 polyubiquitin (**E**, in a 4-15% gradient gel) were performed. Tubulin was used as loading control. As expected, proteasome inhibitors strongly upregulated the levels of ubiquitinated conjugates while reducing free ubiquitin levels. The DUBs inhibitor PR619 also elevated ubiquitinated conjugates levels, although with a lower effectiveness. Increases in the levels of K48 polyubiquitinated proteins are also visible for both proteasome inhibitors and PR619. (**B**, **D**, **F**) Quantification of band intensities relative to control conditions. Statistical significance was assessed by the Kruskal-Wallis test followed by the Dunn´s multiple comparison test. n represents the number of individual experiments. Error bars indicate s.e.m.

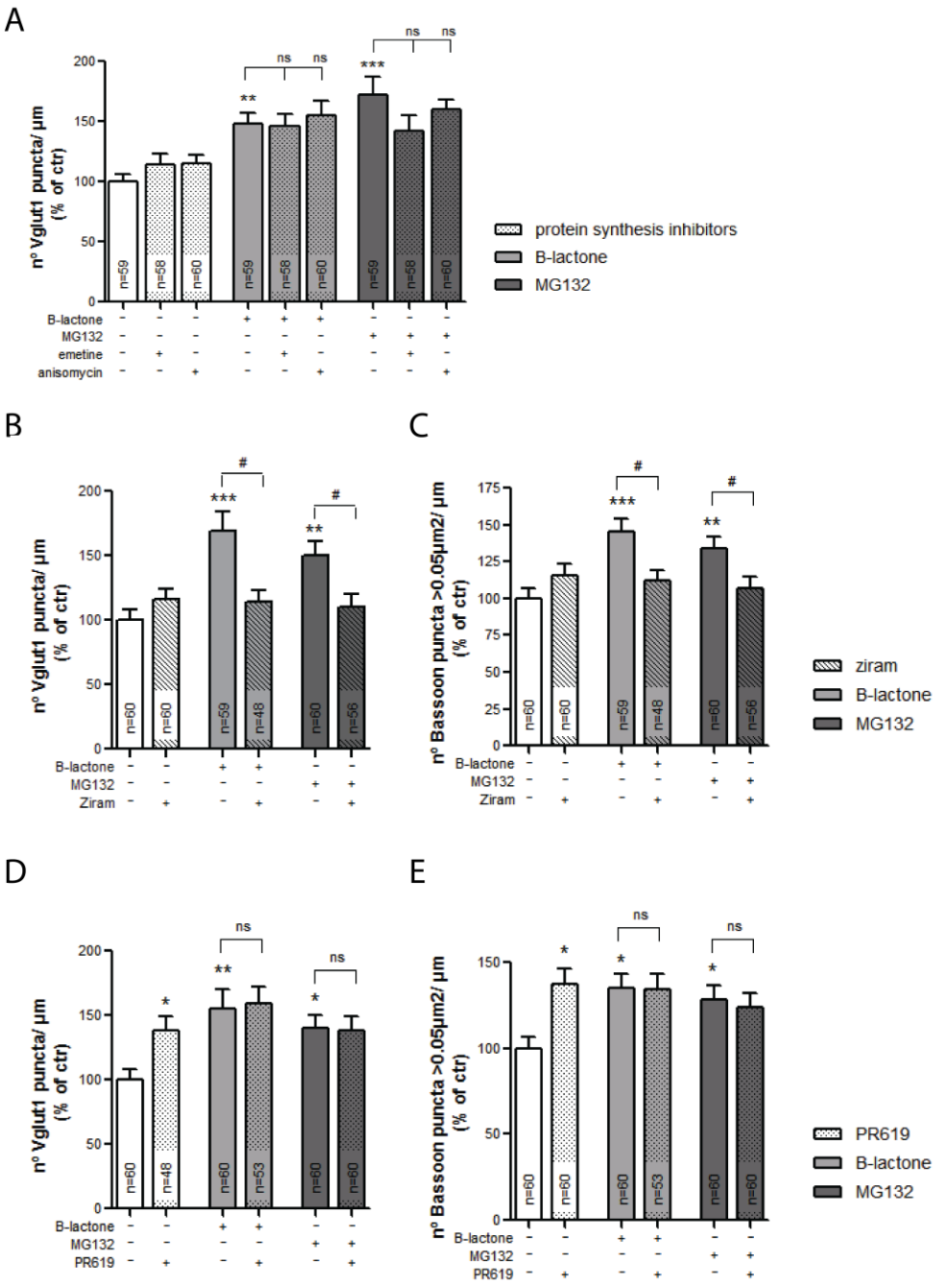

Fig. S4.7 - Clustering of Vglut1 and Bassoon in response to protein synthesis and the UPS inhibitors, PR619 and ziram. (**A**-**E**) Additional presynaptic parameters quantified after axon-specific treatment with (**A**) protein synthesis inhibitors, (**B**, **C**) ziram and (**D**, **E**) PR619, alone or in combination with proteasome inhibitors. Quantitative values of (**A**, **B**, **D**) number of Vglut1 puncta per axonal length and (**C**, **E**) number of Bassoon puncta bigger than 0.05µm^2 per axonal length. Results are expressed as % of control cells and are averaged from at least 5 independent experiments. Statistical significance was assessed by the Kruskal-Wallis test followed by the Dunn´s multiple comparison test (***p<0.001, **p<0.01 and *p<0.05 when compared to control and $^{\#}$p<0.05 between indicated bars). n represents the total number of analyzed microscope FOVs from the axonal side. Error bars indicate s.e.m.

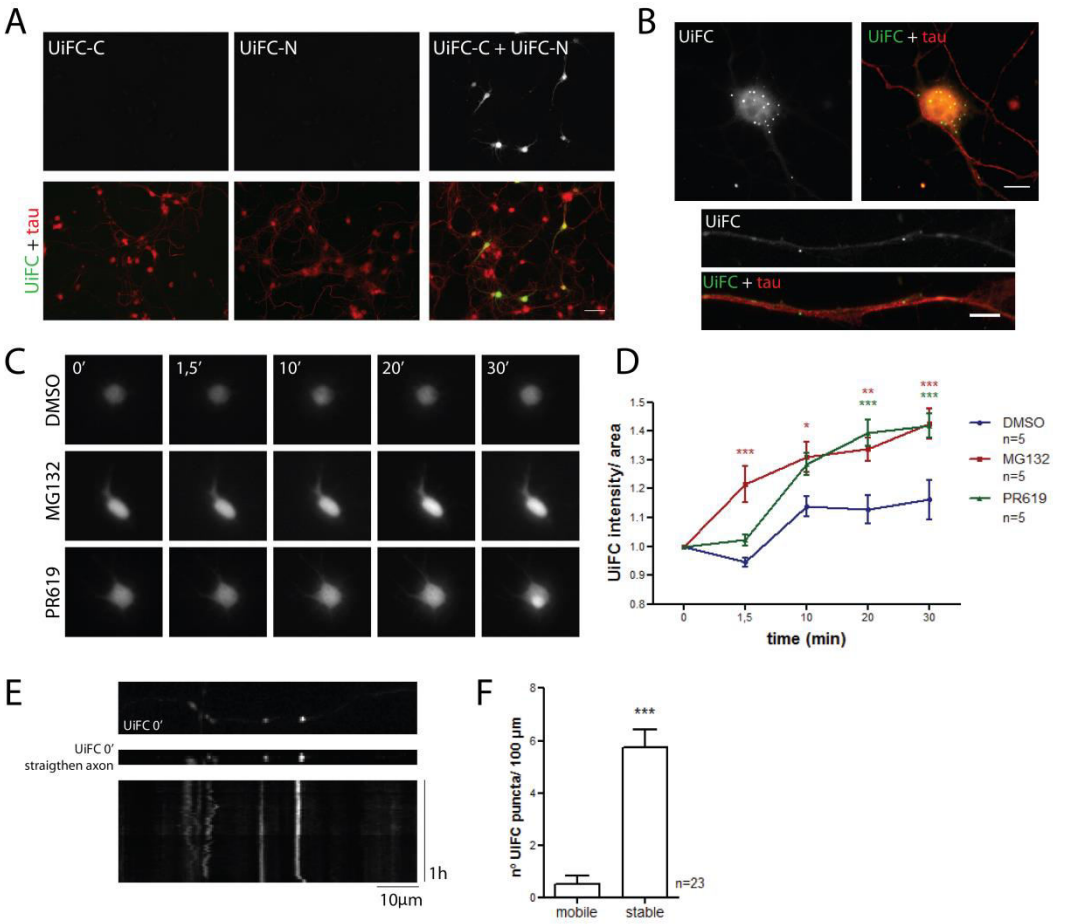

Fig. S4.8 - Validation and characterization of UiFC in neurons. (**A**) The UiFC approach allows for the detection of polyubiquitin chains[415]. Transfection of hippocampal neurons with either UiFC-C or UiFC-N alone did not result in any fluorescent signal; however, venus^{+} neurons can be observed when co-transfection was performed. Tau (red) was used as neuronal marker. Scale bar is 50 µm. (**B**) Top, although most of the neurons had a diffuse UiFC fluorescence (green), some display a punctuate pattern of UiFC distribution in the cell body, which is in agreement with the UiFC aggregates observed in HeLa cells[415] shown to colocalize with K48 polyubiquitin signal. Bottom, in the axonal shaft, UiFC staining was diffuse with occasional UiFC puncta (approximately 5 UiFC puncta/ 100µm). Scale bars are 10 and 5 µm for top and bottom images, respectively. (**C**) Time-lapse imaging of UiFC signal in the cell bodies of hippocampal neurons in response to MG132 (proteasome inhibitor) and PR619 (DUBs inhibitor). Treatment of cells with the aforementioned inhibitors increased UiFC fluorescence, in accordance to the accumulation of K48 ubiquitinated conjugates in cells by these inhibitors (figure S4.6). (**D**) Change in UiFC signal intensity per cell body area. Results are normalized to t0 (0 min) and are averaged from 1 independent experiment. Statistical significance was assessed by 2-way ANOVA (***p<0.001, **p<0.01 and *p<0.05 compared to DMSO at each timepoint). n represents the number of cells. Error bars indicate s.e.m. (**E**) Evaluation of UiFC puncta mobility along axons. In order to characterize UiFC puncta dynamics along the axon, UiFC-expressing axons were imaged every 1 min for 1 h and kymographs were generated. Top, representative segment of an axon at the beginning of the time-lapse. Bottom, representative kymograph from a 1h-movie of UiFC signal. UiFC puncta along the axon were stable. (**F**) Quantification of number of mobile (mean speed greater than 0.05µm/min and net displacement greater than twice their width) and stationary UiFC puncta per axonal length. Statistical analysis by Wilcoxon paired t-test (***p<0.001). n represents the number of axon segments in 1 individual experiment.

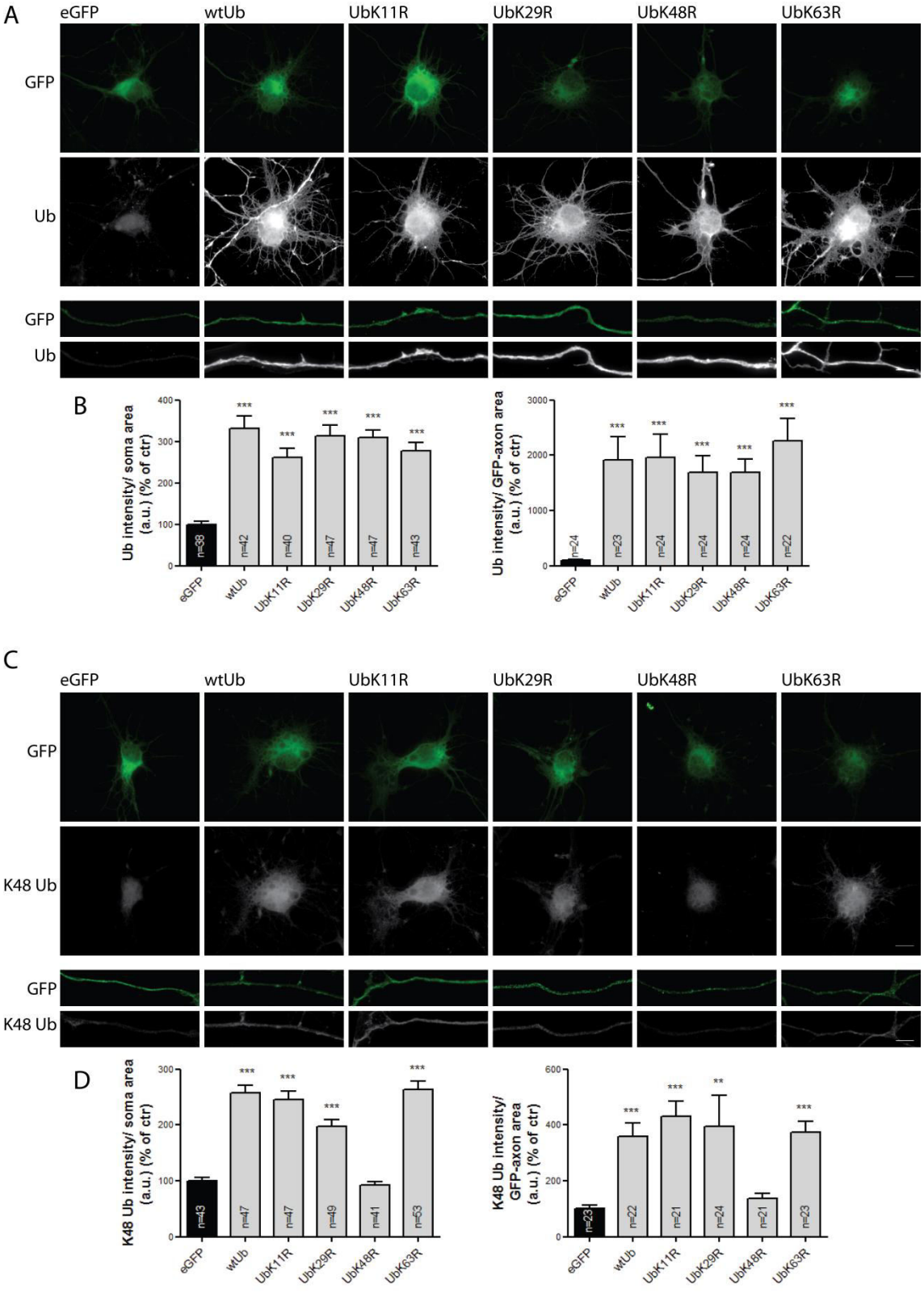

Fig. S4.9 - Expression of Ub results in increased levels of conjugated ubiquitin, which is prevented when the mutant is expressed. (**A**, **C**) Validation of constructs for wtUb and its lysine-specific mutant forms. Neurons were infected with Sindbis virus expressing wtUb, ubiquitin mutants that prevent formation of specific types of polyubiquitin chains (UbK11R, UbK29R, UbK48R and UbK63R) and eGFP as control. Levels of endogenous (**A**) ubiquitin (white) and (**C**) K48 polyubiquitin (white) were evaluated on GFP^+ neurons by immunocytochemistry both at the cell body and axon level. Neurons were plated as

pseudo-explants so that the majority of axons are isolated. Regardless of the mutation, overexpression of wtUb and its mutant forms upregulated levels of Ub in comparison to eGFP. Moreover, conjugation of Ub was enhanced; however, K48 ubiquitination was completely abrogated when the specific lysine was mutated. Scale bars are 10 and 5 µm for top and bottom images, respectively. (**B**, **D**) Quantification of (**B**) ubiquitin and (**D**) K48 polyubiquitin intensity per soma area (left) and per axon area (right). Results are expressed as % of control and are averaged from 2 independent experiments. Statistical significance was assessed by the Kruskal-Wallis test followed by the Dunn´s multiple comparison test (***p<0.001, **p<0.01 when compared to eGFP). n represents the total number of cells (left) or microscope FOVs (right) analyzed. Error bars indicate s.e.m.

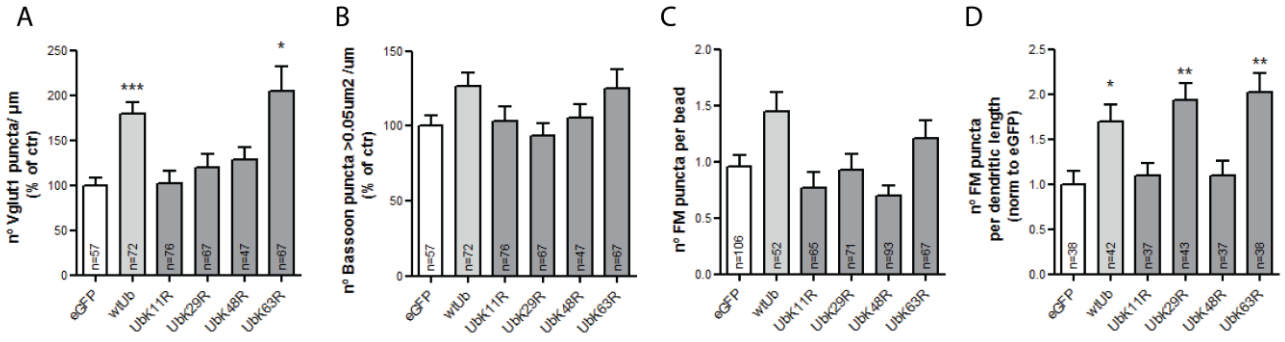

Fig. S4.10 - Effect of wtUb and Ub mutants in presynaptic assembly. (**A**-**D**) Additional presynaptic parameters quantified following expression of wtUb and Ub mutants in hippocampal cultures. Quantitative values of (**A**) number of Vglut1 puncta per axonal length; (**B**) number of Bassoon puncta bigger than 0.05 µm^2 per axonal length; (**C**) number of total FM puncta on beads and (**D**) number of total FM puncta on dendrites. Statistical significance was assessed by the Kruskal-Wallis test followed by the Dunn´s multiple comparison test (***p<0.001, **p<0.01 and *p<0.05 when compared to control). n represents (**A**, **B**) the total number of analyzed microscope FOVs to the axonal side, (**C**) the number of beads and (**D**) the number of dendrites. Error bars indicate s.e.m.

Chapter 5

The Unexplored Role of Polyubiquitination in Presynaptic Release

Maria Joana Pinto, Anne Taylor, Ramiro Almeida

An on-going study

Summary

Depolarization-induced presynaptic release of neurotransmitters is vital for the proper functioning of the nervous system. Proteasomal degradation of key proteins of the SV recycling machinery regulates SV exocytosis; and moreover, altered ubiquitin levels change the release properties of presynaptic terminals. Herein, we explored the functional role of different types of polyubiquitin chains in the kinetics of SV release, by means of styryl FM dye loading and unloading procedures. Our data show that expression of Ub accelerates the rate of stimulus-evoked presynaptic release, which is partially reverted when K11, K29 and K63 polyubiquitination is prevented. We thus predict a functional significance for the attachment of polyubiquitin chains in the regulation of neurotransmitter release.

Introduction

Neurotransmission constitutes the basis of brain function. It is initiated at the presynaptic terminal after arrival of an action potential that triggers the opening of voltage-gated calcium channels, concentrated at the active zone, with a subsequent influx of calcium. Exocytosis of SVs is then triggered and the release of neurotransmitters to the synaptic cleft will generate a postsynaptic response. After fusion, SVs are recycled back and replenished with neurotransmitters as a way of maintaining a responsive pool of SVs within the nerve terminal. Neurotransmitter release is a highly regulated mechanism and relies almost completely on proteins embedded in the CAZ[212]. Formation of the SNARE complex between SV and plasma membrane will prime vesicles for release, constituting the RRP of SVs, which only need the entrance of calcium to initiate fusion. Proteins such as Munc13, Munc18, complexins or RIM1α are important coordinators of this process, guaranteeing that SVs are perfectly linked to the site of fusion and their rapid exocytosis occurs as soon as synaptotagmins sense the steep rise in calcium levels[212,215].

Growing evidence indicates that the UPS is an important modulator of presynaptic release. Ubiquitin is a 76 amino acid peptide that is covalently attached to proteins either as a monomer or as a chain of ubiquitins. It is involved in a multitude of mechanisms within cells from DNA repair, endocytosis, signal transduction, to its well-known role as a tag for proteasome degradation[245,247]. The first clue that Ub has a modulatory role in presynaptic release arose from studies evaluating the effect of proteasome inhibitors in synaptic function. Both in *Aplysia* and *Drosophila*, proteasome inhibition results in rapid strengthening of synaptic transmission[385,386]. Simultaneously to these findings, Dunc13, the Drosophila homolog of Munc13 already known to be implicated in the modulation of the fusion machinery and SV priming[514,515], was identified as a putative proteasome target[385,516]. Presumably, a block in proteasome degradation would result in accumulation of Dunc13 and a subsequent increase in synaptic transmission[385].

In the following years, more intervenients in the events leading to presynaptic neurotransmitter release were added to the list of possible proteasome targets. The synapse-localized E3 ligase SCRAPPER was identified as responsible for the ubiquitination of RIM1α[359], a protein that forms a scaffold in the presynaptic terminal integrating active zone proteins and SVs for the control of neurotransmitter release[178]. Moreover, the levels of other proteins involved in the steps linking calcium rises to SV fusion, such as synaptotagmin, Munc13, Munc18 and CASK, were also shown to be inversely related to levels of SCRAPPER[359]. Another presynaptic scaffolding protein whose levels are regulated by the UPS, liprin-α2, controls the size of the recycling SV pool via recruitment of components of the release machinery[175]. Amazingly, also the cell surface expression of the neuronal N-type calcium channels, $Ca_v2.2$, was shown to be regulated by ubiquitination and degradation[407–409].

In a new twist on the idea of UPS as a regulator of presynaptic release, some studies emphasize a role for ubiquitination. For instance, in rat hippocampal neurons proteasome inhibition for 10 min is sufficient to increase neurotransmitter release, however without changes in Munc13 or Rim1 levels[384]. Because blocking the UPS at a point in which previously ubiquitinated proteins can still be degraded exerts a strikingly equal effect to that of proteasome inhibitors, authors concluded that decreased ubiquitination dynamics is the explanation for the boost in quantal release[384]. Furthermore, the ax^J mice with a loss-of-function mutation in the proteasome-associated deubiquitinating enzyme Usp14, have an inability to mobilize SVs for fusion and a reduced size of the RRP[367]. These changes are associated with reduced levels of protein ubiquitination in the synaptic compartment[258], mainly due to an accelerated loss of ubiquitin by proteasome degradation[259]. These data identify a critical role for ubiquitin homeostasis in presynaptic function, specifically in the release

of neurotransmitters, however no efforts have been made to discern the role of polyubiquitination in this event.

In this preliminary study, we identify a role for polyubiquitin chains in the modulation of presynaptic release. By evaluating the kinetics of stimulus-evoked FM dye release in dissociated cultures, we visualized an increase in the rate of presynaptic release upon expression of Ub. We further identify a role for K11, K29 and K63 polyubiquitin chains in the enhancement of SV pool release. Overall, this set of preliminary results suggests that polyubiquitination may represent a novel, yet unexplored, layer of regulation of presynaptic release.

Results

In order to study presynaptic SV release and evaluate changes in the rate of exocytosis, we used the lipophilic FM 5-95 dye[517,518]. The FM dye was loaded by KCl-mediated depolarization (90mM KCl for 1 min) into presynaptic boutons in hippocampal cultures in the somal compartment of microfluidic devices (figure 5.1A, top images). This stimulus is believed to label the entire pool of recycling SVs, known as the recycling pool[519]. Field stimulation (1200 pulses at 20 Hz for 1 min) was then applied to induce exocytosis of releasable SVs and the unloading of the FM dye (figure 5.1A, middle panel) was live monitored in a spinning disk system by acquiring images every 15 s before, during and after stimulation. Changes in the intensity of individual FM puncta were quantified throughout the time-lapse to evaluate the dynamics of dye release. This procedure was performed to cultures infected with Sindbis virus expressing wtUb or the empty control vector (eGFP) (figure 5.1). By increasing the levels of ubiquitin in neurons, a significant increase in the rate of FM dye unloading was observed (figure 5.1A-D). Ubiquitin accelerated FM release as observed by a steeper decline in FM fluorescence of individual puncta upon electrical stimulation as compared to eGFP (figure 5.1B). Moreover, a robust decrease in the release time constant was observed after expression of Ub, indicating a higher probability of SV content release in presynaptic terminals with higher levels of Ub (figure 5.1C). We also quantified the amount of dye that was released in comparison to the initial amount of dye uptake, and found that Ub-enriched presynaptic terminals released an average of 42% of loaded FM as opposed to eGFP, whose terminals unloaded only 30% of their initial content (figure 5.1D). Collectively, we concluded that increased levels of Ub in neurons alter the kinetics of SV release, potentiating and accelerating action potential-evoked SV pool exocytosis.

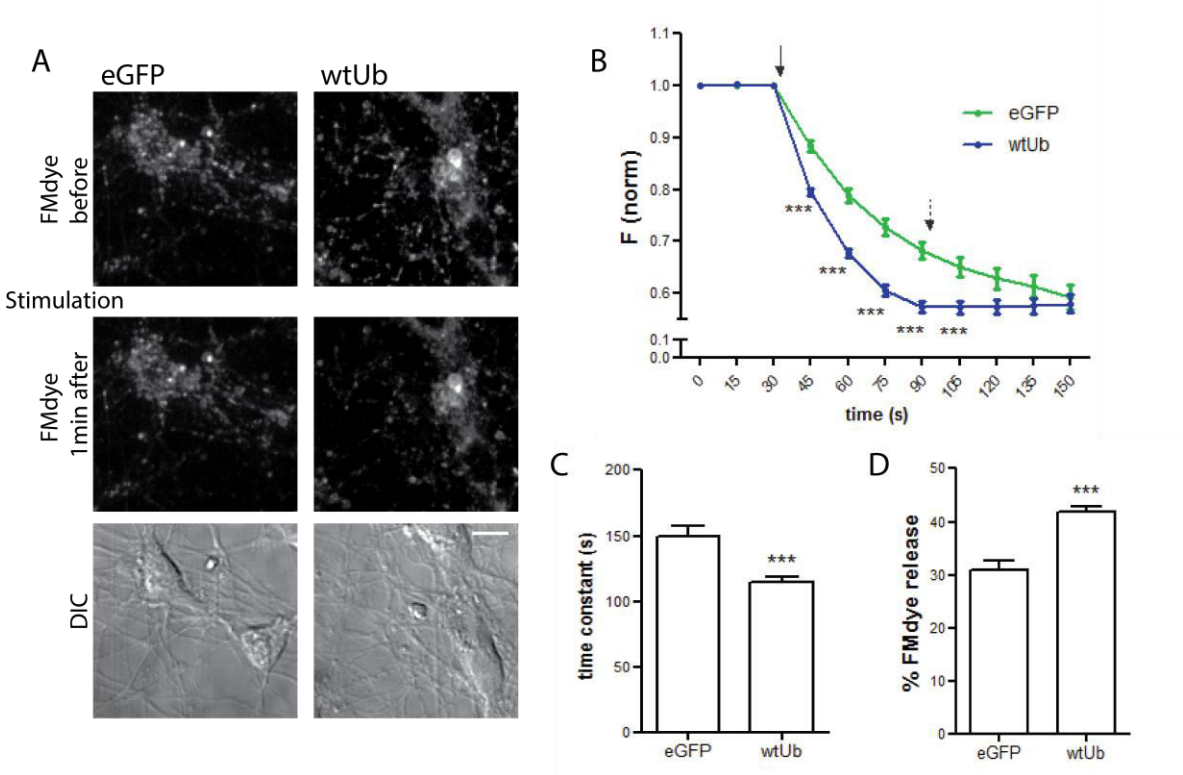

Fig. 5.1 - Overexpression of Ub in hippocampal neurons increases the rate of presynaptic release. (**A**) Kynetics of FM 5-95 dye release upon Ub overexpression. WtUb or the control vector (eGFP) were expressed in dissociated hippocampal neurons for 16-20 h by a Sindbis virus expressing system at DIV 7-9. The protocol for FM dye loading and unloading was performed to evaluate the kynetics of dye

release, as elsewhere reported[419]. Representative images show FM 5-95 dye staining after loading (top) and after 1min of electrical stimulation-induced dye unloading (middle), and the correspondent DIC image (bottom). Upon expression of wtUb, FM dye release in response to stimulation was enhanced. Also, a higher density of FM puncta was observed (discussed in chapter 4, figure 4.9). The scale bar is 10µm. (**B**) Time course of FM 5-95 dye unloading. Neurons were stimulated by 1200 pulses at 20 Hz for 1 min for control (eGFP) and wtUb. Results correspond to FM puncta intensities normalized to the frame preceding stimulation and to the baseline slope. Arrow indicates stimulation. Analysis includes only puncta that unloaded more than 5% of their FM dye content after 1 min of electrical stimulation. Statistical significance was assessed by 2-way ANOVA followed by Bonferroni post-test (***$p<0.001$ at each time point between conditions). (**C**) Average exponential decay time constant, τ, for eGFP and wtUb FM puncta. This value was obtained by fitting the curve of FM unloading kinetics during stimulation to an exponential decay function and calculating the theoretical exponential decay time constant for each punctum individually. (**D**) Amount of FM dye released after 1 min stimulation. The values were calculated in percentage of initial FM dye fluorescence (at the frame preceding stimulation). In C and D, statistical analysis by Mann Whitney test (***$p<0.001$). (**B**, **C**, **D**) Results were averaged from 205 (eGFP) and 517 FM puncta (wtUb) in 2 independent experiments. Error bars indicate s.e.m.

Ubiquitin moieties can be attached to each other at lysine residues with the resulting formation of polyubiquitin chains, whose biological significance is just now beginning to be disclosed[247,248]. To understand whether presynaptic neurotransmitter release is regulated by polyubiquitination, we generated mutant forms of Ub in which specific lysines are mutated into arginines thus preventing formation of polyubiquitin chains on these residues (UbK11R, UbK29R, UbK48R and UbK63R prevent K11, K29, K48 and K63 polyubiquitintion, respectively). The effect of ubiquitin overexpression on the rate of FM unloading was partially reverted when ubiquitination on lysines 11, 29 and 63 was prevented, however cells expressing the UbK48R mutant responded identically to wtUb (figure 5.2). We observed changes in the dynamics of FM release at different time-points following stimulation upon expression of UbK11R (figure 5.2A), UbK29R (figure 5.2D) and UbK63R (figure 5.2J). None of the mutants completely suppressed the effect of wtUb to eGFP basal levels at any of the time-points during stimulation. In contrast, prevention of K48 ubiquitination showed similar patterns of FM unloading to that of wtUb (figure 5.2G), thus showing that formation of this type of chains does not account for the effect of wtUb and that it probably relies on formation of the other types of polyubiquitin chains. We also calculated and plotted the release time constant and the amount of dye released for each mutant in relation to the control eGFP and wtUb (figure 5.2B, E, H, K). In terms of release time constant, the mutants for lysines 11, 29 and 63 (figure 5.2B, E, K, respectively) did not significantly reduce this constant in comparison to eGFP, however their values were different from wtUb. Presynaptic terminals exposed to increased levels of these mutant forms also partially reduced the percentage of dye released induced by wtUb expression (figure 5.2C, F, L). In its turn, the mutant for lysine 48 displayed similar FM release properties to wtUb, both for the release time constant and the percentage of dye released from individual puncta (figure 5.2H, I, respectively). We thus concluded that the effect of Ub expression on the accelerated rate of FM unloading is dependent on the formation of polyubiquitin chains, mainly through lysines 11, 29 and 63. These results unravel a new role for these types of Ub chains in the regulation of presynaptic release.

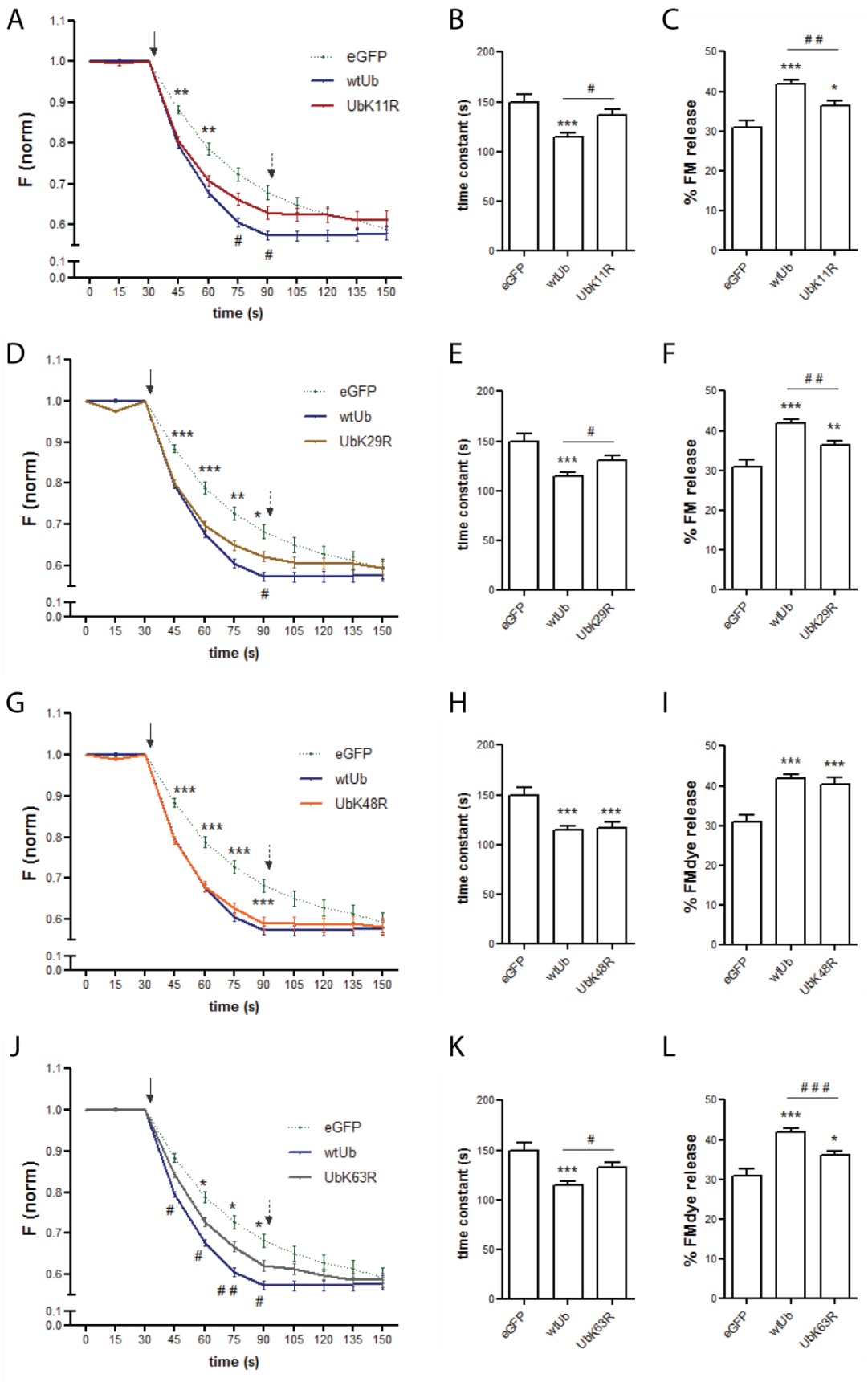

Fig. 5.2 - Polyubiquitination on lysines 11, 29 and 63 regulates presynaptic release. (**A**-**L**) Contribution of linkage-specific polyubiquitin chains to Ub-enhanced FM dye release. Expression of Ub mutant forms

that prevent formation of polyubiquitin chains through lysines 11, 29 and 63 partially reverted the increased rate of FM unloading induced by wtUb. (**A**-**L**) Parameters to evaluate FM unloading kinetics for (**A**, **B**, **C**) UbK11R, (**D**, **E**, **F**) UbK29R, (**G**, **H**, **I**) UbK48R and (**J**, **K**, **L**) UbK63R, in comparison to eGFP and wtUb. (**A**, **D**, **G**, **J**) Time course of FM 5-95 dye unloading triggered by 1200 pulses at 20 Hz for 1 min. Results correspond to FM puncta intensities normalized to the frame preceding stimulation and to the baseline slope. Arrow indicates stimulation. Analysis includes only puncta that unloaded more than 5% of their FM dye content after 1 min of electrical stimulation. Statistical significance was assessed by 2-way ANOVA followed by Bonferroni post-test (***p<0.001, **p<0.01 and *p<0.05 at each time point between eGFP and the Ub mutant; $^{###}$p<0.001, $^{##}$p<0.01 and $^{#}$p<0.05 at each time point between wtUb and the Ub mutant). (**B**, **E**, **H**, **K**) Average exponential decay time constant, τ, for eGFP, wtUb and Ub mutant FM puncta. This value was obtained by fitting the curve of FM unloading kinetics during stimulation to an exponential decay function and calculating the theoretical exponential decay time constant for each punctum individually. Statistical analysis by Kruskal-Wallis test followed by the Dunn´s multiple comparison test (***p<0.01 when compared to eGFP; $^{##}$p<0.01 and $^{#}$p<0.05 between indicated bars). (**C**, **F**, **I**, **L**) Amount of FM dye released after 1 min of stimulation in percentage of initial FM dye fluorescence (at the frame preceding stimulation). Statistical analysis by Kruskal-Wallis test followed by the Dunn´s multiple comparison test (***p<0.01, **p<0.01 and *p<0.05 when compared to eGFP; $^{###}$p<0.001 and $^{##}$p<0.01 between indicated bars). (**A**-**L**) Results were averaged from 205 (eGFP), 517 (wtUb), 252 (UbK11R), 443 (UbK29R), 271 (UbK48R) and 444 (UbK63R) FM puncta in 2 independent experiments. Error bars indicate s.e.m.

Lastly, to understand whether changes in SV pool release properties at presynaptic boutons were due to structural changes in the terminal itself prior to stimulation-induced release, we measured the size of individual FM puncta and their initial dye uptake. There were no changes in the average size of FM puncta between the conditions analyzed (figure 5.3A). We then determined the initial mean fluorescence of FM dye per puncta as a measure of the initial dye uptake, and again, no changes were observed between eGFP, wtUb or its mutant forms (figure 5.3B). This parameter has already been used as an indirect way of evaluating the size of the recycling vesicle pool[412]. In accordance, we observed no changes in the initial pool of recycling vesicles and so this does not account for the differences observed in FM dye unloading kinetics.

Altogether, these results provide evidence that polyubiquitination on lysines 11, 29 and 63 regulates presynaptic neurotransmitter release by affecting the rate of SV pool exocytosis and not the size of the recycling pool of SVs.

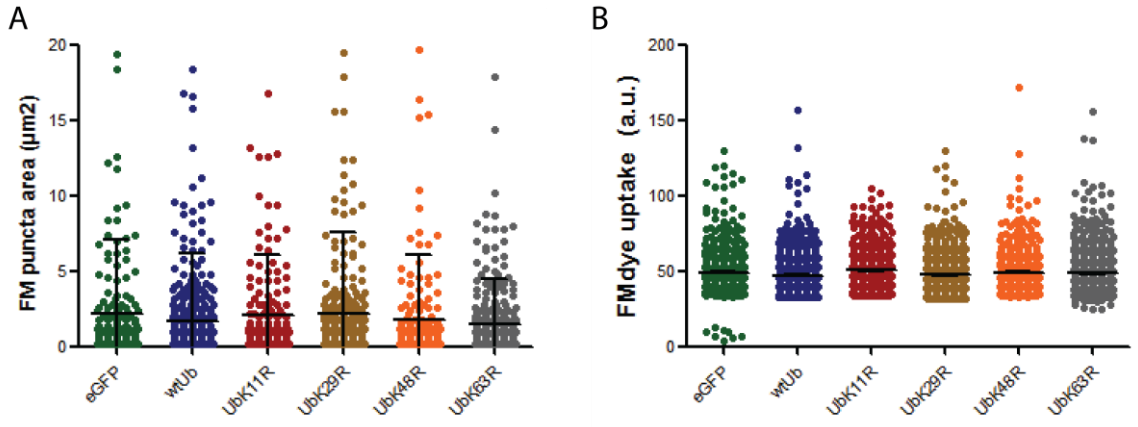

Fig. 5.3 - FM puncta structural properties do not change between experimental conditions. (**A**, **B**) FM puncta area and initial dye uptake in all the experimental conditions. Expression of wtUb or its mutant

forms (UbK11R, UbK29R, UbK48R and UbK63R) did not change the size of FM puncta or initial dye uptake. (**A**) Area of individual FM puncta in the first frame of the time-lapse. (**B**) Mean fluorescence intensity of individual FM puncta at the first frame of the time-lapse as a measure of FM dye uptake. (**A**, **B**) Statistical analysis by Kruskal-Wallis. Results were averaged from 205 (eGFP), 517 (wtUb), 252 (UbK11R), 443 (UbK29R), 271 (UbK48R) and 444 (UbK63R) FM puncta in 2 independent experiments. Error bars indicate s.e.m.

Discussion

In this preliminary study, we uncover a potential role for polyubiquitination as a novel regulator of presynaptic neurotransmitter release. By using dye release experiments, we estimated the rate of SV pool release by analyzing the kinetics of FM dye loss in a population of synaptic terminals that are release competent. We concluded that increasing Ub levels results in an accelerated rate of action potential-induced SV pool exocytosis. Blocking formation of polyubiquitin chains on lysines 11, 29 and 63 partially abrogates this increased release rate, thus suggesting that the effect of elevated Ub levels is mediated by enhanced polyubiquitination of substrates, specifically through K11, K29 and K63 Ub chains.

Currently we have a limited understanding of how Ub regulates synaptic transmission at the presynaptic level. We observed an increased rate of SV pool release upon expression of ubiquitin, which is in agreement with previous findings using the mutant ataxia mice ax^{J} [258,259,367]. These mice are characterized by a loss of free Ub and decreased polyubiquitinated conjugates at the presynaptic compartment. They display severe malformation of the neuromuscular junction and impaired synaptic transmission, which are rescued upon restoration of Ub levels[258,259]. In an attempt for a deeper understanding of the neurotransmission defects of these animals, Miller and colleagues[367] concluded that less SVs are mobilized to sites of fusion and so reduced quantal release is observed. So, in these mice it does seem that decreased levels of Ub correlate with reduced neurotransmitter release. In accordance with these observations, when we overexpress Ub, exactly the opposite outcome is observed, with a higher rate of neurotransmitter release. Therefore, we conclude that ubiquitin-related events are critical for dictating the speed of SVs release at the active zone.

A shared observation is that proteasome inhibitors increase synaptic transmission[359,384–386]. In agreement, when cells were infected with the UbK48R construct, which prevents formation of the polyubiquitin tag for proteasome recognition thus decreasing global rates of protein degradation, an increased rate of presynaptic release was also observed. This fits well with the idea that a halt in degradation will increase levels of proteins of the SV recycling machinery, known to be proteasome targets, thus increasing presynaptic release. Although expression of wtUb and UbK48R result in the same phenotype, the fact that higher levels of wtUb upregulate accumulation of K48 ubiquitinated substrates (see Chapter 4, figure S4.9) thus potentiating their degradation, led us to reason that these two constructs probably alter the rate of SV pool exocytosis through different mechanisms.

Indeed, the partial reversion of Ub phenotype upon expression of the remaining Ub mutant forms (UbK11R, UbK29R and UbK63R), actually gives hints to understanding the dual role of ubiquitin in presynaptic function. These results indicate that formation of polyubiquitin chains through lysines 11, 29 and 63 is required for the increased rate of SVs unloading. We thus assume that higher levels of Ub potentiate formation of these polyubiquitin chains on substrates that will ultimately alter the release properties of SVs. None of the Ub mutant forms completely reverted the effect of wtUb, suggesting that they may exert a combined and cumulative effect, and together account for the total effect of Ub expression on presynaptic release. It would be interesting to address this idea with a triple mutant for lysines 11, 29 and 63. However, we cannot discard the possibility that other types of Ub chains, for instance through lysines 6, 27 or 33 (which were also detected in the brain ubiquitome[243]), might also regulate neurotransmitter release. The generation of mutants for these lysines would probably address this question. Moreover, for further validation of these results, electrophysiological recordings or the use of pH-sensitive fluorescent proteins (e.g. synaptophysin-pHluorin[520]) would be highly instrumental and informative.

Work in synaptosomes revealed that depolarization-dependent Ca^{2+} influx induces a general decrease of the ubiquitinated state of proteins that is not due to protein turnover by the proteasome[387]. Another group concluded that increased neurotransmitter release results from an altered state of a group of dynamically ubiquitinated proteins[384]. Together with our results, these data suggest that an increased polyubiquitinated state of a subset of presynaptic proteins enhances the efficacy of SV release, which is rapidly counteracted by Ca^{2+}-driven intracellular events that inhibit ubiquitination. Hence, presynaptic boutons can modulate their readiness for release by adjusting polyubiquitin tags on substrates. Herein, we propose that these tags are mainly composed of K11, K29 and K63 Ub linkages.

At this stage important questions arise. How does polyubiquitination regulate neurotransmitter presynaptic release? How can it interfere with SV recycling machinery into increasing the rate of exocytosis? We can speculate that polyubiquitination of proteins within the presynaptic terminal may interfere with calcium channels, either increasing their responsiveness to action potentials or their expression at the plasma membrane surface. In fact, calcium channels are highly modulated by multiple mechanisms as a way of regulating synaptic transmission[521] and their surface expression might be tuned by ubiquitination[407–409]. We may also speculate that the attachment of polyubiquitin chains modulate proteins into promoting faster SV exocytosis or facilitating the zippering of SNARE proteins for instance. Indeed, it was recently proposed that ubiquitination may have direct effects on proteins, either altering their conformation, modulating their function or influencing protein-protein interactions[246]. The E3 ligase Rnf13 is actually capable of favoring SNARE assembly by enhancing interaction of SNAP25 with snapin via K29 ubiquitination[360]. Interestingly, SUMOylation, which shares with ubiquitination striking similarities, has been shown to play a central role in the regulation of fast SVs exocytosis[522,523]. Apparently RIM1α switches between a SUMOylated and a non-SUMOylated form. SUMOylation of RIM1α alters its conformation into enhancing interaction with calcium channels, thus facilitating their clustering and higher calcium influx; whilst non-SUMOylated RIM1α participates in the docking and priming of SVs[522]. Due to the nature of ubiquitin signaling and its resemblance with SUMO, it is plausible to predict a similar regulatory role for ubiquitination in presynaptic release.

In conclusion, this preliminary study attributes a novel and potential role for K11, K29 and K63 polyubiquitination in the modulation of presynaptic neurotransmitter release. It would be interesting to investigate the mechanism underlying the regulation of SV pool release by polyubiquitination, regardless how far-reaching it may seem at this moment.

Chapter 6

General Discussion and Future Perspectives

In this work we uncover a prominent role for ubiquitin and the proteasome at the presynaptic level, both for its formation and function. The proteasome is a multicomplex that relies on internal subunits and additional machinery to collect proteins bearing a tag for degradation. Once unfolded, the proteasome will degrade them indiscriminately. In order to guarantee selective degradation of proteins, cells have developed an intricate coding system based on the small molecule ubiquitin. However, ubiquitin range of action is far wider than targeting proteins to the proteasome. Indeed, the diverse forms by which ubiquitin can decorate a substrate exponentially multiply its possible interpretations and outcomes within a cell. Pioneer studies have predicted that synapse formation relies on ubiquitination events. Besides, some studies, mostly in invertebrates, have demonstrated a role for E3 ligases at the nascent presynaptic terminal. Furthermore, efforts have been made to understand the contribution of ubiquitin to neurotransmitter release upon arrival of an action potential.

One of the major questions in the field of presynapse formation is how synaptic material gets trapped in specific subdomains and orderly clustered into a presynaptic bouton. In vertebrates, F-actin and scaffolding proteins have so far been identified as the local players mediating this event. Herein, we contribute considerably to the field by showing that ubiquitin and the proteasome also function locally to control the extent of presynaptic differentiation in the vertebrate CNS. In this work, we also highlight the potential contribution of polyubiquitination for the building of a functional SV release apparatus.

Overall, this work unravels a crucial role for ubiquitin and the proteasome in the lifetime of a presynaptic terminal. Our results support five major findings: i) presynaptogenic factors alter proteasome distribution along the axon with their concentration in catalytically active hot-spots; ii) FGF22 and BDNF-induced presynaptic differentiation require degradation of proteins by the proteasome; iii) increased *on-site* accumulation of polyubiquitinated conjugates in response to proteasome inhibition triggers the assembly of functional presynaptic terminals; iv) proteolytic-related polyubiquitin chains may function transiently as signals for presynaptic clustering and v) polyubiquitination regulate stimulus-evoked neurotransmitter release.

A dynamic proteasome in the axon

Within the axon, the proteasome may suffer changes in its localization and activity status to respond adequately to extracellular factors. Degradation of proteins in cells has to occur in a highly regulated and selective manner; otherwise unwanted proteolysis of functional proteins would affect cell homeostasis. In addition to the specificity conferred by all the UPS machinery and Ub tags, dislocation of the proteasome to the site of degradation also occurs. Indeed, proteasomes are recruited and sequestered in dendritic spines upon depolarization[411], probably as a way of sculpting the content of a synapse in an activity context[457]. It is therefore likely to predict that similar modes of regulation also take place in the axon. The proteasome has very recently been shown to travel along the axon in three distinct types of motion: an active movement at a speed comparable to that of fast axonal transport; a diffusion-driven transport in which the proteasome particle moves adrift (barely changing its net displacement) and proteasome-confined motion[442]. These types of movement account for 20%, 56% and 24% of total proteasome particles[442]. This heterogeneity may grant proteasomes the capability to be rapidly recruited or relocated to specific axonal domains, in order to fulfill local needs for protein degradation. For instance, a rapidly moving proteasome is likely to target distal regions, whilst the diffuse proteasome probably awaits a local “call” to meet proximal demands. On the other hand, it is conceivable that the confined proteasome constitute fixed sites of proteolysis along the

axon to which proteins harboring a degradation tag are taken. To our knowledge, these ideas have not yet been tested in axons.

On chapter 3, we observed an upregulation of proteasome puncta along axons in response to two unrelated presynaptic organizing factors, FGF22 and BDNF. Moreover, distinct spots of catalytically active proteasome appear upon stimulation with these same factors. We thus concluded that a presynaptogenic stimuli alters the distribution pattern of the endogenous proteasome and creates specific hot-spots of proteasome degradation along the axon. However, SV clusters were not specifically formed on sites of accumulated proteasome. We thus hypothesized that proteasomes cluster either at the vicinity of a nascent terminal or at the same location but at a time point previous to SV clustering. The fact that less than 10% of SV clusters colocalize with accumulated proteasome and that live formation of a stable presynaptic cluster is preceded and accompanied by an *on-site* decrease in proteasome degradation (chapter 4) gives support to the former hypothesis. It would be interesting to address these possibilities by performing a live-imaging experiment in which an axon co-expressing the presynaptic marker Vglut1-mCherry and the proteasome reporter CIM5-GFP[411] would be stimulated with FGF22 and BDNF. In addition a construct for the 20S proteasome, α4-YFP[442] for instance, could also be used to evaluate differences in the movement of the regulatory and catalytic proteasome complexes. Furthermore, it would be interesting to ascertain whether axonal redistribution of the proteasome is a shared effect of soluble synaptogenic molecules by performing the same analysis upon bath stimulation with Wnts, semaphorin 4D, netrin, thrombospondins or TGF-β1 (see table 1.1). Furthermore, one could try to evaluate axonal proteasome redistribution during synapse formation in organotypic hippocampal slices expressing the reporters aforementioned, in which the developmental stages are closer to the *in vivo* context. Nevertheless, it is conceivable that axons may use different strategies downstream different presynaptic differentiation factors that result in the same outcome. For instance, we have observed that engagement of transsynaptic complexes upon bead and dendritic contact reduces activity of the local proteasome to trigger presynaptic differentiation, whereas activation of receptors by soluble factors (FGF22 and BDNF) requires proteasome activity. This duality will be discussed ahead.

How the axon can alter proteasome localization remains totally unknown. In dendrites, the proteasome is recruited to spines by autophosphorylated CamKIIα, whose relocation to these structures is sufficient to drag proteasomes along[440]. As previously discussed, it is conceivable that a similar mechanism occurs in axons. To test this hypothesis, live-imaging of proteasome distribution along axons could be performed in combination with a fluorescent form of wt CamKIIα or autophosphorylation-deficient and phospho-mimic CamKIIα constructs, as previously performed[440]. In addition to proteasome redistribution, CamKIIα also activates the proteasome by phosphorylating the proteasome subunit Rpt6[440,466,467]. It is thus equally likely that a similar mechanism underlying proteasome activation occurs downstream activation of TrkB and FGFR2b in axons. Analysis of the phosphorylation level of Rpt6 in response to FGF22 or BDNF would test the truthfulness of this hypothesis. It is also predictable that other site-specific phosphorylation episodes activate the proteasome. In cardiac cells, kinases and phosphatases coordinate proteasome function and a large number of post-translational modifications (PTMs) of proteasome subunits by phosphorylation have been identified[524–526]. By performing a proteasome fractionation technique and analyzing the phosphoproteome by mass spectrometry it was observed that in the heart the 20S proteasome subunits are extensively phosphorylated and modulated by PKA[526]. Similarly, comprehensive characterization of the phosphorylation profile of the proteasomes under basal and FGF22 or BDNF-stimulated developing neuronal cells would enable identification of potential modes of proteasome activity enhancement by synaptogenic cues. Considerable complexity is added by a myriad of PTMs, such as NH_2-terminal

modifications, N-myristolation, clivage, acetylation, ubiquitination, SUMOylation and O-linked *N*-acetylglucosamine, which regulate multiple facets of proteasome function including its catalytic activity and subcellular localization[503,524]. Although phosphorylation is a highly potential candidate due to the kinase nature of the receptors intracellular domain, any of the modifications listed may theoretically underlie the effect of FGF22 and BDNF, and so, are worth exploring in future research projects. Proteasome regulation by PTMs confers an outstanding tool to rapidly modulate proteasome function in order to fulfill cell needs and accordingly of utmost importance in a highly polarized cell as the neuron.

Another possibility by which presynaptogenic factors alter proteasome localization would be direct interaction between the proteasome and the intracellular portion of the activated transmembrane receptor, thus directly accumulating proteasome specifically at sites of receptor enrichment. Although there is no evidence supporting this idea both for TrkB and FGFR2, the TrkA receptor interacts directly with the proteasome subunit β6 and induces its phosphorylation[527]. It would be relevant to address this idea by performing immunoaffinity purification for the intracellular domains of TrkB and FGFR2 and assess their binding to proteasome subunits or alternatively to E3 ligases. Moreover, it would be interesting to perceive whether hotspots of active proteasome are coincident with FGFR2 and TrkB enrichment sites along the axon.

Although we are still lacking a live characterization of proteasome dynamics in the axon during presynaptic formation, this work pioneers the finding that proteasomes are prone to suffer changes in their localization in axons. However, the specific function of proteasome redistribution in presynaptic differentiation remains to be fully delineated. Furthermore, the axonal mechanism underlying proteasome redistribution and enhanced activity is still elusive and deserves close attention in future work.

Disposal of proteins to proceed with presynaptic differentiation

Proteasome activity can trigger presynaptic differentiation by degrading proteins that are preventing its initiation. This strategy confers temporal and spatial specificity to synapse formation and constitutes a prime strategy to allow for correct wiring of the nervous system. An outstanding example is that of ephexin5 at the postsynaptic side[434]. Ephexin5 is an intracellular RhoA GEF that interacts directly with the postsynaptic receptor EphB2 and negatively regulates differentiation of the postsynaptic terminal following activation of this receptor[434]. Binding of EphrinB and activation of the receptor reverts this blocking by ubiquitination and targeting of ephexin5 for degradation[434]. Similarly, formation of presynaptic terminals in *C. elegans* requires downregulation in a manner dependent on E3 ligases of presynaptically-located kinases[350,351]. Whether a similar mechanism also regulates differentiation of the presynaptic terminal in higher organism was until now not investigated. Herein, we provide evidence that FGF22 and BDNF presynaptogenic effect also requires degradation of proteins.

These findings suggest that identification of the candidates undergoing degradation in axons in response to FGF22 and BDNF would be essential for the full clarification of the mechanism downstream activation of their cognate receptors. Moreover, these candidates are likely to represent intra-axonal negative regulators of presynaptic differentiation; hence their identification would give valuable insights to the field. To most of the presynaptic organizing factors, the corresponding downstream pathway is still elusive. It is plausible that some might converge on the same intracellular target, such as removal of the above proposed specific local constraint in presynaptic clustering. Therefore, identification of FGF22 and BDNF targets (or target) for proteolysis will open new avenues of research and possibly identification of

redundant and cooperative intra-axonal pathways that trigger presynaptic assembly. Indeed, along axons formation of an F-actin network that recruits SVs occurs through recruitment of actin regulators and can be initiated at the base of different transmembrane receptors[142,193,194,198,528].

Another possibility would be that predefined pausing sites of SVs, in which an axodendritic synapse preferentially forms[44,46–48], are created by differential degradation of proteins along the axons. Sites at which a protein functioning to restrain synapse formation is continuously degraded would correspondent to these, yet unexplained, specific axonal sites. Asymmetrical proteasomal degradation is in fact observed in axons of cortical neurons throughout development. During axonal outgrowth, the endocannabinoid 2-arachidonoyl glycerol (2-AG) is synthesized in the growth cone and acts as an autocrine factor to facilitate its growth. The enzyme that degrades 2-AG, MGL, is spatially regulated by the proteasome: the growth cone is devoid of MGL as opposed to the axonal shaft, thus allowing axonal progression[435]. At the moment of synaptogenesis, asymmetrical proteasome distribution is lost and the growth cone halts to give place to synapse formation[435].

To identify the possible candidates whose degradation is needed for presynaptic differentiation to proceed, immunoprecipitation with an antibody specific for K48-polyubiquitin linkages[492] of axonal pure preparations followed by mass spectrometry could be performed. Candidates whose downregulation upon FGF22 or BDNF stimuli is sensitive to proteasome inhibition would constitute possible targets that could be further validated. Some studies give us some clues of possible proteins. BDNF decreases in a proteasome activity-dependent manner the amount of some proteins enriched at spines, such as the postsynaptic NMDA receptors subunits NR2B and NR1, A-kinase anchor protein (AKAP), PKA and spinophilin[456]; whereas activation of FGFR2 in skeleton cells triggers ubiquitination and degradation of α5 integrin and PI3K[464,465]. Nevertheless, an axon-directed approach would more precisely reveal which proteins are proteolytically removed in a developing axon exposed to these soluble factors.

An intriguing question remains as to how FGFR2 and TrkB can enhance proteasome-mediated degradation. We have previously discussed the idea that a conserved mechanism of proteasome redistribution and activity through CamKIIα is likely. Notwithstanding, additional mechanisms might lead to enhanced degradation. Interestingly, two independent studies that performed unbiased microarray analysis show that mRNAs coding for several proteasome subunits can be found in axons[474,529]. Notably, in mouse retinal growth cones, collected by laser microdissection, an outstanding number of transcripts for subunits of the 19S and 20S proteasome can be found[529]. Similarly, it was identified in axons of hippocampal neurons grown in microfluidic devices mRNAs for the 20S proteasome subunits β1, β4, β5 and α7[474]. This information in combination with the established idea of local translation in axons, leads us to hypothesize that proteasome subunits might be synthesized in the developing axon. Indeed, both FGF22 and BDNF have been shown to regulate events in the axon through enhanced local protein synthesis[486,530–532]. It is thus conceivable that these factors enhance proteasome activity by upregulating local translation of proteasome subunits that will be integrated into functional complexes. It is interesting to emphasize that the mRNA coding the β1 20S subunit, which we observed to be more catalytically active upon stimulation, can be found in axons. Apart from proteasome subunits, the pool of axonal transcripts also comprises mRNAs for E2s and E3s[529]. They include the F-box protein Fbxo45 whose deletion impairs synapse formation[377] and several proteins of the RNF family whose members play roles in axon growth and presynaptic release[332,360]. Accordingly, it is also possible that rather than enhancing proteasome activity directly, FGF22 and BDNF upregulate ubiquitination of targets for degradation by locally synthesizing E2s and E3s. On the other hand, due to the kinase nature of the intracellular domains of TrkB and FGFR2b, a more rapid effect on E3s activity

could be promoted by phosphorylation. Indeed, E3 ligases localization, activity and substrate preference can be regulated by phosphorylation[315,324,533–535]. Moreover, work in our lab has shown that FGF22-induced presynaptic differentiation is dependent on extracellular-signal-regulated kinase (ERK) and AKT kinases (unpublished data). FGFR2 binds directly to the E3 ligase Cbl during skeletogenesis[465] and TrkA receptor associates with the E3 ligase Nedd4 and phosphorylates it upon NGF binding[536], thus revealing an additional possible mechanism for the activation of E3s through direct binding to the receptors and phosphorylation.

Altogether, these are hypothesis worth exploring to go deeper into the understanding of the intracellular events orchestrating presynaptic differentiation. Site-specific elimination of proteins may either induce presynaptic clustering *per se*, or be part of a cascade of events that leads to formation of presynaptic terminals. An illustrative example of the latter hypothesis is Nedd4-induced downregulation of PTEN, a negative regulator of PI3K, which in turn promotes cytoskeletal rearrangements in the growth cone and enhancement of its braching[345].

A polyubiquitin nest for presynaptic differentiation

Accumulation of polyubiquitinated proteins can act as a local recruitment platform for formation of *en passant* presynaptic terminals. The function of ubiquitin chains as recruiters of molecular machinery to specific locations as a means to execute cellular events has already been described in other cellular events. Some strategies for DNA repair involve recruitment of repair machinery to the site of DNA lesion by the recognition of mono or polyubiquitinated substrates[296–298]. Furthermore, activation of the NF-κB pathway requires recruitment of kinases to a highly polyubiquitinated signaling complex formed by activation of transmembrane receptors[248,299]. In this work we unveil a new potential mechanism for formation of presynaptic clusters involving recruitment and clustering of synaptic material to enriched sites of polyubiquitinated proteins. It will be important to determine how polyubiquitination may promote recruitment of presynaptic material to nascent synaptic sites and how this may functionally cooperate with other *on-site* intracellular events instructing clustering. It is currently believed that formation of an F-actin network recruits SVs to discrete sites along the axon by acting as a scaffold for nascent presynapses[537]. It may be possible that Ub and actin function together to erect a local “hub” for the recruitment of presynaptic material. Indeed, bead-induced presynaptic differentiation promotes both localized F-actin clustering[192] and accumulation of K48 polyubiquitinated conjugates (figure 4.8 and 4.9). In addition, nascent presynapses along axons are associated with enhanced levels of F-actin[191] and increased K48 polyubiquitin signal (figure 4.8). Due to Ub ability to modulate actin monomers and regulators of actin dynamics[538,539], a scenario in which enhanced local polyubiquitination alters cytoskeleton dynamics into favoring presynaptic assembly is also possible. Furthermore, it would be interesting to understand in which precise step of presynaptic assembly an *on-site* polyubiquitinated pool exerts its effect. Does it only promote site-specific deposition of material that will afterwards cluster independently or does it also coordinate assembly?

The concept that *on-site* accumulation of polyubiquitinated proteins triggers formation of presynaptic clusters implies that presynaptic differentiation is dependent on Ub homeostasis. As a matter of fact, development of the presynapse was shown to be controlled by a balance between ubiquitination and deubiquitination in *Drosophila*[363]. Furthermore, decreased synaptic levels of free and conjugated Ub in a mutant mice results in defective presynaptic formation and function, which are rescued by restoring Ub levels[259,260,258]. Contrariwise, transgenic mice overexpressing Ub also display impaired formation of synapses[257], further reinforcing that tightly balanced Ub levels are crucial for proper synaptic development.

Mice have been engineered to lack the polyubiquitin genes Ubb or Ubc with subsequent loss of Ub levels [540–543]. These mice would be instrumental to address the *in vivo* function of Ub for the formation of synapses. In order to specifically deplete neuronal Ub during development, thus discarding its effect on additional tissues or developmental windows, conditional ubiquitin mutant mice could be generated in which Ub genes would be specifically deleted in brain tissues at the 2-3 first postnatal weeks, time at which synapse formation occurs in rodents. On the other hand, assessment of the *in vivo* function of polyubiquitination in presynaptic development would be much more difficult. This could be achieved by the generation of conditional Ub point mutant knock-in mice, as elsewhere reported for a GABA receptor subunit[544], to temporally restrict expression of Ub forms incapable of forming linkage-specific chains.

In this work, we uncover a new potential role for proteolytic-related Ub chains in functioning as signals for presynaptic assembly. In an attempt to further characterize the role of accumulated ubiquitinated conjugates on the formation of presynaptic clusters, Ub mutants that prevent formation of specific Ub linkages were expressed on cells, which allowed us to conclude that Ub chains that normally function to send proteins for proteasomal degradation (K11, K29 and K48) may also trigger formation of functional presynaptic clusters. K48 and K11 Ub chains are well-established as tags for degradation by the proteasome[267,292], while K29 Ub chains have been linked to the proteasome only based on mass spectrometry detection of its upregulation upon proteasome inactivation[277–279]. On the contrary to K11 and K48 Ub linkages, whose specific mutants abolish formation of presynaptic clusters regardless of the experimental conditions, the results for K29 ubiquitination were incoherent between presynaptic clusters being formed on isolated axons or in an axodendritic context. This may indicate us that the main proteasome-related Ub linkages, K11 and K48 chains, constitute the prime signals within the pool of ubiquitinated conjugates that trigger presynaptic differentiation. So far, very few studies have revealed roles for K48 Ub chains other than the classical labeling of proteins destined for the proteasome. K48-linked Ub chains can inactivate the *S. cerevisiae* transcription factor Met4 without targeting it for degradation[545–547] or function as signals for translocating membrane ER proteins to the cytosol by the Ub selective chaperone p97[548,549]. As for K11-linked chains, they appear to be involved in a wider range of cellular processes. Besides its function in ERAD[277,284] and degradation of proteins to govern cell cycle progression[550], K11 Ub chains can also enhance stability of proteins[396], perform a signaling role in the activation of NF-κB downstream TNFR[551], or function as an internalization signal for membrane receptors[552,553]. Herein, we propose a novel role for these two types of Ub linkages in presynaptic differentiation, which are among the Ub chains with higher expression levels in the young *Drosophila* nervous system undergoing synaptogenesis[242] and in the adult rat brain[243].

Ubiquitin signals on substrates may serve a dual role in a developing neuron. An interesting finding tell us that only 5% of total Ub in the brain can be found as polyubiquitin chains on substrates[294], possibly indicating that cells are equipped to respond rapidly to new intracellular polyubiquitination signals, rather than requiring proteins to remain accumulated in their polyubiquitinated state for long periods. In accordance, we propose that proteins that under normal conditions are rapidly directed to the proteasome upon their ubiquitination will remain accumulated in cells in this state if their degradation is momentarily paused. Hereupon, their availability as polyubiquitinated conjugates is extended thus allowing them to exert a different biological function (such as triggering of presynaptic assembly) that precedes their proteasome removal. This model highlights the fact that the same type of Ub chain attached to a protein may engage it into diverse roles. Moreover, it suggests that the outcome of ubiquitination do not depend solely on chain topology, but also on signal duration, localization and available downstream Ub interpreters and effectors. It is also conceivable that a dual role for Ub chains is due to different chain lengths on substrates. Efforts

should be made to better understand the intra-axonal mechanisms that regulate, build and decode Ub signals with a dual regulatory role.

On the previous section, we discussed the possibility that predefined pausing sites of SVs may be defined by differential degradation of proteins along axons. Alternatively, they may represent enriched sites of polyubiquitination. Throughout this work, we made use of a fluorescence complementation approach, UiFC, to detect formation of K48 ubiquitin chains along developing axons. In agreement with our final model on chapter 4, contact with beads induces accumulation of K48 ubiquitin signal on contacting axons (figure 4.9). Additionally, stable puncta of UiFC can be found along axons under basal conditions (figure S4.8). Although we did not explore their biological significance, they constitute hot-spots of accumulation of K48 polyubiquitinated conjugates that remain untouched in cells. It is so plausible to ask whether SVs or active zone material preferentially pause and cluster at these sites. Time-lapse imaging along with a presynaptic marker or recurrent labeling for active terminals with FM dye would address this question. In addition, to further validate our current model, it would be of paramount significance to evaluate appearance of an axonal UiFC puncta at an axodendritic contact in which formation of a presynaptic cluster occurs.

To fully validate the novel concept that an *on-site* pool of polyubiquitinated axonal proteins functions as a signal to give rise to new presynaptic clusters, complete characterization and identification of the involved substrates is undoubtedly needed. We have observed that K48 polyubiquitinated conjugates accumulate at sites of nascent synapses. Our results further suggest that additional chains of different Ub topologies, such as K11 or K29, may also specifically accumulate. Specific antibodies for Ub linkages, which have already been generated and used as tools for characterizing functions of Ub chains[282,554], could be used to stain developing axons. Another important aspect would be to characterize the relative position of polyubiquitinated signals to the presynaptic structure being formed. For instance, in *Drosophila* NMJs ubiquitinated conjugates concentrate surrounding the active zone[472]. One could address this issue by combining information from immunoelectron microscopy strategies with super-resolution fluorescence imaging methods, using brain slices from animals at developmental stages coincident with synaptogenesis and isolated axons treated with proteasome inhibitors or presynaptic clustering-inducing beads. The use of super-resolution approaches has been instrumental to allow for the 3D reconstruction of molecular assemblies at the presynaptic terminal[3,555].

Notwithstanding, identification of the ubiquitinated conjugates featuring presynaptogenic properties would be the key issue to disclose, so that the full mechanism can be understood. A cohort of different approaches involving isolation of ubiquitinated conjugates and subsequent mass spectrometry has been extensively exploited to identify the proteins comprising the cellular ubiquitome[556–559]. Although two different ubiquitin proteomics studies have made efforts to characterize the brain ubiquitome[242,243], a more directed approach would be needed to identify the polyubiquitinated substrates being locally accumulated in axons that could function as local recruiters of presynaptic material. This could be achieved by performing a mass spectrometry analysis of the pool of ubiquitinated proteins present in ultrapure synaptosomes, which would be isolated by using a fluorescence activated synaptosome sorting method recently described[560], or present in presynaptic clusters formed on beads that could be captured by laser microdissection, as elsewhere performed for growth cones[529]. In order to evaluate changes in the presynapse ubiquitome throughout the developmental stages of a presynaptic terminal, synaptosomes could be obtained from brain tissue at different post-natal stages or extraction of axonal material contacting with beads could be performed at different time-points after initial contact. A similar strategy has been used to address changes in the expression level of different classes of proteins in synaptosomes during early development[561].

Furthermore, our results support the hypothesis that a reduction in proteasome activity in specific axonal domains is accompanied with an increased accumulation of ubiquitinated conjugates that in turn trigger presynaptic assembly. Moreover, the presynaptogenic effect of the deubiquitinase inhibitor PR619 is likely to function through the same pathway. Taking this into consideration, identification of proteins whose ubiquitination is enhanced by proteasome inhibition or PR619 in isolated axons would grant a step forward in understanding this Ub-mediated pathway leading to presynaptic differentiation. Gathering information from all the described experimental set-ups could contribute to characterize the composition of an axonal synaptogenic pool of polyubiquitinated proteins, which could then be individually validated as candidates whose ubiquitinated state enhance presynaptic assembly.

Proteins containing UBDs will theoretically serve as the mediators transforming polyubiquitin signals into downstream effects that instruct clustering of presynaptic material. It has been previously discussed that the active zone protein syntenin, the SV protein amphiphysin and the endocytic adaptors epsin1 and Eps15 contain UBDs[403,507–510] and so constitute potential candidates for promoting presynaptic clustering downstream polyubiquitin signals. It is also known that syntenin is required for EphB-induced presynaptic differentiation[132]; however, whether this is dependent on its UBDs is still unknown. Syntenin has the ability to bind to K48-linked chains, co-localizes with ubiquitinated cellular proteins and forms Ub-based molecular hubs by interacting with a set of ubiquitinated proteins linking them to transmembrane proteins in HeLa cells[508]. These evidences further emphasize the potential role of syntenin in presynaptic assembly triggered by polyubiquitin signals, which we believe is worth exploring in detail. On the other hand, our results attribute to K11-linked Ub chains a decisive role in presynaptic differentiation, yet no UBDs capable of specifically recognizing this type of linkage have been identified. K11 chains could either be recognized by the same intracellular machinery as K48 chains, or by a distinct set of axonal proteins. It would be important to identify presynaptic proteins that bind to K11 polyubiquitin and evaluate their requirement in presynaptic differentiation. The fact that: UBDs fold into secondary structural elements; that recognition of Ub domains can occur through diverse and interleaved surfaces and structural elements within a protein; and that the regions flanking interacting domains also adjust binding competence[265], makes it difficult to bioinformatically predict the likelihood of a protein to recognize and bind Ub. Hence, experimental approaches based on direct binding assays for different types of chains have to be performed to detect and characterize potential UBPs in the presynapse.

Overall, we hereby propose a novel model for the coordinated clustering of presynaptic material based on the formation of a nest of polyubiquitinated conjugates at sites of contact with a postsynaptic partner. Future investigation will hopefully further validate this idea and help to provide a detailed description of the full mechanism.

The paradoxical role of the UPS in presynaptic differentiation

Surprisingly, the UPS has an ambiguous role in axonal processes. Evidence show that it can interfere with an event occurring at the developing axon through distinct and antagonistic ways. In terms of growth, first studies indicated that proteasome inhibition increases neurite outgrowth in PC12 cells[562–565] and in *Aplysia* [386]. Later, in PC12 cells proteasome inhibitors were proposed to enhance neurite outgrowth through a mechanism involving activation of ERK/MAPK and PI3K/AKT signaling pathways and phosphorylation and ubiquitination of TrkA receptors[566]. In complete contrast, in primary cultures the proteasome inhibitor lactacystin inhibits the positive effect of NGF on neurite outgrowth[567] and impairs axonal regeneration[568],

thus revealing that protein degradation by the proteasome can also serve as a requisite for axonal extension. Together, these studies predict that the UPS may affect axon outgrowth through opposite pathways. As a matter of fact, whilst proteasomal degradation of some proteins is necessary for axon outgrowth[334,345,569], degradation of other proteins should pause to allow for their accumulation on cells and promotion of axonal growth[332]. In a similar fashion, presynaptic differentiation can be triggered by either enhanced proteasomal degradation of specific proteins[350,351] or restrained by their constitutive removal[348,352]. Indeed, proteasome inhibition increases the number of synaptic contacts formed between *Aplysia* sensory and motor neurons[386]. Overall, it seems that the proteasome does not straightforwardly affect processes in the developing axon, but rather has a double-sided effect.

The results gathered in this work clearly show that the UPS can orchestrate presynaptic differentiation in hippocampal neurons through diverse and antagonistic intracellular pathways. Throughout the course of our work, we found that FGF22 and BDNF required proteasomal degradation to induce presynaptic differentiation and expectedly converge with the effect of the proteasome activator IU1 in the enhancement of presynaptic clustering (chapter 3). Surprisingly, proteasome inhibitors not only revert the effect of FGF22 on isolated axons and but are themselves capable of exerting a presynaptogenic effect, thus meaning that they trigger presynaptic assembly in an antagonistic manner to that of FGF22. We then delved into the understanding of the mechanism underlying the effect of proteasome inhibitors and attributed a role to the resultant pool of polyubiquitinated proteins (which are ordinarily targeted to degradation) in the induction of presynaptic assembly (chapter 4). These findings suggest that interfering with the UPS both positively and negatively upsets the basal balance of protein ubiquitination and degradation, which then leads to presynaptic clustering via distinct routes (figure 6.1). Overall, our results unveil two distinct pathways boosting presynaptic differentiation that involve the UPS: removal of proteins by increased proteasomal degradation or accumulation of polyubiquitinated proteins by reduced proteasome activity (figure 6.1).

The fact that distinct factors induce presynaptic assembly and their combined effect abrogates clustering to basal levels, clearly demonstrates that antagonistic routes involving the same players can result in the same presynaptic outcome. In terms of the effect of FGF22 and proteasome inhibitors on the number of SV clusters in isolated axons and based on the results gathered in this work it is predictable that inhibition of protein degradation prevents FGF22 effect. On the other hand, FGF22 itself may alter the landscape of protein ubiquitination produced by proteasome inhibitors alone thus also canceling their effect when co-applied. An interesting conclusion is that the same neuron can engage into either route and so it contains the required intracellular machinery to respond to both opposite stimuli. Probably the simplest explanation for interpreting this paradox is that axonal UPS can be differently affected downstream activation of different presynaptogenic factors: whilst FGFR2 and TrkB enhance degradation of proteins, other factors might locally diminish proteasome activity (figure 6.1). It remains to be determined which presynaptic inducing factors can negatively alter local UPS activity and how or whether opposite routes to presynaptic assembly can be properly integrated to signal formation of functional presynaptic terminals.

How can we explain this antagonistic function of proteasome and ubiquitin in presynaptic differentiation? The first possibility would be that these different UPS-driven pathways regulate presynaptic assembly at different critical developmental stages. Indeed, the effect of proteasome inhibitors in the number of presynaptic clusters is specific to axons isolated in microfluidic devices, which have a decreased level of maturity due to their deprivation from soma-derived factors. Moreover, older axons in microfluidic devices lose responsiveness to proteasome inhibition. It is thus likely that proteasome inhibition, as opposed to the proteasome-dependent effect of FGF22 or BDNF on presynaptic clustering, works at early

developmental stages. We may speculate that intrinsic changes in the developing axon, for instance in the expression of axonal *on-site* effectors, will render it unresponsive to proteasome inhibition, but still capable of reacting to different cues. A second possibility would be that distinct UPS-mediated pathways leading to presynaptic assembly function at different axonal locations. Engagement of different intracellular signaling pathways in a region specific manner would probably be due to asymmetric distribution of surface receptors and/or intracellular effectors along a growing axon. Indeed, surface receptors and endogenous signaling factors may display a characteristic asymmetric distribution along axons which was shown to be correlated with an important functional significance[570–573].

Even though much remains to be understood and clarified, this work supports the notion that distinct presynaptic organizers act through distinct intracellular routes, rather than converging on the same pathway. Furthermore, it reveals that the UPS can be exploited in more than one manner to induce formation of presynaptic boutons in the same cell.

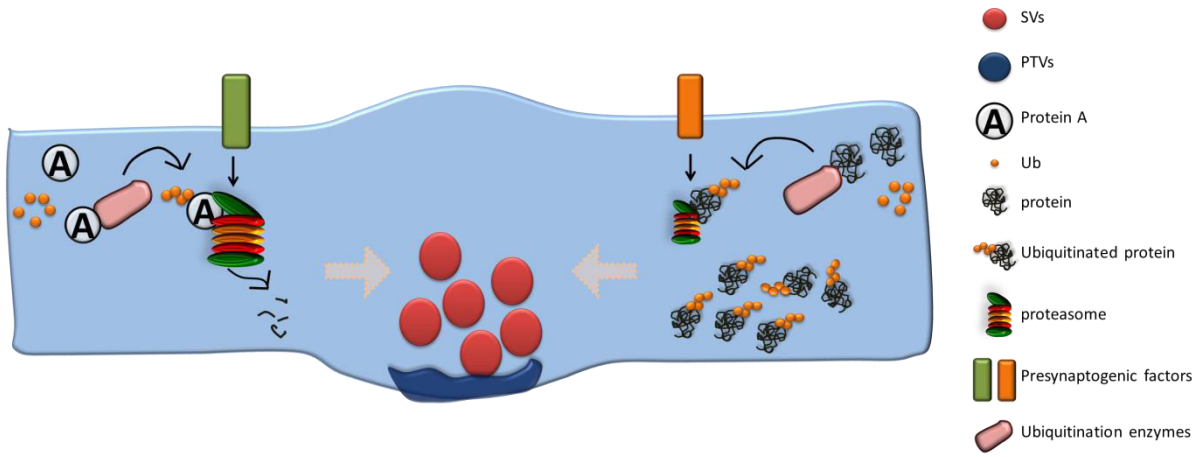

Fig. 6.1 - The proteasome: a double agent in presynaptic differentiation. According to our results, we propose that both activation and inhibition of the proteasome can paradoxically lead to presynaptic differentiation by removal of a specific protein (protein A) or accumulation of proteins in their polyubiquitinated state, respectively. We further hypothesize that an axon undergoing development can be equally submitted to either route depending on the activated surface presynaptogenic factor.

Polyubiquitin enhancers of presynaptic release

Presynaptic release is modulated by posttranslational modifications on presynaptic proteins. So far, these include phosphorylation, acetylation, SUMOylation and ubiquitination, which have been proposed to regulate presynaptic function by altering properties of target proteins. Attachment of phosphate groups to presynaptic proteins such as synapsin[574,575], calcium channels[576,577] and SNAP25[578] can alter presynaptic release either positively and negatively. Whereas phosphorylation of P/Q-type Ca^{2+} channels dissociates them from SNAP-25 and synaptotagmin complex thus decreasing neurotransmitter release[576], phosphorylated N-type Ca^{2+} channels feature increased channel open probability and subsequently higher Ca^{2+} influx[577]. Phosphorylated synapsin, for instance, recruits SVs to the active recycling pool[575] and accordingly more vesicles are ready for membrane fusion. In addition to phosphorylation, acetylation and SUMOylation have recently been proposed to also modulate presynaptic release. In *Drosophila*, the deacetylase HDAC6 targets the active zone protein Bruchpilot and enlarges the RRP[579] and in rat cortical

neurons SUMOylated RIM1α enables fast synaptic vesicle exocytosis, due to its prime role in clustering synaptic Ca^{2+} channels thus enhancing Ca^{2+} influx[522]. Interestingly, presynaptic activity alters levels of proteins covalently tagged with both SUMO and its analogous protein, ubiquitin: KCl-evoked depolarization increases the levels of SUMOylated proteins in presynaptic fractions[523] and decreases the levels of ubiquitinated proteins in synaptosomes[387]. Furthermore, presynaptic terminals contain the machinery required for addition and removal of Ub chains on substrates[240], thus making it possible that Ub also functions as a posttranslational modification capable of modulating release competence. Indeed, a K29 polyubiquitin chain on snapin enhances its ability to interact with SNAP25[360], which then facilitates its association with synaptotagmin and synaptic transmission[388–390]. In this work we further propose that K11, K29 and K63 polyubiquitin tags on presynaptic proteins function as enhancers of presynaptic release.

This preliminary finding that polyubiquitination positively impacts SV release deserves further validation. In order to complement our work with FM dye in presynaptic exocytosis, experiments using a fluorescent pH-sensitive indicator fused to an SV protein, such as synaptopHluorin[520], could be performed. Future work should also be aimed at performing electrophysiological recordings to analyze spontaneous and evoked excitatory and inhibitory currents following expression of wtUb and its mutant forms in primary cultures or slices. Tools to study the function of polyubiquitin chains of different topologies have been limited to linkage-specific antibodies and Ub-replacement strategies (in which overexpressed Ub or its chain formation mutant forms compete with endogenous Ub). It has been recently developed a new strategy to dissect the functional outcome of polyubiquitin signals in cells that involves expression of linkage specific inhibitors[580]. Authors have developed K63-specific sensors that specifically bind to K63 Ub chains and inhibit downstream signaling, and used them to further consolidate the role of this K63 Ub linkage in NF-κB activation[580]. Further development and optimization of these Ub linkage competitive inhibitors would contribute greatly to deciphering the roles of Ub signals in cells and could be exploited to further validate the role of poyubiquitination in presynaptic release or presynaptic differentiation.

Efforts should be made to identify proteins whose ubiquitination enhance presynaptic release. Several components of the SV exocytosis machinery and additional proteins with known roles in presynaptic release, such as RIM1, Munc13, α-synuclein, β-catenin, synaptophysin, syntaxin and calcium channels, have been demonstrated to be targeted for UPS-mediated degradation (see tables 1.2 and 1.3). Nevertheless, much less is known about proteins whose non-proteolytic ubiquitination commits them to improved release performance. In addition to the aforementioned snapin[360], some potential candidates include synaptotagmin, SNAP25, VAMP or the vesicle-fusing ATPase NSF (table 1.3), which are prone to be ubiquitinated in cells. However, modulation of their function in presynaptic release upon ubiquitination has not been addressed, and so would constitute insightful topics for future research. As previously proposed, ubiquitin proteomics to synaptosomes, obtained from adult brain tissue, would allow for the identification of additional ubiquitinated presynaptic substrates as potential targets that transiently harbor polyubiquitin enhancers of presynaptic release. On the other hand, identification of the ubiquitination machinery that adds and removes Ub from substrates is crucial for a deeper understanding of the local mechanisms governing SV release. Tables 1.2 and 1.3 present a comprehensive list of E3s ligases that function in axons and so are likely to play a role in neurotransmitter release. Less is known about potential DUBs. Two-hybrid screenings to identify interacting partners of presynaptic ubiquitinated proteins would eventually be useful for the identification of all the players involved.

Despite the current deep understanding of the mechanism of SV exocytosis, the finding that the UPS is intimately associated with presynaptic release[384,387] suggests that a tight control by Ub is fundamental.

Herein, we underscore a role for K11, K29 and K63 polyubiquitin tags as enhancers of SV release. Transfer of information within the nervous system relies on presynaptic function; hence complete knowledge of the modulatory function of polyubiquitination is of utmost importance.

UPS dysfunctions in neurodevelopmental diseases

Why is it important to go deeper into the understanding of UPS involvement in synapse formation? The proteasome and ubiquitin are abundantly expressed in the brain and are believed to control diverse functions including serving as key regulators of neuronal protein homeostasis[268,270]. Strong links between UPS dysfunction and neurological diseases such as Alzheimer's disease, amyotrophic lateral sclerosis, Huntington's disease, Parkinson's disease, Angelman syndrome (AS), ataxia, schizophrenia, X-linked infantile spinal-muscular atrophy (XL-SMA) have been observed[244]. Generally speaking, neurodegenerative diseases are characterized by accumulation of ubiquitinated protein aggregates that the cell is incapable of degrading due to an aberrant tagging of proteins for degradation and/or their impaired removal by the proteasome[244]. Because this work highlights the involvement of the UPS as a crucial player during development of the presynapse, we will focus this brief section on disorders that affect the developing brain.

In order to understand the dysfunctional background of ataxia, in which muscle coordination is lacking, researchers have been paying close attention to the spontaneously arising ataxia (ax^J) mice. These animals exhibit severe resting tremor at 2-3 weeks old followed by hindlimb paralysis and death early in development[260]. These defects are the result of a loss-of-function mutation in the DUB Usp14, which recycles Ub from substrates before their proteasome removal. In agreement, reduced levels of monomeric Ub are observed in brain tissue of the mutant mice[581] in which the synaptic compartment was shown to be particularly vulnerable[258]. These mice display severe synaptic structural and functional defects at the NMJ that are rescued by neuron-specific overexpression of wtUsp14 or Ub[258,259]. Overall, these findings indicate that fluctuations in synaptic Ub levels may constitute a potential cause for the progression of neuronal disorders. This hypothesis is further fortified by analysis to the gracile axonal dystrophy (gad) mice, which have a spontaneous mutation in the DUB UCH-L1[582] and exhibit severe sensory ataxia at early stages caused by axonal degeneration in the gracile tract[583]. Similarly to ax^J mice, in gad mice reduced levels of monomeric Ub are observed in neurons[262]; moreover, inhibition of UCH-L1 decreases Ub levels and alters synaptic structure which are restored upon Ub overexpression[261]. Interestingly, mutations[584,585], reduced levels[586,587] and PTMs[586,588] in UCH-L1 have been linked to PD and AD, thus further reinforcing that inability to maintain steady-state levels of Ub in neurons underlies development of neurological defects.

Besides mutations DUBs, mutations in the E1-ubiquitin activating enzyme have also been associated to the onset of neurodevelopmental diseases. In XL-SMA, characterized by pre-natal loss of anterior horn cells in the spinal cord and brainstem that is probably linked to defective development of the motor unit and premature death[589], a point mutation in the gene coding for the E1 enzyme was reported[590]. Surprisingly, disruption of Ub homeostasis due to reduced levels of the E1 enzyme was also proposed to underlie the neuromuscular pathogenesis of proximal spinal muscular atrophy (SMA)[591], which is widely known to be caused by deletion of the survival motor neuron 1 (SMN1) gene[592,593]. This disease is characterized by loss of motor neurons and concomitant defects in synaptic structure and connectivity at the NMJ[594–596]. Moreover, upon reduced SMN protein, the earliest cellular defect comprises an arrest in the postnatal development of NMJs, with anomalies at both post and presynaptic terminals[597]. Taken together, these findings indicate that anomalous UPS function at the synaptic level is likely to contribute to the onset of several forms of SMA.

The progressive mental disorder schizophrenia is also associated to dysfunctions in the UPS. Despite some controversy, the neuronal abnormalities in schizophrenia are believed to result from aberrant neurodevelopment[598]. Interestingly, gene expression profiling revealed decreased expression of genes involved in ubiquitin signaling, including proteasome subunits and ubiquitin[599,600]. In agreement, postmortem samples of subjects with schizophrenia exhibit overall reduction of protein ubiquitination, monomeric free Ub, K48-linked ubiquitination and decreased levels of E1 activating enzyme and the E3 ligase Nedd4[601], thus further reinforcing that UPS function is downregulated in schizophrenia.

AS is a neurological disorder characterized by developmental delay, severe intellectual disability, absent speech, exuberant behavior, motor impairment and epilepsy[602]. The possible causes for the neurological phenotype of AS are not yet completely known. AS mice models show impaired brain activity and altered activity of kinases critical for synaptic plasticity[603,604], thus suggesting that it results from abnormalities at the level of synaptic potentiation and plasticity. Another eminent possibility is an abnormal formation of synapses, which is in agreement with the lack of an observable window of normal development in AS patients[605]. Interestingly, the gene involved in AS, UBE3A (that codes for the an ubiquitin ligase), is also implicated in the pathogenesis of other neurodevelopmental diseases known to result from abnormalities at the synapse formation level, such as autism[606,607] and Rett syndrome[608]. At the postsynaptic side, Ube3A was already shown to regulate excitatory synapse development by controlling the levels of AMPA receptors through targeting Arc, an important regulator of receptors internalization[609]. In agreement, mice with maternal deficiency for E6AP display an abnormal dendritic spine development[394]. Ube3A was shown to co-localize with a presynaptic marker in axons of immature hippocampal neurons[394], thus suggesting that AS may also feature a deficient development of the presynaptic terminal due to an impaired control of UPS. Mice engineered to lack expression of the maternal Ube3A copy display impaired long-term potentiation[603], impaired excitatory synaptic transmission[610,611] and decreased experience-dependent maturation of neuronal circuits[612]. Overall, brain function is highly compromised early in development, thus further suggesting that initial wiring of neuronal circuits does not occur properly. Importantly, Ube3A expression is upregulated by neuronal activity and enhanced in response to environmental stimuli that trigger experience-dependent synaptic development[609]. Altogether, these studies suggest a scenario in which Ube3A acts at neurites during development of the central nervous system to accurately govern the establishment of synaptic connections perfectly integrated in neuronal circuits and concomitantly regulation of brain activity. Therefore, its loss in AS will hamper normal brain development in different brain regions, which most probably underlies its cognitive and motor dysfunctional features.

Overall, proteasome malfunctioning and defects in Ub signaling lead to diverse brain disorders, with a particular emphasizes on neurodevelopment diseases. This substantial prevalence as a causative factor for the pathogenesis of neurological diseases makes it apparent the need to fully understand and characterize the physiological role of the UPS. Herein, we contributed considerably to the current knowledge on the involvement of Ub and the proteasome in presynaptic development and function.

Chapter 7

References

1. Siksou, L. *et al.* Three-dimensional architecture of presynaptic terminal cytomatrix. *J. Neurosci.* **27,** 6868–77 (2007).

2. Fernández-Busnadiego, R. *et al.* Quantitative analysis of the native presynaptic cytomatrix by cryoelectron tomography. *J. Cell Biol.* **188,** 145–56 (2010).

3. Wilhelm, B. G. *et al.* Composition of isolated synaptic boutons reveals the amounts of vesicle trafficking proteins. *Science* **344,** 1023–8 (2014).

4. Fernández-Busnadiego, R. *et al.* Insights into the molecular organization of the neuron by cryo-electron tomography. *J. Electron Microsc.* **60 Suppl 1,** S137–48 (2011).

5. Takamori, S. *et al.* Molecular anatomy of a trafficking organelle. *Cell* **127,** 831–46 (2006).

6. Zhai, R. G. & Bellen, H. J. The architecture of the active zone in the presynaptic nerve terminal. *Physiology* **19,** 262–70 (2004).

7. Phillips, G. R. *et al.* The Presynaptic Particle Web : Ultrastructure , Composition , Dissolution , and Reconstitution. **32,** 63–77 (2001).

8. Gundelfinger, E. D. & Fejtova, A. Molecular organization and plasticity of the cytomatrix at the active zone. *Curr. Opin. Neurobiol.* **22,** 423–30 (2012).

9. Fejtova, A. & Gundelfinger, E. D. Molecular organization and assembly of the presynaptic active zone of neurotransmitter release. *Results Probl. Cell Differ.* **43,** 49–68 (2006).

10. Boyken, J. *et al.* Molecular profiling of synaptic vesicle docking sites reveals novel proteins but few differences between glutamatergic and GABAergic synapses. *Neuron* **78,** 285–97 (2013).

11. Weingarten, J. *et al.* The proteome of the presynaptic active zone from mouse brain. *Mol. Cell. Neurosci.* **59,** 106–18 (2014).

12. Friedman, H. V. *et al.* Assembly of new individual excitatory synapses: time course and temporal order of synaptic molecule recruitment. *Neuron* **27,** 57–69 (2000).

13. Bresler, T. *et al.* Postsynaptic density assembly is fundamentally different from presynaptic active zone assembly. *J. Neurosci.* **24,** 1507–20 (2004).

14. Ahmari, S. E. *et al.*Assembly of presynaptic active zones from cytoplasmic transport packets. *Nat. Neurosci.* **3,** 445–51 (2000).

15. Okabe, S. *et al.* Spine formation and correlated assembly of presynaptic and postsynaptic molecules. *J. Neurosci.* **21,** 6105–14 (2001).

16. Maday, S. *et al.*Axonal Transport: Cargo-Specific Mechanisms of Motility and Regulation. *Neuron* **84,** 292–309 (2014).

17. Goldstein, A. Y. N., Wang, X. & Schwarz, T. L. Axonal transport and the delivery of pre-synaptic components. *Curr. Opin. Neurobiol.* **18,** 495–503 (2008).

18. Hirokawa, N., Niwa, S. & Tanaka, Y. Molecular motors in neurons: transport mechanisms and roles in brain function, development, and disease. *Neuron* **68,** 610–38 (2010).

19. Kraszewski, K. *et al.* Synaptic vesicle dynamics in living cultured hippocampal neurons visualized with CY3-conjugated antibodies directed against the lumenal domain of synaptotagmin. *J. Neurosci.* **15,** 4328–42 (1995).

20. Zhai, R. G. *et al.* Assembling the Presynaptic Active Zone : A Characterization of an Active Zone Precursor Vesicle. *Neuron* **29,** 131–143 (2001).

21. Shapira, M. *et al.* Unitary Assembly of Presynaptic Active Zones from Piccolo-Bassoon Transport Vesicles. *Neuron* **38,** 237–252 (2003).

22. Dresbach, T. *et al.* Assembly of active zone precursor vesicles: obligatory trafficking of presynaptic cytomatrix proteins Bassoon and Piccolo via a trans-Golgi compartment. *J. Biol. Chem.* **281,** 6038–47 (2006).

23. Maas, C. *et al.* Formation of Golgi-derived active zone precursor vesicles. *J. Neurosci.* **32,** 11095–108 (2012).

24. Sadakata, T. *et al.* CAPS1 deficiency perturbs dense-core vesicle trafficking and Golgi structure and reduces presynaptic release probability in the mouse brain. *J. Neurosci.* **33,** 17326–34 (2013).

25. Tanizawa, Y. *et al.* Inositol monophosphatase regulates localization of synaptic components and behavior in the mature nervous system of C. elegans. *Genes Dev.* **20,** 3296–310 (2006).

26. Kimata, T. *et al.* Synaptic polarity depends on phosphatidylinositol signaling regulated by myo-inositol monophosphatase in Caenorhabditis elegans. *Genetics* **191,** 509–21 (2012).

27. Sakaguchi-Nakashima, A. *et al.* LRK-1, a C. elegans PARK8-related kinase, regulates axonal-dendritic polarity of SV proteins. *Curr. Biol.* **17,** 592–8 (2007).

28. Bisbal, M. *et al.* Protein kinase d regulates trafficking of dendritic membrane proteins in developing neurons. *J. Neurosci.* **28,** 9297–308 (2008).

29. Okada, Y. *et al.* The neuron-specific kinesin superfamily protein KIF1A is a unique monomeric motor for anterograde axonal transport of synaptic vesicle precursors. *Cell* **81,** 769–80 (1995).

30. Yonekawa, Y. *et al.* Defect in synaptic vesicle precursor transport and neuronal cell death in KIF1A motor protein-deficient mice. *J. Cell Biol.* **141,** 431–41 (1998).

31. Nakamura, N. *et al.* KIF1Bbeta2, capable of interacting with CHP, is localized to synaptic vesicles. *J. Biochem.* **132,** 483–91 (2002).

32. Cai, *et al.* Syntabulin-kinesin-1 family member 5B-mediated axonal transport contributes to activity-dependent presynaptic assembly. *J. Neurosci.* **27,** 7284–96 (2007).

33. Su, Q. *et al.* Syntabulin is a microtubule-associated protein implicated in syntaxin transport in neurons. *Nat. Cell Biol.* **6,** 941–53 (2004).

34. Ma, H. *et al.* KIF5B motor adaptor syntabulin maintains synaptic transmission in sympathetic neurons. *J. Neurosci.* **29,** 13019–29 (2009).

35. Shin, H. *et al.* Association of the kinesin motor KIF1A with the multimodular protein liprin-alpha. *J. Biol. Chem.* **278,** 11393–401 (2003).

36. Miller, K. E. *et al.* Direct observation demonstrates that Liprin-alpha is required for trafficking of synaptic vesicles. *Curr. Biol.* **15,** 684–9 (2005).

37. Zheng, Q. *et al.* The vesicle protein SAM-4 regulates the processivity of synaptic vesicle transport. *PLoS Genet.* **10,** e1004644 (2014).

38. Easley-Neal, C. *et al.* Late recruitment of synapsin to nascent synapses is regulated by Cdk5. *Cell Rep.* **3,** 1199–212 (2013).

39. Roy, S. Seeing the unseen: the hidden world of slow axonal transport. *Neuroscientist* **20,** 71–81 (2014).

40. Scott, D. A., Das, U., Tang, Y. & Roy, S. Mechanistic logic underlying the axonal transport of cytosolic proteins. *Neuron* **70,** 441–54 (2011).

41. Koushika, S. P. *et al.* Mutations in Caenorhabditis elegans cytoplasmic dynein components reveal specificity of neuronal retrograde cargo. *J. Neurosci.* **24,** 3907–16 (2004).

42. Fejtova, A. *et al.* Dynein light chain regulates axonal trafficking and synaptic levels of Bassoon. *J. Cell Biol.* **185,** 341–55 (2009).

43. Ou, C-Y. *et al.* Two cyclin-dependent kinase pathways are essential for polarized trafficking of presynaptic components. *Cell* **141,** 846–58 (2010).

44. Bury, L. A. D. & Sabo, S. L. Coordinated trafficking of synaptic vesicle and active zone proteins prior to synapse formation. *Neural Dev.* **6,** 24 (2011).

45. Wu, Y. E. *et al.* The balance between capture and dissociation of presynaptic proteins controls the spatial distribution of synapses. *Neuron* **78,** 994–1011 (2013).

46. Krueger, S. R. *et al.* The presynaptic release apparatus is functional in the absence of dendritic contact and highly mobile within isolated axons. *Neuron* **40,** 945–57 (2003).

47. Ratnayaka, A. *et al.* Extrasynaptic vesicle recycling in mature hippocampal neurons. *Nat. Commun.* **2,** 531 (2011).

48. Sabo, S. L. *et al.* Formation of presynaptic terminals at predefined sites along axons. *J. Neurosci.* **26,** 10813–25 (2006).

49. TerBush, D. R. & Novick, P. Sec6, Sec8, and Sec15 are components of a multisubunit complex which localizes to small bud tips in Saccharomyces cerevisiae. *J. Cell Biol.* **130,** 299–312 (1995).

50. TerBush, D. R. *et al.* The Exocyst is a multiprotein complex required for exocytosis in Saccharomyces cerevisiae. *EMBO J.* **15,** 6483–94 (1996).

51. Hazuka, C. D. *et al.* The sec6/8 complex is located at neurite outgrowth and axonal synapse-assembly domains. *J. Neurosci.* **19,** 1324–34 (1999).

52. Washbourne, P. *et al.* Rapid recruitment of NMDA receptor transport packets to nascent synapses. *Nat. Neurosci.* **5,** 751–9 (2002).

53. Washbourne, P. *et al.* Cycling of NMDA receptors during trafficking in neurons before synapse formation. *J. Neurosci.* **24,** 8253–64 (2004).

54. Sans, N. *et al.* NMDA receptor trafficking through an interaction between PDZ proteins and the exocyst complex. *Nat. Cell Biol.* **5,** 520–30 (2003).

55. Gerges, N. Z. *et al.* Dual role of the exocyst in AMPA receptor targeting and insertion into the postsynaptic membrane. *EMBO J.* **25,** 1623–34 (2006).

56. Teodoro, R. O. *et al.* Ral mediates activity-dependent growth of postsynaptic membranes via recruitment of the exocyst. *EMBO J.* **32,** 2039–55 (2013).

57. Pike, L. J. Rafts defined: a report on the Keystone Symposium on Lipid Rafts and Cell Function. *J. Lipid Res.* **47,** 1597–8 (2006).

58. Pristerà, A. *et al.* Association between tetrodotoxin resistant channels and lipid rafts regulates sensory neuron excitability. *PLoS One* **7,** e40079 (2012).

59. Kamiguchi, H. The region-specific activities of lipid rafts during axon growth and guidance. *J. Neurochem.* **98,** 330–5 (2006).

60. Guirland, C. & Zheng, J. Q. Membrane lipid rafts and their role in axon guidance. *Adv. Exp. Med. Biol.* **621,** 144–55 (2007).

61. Solis, G. P. *et al.* Reggie/flotillin proteins are organized into stable tetramers in membrane microdomains. *Biochem. J.* **403,** 313–22 (2007).

62. Swanwick, C. C. *et al.* Flotillin-1 promotes formation of glutamatergic synapses in hippocampal neurons. *Dev. Neurobiol.* **70,** 875–83 (2010).

63. Suzuki, S. *et al.* Brain-derived neurotrophic factor regulates cholesterol metabolism for synapse development. *J. Neurosci.* **27,** 6417–27 (2007).

64. Suzuki, T. *et al.* Association of membrane rafts and postsynaptic density: proteomics, biochemical, and ultrastructural analyses. *J. Neurochem.* **119,** 64–77 (2011).

65. Liu, Q. *et al.* Specific interaction of postsynaptic densities with membrane rafts isolated from synaptic plasma membranes. *J. Neurogenet.* **27,** 43–58 (2013).

66. Klassen, M. P. *et al.* An Arf-like small G protein, ARL-8, promotes the axonal transport of presynaptic cargoes by suppressing vesicle aggregation. *Neuron* **66,** 710–23 (2010).

67. Gerrow, K. *et al.* A preformed complex of postsynaptic proteins is involved in excitatory synapse development. *Neuron* **49,** 547–62 (2006).

68. Ziv, N. E. & Garner, C. C. Cellular and molecular mechanisms of presynaptic assembly. *Nat. Rev. Neurosci.* **5,** 385–99 (2004).

69. Bury, L. A. & Sabo, S. L. Dynamic mechanisms of neuroligin-dependent presynaptic terminal assembly in living cortical neurons. *Neural Dev.* **9,** 13 (2014).

70. Johnson-Venkatesh, E. M. & Umemori, H. Secreted factors as synaptic organizers. *Eur. J. Neurosci.* **32,** 181–90 (2010).

71. Siddiqui, T. J. & Craig, A. M. Synaptic organizing complexes. *Curr. Opin. Neurobiol.* **21,** 132–43 (2011).

72. Chia, P. H. *et al.* Cell biology in neuroscience: cellular and molecular mechanisms underlying presynapse formation. *J. Cell Biol.* **203,** 11–22 (2013).

73. Ushkaryov, Y. A. *et al.* Neurexins: synaptic cell surface proteins related to the alpha-latrotoxin receptor and laminin. *Science* **257,** 50–6 (1992).

74. Fannon, A. M. & Colman, D. R. A model for central synaptic junctional complex formation based on the differential adhesive specificities of the cadherins. *Neuron* **17,** 423–34 (1996).

75. Martínez, a *et al.* TrkB and TrkC signaling are required for maturation and synaptogenesis of hippocampal connections. *J. Neurosci.* **18,** 7336–50 (1998).

76. O'Brien, R. J. *et al.* Synaptic clustering of AMPA receptors by the extracellular immediate-early gene product Narp. *Neuron* **23,** 309–23 (1999).

77. Scheiffele, P. *et al.* Neuroligin expressed in nonneuronal cells triggers presynaptic development in contacting axons. *Cell* **101,** 657–69 (2000).

78. Dean, C. *et al.* Neurexin mediates the assembly of presynaptic terminals. *Nat. Neurosci.* **6,** 708–16 (2003).

79. Levinson, J. N. *et al.* Neuroligins mediate excitatory and inhibitory synapse formation: involvement of PSD-95 and neurexin-1beta in neuroligin-induced synaptic specificity. *J. Biol. Chem.* **280,** 17312–9 (2005).

80. Graf, E. R. *et al.* Neurexins induce differentiation of GABA and glutamate postsynaptic specializations via neuroligins. *Cell* **119,** 1013–26 (2004).

81. Chih, B. *et al.* Control of excitatory and inhibitory synapse formation by neuroligins. *Science* **307,** 1324–8 (2005).

82. Fogel, A. I. *et al.* SynCAMs organize synapses through heterophilic adhesion. *J. Neurosci.* **27,** 12516–30 (2007).

83. Biederer, T. *et al.* SynCAM, a synaptic adhesion molecule that drives synapse assembly. *Science* **297,** 1525–31 (2002).

84. Takahashi, H. *et al.* Postsynaptic TrkC and presynaptic PTPσ function as a bidirectional excitatory synaptic organizing complex. *Neuron* **69,** 287–303 (2011).

85. Woo, J. *et al.* Trans-synaptic adhesion between NGL-3 and LAR regulates the formation of excitatory synapses. *Nat. Neurosci.* **12,** 428–37 (2009).

86. Kwon, S-K. *et al.* Trans-synaptic adhesions between netrin-G ligand-3 (NGL-3) and receptor tyrosine phosphatases LAR, protein-tyrosine phosphatase delta (PTPdelta), and PTPsigma via specific domains regulate excitatory synapse formation. *J. Biol. Chem.* **285,** 13966–78 (2010).

87. Yoshida, T. *et al.* IL-1 receptor accessory protein-like 1 associated with mental retardation and autism mediates synapse formation by trans-synaptic interaction with protein tyrosine phosphatase δ. *J. Neurosci.* **31,** 13485–99 (2011).

88. Yoshida, T. *et al.* Interleukin-1 receptor accessory protein organizes neuronal synaptogenesis as a cell adhesion molecule. *J. Neurosci.* **32,** 2588–600 (2012).

89. Takahashi, H. *et al.* Selective control of inhibitory synapse development by Slitrk3-PTPδ trans-synaptic interaction. *Nat. Neurosci.* **15,** 389–98 (2012).

90. Takahashi, H. & Craig, A. M. Protein tyrosine phosphatases PTPδ, PTPσ, and LAR: presynaptic hubs for synapse organization. *Trends Neurosci.* **36,** 522–34 (2013).

91. Pettem, K. L. *et al.* The specific α-neurexin interactor calsyntenin-3 promotes excitatory and inhibitory synapse development. *Neuron* **80,** 113–28 (2013).

92. Um, J. W. *et al.* Calsyntenins function as synaptogenic adhesion molecules in concert with neurexins. *Cell Rep.* **6,** 1096–109 (2014).

93. De Wit, J. *et al.* LRRTM2 interacts with Neurexin1 and regulates excitatory synapse formation. *Neuron* **64,** 799–806 (2009).

94. Uemura, T. *et al.* Trans-synaptic interaction of GluRdelta2 and Neurexin through Cbln1 mediates synapse formation in the cerebellum. *Cell* **141,** 1068–79 (2010).

95. Yasumura, M. *et al.* Glutamate receptor δ1 induces preferentially inhibitory presynaptic differentiation of cortical neurons by interacting with neurexins through cerebellin precursor protein subtypes. *J. Neurochem.* **121,** 705–16 (2012).

96. Matsuda, K. *et al.* Cbln1 is a ligand for an orphan glutamate receptor delta2, a bidirectional synapse organizer. *Science* **328,** 363–8 (2010).

97. Matsuda, K. & Yuzaki, M. Cbln family proteins promote synapse formation by regulating distinct neurexin signaling pathways in various brain regions. *Eur. J. Neurosci.* **33,** 1447–61 (2011).

98. De Wit, J. & Ghosh, A. Control of neural circuit formation by leucine-rich repeat proteins. *Trends Neurosci.* **37,** 539–50 (2014).

99. Umemori, H. *et al.* FGF22 and its close relatives are presynaptic organizing molecules in the mammalian brain. *Cell* **118,** 257–70 (2004).

100. Linhoff, M. W. *et al.* An unbiased expression screen for synaptogenic proteins identifies the LRRTM protein family as synaptic organizers. *Neuron* **61,** 734–49 (2009).

101. Sharma, K. *et al.* High-throughput genetic screen for synaptogenic factors: identification of LRP6 as critical for excitatory synapse development. *Cell Rep.* **5,** 1330–41 (2013).

102. Paradis, S. *et al.* An RNAi-based approach identifies molecules required for glutamatergic and GABAergic synapse development. *Neuron* **53,** 217–32 (2007).

103. Terauchi, A. *et al.* Distinct FGFs promote differentiation of excitatory and inhibitory synapses. *Nature* **465,** 783–7 (2010).

104. Sia, G-M. *et al.* Interaction of the N-terminal domain of the AMPA receptor GluR4 subunit with the neuronal pentraxin NP1 mediates GluR4 synaptic recruitment. *Neuron* **55,** 87–102 (2007).

105. Pfrieger, F. W. & Barres, B. A. Synaptic efficacy enhanced by glial cells in vitro. *Science* **277,** 1684–7 (1997).

106. Nägler, K. *et al.* Glia-derived signals induce synapse formation in neurones of the rat central nervous system. *J. Physiol.* **533,** 665–79 (2001).

107. Ullian, E. M. *et al.* Control of synapse number by glia. *Science* **291,** 657–61 (2001).

108. Christopherson, K. S. *et al.* Thrombospondins are astrocyte-secreted proteins that promote CNS synaptogenesis. *Cell* **120,** 421–33 (2005).

109. Mauch, D. H. *et al.* CNS synaptogenesis promoted by glia-derived cholesterol. *Science* **294,** 1354–7 (2001).

110. Goritz, C. *et al.* Multiple mechanisms mediate cholesterol-induced synaptogenesis in a CNS neuron. *Mol. Cell. Neurosci.* **29,** 190–201 (2005).

111. Xu, J., Xiao, N. & Xia, J. Thrombospondin 1 accelerates synaptogenesis in hippocampal neurons through neuroligin 1. *Nat. Neurosci.* **13,** 22–4 (2010).

112. Eroglu, C. *et al.* Gabapentin receptor alpha2delta-1 is a neuronal thrombospondin receptor responsible for excitatory CNS synaptogenesis. *Cell* **139,** 380–92 (2009).

113. Kucukdereli, H. *et al.* Control of excitatory CNS synaptogenesis by astrocyte-secreted proteins Hevin and SPARC. *Proc. Natl. Acad. Sci. U. S. A.* **108,** E440-E449 (2011).

114. Ledda, F. *et al.* GDNF and GFRalpha1 promote formation of neuronal synapses by ligand-induced cell adhesion. *Nat. Neurosci.* **10,** 293–300 (2007).

115. Garrett, A. M. & Weiner, J. A. Control of CNS synapse development by {gamma}-protocadherin-mediated astrocyte-neuron contact. *J. Neurosci.* **29,** 11723–31 (2009).

116. Chih, B. *et al.* Alternative splicing controls selective trans-synaptic interactions of the neuroligin-neurexin complex. *Neuron* **51,** 171–8 (2006).

117. Varoqueaux, F. *et al.* Neuroligins determine synapse maturation and function. *Neuron* **51,** 741–54 (2006).

118. Sara, Y. *et al.* Selective capability of SynCAM and neuroligin for functional synapse assembly. *J. Neurosci.* **25,** 260–70 (2005).

119. Dahlhaus, R. *et al.* Overexpression of the cell adhesion protein neuroligin-1 induces learning deficits and impairs synaptic plasticity by altering the ratio of excitation to inhibition in the hippocampus. *Hippocampus* **20,** 305–22 (2010).

120. Hines, R. M. *et al.* Synaptic imbalance, stereotypies, and impaired social interactions in mice with altered neuroligin 2 expression. *J. Neurosci.* **28,** 6055–67 (2008).

121. Hirai, H. *et al.* Cbln1 is essential for synaptic integrity and plasticity in the cerebellum. *Nat. Neurosci.* **8,** 1534–41 (2005).

122. Uemura, T. & Mishina, M. The amino-terminal domain of glutamate receptor delta2 triggers presynaptic differentiation. *Biochem. Biophys. Res. Commun.* **377,** 1315–9 (2008).

123. Ito-Ishida, A. *et al.* Cbln1 regulates rapid formation and maintenance of excitatory synapses in mature cerebellar Purkinje cells in vitro and in vivo. *J. Neurosci.* **28,** 5920–30 (2008).

124. Ko, J. *et al.* LRRTM2 functions as a neurexin ligand in promoting excitatory synapse formation. *Neuron* **64,** 791–8 (2009).

125. De Wit, J. *et al.* Unbiased discovery of glypican as a receptor for LRRTM4 in regulating excitatory synapse development. *Neuron* **79,** 696–711 (2013).

126. Siddiqui, T. J. *et al.* An LRRTM4-HSPG complex mediates excitatory synapse development on dentate gyrus granule cells. *Neuron* **79,** 680–95 (2013).

127. Robbins, E. M. *et al.* SynCAM 1 adhesion dynamically regulates synapse number and impacts plasticity and learning. *Neuron* **68,** 894–906 (2010).

128. Kim, S. *et al.* NGL family PSD-95-interacting adhesion molecules regulate excitatory synapse formation. *Nat. Neurosci.* **9,** 1294–301 (2006).

129. Soto, F. *et al.* NGL-2 regulates pathway-specific neurite growth and lamination, synapse formation, and signal transmission in the retina. *J. Neurosci.* **33,** 11949–59 (2013).

130. Yasumura, M. *et al.* IL1RAPL1 knockout mice show spine density decrease, learning deficiency, hyperactivity and reduced anxiety-like behaviours. *Sci. Rep.* **4,** 6613 (2014).

131. Kayser, M. S. *et al.* Intracellular and trans-synaptic regulation of glutamatergic synaptogenesis by EphB receptors. *J. Neurosci.* **26,** 12152–64 (2006).

132. McClelland, A. C. *et al.* Ephrin-B1 and ephrin-B2 mediate EphB-dependent presynaptic development via syntenin-1. *Proc. Natl. Acad. Sci. U. S. A.* **106,** 20487–92 (2009).

133. Aoto, J. *et al.* Postsynaptic ephrinB3 promotes shaft glutamatergic synapse formation. *J. Neurosci.* **27,** 7508–19 (2007).

134. McClelland, A. C. *et al.* Trans-synaptic EphB2-ephrin-B3 interaction regulates excitatory synapse density by inhibition of postsynaptic MAPK signaling. *Proc. Natl. Acad. Sci. U. S. A.* **107,** 8830–5 (2010).

135. Xu, N-J. *et al.* A dual shaping mechanism for postsynaptic ephrin-B3 as a receptor that sculpts dendrites and synapses. *Nat. Neurosci.* **14,** 1421–9 (2011).

136. Togashi, H. *et al.* Cadherin Regulates Dendritic Spine Morphogenesis. *Neuron* **35,** 77–89 (2002).

137. Stan, a *et al.* Essential cooperation of N-cadherin and neuroligin-1 in the transsynaptic control of vesicle accumulation. *Proc. Natl. Acad. Sci. U. S. A.* **107,** 11116–21 (2010).

138. Mah, W. *et al.* Selected SALM (synaptic adhesion-like molecule) family proteins regulate synapse formation. *J. Neurosci.* **30,** 5559–68 (2010).

139. O'Sullivan, M. L. *et al.* FLRT proteins are endogenous latrophilin ligands and regulate excitatory synapse development. *Neuron* **73,** 903–10 (2012).

140. Wang, Z. *et al.* Presynaptic and postsynaptic interaction of the amyloid precursor protein promotes peripheral and central synaptogenesis. *J. Neurosci.* **29,** 10788–801 (2009).

141. Manitt, C. *et al.* Netrin participates in the development of retinotectal synaptic connectivity by modulating axon arborization and synapse formation in the developing brain. *J. Neurosci.* **29,** 11065–77 (2009).

142. Goldman, J. S. *et al.* Netrin-1 promotes excitatory synaptogenesis between cortical neurons by initiating synapse assembly. *J. Neurosci.* **33,** 17278–89 (2013).

143. Kuzirian, M. S. *et al.* The class 4 semaphorin Sema4D promotes the rapid assembly of GABAergic synapses in rodent hippocampus. *J. Neurosci.* **33,** 8961–73 (2013).

144. Raissi, A. J. *et al.* Sema4D localizes to synapses and regulates GABAergic synapse development as a membrane-bound molecule in the mammalian hippocampus. *Mol. Cell. Neurosci.* **57,** 23–32 (2013).

145. Singh, R. *et al.* Fibroblast growth factor 22 contributes to the development of retinal nerve terminals in the dorsal lateral geniculate nucleus. *Front. Mol. Neurosci.* **4,** 61 (2012).

146. Krylova, O. *et al.* WNT-3, expressed by motoneurons, regulates terminal arborization of neurotrophin-3-responsive spinal sensory neurons. *Neuron* **35,** 1043–56 (2002).

147. Hall, A. C. *et al.* Axonal Remodeling and Synaptic Differentiation in the Cerebellum Is Regulated by WNT-7a Signaling. *Cell* **100,** 525–535 (2000).

148. Sahores, M. *et al.* Frizzled-5, a receptor for the synaptic organizer Wnt7a, regulates activity-mediated synaptogenesis. *Development* **137,** 2215–25 (2010).

149. Ciani, L. *et al.* Wnt7a signaling promotes dendritic spine growth and synaptic strength through Ca^{2+}/Calmodulin-dependent protein kinase II. *Proc. Natl. Acad. Sci. U. S. A.* **108,** 10732–7 (2011).

150. Cuitino, L. *et al.* Wnt-5a modulates recycling of functional GABAA receptors on hippocampal neurons. *J. Neurosci.* **30,** 8411–20 (2010).

151. O'Brien, R. *et al.* Synaptically targeted narp plays an essential role in the aggregation of AMPA receptors at excitatory synapses in cultured spinal neurons. *J. Neurosci.* **22,** 4487–98 (2002).

152. Collin, C. *et al.* Neurotrophins act at presynaptic terminals to activate synapses among cultured hippocampal neurons. *Eur. J. Neurosci.* **13,** 1273–1282 (2001).

153. Pozzo-Miller, L. D. *et al.* Impairments in high-frequency transmission, synaptic vesicle docking, and synaptic protein distribution in the hippocampus of BDNF knockout mice. *J. Neurosci.* **19,** 4972–83 (1999).

154. Genoud, C. *et al.* Altered synapse formation in the adult somatosensory cortex of brain-derived neurotrophic factor heterozygote mice. *J. Neurosci.* **24,** 2394–400 (2004).

155. Luikart, B. W. *et al.* TrkB has a cell-autonomous role in the establishment of hippocampal Schaffer collateral synapses. *J. Neurosci.* **25,** 3774–86 (2005).

156. Parkhurst, C. N. *et al.* Microglia promote learning-dependent synapse formation through brain-derived neurotrophic factor. *Cell* **155,** 1596–609 (2013).

157. Gómez-Casati, M. E. *et al.* Nonneuronal cells regulate synapse formation in the vestibular sensory epithelium via erbB-dependent BDNF expression. *Proc. Natl. Acad. Sci. U. S. A.* **107,** 17005–10 (2010).

158. Elmariah, S. B. *et al.* Postsynaptic TrkB-mediated signaling modulates excitatory and inhibitory neurotransmitter receptor clustering at hippocampal synapses. *J. Neurosci.* **24,** 2380–93 (2004).

159. Rico, B. *et al.* TrkB receptor signaling is required for establishment of GABAergic synapses in the cerebellum. *Nat. Neurosci.* **5,** 225–33 (2002).

160. Elmariah, S. B. *et al.* Astrocytes regulate inhibitory synapse formation via Trk-mediated modulation of postsynaptic GABAA receptors. *J. Neurosci.* **25,** 3638–50 (2005).

161. Diniz, L. P. *et al.* Astrocyte-induced synaptogenesis is mediated by transforming growth factor β signaling through modulation of D-serine levels in cerebral cortex neurons. *J. Biol. Chem.* **287,** 41432–45 (2012).

162. Allen, N. J. *et al.* Astrocyte glypicans 4 and 6 promote formation of excitatory synapses via GluA1 AMPA receptors. *Nature* **486,** 410–4 (2012).

163. Terauchi, A. *et al.* Selective synaptic targeting of the excitatory and inhibitory presynaptic organizers FGF22 and FGF7. *J. Cell Sci.* **128,** 281–92 (2015).

164. Hughes, E. G. *et al.* Astrocyte secreted proteins selectively increase hippocampal GABAergic axon length, branching, and synaptogenesis. *Mol. Cell. Neurosci.* **43,** 136–45 (2010).

165. Duan, Y. *et al.* Semaphorin 5A inhibits synaptogenesis in early postnatal- and adult-born hippocampal dentate granule cells. *Elife* **3,** (2014).

166. Tran, T. S. *et al.* Secreted semaphorins control spine distribution and morphogenesis in the postnatal CNS. *Nature* **462,** 1065–9 (2009).

167. Bury, L. A. D. & Sabo, S. L. How it's made: the synapse. *Mol. Interv.* **10,** 282–92 (2010).

168. Zhen, M. & Jin, Y. The liprin protein SYD-2 regulates the differentiation of presynaptic termini in C. elegans. *Nature* **401,** 371–5 (1999).

169. Dai, Y. *et al.* SYD-2 Liprin-alpha organizes presynaptic active zone formation through ELKS. *Nat. Neurosci.* **9,** 1479–87 (2006).

170. Patel, M. R. *et al.* Hierarchical assembly of presynaptic components in defined C. elegans synapses. *Nat. Neurosci.* **9,** 1488–98 (2006).

171. Kittelmann, M. *et al.* Liprin-α/SYD-2 determines the size of dense projections in presynaptic active zones in C. elegans. *J. Cell Biol.* **203,** 849–63 (2013).

172. Stigloher, C. *et al.* The presynaptic dense projection of the Caenorhabditis elegans cholinergic neuromuscular junction localizes synaptic vesicles at the active zone through SYD-2/liprin and UNC-10/RIM-dependent interactions. *J. Neurosci.* **31,** 4388–96 (2011).

173. Patel, M. R. & Shen, K. RSY-1 is a local inhibitor of presynaptic assembly in C. elegans. *Science* **323,** 1500–3 (2009).

174. Wentzel, C. *et al.* mSYD1A, a mammalian synapse-defective-1 protein, regulates synaptogenic signaling and vesicle docking. *Neuron* **78,** 1012–23 (2013).

175. Spangler, S. a *et al.* Liprin-α2 promotes the presynaptic recruitment and turnover of RIM1/CASK to facilitate synaptic transmission. *J. Cell Biol.* **201,** 915–28 (2013).

176. Pulido, R. *et al.* The LAR/PTP delta/PTP sigma subfamily of transmembrane protein-tyrosine-phosphatases: multiple human LAR, PTP delta, and PTP sigma isoforms are expressed in a tissue-specific manner and associate with the LAR-interacting protein LIP.1. *Proc. Natl. Acad. Sci. U. S. A.* **92,** 11686–90 (1995).

177. Kaeser, P. S. *et al.* RIM proteins tether Ca2+ channels to presynaptic active zones via a direct PDZ-domain interaction. *Cell* **144,** 282–95 (2011).

178. Schoch, S. *et al.* RIM1alpha forms a protein scaffold for regulating neurotransmitter release at the active zone. *Nature* **415,** 321–6 (2002).

179. Wang, Y. *et al.* A family of RIM-binding proteins regulated by alternative splicing: Implications for the genesis of synaptic active zones. *Proc. Natl. Acad. Sci. U. S. A.* **99,** 14464–9 (2002).

180. Hata, Y. *et al.* CASK: a novel dlg/PSD95 homolog with an N-terminal calmodulin-dependent protein kinase domain identified by interaction with neurexins. *J. Neurosci.* **16,** 2488–94 (1996).

181. Olsen, O. *et al.* Neurotransmitter release regulated by a MALS-liprin-alpha presynaptic complex. *J. Cell Biol.* **170,** 1127–34 (2005).

182. Zhang, Y. *et al.* The scaffolding protein CASK mediates the interaction between rabphilin3a and beta-neurexins. *FEBS Lett.* **497,** 99–102 (2001).

183. Maximov, A. & Bezprozvanny, I. Synaptic targeting of N-type calcium channels in hippocampal neurons. *J. Neurosci.* **22,** 6939–52 (2002).

184. Chen, J. *et al.* Calcium channels link the muscle-derived synapse organizer laminin β2 to Bassoon and CAST/Erc2 to organize presynaptic active zones. *J. Neurosci.* **31,** 512–25 (2011).

185. Biederer, T. & Sudhof, T. C. CASK and protein 4.1 support F-actin nucleation on neurexins. *J. Biol. Chem.* **276,** 47869–76 (2001).

186. Atasoy, D. *et al.* Deletion of CASK in mice is lethal and impairs synaptic function. *Proc. Natl. Acad. Sci. U. S. A.* **104,** 2525–30 (2007).

187. Mukherjee, K. *et al.* Piccolo and bassoon maintain synaptic vesicle clustering without directly participating in vesicle exocytosis. *Proc. Natl. Acad. Sci. U. S. A.* **107,** 6504–9 (2010).

188. Zhai, R. *et al.* Temporal appearance of the presynaptic cytomatrix protein bassoon during synaptogenesis. *Mol. Cell. Neurosci.* **15,** 417–28 (2000).

189. Lanore, F. *et al.* Impaired development of hippocampal mossy fibre synapses in mouse mutants for the presynaptic scaffold protein Bassoon. *J. Physiol.* **588,** 2133–45 (2010).

190. Zhang, W. & Benson, D. L. Stages of synapse development defined by dependence on F-actin. *J. Neurosci.* **21,** 5169–81 (2001).

191. Zhang, W. & Benson, D. L. Developmentally regulated changes in cellular compartmentation and synaptic distribution of actin in hippocampal neurons. *J. Neurosci. Res.* **69,** 427–36 (2002).

192. Lucido, A. L. *et al.* Rapid assembly of functional presynaptic boutons triggered by adhesive contacts. *J. Neurosci.* **29,** 12449–66 (2009).

193. Chia, P. H. *et al.* NAB-1 instructs synapse assembly by linking adhesion molecules and F-actin to active zone proteins. *Nat. Neurosci.* **15,** 234–42 (2012).

194. Chia, P. H. *et al.* Local F-actin network links synapse formation and axon branching. *Cell* **156,** 208–20 (2014).

195. Stavoe, A. K. H. & Colón-Ramos, D. A. Netrin instructs synaptic vesicle clustering through Rac GTPase, MIG-10, and the actin cytoskeleton. *J. Cell Biol.* **197,** 75–88 (2012).

196. Bamji, S. X. *et al.* Role of beta-catenin in synaptic vesicle localization and presynaptic assembly. *Neuron* **40,** 719–31 (2003).

197. Sun, Y. *et al.* Scribble interacts with beta-catenin to localize synaptic vesicles to synapses. *Mol. Biol. Cell* **20,** 3390–400 (2009).

198. Sun, Y. & Bamji, S. X. β-Pix modulates actin-mediated recruitment of synaptic vesicles to synapses. *J. Neurosci.* **31,** 17123–33 (2011).

199. Waites, C. L. *et al.* Piccolo regulates the dynamic assembly of presynaptic F-actin. *J. Neurosci.* **31,** 14250–63 (2011).

200. Lou, H. *et al.* Carboxypeptidase E cytoplasmic tail mediates localization of synaptic vesicles to the pre-active zone in hypothalamic pre-synaptic terminals. *J. Neurochem.* **114,** 886–96 (2010).

201. Bamji, S. X. *et al.* BDNF mobilizes synaptic vesicles and enhances synapse formation by disrupting cadherin-beta-catenin interactions. *J. Cell Biol.* **174,** 289–99 (2006).

202. Menna, E. *et al.* Eps8 regulates axonal filopodia in hippocampal neurons in response to brain-derived neurotrophic factor (BDNF). *PLoS Biol.* **7,** e1000138 (2009).

203. Gallo, G. Mechanisms underlying the initiation and dynamics of neuronal filopodia: from neurite formation to synaptogenesis. *Int. Rev. Cell Mol. Biol.* **301,** 95–156 (2013).

204. Bouwman, J. *et al.* Quantification of synapse formation and maintenance in vivo in the absence of synaptic release. *Neuroscience* **126,** 115–26 (2004).

205. Kerschensteiner, D. *et al*. Neurotransmission selectively regulates synapse formation in parallel circuits in vivo. *Nature* **460,** 1016–20 (2009).

206. Sceniak, M. P. *et al.* Facilitation of neocortical presynaptic terminal development by NMDA receptor activation. *Neural Dev.* **7,** 8 (2012).

207. Royle, S. J. & Lagnado, L. Clathrin-mediated endocytosis at the synaptic terminal: bridging the gap between physiology and molecules. *Traffic* **11,** 1489–97 (2010).

208. Saheki, Y. & De Camilli, P. Synaptic vesicle endocytosis. *Cold Spring Harb. Perspect. Biol.* **4,** a005645 (2012).

209. McMahon, H. T. & Boucrot, E. Molecular mechanism and physiological functions of clathrin-mediated endocytosis. *Nat. Rev. Mol. Cell Biol.* **12,** 517–33 (2011).

210. He, L. & Wu, L.-G. The debate on the kiss-and-run fusion at synapses. *Trends Neurosci.* **30,** 447–55 (2007).

211. Alabi, A. A. & Tsien, R. W. Perspectives on kiss-and-run: role in exocytosis, endocytosis, and neurotransmission. *Annu. Rev. Physiol.* **75,** 393–422 (2013).

212. Jahn, R. & Fasshauer, D. Molecular machines governing exocytosis of synaptic vesicles. *Nature* **490,** 201–7 (2012).

213. Rizzoli, S. O. & Betz, W. J. Synaptic vesicle pools. *Nat. Rev. Neurosci.* **6,** 57–69 (2005).

214. Ratnayaka, A. *et al.* Recruitment of resting vesicles into recycling pools supports NMDA receptor-dependent synaptic potentiation in cultured hippocampal neurons. *J. Physiol.* **590,** 1585–97 (2012).

215. Südhof, T. C. & Rizo, J. Synaptic vesicle exocytosis. *Cold Spring Harb. Perspect. Biol.* **3,** a005637 (2011).

216. Südhof, T. C. Neurotransmitter release: the last millisecond in the life of a synaptic vesicle. *Neuron* **80,** 675–90 (2013).

217. Söllner, T. *et al.* SNAP receptors implicated in vesicle targeting and fusion. *Nature* **362,** 318–24 (1993).

218. Sutton, R. B. *et al.* Crystal structure of a SNARE complex involved in synaptic exocytosis at 2.4 A resolution. *Nature* **395,** 347–53 (1998).

219. Stein, A. *et al.* Helical extension of the neuronal SNARE complex into the membrane. *Nature* **460,** 525–8 (2009).

220. Hanson, P. I. *et al.* Neurotransmitter release - four years of SNARE complexes. *Curr. Opin. Neurobiol.* **7,** 310–5 (1997).

221. Sørensen, J. B. *et al.* Sequential N- to C-terminal SNARE complex assembly drives priming and fusion of secretory vesicles. *EMBO J.* **25,** 955–966 (2006).

222. Dulubova, I. *et al.* A conformational switch in syntaxin during exocytosis: role of munc18. *EMBO J.* **18,** 4372–82 (1999).

223. Dulubova, I. *et al.* Munc18-1 binds directly to the neuronal SNARE complex. *Proc. Natl. Acad. Sci. U. S. A.* **104,** 2697–702 (2007).

224. Gerber, S. H. *et al.* Conformational switch of syntaxin-1 controls synaptic vesicle fusion. *Science* **321,** 1507–10 (2008).

225. Deák, F. *et al.* Munc18-1 binding to the neuronal SNARE complex controls synaptic vesicle priming. *J. Cell Biol.* **184,** 751–64 (2009).

226. Khvotchev, M. *et al.* Dual modes of Munc18-1/SNARE interactions are coupled by functionally critical binding to syntaxin-1 N terminus. *J. Neurosci.* **27,** 12147–55 (2007).

227. Augustin, I. *et al.* Munc13-1 is essential for fusion competence of glutamatergic synaptic vesicles. *Nature* **400,** 457–61 (1999).

228. Ma, C. *et al.* Reconstitution of the vital functions of Munc18 and Munc13 in neurotransmitter release. *Science* **339,** 421–5 (2013).

229. Chen, X. *et al.* Three-dimensional structure of the complexin/SNARE complex. *Neuron* **33,** 397–409 (2002).

230. Fernández-Chacón, R. *et al.* Synaptotagmin I functions as a calcium regulator of release probability. *Nature* **410,** 41–9 (2001).

231. Reim, K. *et al.* Complexins regulate a late step in Ca2+-dependent neurotransmitter release. *Cell* **104,** 71–81 (2001).

232. Söllner, T. *et al.* E. A protein assembly-disassembly pathway in vitro that may correspond to sequential steps of synaptic vesicle docking, activation, and fusion. *Cell* **75,** 409–18 (1993).

233. Burré, J. *et al.* Alpha-synuclein promotes SNARE-complex assembly in vivo and in vitro. *Science* **329,** 1663–7 (2010).

234. Sharma, M. *et al.* CSPα promotes SNARE-complex assembly by chaperoning SNAP-25 during synaptic activity. *Nat. Cell Biol.* **13,** 30–9 (2011).

235. Han, Y. *et al.* RIM determines Ca^2+ channel density and vesicle docking at the presynaptic active zone. *Neuron* **69,** 304–16 (2011).

236. Wang, Y. *et al.* Rim is a putative Rab3 effector in regulating synaptic-vesicle fusion. *Nature* **388,** 593–8 (1997).

237. Gracheva, E. O. *et al.* Direct interactions between C. elegans RAB-3 and Rim provide a mechanism to target vesicles to the presynaptic density. *Neurosci. Lett.* **444,** 137–42 (2008).

238. Fernández-Busnadiego, R. *et al.* Cryo-electron tomography reveals a critical role of RIM1α in synaptic vesicle tethering. *J. Cell Biol.* **201,** 725–40 (2013).

239. Deng, L. *et al.* RIM proteins activate vesicle priming by reversing autoinhibitory homodimerization of Munc13. *Neuron* **69,** 317–31 (2011).

240. Schrimpf, S. P. *et al.* Proteomic analysis of synaptosomes using isotope-coded affinity tags and mass spectrometry. *Proteomics* **5,** 2531–41 (2005).

241. Kawabe, H. & Brose, N. The role of ubiquitylation in nerve cell development. *Nat. Rev. Neurosci.* **12,** 251–68 (2011).

242. Franco, M. *et al.* A novel strategy to isolate ubiquitin conjugates reveals wide role for ubiquitination during neural development. *Mol. Cell. Proteomics* **10,** M110.002188 (2011).

243. Na, C. H. *et al.* Synaptic protein ubiquitination in rat brain revealed by antibody-based ubiquitome analysis. *J. Proteome Res.* **11,** 4722–32 (2012).

244. Hegde, A. N. & Upadhya, S. C. Role of ubiquitin-proteasome-mediated proteolysis in nervous system disease. *Biochim. Biophys. Acta* **1809,** 128–140 (2010).

245. Komander, D. & Rape, M. The ubiquitin code. *Annu. Rev. Biochem.* **81,** 203–29 (2012).

246. Chernorudskiy, A. L. & Gainullin, M. R. Ubiquitin system: direct effects join the signaling. *Sci. Signal.* **6,** pe22 (2013).

247. Sadowski, M. *et al.* Protein monoubiquitination and polyubiquitination generate structural diversity to control distinct biological processes. *IUBMB Life* **64,** 136–42 (2012).

248. Kulathu, Y. & Komander, D. Atypical ubiquitylation - the unexplored world of polyubiquitin beyond Lys48 and Lys63 linkages. *Nat. Rev. Mol. Cell Biol.* **13,** 508–23 (2012).

249. Husnjak, K. & Dikic, I. Ubiquitin-binding proteins: decoders of ubiquitin-mediated cellular functions. *Annu. Rev. Biochem.* **81,** 291–322 (2012).

250. Haas, A. L. *et al.* Ubiquitin-activating enzyme. Mechanism and role in protein-ubiquitin conjugation. *J. Biol. Chem.* **257,** 2543–8 (1982).

251. Pickart, C. M. Mechanisms underlying ubiquitination. *Annu. Rev. Biochem.* **70,** 503–33 (2001).

252. Metzger, M. B. *et al.* HECT and RING finger families of E3 ubiquitin ligases at a glance. *J. Cell Sci.* **125,** 531–7 (2012).

253. Willems, A. R. *et al.* A hitchhiker's guide to the cullin ubiquitin ligases: SCF and its kin. *Biochim. Biophys. Acta* **1695,** 133–70 (2004).

254. Barford, D. Structure, function and mechanism of the anaphase promoting complex (APC/C). *Q. Rev. Biophys.* **44,** 153–90 (2011).

255. Ristic, G. *et al.* An optimal ubiquitin-proteasome pathway in the nervous system: the role of deubiquitinating enzymes. *Front. Mol. Neurosci.* **7,** 72 (2014).

256. Park, C-W. & Ryu, K-Y. Cellular ubiquitin pool dynamics and homeostasis. *BMB Rep.* **47,** 475–82 (2014).

257. Hallengren, J. *et al.* Neuronal ubiquitin homeostasis. *Cell Biochem. Biophys.* **67,** 67–73 (2013).

258. Chen, P-C. *et al.* The proteasome-associated deubiquitinating enzyme Usp14 is essential for the maintenance of synaptic ubiquitin levels and the development of neuromuscular junctions. *J. Neurosci.* **29,** 10909–19 (2009).

259. Chen, P-C. *et al.* Ubiquitin homeostasis is critical for synaptic development and function. *J. Neurosci.* **31,** 17505–13 (2011).

260. Wilson, S. M. *et al.* Synaptic defects in ataxia mice result from a mutation in Usp14, encoding a ubiquitin-specific protease. *Nat. Genet.* **32,** 420–5 (2002).

261. Cartier, A. E. *et al.* Regulation of synaptic structure by ubiquitin C-terminal hydrolase L1. *J. Neurosci.* **29,** 7857–68 (2009).

262. Osaka, H. *et al.* Ubiquitin carboxy-terminal hydrolase L1 binds to and stabilizes monoubiquitin in neuron. *Hum. Mol. Genet.* **12,** 1945–58 (2003).

263. Ohtake, F. *et al.* Ubiquitin acetylation inhibits polyubiquitin chain elongation. *EMBO Rep.* **16,** 192–201 (2014).

264. Ikeda, F. *et al.* What determines the specificity and outcomes of ubiquitin signaling? *Cell* **143,** 677–81 (2010).

265. Dikic, I. *et al.* Ubiquitin-binding domains - from structures to functions. *Nat. Rev. Mol. Cell Biol.* **10,** 659–71 (2009).

266. Grabbe, C. & Dikic, I. Functional roles of ubiquitin-like domain (ULD) and ubiquitin-binding domain (UBD) containing proteins. *Chem. Rev.* **109,** 1481–94 (2009).

267. Thrower, J. S. *et al.* Recognition of the polyubiquitin proteolytic signal. *EMBO J.* **19,** 94–102 (2000).

268. Yi, J. J. & Ehlers, M. D. Emerging Roles for Ubiquitin and Protein Degradation in Neuronal Function. *Pharmacol. Rev.* **59,** 14–39 (2007).

269. Tai, H.-C. & Schuman, E. M. Ubiquitin, the proteasome and protein degradation in neuronal function and dysfunction. *Nat. Rev. Neurosci.* **9,** 826–38 (2008).

270. Bingol, B. & Sheng, M. Deconstruction for reconstruction: the role of proteolysis in neural plasticity and disease. *Neuron* **69,** 22–32 (2011).

271. Wolf, D. H. & Hilt, W. The proteasome: a proteolytic nanomachine of cell regulation and waste disposal. *Biochim. Biophys. Acta* **1695,** 19–31 (2004).

272. Kish-Trier, E. & Hill, C. P. Structural biology of the proteasome. *Annu. Rev. Biophys.* **42,** 29–49 (2013).

273. Yao, T. & Cohen, R. E. A cryptic protease couples deubiquitination and degradation by the proteasome. *Nature* **419,** 403–7 (2002).

274. Lee, B-H. *et al.* Enhancement of proteasome activity by a small-molecule inhibitor of USP14. *Nature* **467,** 179–84 (2010).

275. Tanaka, K. The proteasome: from basic mechanisms to emerging roles. *Keio J. Med.* **62,** 1–12 (2013).

276. Lin, A. W. & Man, H-Y. Ubiquitination of neurotransmitter receptors and postsynaptic scaffolding proteins. *Neural Plast.* **2013,** 432057 (2013).

277. Xu, P. *et al.* Quantitative proteomics reveals the function of unconventional ubiquitin chains in proteasomal degradation. *Cell* **137,** 133–45 (2009).

278. Dammer, E. B. *et al.* Polyubiquitin linkage profiles in three models of proteolytic stress suggest the etiology of Alzheimer disease. *J. Biol. Chem.* **286,** 10457–65 (2011).

279. Bedford, L. *et al.* Diverse polyubiquitin chains accumulate following 26S proteasomal dysfunction in mammalian neurones. *Neurosci. Lett.* **491,** 44–7 (2011).

280. Kirkpatrick, D. S. *et al.* Quantitative analysis of in vitro ubiquitinated cyclin B1 reveals complex chain topology. *Nat. Cell Biol.* **8,** 700–10 (2006).

281. Jin, L. *et al.* Mechanism of ubiquitin-chain formation by the human anaphase-promoting complex. *Cell* **133,** 653–65 (2008).

282. Matsumoto, M. L. *et al.* K11-linked polyubiquitination in cell cycle control revealed by a K11 linkage-specific antibody. *Mol. Cell* **39,** 477–84 (2010).

283. Dimitrova, Y. N. *et al.* Direct ubiquitination of beta-catenin by Siah-1 and regulation by the exchange factor TBL1. *J. Biol. Chem.* **285,** 13507–16 (2010).

284. Locke, M. *et al.* Lys11- and Lys48-linked ubiquitin chains interact with p97 during endoplasmic-reticulum-associated degradation. *Biochem. J.* **459,** 205–16 (2014).

285. Kim, H. T. *et al.* Certain pairs of ubiquitin-conjugating enzymes (E2s) and ubiquitin-protein ligases (E3s) synthesize nondegradable forked ubiquitin chains containing all possible isopeptide linkages. *J. Biol. Chem.* **282,** 17375–86 (2007).

286. Saeki, Y. *et al.* Lysine 63-linked polyubiquitin chain may serve as a targeting signal for the 26S proteasome. *EMBO J.* **28,** 359–71 (2009).

287. Jacobson, A. D. *et al.* The lysine 48 and lysine 63 ubiquitin conjugates are processed differently by the 26 s proteasome. *J. Biol. Chem.* **284,** 35485–94 (2009).

288. Nathan, J. A. *et al.* Why do cellular proteins linked to K63-polyubiquitin chains not associate with proteasomes? *EMBO J.* **32,** 552–65 (2013).

289. Schimmel, J. *et al.* The ubiquitin-proteasome system is a key component of the SUMO-2/3 cycle. *Mol. Cell. Proteomics* **7,** 2107–22 (2008).

290. Tatham, M. H. *et al.* RNF4 is a poly-SUMO-specific E3 ubiquitin ligase required for arsenic-induced PML degradation. *Nat. Cell Biol.* **10,** 538–46 (2008).

291. Xu, Y. *et al.* Structural insight into SUMO chain recognition and manipulation by the ubiquitin ligase RNF4. *Nat. Commun.* **5,** 4217 (2014).

292. Kravtsova-Ivantsiv, Y. & Ciechanover, A. Non-canonical ubiquitin-based signals for proteasomal degradation. *J. Cell Sci.* **125,** 539–48 (2012).

293. Meyer, H.-J. & Rape, M. Enhanced protein degradation by branched ubiquitin chains. *Cell* **157,** 910–21 (2014).

294. Kaiser, S. E. *et al.* Protein standard absolute quantification (PSAQ) method for the measurement of cellular ubiquitin pools. *Nat. Methods* **8,** 691–6 (2011).

295. Erpapazoglou, Z. *et al.* Versatile roles of k63-linked ubiquitin chains in trafficking. *Cells* **3,** 1027–88 (2014).

296. Huang, T. T. & D'Andrea, A. D. Regulation of DNA repair by ubiquitylation. *Nat. Rev. Mol. Cell Biol.* **7,** 323–34 (2006).

297. Ulrich, H. D. Ubiquitin and SUMO in DNA repair at a glance. *J. Cell Sci.* **125,** 249–54 (2012).

298. Jackson, S. P. & Durocher, D. Regulation of DNA damage responses by ubiquitin and SUMO. *Mol. Cell* **49,** 795–807 (2013).

299. Skaug, B. *et al.* The role of ubiquitin in NF-kappaB regulatory pathways. *Annu. Rev. Biochem.* **78,** 769–96 (2009).

300. Haglund, K. *et al.* Multiple monoubiquitination of RTKs is sufficient for their endocytosis and degradation. *Nat. Cell Biol.* **5,** 461–6 (2003).

301. Haglund, K. *et al.* Distinct monoubiquitin signals in receptor endocytosis. *Trends Biochem. Sci.* **28,** 598–603 (2003).

302. Stringer, D. K. & Piper, R. C. A single ubiquitin is sufficient for cargo protein entry into MVBs in the absence of ESCRT ubiquitination. *J. Cell Biol.* **192,** 229–42 (2011).

303. Su, H. *et al.* Activation of the cAMP/PKA pathway induces UT-A1 urea transporter monoubiquitination and targets it for lysosomal degradation. *Am. J. Physiol. Renal Physiol.* **305,** F1775–82 (2013).

304. Huang, F. *et al.* Differential regulation of EGF receptor internalization and degradation by multiubiquitination within the kinase domain. *Mol. Cell* **21,** 737–48 (2006).

305. Huang, F. *et al.* EGF receptor ubiquitination is not necessary for its internalization. *Proc. Natl. Acad. Sci. U. S. A.* **104,** 16904–9 (2007).

306. Chastagner, P. *et al.* Itch/AIP4 mediates Deltex degradation through the formation of K29-linked polyubiquitin chains. *EMBO Rep.* **7,** 1147–53 (2006).

307. Haugsten E. M. *et al.* Ubiquitination of Fibroblast Growth Factor Receptor 1 Is Required for Its Intracellular Sorting but Not for Its Endocytosis. *Mol. Biol. Cell* **19,** 3390 –3403 (2008).

308. Persaud, A. *et al.* Nedd4-1 binds and ubiquitylates activated FGFR1 to control its endocytosis and function. *EMBO J.* **30,** 3259–73 (2011).

309. Al-Hakim, A. K. *et al.* Control of AMPK-related kinases by USP9X and atypical Lys(29)/Lys(33)-linked polyubiquitin chains. *Biochem. J.* **411,** 249–60 (2008).

310. Geisler, S. *et al.* PINK1/Parkin-mediated mitophagy is dependent on VDAC1 and p62/SQSTM1. *Nat. Cell Biol.* **12,** 119–31 (2010).

311. Fei, C. *et al.* Smurf1-mediated Lys29-linked nonproteolytic polyubiquitination of axin negatively regulates Wnt/β-catenin signaling. *Mol. Cell. Biol.* **33,** 4095–105 (2013).

312. Hamilton, A. M. & Zito, K. Breaking it down: the ubiquitin proteasome system in neuronal morphogenesis. *Neural Plast.* **2013,** 196848 (2013).

313. Yan, D. *et al.* Requirement of dendritic Akt degradation by the ubiquitin-proteasome system for neuronal polarity. *J. Cell Biol.* **174,** 415–24 (2006).

314. Schwamborn, J. C. *et al.* Ubiquitination of the GTPase Rap1B by the ubiquitin ligase Smurf2 is required for the establishment of neuronal polarity. *EMBO J.* **26,** 1410–22 (2007).

315. Cheng, P. *et al.* Phosphorylation of E3 ligase Smurf1 switches its substrate preference in support of axon development. *Neuron* **69,** 231–43 (2011).

316. Lin, M-Y. *et al.* PDZ-RhoGEF ubiquitination by Cullin3-KLHL20 controls neurotrophin-induced neurite outgrowth. *J. Cell Biol.* **193,** 985–94 (2011).

317. Shi, S-H. *et al.* Hippocampal neuronal polarity specified by spatially localized mPar3/mPar6 and PI 3-kinase activity. *Cell* **112,** 63–75 (2003).

318. Jiang, H. *et al.* Both the establishment and the maintenance of neuronal polarity require active mechanisms: critical roles of GSK-3beta and its upstream regulators. *Cell* **120,** 123–35 (2005).

319. Yoshimura, T. *et al.* GSK-3beta regulates phosphorylation of CRMP-2 and neuronal polarity. *Cell* **120,** 137–49 (2005).

320. Bae, S. *et al.* Akt is negatively regulated by the MULAN E3 ligase. *Cell Res.* **22,** 873–85 (2012).

321. Kannan, M. *et al.* The E3 ligase Cdh1-anaphase promoting complex operates upstream of the E3 ligase Smurf1 in the control of axon growth. *Development* **139,** 3600–12 (2012).

322. Yang, Y. *et al.* The dynamic ubiquitin ligase duo: Cdh1-APC and Cdc20-APC regulate neuronal morphogenesis and connectivity. *Curr. Opin. Neurobiol.* **20,** 92–9 (2010).

323. Konishi, Y. *et al.* Cdh1-APC controls axonal growth and patterning in the mammalian brain. *Science* **303,** 1026–30 (2004).

324. Huynh, M. A. *et al.* Regulation of Cdh1-APC function in axon growth by Cdh1 phosphorylation. *J. Neurosci.* **29,** 4322–7 (2009).

325. Stegmüller, J. *et al.* TGFbeta-Smad2 signaling regulates the Cdh1-APC/SnoN pathway of axonal morphogenesis. *J. Neurosci.* **28,** 1961–9 (2008).

326. Wan, Y. *et al.* The anaphase-promoting complex mediates TGF-beta signaling by targeting SnoN for destruction. *Mol. Cell* **8,** 1027–39 (2001).

327. Stroschein, S. L. *et al.* Smad3 recruits the anaphase-promoting complex for ubiquitination and degradation of SnoN. *Genes Dev.* **15,** 2822–36 (2001).

328. Stegmüller, J. *et al.* Cell-intrinsic regulation of axonal morphogenesis by the Cdh1-APC target SnoN. *Neuron* **50,** 389–400 (2006).

329. Lasorella, A. *et al.* Degradation of Id2 by the anaphase-promoting complex couples cell cycle exit and axonal growth. *Nature* **442,** 471–4 (2006).

330. Ikeuchi, Y. *et al.* A SnoN-Ccd1 pathway promotes axonal morphogenesis in the mammalian brain. *J. Neurosci.* **29,** 4312–21 (2009).

331. Rosso, S. *et al.* LIMK1 regulates Golgi dynamics, traffic of Golgi-derived vesicles, and process extension in primary cultured neurons. *Mol. Biol. Cell* **15,** 3433–49 (2004).

332. Tursun, B. *et al.* The ubiquitin ligase Rnf6 regulates local LIM kinase 1 levels in axonal growth cones. *Genes Dev.* **19,** 2307–19 (2005).

333. Jiménez, C. *et al.* Role of the PI3K regulatory subunit in the control of actin organization and cell migration. *J. Cell Biol.* **151,** 249–62 (2000).

334. Christie, K. J. *et al.* Disruption of E3 ligase NEDD4 in peripheral neurons interrupts axon outgrowth: Linkage to PTEN. *Mol. Cell. Neurosci.* **50,** 179–92 (2012).

335. Po, M. D. *et al.* PHRs: bridging axon guidance, outgrowth and synapse development. *Curr. Opin. Neurobiol.* **20,** 100–7 (2010).

336. Bloom, A. J. *et al.* The requirement for Phr1 in CNS axon tract formation reveals the corticostriatal boundary as a choice point for cortical axons. *Genes Dev.* **21,** 2593–606 (2007).

337. Lewcock, J. W. *et al.* The ubiquitin ligase Phr1 regulates axon outgrowth through modulation of microtubule dynamics. *Neuron* **56,** 604–20 (2007).

338. Hendricks, M. & Jesuthasan, S. PHR regulates growth cone pausing at intermediate targets through microtubule disassembly. *J. Neurosci.* **29,** 6593–8 (2009).

339. Bhat, J. M. *et al.* PLR-1, a putative E3 ubiquitin ligase, controls cell polarity and axonal extensions in C. elegans. *Dev. Biol.* **398,** 44–56 (2015).

340. Vandewalle, J. *et al.* Ubiquitin ligase HUWE1 regulates axon branching through the Wnt/β-catenin pathway in a Drosophila model for intellectual disability. *PLoS One* **8,** e81791 (2013).

341. Packard, M. *et al.* The Drosophila Wnt, wingless, provides an essential signal for pre- and postsynaptic differentiation. *Cell* **111,** 319–30 (2002).

342. Purro, S. A. *et al.* Wnt regulates axon behavior through changes in microtubule growth directionality: a new role for adenomatous polyposis coli. *J. Neurosci.* **28,** 8644–54 (2008).

343. Gao, C. & Chen, Y-G. Dishevelled: The hub of Wnt signaling. *Cell. Signal.* **22,** 717–27 (2010).

344. Wang, Z. *et al.* The EBAX-type Cullin-RING E3 ligase and Hsp90 guard the protein quality of the SAX-3/Robo receptor in developing neurons. *Neuron* **79,** 903–16 (2013).

345. Drinjakovic, J. *et al.* E. E3 Ligase Nedd4 Promotes Axon Branching by Downregulating PTEN. *Neuron* **65,** 341–357 (2010).

346. Ing, B. *et al.* Regulation of Commissureless by the ubiquitin ligase DNedd4 is required for neuromuscular synaptogenesis in Drosophila melanogaster. *Mol. Cell. Biol.* **27,** 481–96 (2007).

347. Zhong, Y. *et al.* A splice isoform of DNedd4, DNedd4-long, negatively regulates neuromuscular synaptogenesis and viability in Drosophila. *PLoS One* **6,** e27007 (2011).

348. Van Roessel, P. *et al.* Independent regulation of synaptic size and activity by the anaphase-promoting complex. *Cell* **119,** 707–18 (2004).

349. Yang, Y. *et al.* A Cdc20-APC Ubiquitin Signaling Pathway Regulates Presynaptic Differentiation. *Science* **326,** 575–578 (2010).

350. Liao, E. H. *et al.* An SCF-like ubiquitin ligase complex that controls presynaptic differentiation. *Nature* **430,** 345–350 (2004).

351. Nakata, K. *et al.* Regulation of a DLK-1 and p38 MAP kinase pathway by the ubiquitin ligase RPM-1 is required for presynaptic development. *Cell* **120,** 407–20 (2005).

352. Collins, C. A. *et al.*. Highwire restrains synaptic growth by attenuating a MAP kinase signal. *Neuron* **51,** 57–69 (2006).

353. Wu, C. *et al.* DFsn collaborates with Highwire to down-regulate the Wallenda/DLK kinase and restrain synaptic terminal growth. *Neural Dev.* **2,** 16 (2007).

354. Shin, J. E. & DiAntonio, A. Highwire regulates guidance of sister axons in the Drosophila mushroom body. *J. Neurosci.* **31,** 17689–700 (2011).

355. Opperman, K. J. & Grill, B. RPM-1 is localized to distinct subcellular compartments and regulates axon length in GABAergic motor neurons. *Neural Dev.* **9,** 10 (2014).

356. Xiong, X. *et al.* The Highwire ubiquitin ligase promotes axonal degeneration by tuning levels of Nmnat protein. *PLoS Biol.* **10,** e1001440 (2012).

357. Babetto, E. *et al.* The Phr1 ubiquitin ligase promotes injury-induced axon self-destruction. *Cell Rep.* **3,** 1422–9 (2013).

358. Ding, M. C *et al.* Spatial regulation of an E3 ubiquitin ligase directs selective synapse elimination. *Science* **317,** 947–51 (2007).

359. Yao, I. *et al.* SCRAPPER-dependent ubiquitination of active zone protein RIM1 regulates synaptic vesicle release. *Cell* **130,** 943–57 (2007).

360. Zhang, Q. *et al.* E3 ubiquitin ligase RNF13 involves spatial learning and assembly of the SNARE complex. *Cell. Mol. Life Sci.* **70,** 153–65 (2013).

361. Tada, H. *et al.* Fbxo45, a novel ubiquitin ligase, regulates synaptic activity. *J. Biol. Chem.* **285,** 3840–9 (2010).

362. Sun, Y. *et al.* The F-box protein MEC-15 (FBXW9) promotes synaptic transmission in GABAergic motor neurons in C. elegans. *PLoS One* **8,** e59132 (2013).

363. DiAntonio, A. *et al.* Ubiquitination-dependent mechanisms regulate synaptic growth and function. *Nature* **412,** (2001).

364. Bao, H. *et al.* The Drosophila epsin 1 is required for ubiquitin-dependent synaptic growth and function but not for synaptic vesicle recycling. *Traffic* **9,** 2190–205 (2008).

365. Yuasa-Kawada, J. *et al.* Midline crossing and Slit responsiveness of commissural axons require USP33. *Nat. Neurosci.* **12,** 1087–9 (2009).

366. Anckar, J. & Bonni, A. Regulation of neuronal morphogenesis and positioning by ubiquitin-specific proteases in the cerebellum. *PLoS One* **10,** e0117076 (2015).

367. Bhattacharyya, B. J. *et al*. Altered neurotransmitter release machinery in mice deficient for the deubiquitinating enzyme Usp14. *Am. J. Physiol. Cell Physiol.* **302,** C698–708 (2012).

368. Uthaman, S. B. *et al.* A mechanism distinct from highwire for the Drosophila ubiquitin conjugase bendless in synaptic growth and maturation. *J. Neurosci.* **28,** 8615–23 (2008).

369. Trujillo, G. *et al.* A Ubiquitin E2 Variant Protein Acts in Axon Termination and Synaptogenesis in Caenorhabditis elegans. *Genetics* **186,** 135–45 (2010).

370. Campbell, D. S. & Holt, C. E. Chemotropic responses of retinal growth cones mediated by rapid local protein synthesis and degradation. *Neuron* **32,** 1013–26 (2001).

371. Kim, T.-H. *et al.* Netrin induces down-regulation of its receptor, Deleted in Colorectal Cancer, through the ubiquitin-proteasome pathway in the embryonic cortical neuron. *J. Neurochem.* **95,** 1–8 (2005).

372. Nguyen-Ba-Charvet, K. T. & Chédotal, A. Role of Slit proteins in the vertebrate brain. *J. Physiol. Paris* **96,** 91–8 (2002)

373. Myat, A. *et al.* Drosophila Nedd4, a ubiquitin ligase, is recruited by Commissureless to control cell surface levels of the roundabout receptor. *Neuron* **35,** 447–59 (2002).

374. Wan, H. I. *et al.* Highwire regulates synaptic growth in Drosophila. *Neuron* **26,** 313–29 (2000).

375. Brace, E. J. *et al.* SkpA restrains synaptic terminal growth during development and promotes axonal degeneration following injury. *J. Neurosci.* **34,** 8398–410 (2014).

376. Wise, A. *et al.* Drosophila-Cdh1 (Rap/Fzr) a regulatory subunit of APC/C is required for synaptic morphology, synaptic transmission and locomotion. *Int. J. Dev. Neurosci.* **31,** 624–33 (2013).

377. Saiga, T. *et al.* Fbxo45 forms a novel ubiquitin ligase complex and is required for neuronal development. *Mol. Cell. Biol.* **29,** 3529–43 (2009).

378. Burgess, R. W. *et al.* Evidence for a conserved function in synapse formation reveals Phr1 as a candidate gene for respiratory failure in newborn mice. *Mol. Cell. Biol.* **24,** 1096–105 (2004).

379. Yamada, T. *et al.* Sumoylated MEF2A coordinately eliminates orphan presynaptic sites and promotes maturation of presynaptic boutons. *J. Neurosci.* **33,** 4726–40 (2013).

380. Wolf, B. *et al.* Commissureless endocytosis is correlated with initiation of neuromuscular synaptogenesis. *Development* **125,** 3853–63 (1998).

381. Liu, Y. *et al.* Abnormal development of the neuromuscular junction in Nedd4-deficient mice. *Dev. Biol.* **330,** 153–66 (2009).

382. Tsai, N-P. *et al.* Multiple autism-linked genes mediate synapse elimination via proteasomal degradation of a synaptic scaffold PSD-95. *Cell* **151,** 1581–94 (2012).

383. Zang, S. *et al.* Nicotinamide mononucleotide adenylyltransferase maintains active zone structure by stabilizing Bruchpilot. *EMBO Rep.* **14,** 87–94 (2013).

384. Rinetti, G. V & Schweizer, F. E. Ubiquitination acutely regulates presynaptic neurotransmitter release in mammalian neurons. *J. Neurosci.* **30,** 3157–66 (2010).

385. Speese, S. D. *et al.* The Ubiquitin Proteasome System Acutely Regulates Presynaptic Protein Turnover and Synaptic Efficacy. *Curr. Biol.* **13,** 899–910 (2003).

386. Zhao, Y. *et al.* The Ubiquitin Proteasome System Functions as an Inhibitory Constraint on Synaptic Strengthening. *Curr. Biol.* **13,** 887–898 (2003).

387. Chen, H. *et al.* Rapid Ca 2^{2+} -dependent decrease of protein ubiquitination at synapses. **100,** 2–7 (2003).

388. Ilardi, J. M. *et al.* Snapin: a SNARE-associated protein implicated in synaptic transmission. *Nat. Neurosci.* **2,** 119–24 (1999).

389. Pan, P-Y. *et al.* Snapin facilitates the synchronization of synaptic vesicle fusion. *Neuron* **61,** 412–24 (2009).

390. Tian, J-H. *et al.* The role of Snapin in neurosecretion: snapin knock-out mice exhibit impaired calcium-dependent exocytosis of large dense-core vesicles in chromaffin cells. *J. Neurosci.* **25,** 10546–55 (2005).

391. Waites, C. L. *et al.* Bassoon and Piccolo maintain synapse integrity by regulating protein ubiquitination and degradation. *EMBO J.* **32,** 954–69 (2013).

392. Shen, J. Impaired neurotransmitter release in Alzheimer's and Parkinson's diseases. *Neurodegener. Dis.* **7,** 80–3 (2010).

393. Itier, J-M. *et al.* Parkin gene inactivation alters behaviour and dopamine neurotransmission in the mouse. *Hum. Mol. Genet.* **12,** 2277–91 (2003).

394. Dindot, S. V. *et al.* The Angelman syndrome ubiquitin ligase localizes to the synapse and nucleus, and maternal deficiency results in abnormal dendritic spine morphology. *Hum. Mol. Genet.* **17,** 111–8 (2008).

395. Chen, F. *et al.* Ubiquitin carboxyl-terminal hydrolase L1 is required for maintaining the structure and function of the neuromuscular junction. *Proc. Natl. Acad. Sci. U. S. A.* **107,** 1636–41 (2010).

396. Hay-Koren, A. *et al.* The EDD E3 ubiquitin ligase ubiquitinates and up-regulates beta-catenin. *Mol. Biol. Cell* **22,** 399–411 (2011).

397. Wheeler, T. C. *et al.* Regulation of synaptophysin degradation by mammalian homologues of seven in absentia. *J. Biol. Chem.* **277,** 10273–82 (2002).

398. Nagano, Y. *et al.* Siah-1 facilitates ubiquitination and degradation of synphilin-1. *J. Biol. Chem.* **278,** 51504–14 (2003).

399. Liani, E. *et al.* Ubiquitylation of synphilin-1 and alpha-synuclein by SIAH and its presence in cellular inclusions and Lewy bodies imply a role in Parkinson's disease. *Proc. Natl. Acad. Sci. U. S. A.* **101,** 5500–5 (2004).

400. Hu, G. *et al.* Mammalian homologs of seven in absentia regulate DCC via the ubiquitin-proteasome pathway. *Genes Dev.* **11,** 2701–14 (1997).

401. Rott, R. *et al.* α-Synuclein fate is determined by USP9X-regulated monoubiquitination. *Proc. Natl. Acad. Sci. U. S. A.* **108,** 18666–71 (2011).

402. Chin, L-S. *et al.* Staring, a novel E3 ubiquitin-protein ligase that targets syntaxin 1 for degradation. *J. Biol. Chem.* **277,** 35071–9 (2002).

403. Okumura, F. *et al.* MDA-9/syntenin interacts with ubiquitin via a novel ubiquitin-binding motif. *Mol. Cell. Biochem.* **352,** 163–72 (2011).

404. Huynh, D. P. *et al.* The autosomal recessive juvenile Parkinson disease gene product, parkin, interacts with and ubiquitinates synaptotagmin XI. *Hum. Mol. Genet.* **12,** 2587–97 (2003).

405. Zhang, Y. *et al.* Parkin functions as an E2-dependent ubiquitin- protein ligase and promotes the degradation of the synaptic vesicle-associated protein, CDCrel-1. *Proc. Natl. Acad. Sci. U. S. A.* **97,** 13354–9 (2000).

406. Fallon, L. *et al.* A regulated interaction with the UIM protein Eps15 implicates parkin in EGF receptor trafficking and PI(3)K-Akt signalling. *Nat. Cell Biol.* **8,** 834–42 (2006).

407. Marangoudakis, S. *et al.* Differential ubiquitination and proteasome regulation of Ca(V)2.2 N-type channel splice isoforms. *J. Neurosci.* **32,** 10365–9 (2012).

408. Gandini, M. A. *et al.* CaV2.2 channel cell surface expression is regulated by the light chain 1 (LC1) of the microtubule-associated protein B (MAP1B) via UBE2L3-mediated ubiquitination and degradation. *Pflugers Arch.* **466,** 2113–26 (2014).

409. Ferron, L. *et al.* Fragile X mental retardation protein controls synaptic vesicle exocytosis by modulating N-type calcium channel density. *Nat. Commun.* **5,** 3628 (2014).

410. Sun, Q. & Kelly, G. M. Post-translational modification of CASK leads to its proteasome-dependent degradation. *Int. J. Biochem. Cell Biol.* **42,** 90–7 (2010).

411. Bingol, B. & Schuman, E. M. Activity-dependent dynamics and sequestration of proteasomes in dendritic spines. *Nature* **441,** 1144–8 (2006).

412. Willeumier, K. *et al.* Proteasome Inhibition Triggers Activity-Dependent Increase in the Size of the Recycling Vesicle Pool in Cultured Hippocampal Neurons. *J. Neurosci.* **26,** 11333–11341 (2009).

413. Herzog, E. *et al.* In vivo imaging of intersynaptic vesicle exchange using VGLUT1 Venus knock-in mice. *J. Neurosci.* **31,** 15544–59 (2011).

414. Dantuma, N. P. *et al.* Short-lived green fluorescent proteins for quantifying ubiquitin / proteasome- dependent proteolysis in living cells. **18,** 538-543 (2000).

415. Chen, Z. *et al.* Ubiquitination-induced fluorescence complementation (UiFC) for detection of K48 ubiquitin chains in vitro and in live cells. *PLoS One* **8,** e73482 (2013).

416. Wu, K. Y. *et al.* Local translation of RhoA regulates growth cone collapse. *Nature* **436,** 1020–4 (2005).

417. Taylor, A. M. *et al.* Microfluidic Multicompartment Device for Neuroscience Research. *Langmuir* **19,** 1551–1556 (2003).

418. Ribeiro, L. F. *et al.* Ghrelin triggers the synaptic incorporation of AMPA receptors in the hippocampus. *Proc. Natl. Acad. Sci. U. S. A.* **111,** E149–58 (2014).

419. Taylor, A. M. *et al.* Axonal translation of β-catenin regulates synaptic vesicle dynamics. *J. Neurosci.* **33,** 5584–9 (2013).

420. Steward, O. & Falk, P. M. Selective localization of polyribosomes beneath developing synapses: a quantitative analysis of the relationships between polyribosomes and developing synapses in the hippocampus and dentate gyrus. *J. Comp. Neurol.* **314,** 545–57 (1991).

421. Jin, Y. & Garner, C. C. Molecular mechanisms of presynaptic differentiation. *Annu. Rev. Cell Dev. Biol.* **24,** 237–62 (2008).

422. Leal, G. *et al.* Regulation of hippocampal synaptic plasticity by BDNF. *Brain Res.* **14,** 01421-8 (2014).

423. Rubio, N. Mouse astrocytes store and deliver brain-derived neurotrophic factor using the non-catalytic gp95trkB receptor. *Eur. J. Neurosci.* **9,** 1847–53 (1997).

424. Alsina, B. *et al.* Visualizing synapse formation in arborizing optic axons in vivo: dynamics and modulation by BDNF. *Nat. Neurosci.* **4,** 1093–101 (2001).

425. Fox, M. A. *et al.* Distinct target-derived signals organize formation, maturation, and maintenance of motor nerve terminals. *Cell* **129,** 179–93 (2007).

426. Jones, K. & Basson, M. A. FGF ligands emerge as potential specifiers of synaptic identity. *Cellscience* **7,** 33–42 (2010).

427. Sone, M. *et al.* Synaptic development is controlled in the periactive zones of Drosophila synapses. *Development* **127,** 4157–68 (2000).

428. Somers, D. E. & Fujiwara, S. Thinking outside the F-box: novel ligands for novel receptors. *Trends Plant Sci.* **14,** 206–13 (2009).

429. Schaefer, A. M. *et al.* Rpm-1, a conserved neuronal gene that regulates targeting and synaptogenesis in C. elegans. *Neuron* **26,** 345–56 (2000).

430. Zhen, M. *et al.* Regulation of Presynaptic Terminal Organization by C. elegans RPM-1, a Putative Guanine Nucleotide Exchanger with a RING-H2 Finger Domain. *Neuron* **26,** 331–343 (2000).

431. Upadhya, S. C. *et al.* Differential regulation of proteasome activity in the nucleus and the synaptic terminals. *Neurochem. Int.* **48,** 296–305 (2006).

432. Segref, A. & Hoppe, T. Think locally: control of ubiquitin-dependent protein degradation in neurons. *EMBO Rep.* **10,** 44–50 (2009).

433. Banerjee, S. *et al.* A coordinated local translational control point at the synapse involving relief from silencing and MOV10 degradation. *Neuron* **64,** 871–84 (2009).

434. Margolis, S. S. *et al.* EphB-Mediated Degradation of the RhoA GEF Ephexin5 Relieves a Developmental Brake on Excitatory Synapse Formation. *Cell* **143,** 442–455 (2010).

435. Keimpema, E. *et al.* Differential subcellular recruitment of monoacylglycerol lipase generates spatial specificity of 2-arachidonoyl glycerol signaling during axonal pathfinding. *J. Neurosci.* **30,** 13992–4007 (2010).

436. Reits, E. & Benham, A. Dynamics of proteasome distribution in living cells. *EMBO J* **16,** 6087–6094 (1997).

437. Gordon, C. The intracellular localization of the proteasome. *Curr. Top. Microbiol. Immunol.* **268,** 175–84 (2002).

438. Girão, H. *et al.* Subcellular redistribution of components of the ubiquitin-proteasome pathway during lens differentiation and maturation. *Invest. Ophthalmol. Vis. Sci.* **46,** 1386–92 (2005).

439. Boisvert, F-M. *et al.* A quantitative proteomics analysis of subcellular proteome localization and changes induced by DNA damage. *Mol. Cell. Proteomics* **9,** 457–70 (2010).

440. Bingol, B. *et al.* Autophosphorylated CaMKIIalpha acts as a scaffold to recruit proteasomes to dendritic spines. *Cell* **140,** 567–78 (2010).

441. Haas, K. F. & Broadie, K. Roles of ubiquitination at the synapse. *Biochim Biophys Acta* **1779,** 495–506 (2009).

442. Otero, M. G. *et al.* Fast axonal transport of the proteasome complex depends on membrane interaction and molecular motor function. *J. Cell Sci.* **127,** 1537–49 (2014).

443. Zhang, X. *et al.* Receptor specificity of the fibroblast growth factor family. The complete mammalian FGF family. *J. Biol. Chem.* **281,** 15694–700 (2006).

444. Fryer, R. H. *et al.* Developmental and mature expression of full-length and truncated TrkB receptors in the rat forebrain. *J. Comp. Neurol.* **374,** 21–40 (1996).

445. Yan, Q. *et al.* Immunocytochemical localization of TrkB in the central nervous system of the adult rat. *J. Comp. Neurol.* **378,** 135–57 (1997).

446. Berkers, C. R. *et al.* Activity probe for in vivo profiling of the specificity of proteasome inhibitor bortezomib. *Nat. Methods* **2,** 357–362 (2005).

447. Berkers, C. R. *et al.* Profiling Proteasome Activity in Tissue with Fluorescent Probes. **4,** 739–748 (2007).

448. Zhang, S. *et al.* Covalent complexes of proteasome model with peptide aldehyde inhibitors MG132 and MG101: docking and molecular dynamics study. *J. Mol. Model.* **15,** 1481–90 (2009).

449. Verdoes, M. *et al.* A fluorescent broad-spectrum proteasome inhibitor for labeling proteasomes in vitro and in vivo. *Chem. Biol.* **13,** 1217–26 (2006).

450. Unno, M. *et al.* The structure of the mammalian 20S proteasome at 2.75 A resolution. *Structure* **10,** 609–18 (2002).

451. Mann, F. *et al.* B-type Eph receptors and ephrins induce growth cone collapse through distinct intracellular pathways. *J. Neurobiol.* **57,** 323–36 (2003).

452. Fenteany, G. *et al.* Inhibition of proteasome activities and subunit-specific amino-terminal threonine modification by lactacystin. *Science* **268,** 726–31 (1995).

453. Dick, L. R. *et al.* Mechanistic studies on the inactivation of the proteasome by lactacystin in cultured cells. *J. Biol. Chem.* **272,** 182–8 (1997).

454. Taylor, A. M. *et al.* A microfluidic culture platform for CNS axonal injury, regeneration and transport. *Nat. Methods* **2,** 599–605 (2005).

455. Sia, S. K. & Whitesides, G. M. Microfluidic devices fabricated in poly(dimethylsiloxane) for biological studies. *Electrophoresis* **24,** 3563–76 (2003).

456. Jia, J-M. *et al.* Brain-derived neurotrophic factor-tropomyosin-related kinase B signaling contributes to activity-dependent changes in synaptic proteins. *J. Biol. Chem.* **283,** 21242–50 (2008).

457. Ehlers, M. D. Activity level controls postsynaptic composition and signaling via the ubiquitin-proteasome system. *Nat. Neurosci.* **6,** 231–42 (2003).

458. Bence, N. F. *et al.* Impairment of the ubiquitin-proteasome system by protein aggregation. *Science* **292,** 1552–5 (2001).

459. Gilon, T. *et al*. Degradation signals for ubiquitin system proteolysis in Saccharomyces cerevisiae. *EMBO J.* **17,** 2759–66 (1998).

460. Bence, N. F. *et al.* Application and analysis of the GFPu family of ubiquitin-proteasome system reporters. *Methods Enzymol.* **399,** 481–90 (2005).

461. Santos, A. R. *et al.* Differential Role of the Proteasome in the Early and Late Phases of BDNF-Induced Facilitation of LTP. *J. Neurosci.* **35,** 3319–29 (2015).

462. Li, B. *et al.* FGF-2 prevents cancer cells from ER stress-mediated apoptosis via enhancing proteasome-mediated Nck degradation. *Biochem. J.* **452,** 139–45 (2013).

463. Mariotti, M. *et al*. The tyrosine phosphatase HD-PTP is regulated by FGF-2 through proteasome degradation. *Front. Biosci.* **11,** 2138–43 (2006).

464. Kaabeche, K. *et al.* Cbl-mediated ubiquitination of alpha5 integrin subunit mediates fibronectin-dependent osteoblast detachment and apoptosis induced by FGFR2 activation. *J. Cell Sci.* **118,** 1223–32 (2005).

465. Dufour, C. *et al.* FGFR2-Cbl interaction in lipid rafts triggers attenuation of PI3K/Akt signaling and osteoblast survival. *Bone* **42,** 1032–9 (2008).

466. Djakovic, S. N. *et al.* Regulation of the proteasome by neuronal activity and calcium/calmodulin-dependent protein kinase II. *J. Biol. Chem.* **284,** 26655–65 (2009).

467. Djakovic, S. N. *et al.* Phosphorylation of Rpt6 regulates synaptic strength in hippocampal neurons. *J. Neurosci.* **32,** 5126–31 (2012).

468. Slonimsky, J. D. *et al.* Role for calcium/calmodulin-dependent protein kinase II in the p75-mediated regulation of sympathetic cholinergic transmission. *Proc. Natl. Acad. Sci. U. S. A.* **103,** 2915–9 (2006).

469. Blanquet, P. *et al*. A calcium/calmodulin kinase pathway connects brain-derived neurotrophic factor to the cyclic amp-responsive transcription factor in the rat hippocampus. *Neuroscience* **118,** 477–490 (2003).

470. Tao-Cheng, J-H. *et al.* Changes in the distribution of calcium calmodulin-dependent protein kinase II at the presynaptic bouton after depolarization. *Brain Cell Biol.* **35,** 117–24 (2006).

471. Soppet, D. *et al.* The neurotrophic factors brain-derived neurotrophic factor and neurotrophin-3 are ligands for the trkB tyrosine kinase receptor. *Cell* **65,** 895–903 (1991).

472. Tian, X. & Wu, C. The role of ubiquitin-mediated pathways in regulating synaptic development, axonal degeneration and regeneration: insights from fly and worm. *J. Physiol.* **591,** 3133–43 (2013).

473. Millet, L. J. *et al.*. Guiding neuron development with planar surface gradients of substrate cues deposited using microfluidic devices. *Lab Chip* **10,** 1525-35 (2010).

474. Taylor, A. M. *et al.* Axonal mRNA in uninjured and regenerating cortical mammalian axons. *J. Neurosci.* **29,** 4697–707 (2009).

475. Szelechowski, M. *et al.* A viral peptide that targets mitochondria protects against neuronal degeneration in models of Parkinson's disease. *Nat. Commun.* **5,** 5181 (2014).

476. Cristovão, G. *et al.* Activation of microglia bolsters synapse formation. *Front. Cell. Neurosci.* **8,** 153 (2014).

477. Suo, D. *et al.* Coronin-1 is a neurotrophin endosomal effector that is required for developmental competition for survival. *Nat. Neurosci.* **17,** 36–45 (2014).

478. Fletcher, T. L. *et al.* Synaptogenesis in hippocampal cultures: evidence indicating that axons and dendrites become competent to form synapses at different stages of neuronal development. *J. Neurosci.* **14,** 6695–706 (1994).

479. Waters, J. C. Accuracy and precision in quantitative fluorescence microscopy. *J. Cell Biol.* **185,** 1135–48 (2009).

480. Nakamura, Y. *et al.* Role of neuropsin in formation and maturation of Schaffer-collateral L1cam-immunoreactive synaptic boutons. *J. Cell Sci.* **119,** 1341–9 (2006).

481. Shen, W. *et al.* Activity-induced rapid synaptic maturation mediated by presynaptic cdc42 signaling. *Neuron* **50,** 401–14 (2006).

482. Taylor, A. M. *et al.* Microfluidic local perfusion chambers for the visualization and manipulation of synapses. *Neuron* **66,** 57–68 (2010).

483. Prokop, A. *et al.* Presynaptic development at the Drosophila neuromuscular junction: assembly and localization of presynaptic active zones. *Neuron* **17,** 617–26 (1996).

484. McAllister, A. K. Dynamic aspects of CNS synapse formation. *Annu. Rev. Neurosci.* **30,** 425–50 (2007).

485. Jiang, X. *et al.* A role for the ubiquitin-proteasome system in activity-dependent presynaptic silencing. *J. Neurosci.* **30,** 1798–809 (2010).

486. Pedro, J.R. *et al.* Intra-axonal translation of beta-actin is required for presynaptic differentiation. *FENS* (2014) (poster).

487. Lyles, V. *et al.* Synapse formation and mRNA localization in cultured Aplysia neurons. *Neuron* **49,** 349–56 (2006).

488. Nalavadi, V. C. *et al.* Dephosphorylation-induced ubiquitination and degradation of FMRP in dendrites: a role in immediate early mGluR-stimulated translation. *J. Neurosci.* **32,** 2582–7 (2012).

489. Chou, A. P. *et al.* Ziram causes dopaminergic cell damage by inhibiting E1 ligase of the proteasome. *J. Biol. Chem.* **283,** 34696–703 (2008).

490. Altun, M. *et al.* Activity-based chemical proteomics accelerates inhibitor development for deubiquitylating enzymes. *Chem. Biol.* **18,** 1401–12 (2011).

491. Seiberlich, V. *et al.* The small molecule inhibitor PR-619 of deubiquitinating enzymes affects the microtubule network and causes protein aggregate formation in neural cells: implications for neurodegenerative diseases. *Biochim. Biophys. Acta* **1823,** 2057–68 (2012).

492. Newton, K. *et al.* Ubiquitin chain editing revealed by polyubiquitin linkage-specific antibodies. *Cell* **134,** 668–78 (2008).

493. Mody, M. *et al.* Genome-wide gene expression profiles of the developing mouse hippocampus. *Proc. Natl. Acad. Sci. U. S. A.* **98,** 8862–7 (2001).

494. Peng, J. *et al.* A proteomics approach to understanding protein ubiquitination. *Nat. Biotechnol.* **21,** 921–6 (2003).

495. Budhavarapu, V. N. *et al.* Regulation of E2F1 by APC/C Cdh1 via K11 linkage-specific ubiquitin chain formation. *Cell Cycle* **11,** 2030–8 (2012).

496. Kim, W. *et al.* Systematic and quantitative assessment of the ubiquitin-modified proteome. *Mol. Cell* **44,** 325–40 (2011).

497. Wagner, S. A. *et al.* A proteome-wide, quantitative survey of in vivo ubiquitylation sites reveals widespread regulatory roles. *Mol. Cell. Proteomics* **10,** M111.013284 (2011).

498. Petersen, A. *et al.* Changes in Activity and Kinetic Properties of the Proteasome in Different Rat Organs during Development and Maturation. *Curr. Gerontol. Geriatr. Res.* 230697 (2010).

499. Sakanaka, C. *et al.* Bridging of beta-catenin and glycogen synthase kinase-3beta by axin and inhibition of beta-catenin-mediated transcription. *Proc. Natl. Acad. Sci. U. S. A.* **95,** 3020–3 (1998).

500. Hart, M. *et al.* The F-box protein beta-TrCP associates with phosphorylated beta-catenin and regulates its activity in the cell. *Curr. Biol.* **9,** 207–10 (1999).

501. Aberle, H. *et al.* beta-catenin is a target for the ubiquitin-proteasome pathway. *EMBO J.* **16,** 3797–804 (1997).

502. Willert, K. *et al.* Wnt-induced dephosphorylation of axin releases beta-catenin from the axin complex. *Genes Dev.* **13,** 1768–73 (1999).

503. Glickman, M. H. & Raveh, D. Proteasome plasticity. *FEBS Lett.* **579,** 3214–23 (2005).

504. Caldeira, M. V *et al.* Excitotoxic stimulation downregulates the ubiquitin-proteasome system through activation of NMDA receptors in cultured hippocampal neurons. *Biochim. Biophys. Acta* **1832,** 263–74 (2013).

505. Tai, H-C., *et al.* Characterization of the Brain 26S Proteasome and its Interacting Proteins. *Front. Mol. Neurosci.* **3,** 1–19 (2010).

506. Huang, Q. *et al.* Negative regulation of 26S proteasome stability via calpain-mediated cleavage of Rpn10 subunit upon mitochondrial dysfunction in neurons. *J. Biol. Chem.* **288,** 12161–74 (2013).

507. Stamenova, S. D. *et al.* Ubiquitin binds to and regulates a subset of SH3 domains. *Mol. Cell* **25,** 273–84 (2007).

508. Rajesh, S. *et al.* Binding to syntenin-1 protein defines a new mode of ubiquitin-based interactions regulated by phosphorylation. *J. Biol. Chem.* **286,** 39606–14 (2011).

509. Hofmann, K. & Falquet, L. A ubiquitin-interacting motif conserved in components of the proteasomal and lysosomal protein degradation systems. *Trends Biochem. Sci.* **26,** 347–50 (2001).

510. Polo, S. *et al.* A single motif responsible for ubiquitin recognition and monoubiquitination in endocytic proteins. *Nature* **416,** 451–5 (2002).

511. Majumdar, A. *et al.* Drosophila homologue of Eps15 is essential for synaptic vesicle recycling. *Exp. Cell Res.* **312,** 2288–98 (2006).

512. Koh, T-W. *et al.* Eps15 and Dap160 control synaptic vesicle membrane retrieval and synapse development. *J. Cell Biol.* **178,** 309–22 (2007).

513. Jakobsson, J. *et al.* Role of epsin 1 in synaptic vesicle endocytosis. *Proc. Natl. Acad. Sci. U. S. A.* **105,** 6445–50 (2008).

514. Betz, A. *et al.* Munc13-1 is a presynaptic phorbol ester receptor that enhances neurotransmitter release. *Neuron* **21,** 123–36 (1998).

515. Ashery, U. *et al.* Munc13-1 acts as a priming factor for large dense-core vesicles in bovine chromaffin cells. *EMBO J.* **19,** 3586–96 (2000).

516. Aravamudan, B. & Broadie, K. Synaptic Drosophila UNC-13 is regulated by antagonistic G-protein pathways via a proteasome-dependent degradation mechanism. *J. Neurobiol.* **54,** 417–38 (2003).

517. Kavalali, E. T. & Jorgensen, E. M. Visualizing presynaptic function. *Nat. Neurosci.* **17,** 10–6 (2014).

518. Gaffield, M. A. & Betz, W. J. Imaging synaptic vesicle exocytosis and endocytosis with FM dyes. *Nat. Protoc.* **1,** 2916–21 (2006).

519. Ryan, T. A. *et al.* The kinetics of synaptic vesicle recycling measured at single presynaptic boutons. *Neuron* **11,** 713–24 (1993).

520. Burrone, J. *et al.* Studying vesicle cycling in presynaptic terminals using the genetically encoded probe synaptopHluorin. *Nat. Protoc.* **1,** 2970–8 (2006).

521. Catterall, W. A. & Few, A. P. Calcium channel regulation and presynaptic plasticity. *Neuron* **59,** 882–901 (2008).

522. Girach, F. *et al.* RIM1α SUMOylation is required for fast synaptic vesicle exocytosis. *Cell Rep.* **5,** 1294–301 (2013).

523. Feligioni, M. *et al.* Protein SUMOylation modulates calcium influx and glutamate release from presynaptic terminals. *Eur. J. Neurosci.* **29,** 1348–56 (2009).

524. Scruggs, S. B. *et al.* Post-translational modification of cardiac proteasomes: functional delineation enabled by proteomics. *AJP Hear. Circ. Physiol.* **303,** H9–H18 (2012).

525. Cui, Z. *et al.* Regulation of cardiac proteasomes by ubiquitination, SUMOylation, and beyond. *J. Mol. Cell. Cardiol.* **71,** 32–42 (2014).

526. Lu, H. *et al.* Revealing the Dynamics of the 20 S Proteasome Phosphoproteome: A Combined CID and Electron Transfer Dissociation Approach. *Mol. Cell. Proteomics* **7,** 2073–2089 (2008).

527. MacDonald, J. I. *et al.* Activity-dependent interaction of the intracellular domain of rat trkA with intermediate filament proteins, the beta-6 proteasomal subunit, Ras-GRF1, and the p162 subunit of eIF3. *J. Mol. Neurosci.* **13,** 141–58 (1999).

528. Guan, H. & Maness, P. F. Perisomatic GABAergic innervation in prefrontal cortex is regulated by ankyrin interaction with the L1 cell adhesion molecule. *Cereb. Cortex* **20,** 2684–93 (2010).

529. Zivraj, K. H. *et al.* Subcellular profiling reveals distinct and developmentally regulated repertoire of growth cone mRNAs. *J. Neurosci.* **30,** 15464–78 (2010).

530. Zhang, X. H. & Poo, M. Localized synaptic potentiation by BDNF requires local protein synthesis in the developing axon. *Neuron* **36,** 675–88 (2002).

531. Sasaki, Y. *et al.* Phosphorylation of zipcode binding protein is required for BDNF signaling of local β-actin synthesis and growth cone turning. *J. Neurosci.* **30,** 9349–9358 (2011).

532. Ji, S-J. & Jaffrey, S. R. Intra-axonal translation of SMAD1/5/8 mediates retrograde regulation of trigeminal ganglia subtype specification. *Neuron* **74,** 95–107 (2012).

533. Puram, S. V *et al.* A CaMKIIβ signaling pathway at the centrosome regulates dendrite patterning in the brain. *Nat. Neurosci.* **14,** 973–83 (2011).

534. Persaud, A. *et al.* Tyrosine phosphorylation of NEDD4 activates its ubiquitin ligase activity. *Sci. Signal.* **7,** ra95 (2014).

535. Kane, L. A. *et al.* PINK1 phosphorylates ubiquitin to activate Parkin E3 ubiquitin ligase activity. *J. Cell Biol.* **205,** 143–53 (2014).

536. Arévalo, J. C. *et al.* Cell survival through Trk neurotrophin receptors is differentially regulated by ubiquitination. *Neuron* **50,** 549–59 (2006).

537. Nelson, J. C., Stavoe, A. K. H. & Colón-Ramos, D. A. The actin cytoskeleton in presynaptic assembly. *Cell Adh. Migr.* **7,** 379–87

538. Terman, J. R. & Kashina, A. Post-translational modification and regulation of actin. *Curr. Opin. Cell Biol.* **25,** 30–8 (2013).

539. Schaefer, A. *et al.* Ubiquitin links to cytoskeletal dynamics, cell adhesion and migration. *Biochem. J.* **442,** 13–25 (2012).

540. Ryu, K-Y. *et al.* Hypothalamic neurodegeneration and adult-onset obesity in mice lacking the Ubb polyubiquitin gene. *Proc. Natl. Acad. Sci. U. S. A.* **105,** 4016–21 (2008).

541. Ryu, K-Y. *et al.* The mouse polyubiquitin gene UbC is essential for fetal liver development, cell-cycle progression and stress tolerance. *EMBO J.* **26,** 2693–706 (2007).

542. Ryu, K-Y. *et al.* The mouse polyubiquitin gene Ubb is essential for meiotic progression. *Mol. Cell. Biol.* **28,** 1136–46 (2008).

543. Ryu, K-Y. *et al.* Perturbation of the Hematopoietic System during Embryonic Liver Development Due to Disruption of Polyubiquitin Gene Ubc in Mice. *PLoS One* **7,** e32956 (2012).

544. Skvorak, K. *et al.* Production of conditional point mutant knockin mice. *Genesis* **44,** 345–53 (2006).

545. Kaiser, P. *et al.* Regulation of transcription by ubiquitination without proteolysis: Cdc34/SCF(Met30)-mediated inactivation of the transcription factor Met4. *Cell* **102,** 303–14 (2000).

546. Kuras, L. *et al.* Dual regulation of the met4 transcription factor by ubiquitin-dependent degradation and inhibition of promoter recruitment. *Mol. Cell* **10,** 69–80 (2002).

547. Flick, K. *et al.* A ubiquitin-interacting motif protects polyubiquitinated Met4 from degradation by the 26S proteasome. *Nat. Cell Biol.* **8,** 509–15 (2006).

548. Ye, Y. *et al.* The AAA ATPase Cdc48/p97 and its partners transport proteins from the ER into the cytosol. *Nature* **414,** 652–6 (2001).

549. Ye, Y., *et al.* Function of the p97-Ufd1-Npl4 complex in retrotranslocation from the ER to the cytosol: dual recognition of nonubiquitinated polypeptide segments and polyubiquitin chains. *J. Cell Biol.* **162,** 71–84 (2003).

550. Wickliffe, K. E. *et al.* K11-linked ubiquitin chains as novel regulators of cell division. *Trends Cell Biol.* **21,** 656–63 (2011).

551. Dynek, J. N. *et al.* c-IAP1 and UbcH5 promote K11-linked polyubiquitination of RIP1 in TNF signalling. *EMBO J.* **29,** 4198–209 (2010).

552. Boname, J. M. *et al.* Efficient internalization of MHC I requires lysine-11 and lysine-63 mixed linkage polyubiquitin chains. *Traffic* **11,** 210–20 (2010).

553. Goto, E. *et al.* Contribution of lysine 11-linked ubiquitination to MIR2-mediated major histocompatibility complex class I internalization. *J. Biol. Chem.* **285,** 35311–9 (2010).

554. Wang, H. *et al.* Analysis of nondegradative protein ubiquitylation with a monoclonal antibody specific for lysine-63-linked polyubiquitin. *Proc. Natl. Acad. Sci. U. S. A.* **105,** 20197–202 (2008).

555. Dani, A. *et al.* Super-resolution Imaging of Chemical Synapses in the Brain. **68,** 843–856 (2010).

556. Mayor, U. & Peng, J. Deciphering tissue-specific ubiquitylation by mass spectrometry. *Methods Mol. Biol.* **832,** 65–80 (2012).

557. Matsumoto, M. *et al.* Large-scale analysis of the human ubiquitin-related proteome. *Proteomics* **5,** 4145–51 (2005).

558. Kirkpatrick, D. S. *et al.* Proteomic identification of ubiquitinated proteins from human cells expressing His-tagged ubiquitin. *Proteomics* **5,** 2104–11 (2005).

559. Meierhofer, D. *et al.* Quantitative analysis of global ubiquitination in HeLa cells by mass spectrometry. *J. Proteome Res.* **7,** 4566–76 (2008).

560. Biesemann, C. *et al.* Proteomic screening of glutamatergic mouse brain synaptosomes isolated by fluorescence activated sorting. *EMBO J.* **33,** 157–70 (2014).

561. McClatchy, D. B. *et al.* Quantification of the synaptosomal proteome of the rat cerebellum during post-natal development. *Genome Res.* **17,** 1378–88 (2007).

562. Tsubuki, S. *et al.* Purification and characterization of a Z-Leu-Leu-Leu-MCA degrading protease expected to regulate neurite formation: a novel catalytic activity in proteasome. *Biochem. Biophys. Res. Commun.* **196,** 1195–201 (1993).

563. Ohtani-Kaneko, R. *et al.* Proteasome inhibitors which induce neurite outgrowth from PC12h cells cause different subcellular accumulations of multi-ubiquitin chains. *Neurochem. Res.* **23,** 1435–43 (1998).

564. Inoue, M. *et al.* TMC-95A, a reversible proteasome inhibitor, induces neurite outgrowth in PC12 cells. *Bioorg. Med. Chem. Lett.* **14,** 663–5 (2004).

565. Klimaschewski, L. *et al.* Constitutively expressed catalytic proteasomal subunits are up-regulated during neuronal differentiation and required for axon initiation, elongation and maintenance. *J. Neurochem.* **96,** 1708–17 (2006).

566. Song, E. J. *et al.* Proteasome inhibition induces neurite outgrowth through posttranslational modification of TrkA receptor. *Int. J. Biochem. Cell Biol.* **41,** 539–45 (2009).

567. Laser, H. *et al.* Proteasome inhibition arrests neurite outgrowth and causes 'dying-back' degeneration in primary culture. *J. Neurosci. Res.* **74,** 906–16 (2003).

568. Verma, P. *et al.* Axonal protein synthesis and degradation are necessary for efficient growth cone regeneration. *J. Neurosci.* **25,** 331–42 (2005).

569. Bryan, B. *et al.* Ubiquitination of RhoA by Smurf1 promotes neurite outgrowth. *FEBS Lett.* **579,** 1015–9 (2005).

570. Zschätzsch, M. *et al.* Regulation of branching dynamics by axon-intrinsic asymmetries in Tyrosine Kinase Receptor signaling. *Elife* **3,** e01699 (2014).

571. Ketschek, A. & Gallo, G. Nerve growth factor induces axonal filopodia through localized microdomains of phosphoinositide 3-kinase activity that drive the formation of cytoskeletal precursors to filopodia. *J. Neurosci.* **30,** 12185–97 (2010).

572. Tang, F. Netrin-1 Induces Axon Branching in Developing Cortical Neurons by Frequency-Dependent Calcium Signaling Pathways. *J. Neurosci.* **25,** 6702–6715 (2005).

573. Hutchins, B. I. & Kalil, K. Differential outgrowth of axons and their branches is regulated by localized calcium transients. *J. Neurosci.* **28,** 143–53 (2008).

574. Xue, J-F. *et al.* Ginsenoside Rb1 promotes neurotransmitter release by modulating phosphorylation of synapsins through a cAMP-dependent protein kinase pathway. *Brain Res.* **1106,** 91–98 (2006).

575. Verstegen, A. M. J. *et al.* Phosphorylation of synapsin I by cyclin-dependent kinase-5 sets the ratio between the resting and recycling pools of synaptic vesicles at hippocampal synapses. *J. Neurosci.* **34,** 7266–80 (2014).

576. Tomizawa, K. *et al.* Cdk5/p35 regulates neurotransmitter release through phosphorylation and downregulation of P/Q-type voltage-dependent calcium channel activity. *J. Neurosci.* **22,** 2590–7 (2002).

577. Su, S. C. *et al.* Regulation of N-type voltage-gated calcium channels and presynaptic function by cyclin-dependent kinase 5. *Neuron* **75,** 675–87 (2012).

578. Houeland, G. *et al.* PKC modulation of transmitter release by SNAP-25 at sensory-to-motor synapses in aplysia. *J. Neurophysiol.* **97,** 134–43 (2007).

579. Miskiewicz, K. *et al.* HDAC6 is a Bruchpilot deacetylase that facilitates neurotransmitter release. *Cell Rep.* **8,** 94–102 (2014).

580. Sims, J. J. *et al.* Polyubiquitin-sensor proteins reveal localization and linkage-type dependence of cellular ubiquitin signaling. *Nat. Methods* **9,** 303–9 (2012).

581. Anderson, C. *et al.* Loss of Usp14 results in reduced levels of ubiquitin in ataxia mice. *J. Neurochem.* **95,** 724–731 (2005).

582. Saigoh, K. *et al.* Intragenic deletion in the gene encoding ubiquitin carboxy-terminal hydrolase in gad mice. *Nat. Genet.* **23,** 47–51 (1999).

583. Kikuchi, T. *et al.* Axonal degeneration of ascending sensory neurons in gracile axonal dystrophy mutant mouse. *Acta Neuropathol.* **80,** 145–51 (1990).

584. Leroy, E. *et al.* The ubiquitin pathway in Parkinson's disease. *Nature* **395,** 451–2 (1998).

585. Xue, S. & Jia, J. Genetic association between Ubiquitin Carboxy-terminal Hydrolase-L1 gene S18Y polymorphism and sporadic Alzheimer's disease in a Chinese Han population. *Brain Res.* **1087,** 28–32 (2006).

586. Choi, J. *et al.* Oxidative modifications and down-regulation of ubiquitin carboxyl-terminal hydrolase L1 associated with idiopathic Parkinson's and Alzheimer's diseases. *J. Biol. Chem.* **279,** 13256–64 (2004).

587. Barrachina, M. *et al.* Reduced ubiquitin C-terminal hydrolase-1 expression levels in dementia with Lewy bodies. *Neurobiol. Dis.* **22,** 265–273 (2006).

588. Liu, Z. *et al.* Membrane-associated farnesylated UCH-L1 promotes alpha-synuclein neurotoxicity and is a therapeutic target for Parkinson's disease. *Proc. Natl. Acad. Sci. U. S. A.* **106,** 4635–40 (2009).

589. Dressman, D. *et al.* X-linked infantile spinal muscular atrophy: clinical definition and molecular mapping. *Genet. Med.* **9,** 52–60 (2007).

590. Ramser, J. *et al.* Rare Missense and Synonymous Variants in UBE1 Are Associated with X-Linked Infantile Spinal Muscular Atrophy. *Am. J. Hum. Genet.* **82,** 188–193 (2008).

591. Wishart, T. M. *et al.* Dysregulation of ubiquitin homeostasis and β-catenin signaling promote spinal muscular atrophy. *J. Clin. Invest.* **124,** 1821–34 (2014).

592. Lefebvre, S. *et al.* Identification and characterization of a spinal muscular atrophy-determining gene. *Cell* **80,** 155–65 (1995).

593. Wirth, B. An update of the mutation spectrum of the survival motor neuron gene (SMN1) in autosomal recessive spinal muscular atrophy (SMA). *Hum. Mutat.* **15,** 228–37 (2000).

594. Ling, K. K. Y. *et al.* Synaptic Defects in the Spinal and Neuromuscular Circuitry in a Mouse Model of Spinal Muscular Atrophy. *PLoS One* **5,** e15457 (2010).

595. Mentis, G. Z. *et al.* Early functional impairment of sensory-motor connectivity in a mouse model of spinal muscular atrophy. *Neuron* **69,** 453–67 (2011).

596. Murray, L. M. *et al.* Selective vulnerability of motor neurons and dissociation of pre- and post-synaptic pathology at the neuromuscular junction in mouse models of spinal muscular atrophy. *Hum. Mol. Genet.* **17,** 949–962 (2007).

597. Kariya, S. *et al.* Reduced SMN protein impairs maturation of the neuromuscular junctions in mouse models of spinal muscular atrophy. *Hum. Mol. Genet.* **17,** 2552–69 (2008).

598. Gupta, S. & Kulhara, P. What is schizophrenia: A neurodevelopmental or neurodegenerative disorder or a combination of both? A critical analysis. *Indian J. Psychiatry* **52,** 21–7 (2010).

599. Middleton, F. A. *et al.* Gene expression profiling reveals alterations of specific metabolic pathways in schizophrenia. *J. Neurosci.* **22,** 2718–29 (2002).

600. Altar, C. A. *et al.* Deficient hippocampal neuron expression of proteasome, ubiquitin, and mitochondrial genes in multiple schizophrenia cohorts. *Biol. Psychiatry* **58,** 85–96 (2005).

601. Rubio, M. D. *et al.* Dysfunction of the ubiquitin proteasome and ubiquitin-like systems in schizophrenia. *Neuropsychopharmacology* **38,** 1910–20 (2013).

602. Dan, B. Angelman syndrome: current understanding and research prospects. *Epilepsia* **50,** 2331–9 (2009).

603. Jiang, Y. *et al.* Mutation of the Angelman Ubiquitin Ligase in Mice Causes Increased Cytoplasmic p53 and Deficits of Contextual Learning and Long-Term Potentiation. *Neuron* **21,** 799–811 (1998).

604. Weeber, E. J. *et al.* Derangements of Hippocampal Calcium / Calmodulin- Dependent Protein Kinase II in a Mouse Model for Angelman Mental Retardation Syndrome. **23,** 2634–2644 (2003).

605. Clayton-Smith, J. Clinical research on Angelman syndrome in the United Kingdom: observations on 82 affected individuals. *Am. J. Med. Genet.* **46,** 12–5 (1993).

606. Baron, C. A. *et al.* Genomic and functional profiling of duplicated chromosome 15 cell lines reveal regulatory alterations in UBE3A-associated ubiquitin-proteasome pathway processes. *Hum. Mol. Genet.* **15,** 853–69 (2006).

607. Glessner, J. T. *et al.* Autism genome-wide copy number variation reveals ubiquitin and neuronal genes. *Nature* **459,** 569–73 (2009).

608. Makedonski, K., Abuhatzira, L., Kaufman, Y., Razin, A. & Shemer, R. MeCP2 deficiency in Rett syndrome causes epigenetic aberrations at the PWS/AS imprinting center that affects UBE3A expression. *Hum. Mol. Genet.* **14,** 1049–58 (2005).

609. Greer, P. L. *et al.* The Angelman Syndrome protein Ube3A regulates synapse development by ubiquitinating arc. *Cell* **140,** 704–16 (2010).

610. Hayrapetyan, V. *et al.* Region-specific impairments in striatal synaptic transmission and impaired instrumental learning in a mouse model of Angelman syndrome. *Eur. J. Neurosci.* **39,** 1018–25 (2014).

611. Wallace, M. L., Burette, A. C., Weinberg, R. J. & Philpot, B. D. Maternal loss of Ube3a produces an excitatory/inhibitory imbalance through neuron type-specific synaptic defects. *Neuron* **74,** 793–800 (2012).

612. Yashiro, K. *et al.* Ube3a is required for experience-dependent maturation of the neocortex. *Nat. Neurosci.* **12,** 777–83 (2009).